

FINAL REPORT

RIVERS FOR LIFE: SYNTHESIS PROJECT

*Ecological dynamics and instream flow needs: a program synthesis
and assessment of the remaining challenges for the SSRB*

AI1854
March 15, 2018

Principle Investigator:

John R. Post – Biological Sciences, University of Calgary, jrpost@ucalgary.ca

Contributing Investigators:

Bernhard Mayer – GeoSciences, University of Calgary, bmayer@ucalgary.ca

Stewart Rood – Biological Sciences, University of Lethbridge, rood@uleth.ca

Nilo Sinnatamby – Biological Sciences, University of Calgary, ramila.sinnatamby@ucalgary.ca

Anne Farineau – Biological Sciences, University of Calgary, anne.farineau@ucalgary.ca

Veronique Fau – GeoSciences, University of Calgary, vfau@ucalgary.ca

Alberta Innovates and Her Majesty the Queen in right of Alberta make no warranty, express or implied, nor assume any legal liability or responsibility for the accuracy, completeness, or usefulness of any information contained in this publication, nor for any use thereof that infringes on privately owned rights. The views and opinions of the author expressed herein do not necessarily reflect those of Alberta Innovates or Her Majesty the Queen in right of Alberta. The directors, officers, employees, agents and consultants of Alberta Innovates and the Government of Alberta are exempted, excluded and absolved from all liability for damage or injury, howsoever caused, to any person in connection with or arising out of the use by that person for any purpose of this publication or its contents.

Summary of the Scope of the Project:

One of the most difficult decisions that water managers face is to determine how much of the flow regime of a river can be altered without causing species extinctions or the loss of ecosystem functions and the economic services that we derive from our rivers. Existing tools are incomplete and our challenge has been to create a critical conceptual framework and effective modelling applications to ensure that Alberta's rivers are protected, yet managed effectively to support sustainable economic development.

We have made major strides in our understanding of Instream Flow Needs in the South Saskatchewan River Basin (SSRB) throughout our Rivers for Life program (see extensive summaries in our Final Report; Post et al. July 2013). We have developed diagnostic and simulation tools, developed both basin scale and reach scale analyses of mechanistic linkages across physical and biological processes and explored the concept of functional flows, all focused on the SSRB. Now that the pieces of primary research have been disseminated in the scientific literature, it is time to synthesize the new knowledge and assess its application to science-based policy development for the SSRB.

Specific Objectives:

1. To synthesize our current understanding of all physical and biological aspects of ecological functional flows of the SSRB
2. To assess the applicability of bioenergetics approaches to determining instream flow needs of fishes and impacts of climate change on SSRB fish communities
3. To critically evaluate our new isotopic and toxicological tools for tracing nutrients and pollutants in the SSRB
4. Identify knowledge gaps, develop a priority research agenda, and to facilitate application of results to instream flow issues in the SSRB and Alberta

EXECUTIVE SUMMARY

Environmental flows, defined as the ‘quantity, timing and quality of water flows required to sustain freshwater and estuarine ecosystems and the human livelihood and well-being that depend on these ecosystems’ (Brisbane Declaration 2007) is a fundamental principle used to guide water allocation decisions to manage healthy rivers and estuaries. Though internationally accepted in principle, the implementation of water management and the methods used to determine when and how much water extraction is permitted, has varied widely both in time and by jurisdiction (Tharme 2003). There is now general consensus that maintaining the natural flow regime rather than a minimum flow is vital to maintaining ecosystem function (Poff and Zimmerman 2010), however, understanding hydroecological relationships, which can vary within and among regions and sites, and over time, remains a fundamental challenge (Poff et al. 2017). This challenge is exacerbated by the vast number of physical, chemical and biological elements that are interconnected and must be considered together to determine impacts of anthropogenic alterations to the quantity, timing and quality of flows. Adding to this complexity is the involvement of multiple stressors acting upon any one system. Three key physicochemical factors that tend to vary both naturally and anthropogenically in a system and must be considered in determining environmental flows are discharge, water temperature and nutrients.

To address the challenge of understanding hydroecological relationships in the South Saskatchewan River Basin under varying discharge, temperature and nutrient conditions, the Rivers for Life: Synthesis Project synthesized our current understanding of physical and biological aspects of environmental flows. We also applied isotopic tools to determine the source and downstream impact of nutrient inputs, and assessed the impact of nutrients and flooding on macrophyte and algae biomass and consequent dissolved oxygen fluctuations. The nine papers each contribute to the understanding of spatial and temporal variation in water quantity, timing and quality, or hydroecological relationships in the South Saskatchewan River Basin.

Water Quantity, Timing & Quality

Rood et al. (2016) tested the hypothesis that climate change is amplifying the water cycle and intensifying river floods by assessing historic trends in the magnitude, duration and timing of annual peak flows from rivers that drain the Rocky Mountains, including the Red Deer, Bow and Oldman Rivers. Authors found that 7 of 30 free-flowing rivers, and 3 of 5 moderately regulated rivers reflected declining trends, 1 river reflected an increase, and the remaining rivers showed no trend. In general, they found a decrease in flood events in recent decades rather than the intensifying that was hypothesized by climate change predictions. Reasons for the decline were suggested to be an overall decrease in flows, a decrease in winter precipitation or an advancement of spring snowmelt.

A much underdeveloped area of understanding with respect to environmental flows is the role of groundwater in streamflows (Acreman et al. 2014). **Jasechko et al. (2017)** assessed $\delta^{18}\text{O}$ and $\delta^2\text{H}$ values of thousands of rain, snow, groundwater and streamflow samples in the Nelson River basin, which includes the South Saskatchewan River Basin (SSRB) to gain an understanding of the role of groundwater recharge and streamflow generation. Authors found that the amount of precipitation that makes its way into aquifers is 1.3-5x higher during the cold, winter months relative to warm, summer months. The implication of this finding is that changes to winter water balance may have a disproportionate impact on groundwater recharge, which is highly relevant when considering predicted climate change scenarios. Further, authors found that young streamflow (precipitation that becomes streamflow in less than 2.3 months), contributes to 27% of annual streamflow on average, but that the percentage varies greatly among tributaries so that a larger percent of young streamflow contributes to flow in flat catchments (e.g. prairies) vs. tributaries in steep catchments (e.g. mountains). The implication of this finding is that precipitation is likely able to mobilize fertilizers more quickly in flat prairie landscapes that tend to contain more agriculture.

Similarly, relatively little scientific study has been conducted on water quality in groundwater. Work by **Humez et al. (2016)** has contributed to the current understanding of groundwater quality in Alberta. Authors aimed to develop a baseline of methane in Alberta groundwater so that the impact of any future spills could be evaluated appropriately. The study found low concentrations of methane in shallow groundwater in all but 28 of 168 samples. They found that methane concentrations generally increased with sample depth, and were likely to be higher in aquifers associated with coal seams and shale. However, stable isotope analysis identified a common source for all methane in groundwater samples in Alberta, with a biogenic origin via CO₂ reduction.

Nutrient loadings to rivers from anthropogenic sources are a common concern in many watersheds and nutrient assessments are included in environmental flow assessments to maintain water quality. In order to manage nutrients in a system, it is important to identify the various sources and their downstream effects. While nutrient concentrations have been monitored for a number of decades in many watersheds (Sosiak 2003), determining sources, particularly when there are multiple potential sources, is more of a challenge. **Chao et al. (in prep.)** used physical, chemical and isotopic methods to identify and quantify sources of nitrate to the Bow River. Authors found that nitrate flux increased dramatically within the City of Calgary. Nitrate stable isotope values ($\delta^{15}\text{N}$, $\delta^{18}\text{O}$) were instrumental in identifying nitrate sources. $\delta^{15}\text{N}$ and $\delta^{18}\text{O}$ values in the headwater region was largely consistent with forest soil-derived nitrate, whereas downstream of the wastewater treatment plant (WWTP) outflows, $\delta^{15}\text{N}$ and $\delta^{18}\text{O}$ values from water samples were consistent with wastewater effluent stable isotope values. Below the City of Calgary, 84-92 % of the nitrate load was attributed to WWTP effluent.

Impacts of Variability in Water Quantity, Timing and Quality on Ecological Processes

A key component of many environmental flow assessments is determining the proportion of natural flow that must be maintained in a channel to maintain healthy fish populations. To do so, it is the relationship between flow and fish productivity must be characterized. Many scientific studies and

environmental flow assessments have relied strictly on establishing relationships between hydrology and fish production based on habitat suitability curves (Clipperton et al. 2003; Rosenfeld et al. 2007; Laliberte et al. 2014). However, a common criticism of such methods is that they often fail to accurately predict fish abundances, and that habitat selection and fitness associations are rarely supported (Rosenfeld 2003). Bioenergetics models that combine hydraulic models with drift transport and drift-foraging behaviour of the fish to predict fish productivity have shown promise in overcoming those previous shortfalls (Hayes et al. 2007; Wall et al. 2016). Using a free-flowing fourth order tributary of the Bow River, Jumpingpound Creek, as a model reach, **Laliberte et al. (2016)** demonstrated the impact of seasonal variation in discharge, water temperature and prey drift density on fish productivity. Results illustrated that when energy requirements increased (during high discharge and/or high water temperature), higher prey drift densities were required to support fish production. In particular, adult fish were less likely to be productive in the stream reach because of higher prey densities required to meet their higher metabolic needs. The relationship between discharge, temperature, prey availability and fish productivity demonstrated by **Laliberte et al (2016)**, can be extended to predict likely fish productivity in other areas of the SSRB, as well as under anthropogenic alteration (e.g. regulated flow, climate change, nutrient inputs).

The Lower Bow River contains a world-class rainbow trout fishery with an estimated annual economic value of \$24.5 million CAD (Crowe-Swords 2016). While the fishery has functionally operated as a catch-and-release fishery since 2006, its proximity to the City of Calgary and its international reputation as one of the best fly fishing locations in the world results in a high effort fishery with approximately 161 angler hours/ha (Ripley and Council 2006). Rainbow trout were introduced into the Bow River, however, this now naturalized species, is considered economically and recreationally significant, has been the focus of scientific study (Rhodes 2005; Post et al. 2006; Askey et al. 2007), and is managed by the provincial government to maintain a healthy fishery (Sosiak 1987; Ripley and Council 2006). **Cahill et al. (submitted)**

identified a 43-50% decline in adult rainbow trout over a 10 year period, based on population abundance estimates conducted on the Bow River between 2003 and 2013. The Bow River rainbow trout fishery faces a number of stressors that may contribute individually, or in concert, to the declining numbers observed. Three of the key potential stressors identified are (1) whirling disease (Canadian Food Inspection Agency 2016), which has had detrimental effects on rainbow trout populations elsewhere (Nehring and Walker 1996; Vincent 1996), (2) extreme flooding events that occurred in 2005 and 2013 on the Bow River (Veiga et al. 2015), and high angling effort via release mortality (Post et al. 2003; Bartholomew and Bohnsack 2005). Of those potential stressors, only angling can be actively managed. As such, **Cahill et al. (submitted)** suggest effort restrictions as a key management strategy for inland recreational fisheries under multiple stressors, such as the Bow River rainbow trout fishery. Prior to this recent work by **Cahill et al. (submitted)**, the Bow River rainbow trout fishery was not considered to be in decline, let alone exhibit declines of a magnitude that are consistent with threatened or endangered classifications by The Committee on the Status of Endangered Wildlife in Canada (COSEWIC 2018).

Mee et al. (2016) determined the key physicochemical variables that drive fish species distribution throughout the main stem rivers in the SSRB. Authors found that the total number of fish species present increased with distance from the headwaters, consistent with the theory of species addition (Rahel and Hubert 1991). Of the various physical and chemical variables that were included in the analysis, mean July water temperature was the most common driver of species distribution (**Mee et al. 2016**). Authors also found distinct shifts in the fish community composition that occurred at locations along the river with mean July water temperatures of approximately 15 °C and 19-20 °C; a pattern that was consistent across all main stems. The species that comprised each community were typically consistent with known species thermal preferences.

Given the importance of water temperature in determining current fish species distributions along the SSRB main stem rivers (Mee et al. 2016), **Mee et al (in prep.)** used forecasted water temperatures to

predict species distribution in 2040 and 2080. In general, authors found contractions in the distribution of fish with colder thermal preferences (e.g. Cutthroat trout, bull trout), mixed responses in fish species with cool thermal preferences (e.g. little change in rainbow trout, local extinctions of spoonhead sculpin), and potential upstream movement of many fish with warmer thermal tolerances (e.g. walleye).

Sinnatamby et al. (in prep.) combined published, public and new data to assess ecological responses to spatial and temporal variation in discharge, temperature and nutrients in the Bow River. Authors demonstrate that variability observed in the Bow River's physical, hydrological, thermal and nutrient characteristics are a reflection of both natural and anthropogenic drivers. The observed variation can be interpreted spatially, where the most pristine reach is the headwater reach and the region of greatest anthropogenic alteration is the mid-reach area extending from Kananaskis Dam to Highwood River which is characterised by a number of dams, reservoirs, increased population density and municipal nutrient inputs. A similar pattern was mirrored in the riparian abundance as well. **Sinnatamby et al. (in prep.)** presents a number of Bow River ecological case studies that inform our current understanding of hydroecological relationships in the Bow River under varying physical and chemical drivers. Authors update our understanding of the relationships between nutrient inputs, discharge, aquatic vegetation biomass, and diel dissolved oxygen fluctuations, factors that contribute to fish biomass and species abundance distributions, and present a small-scale assessment of how seasonal variations in discharge, temperature and prey densities impact fish productivity.

Advances in Environmental Flows Science in the SSRB

In order to manage the numerous challenges that face the SSRB, and any complex watershed, it is necessary to disentangle the drivers of the observed variation. The use of long-term records, and new analytical and statistical techniques in recent studies on the SSRB have advanced our progress to this end.

The availability of century-long stream gauge records throughout the Rocky Mountains allowed **Rood et al (2016)** the temporal and spatial breadth of data required to assess changes in flood characteristics

while limiting the impact of land use and providing a regional context. Annual variation in macrophyte and epilithic algae biomass in the Bow River has been assessed a number of times in the past (Sosiak 2003; Taube et al. 2016). However, with each iteration of analysis and as the data set grows, new connections between these complex variables can be identified. In the present analysis, **Sinnatamby et al. (in prep.)** presents updated aquatic vegetation biomass data alongside newer diel dissolved oxygen fluctuation data. The results suggest a promising link between epiphytic algae biomass, rather than macrophyte biomass, and dissolved oxygen fluctuations.

Application of new Bayesian statistical methods to an existing data set of rainbow trout population estimates allowed **Cahill et al. (submitted)** to identify a decline in the Bow River rainbow trout fishery that was not previously recognized using traditional statistical methods. Development of analytical methods for boron stable isotopes in river water samples, and application of isotopic biplots comparing boron stable isotope values of river water samples to potential sources (**Sinnatamby et al. in prep.**) has allowed for further elucidation of nutrient sources compared using nitrate alone (**Chao et al. in prep.**). Determination of the importance of water temperature to fish species distribution using decades of presence-absence data (**Mee et al. 2016**) and application of climate change models has allowed **Mee et al. (in prep.)** to predict future species distributions and identify species particularly at risk to predicted thermal changes.

Remaining Challenges for the SSRB

The SSRB still faces a number of challenges with respect to environmental flows. With increasing predicted impacts of climate change, and a growing human population, the demand for water is expected to increase. For example, whereas work presented here addresses predicted changes in temperature, uncertainty remains regarding ecological outcomes to changes in precipitation, flow and receding glaciers also predicted with climate change. While environmental flows address issues of water quantity, timing and quality, implications of multiple existing stressors, some of which are not typically considered in environmental flow assessments (e.g. angling pressure) are likely to complicate assessments or confound

results. As such, interactions between stressors remains a key area that requires further study. Based on the advancements that have occurred in this field, and specifically in the SSRB, long-term data sets, analytical and statistical methods, and mechanistic modelling under different scenarios are likely to contribute should be maintained and developed further.

REFERENCES

- Acreman, M.C., Overton, I.C., King, J., Wood, P.J., Cowx, I.G., Dunbar, M.J., Kendy, E., and Young, W.J. 2014. The changing role of ecohydrological science in guiding environmental flows. *Hydrological Sciences Journal-Journal Des Sciences Hydrologiques* **59**(3-4): 433-450.
- Askey, P.J., Hogberg, L.K., Post, J.R., Jackson, L.J., Rhodes, T., and Thompson, M.S. 2007. Spatial patterns in fish biomass and relative trophic level abundance in a wastewater enriched river. *Ecol. Freshwat. Fish* **16**(3): 343-353.
- Bartholomew, A., and Bohnsack, J. 2005. A review of catch-and-release angling mortality with implications for no-take reserves. *Rev. Fish Biol. Fish.* **15**(1-2): 129-154.
- Brisbane Declaration. 2007. Summary findings and a global action agenda of the 10th International River Symposium and International Environmental Flows Conference, 2-6 September 2007. Available at: <http://www.watercentre.org/news/declaration>. Brisbane, Australia.
- Cahill, C., Mogenson, S., Wilson, K., Cantin, A., Sinnatamby, R.N., Paul, A., Christensen, P., Reilly, R., Winkel, L., Farineau, A., and Post, J.R. submitted. Multiple challenges confront a high-effort inland recreational fishery in decline. *Can. J. Fish. Aquat. Sci.*
- Canadian Food Inspection Agency. 2016. Confirmed detections of whirling disease - Alberta 2016.[online]. Available from <http://www.inspection.gc.ca/animals/aquatic-animals/diseases/reportable/whirling-disease/alberta-2016/eng/1473443992952/1473443993551> [cited March 10 2018].
- Chao, J., Kruk, M., Mayer, B., and Ryan, M.C. in prep. Isotopic apportionment of nitrate sources in the Bow River Alberta, Canada.
- Clipperton, G.K., Koning, C.W., Locke, A.G.H., Mahoney, J.M., and Quazi, B. 2003. Instream flow needs determinations for the South Saskatchewan River Basin, Alberta, Canada. Alberta Government, Alberta.
- COSEWIC. 2018. COSEWIC wildlife species assessment: quantitative criteria and guidelines [online]. Available from <https://www.canada.ca/en/environment-climate-change/services/committee-status-endangered-wildlife/wildlife-species-assessment-process-categories-guidelines/quantitative-criteria.html> [cited March 10 2018].
- Crowe-Swords, P. 2016. The economic importance of recreational river use to the City of Calgary. Calgary River Users Alliance.
- Hayes, J.W., Hughes, N.F., and Kelly, L.H. 2007. Process-based modelling of invertebrate drift transport, net energy intake and reach carrying capacity for drift-feeding salmonids. *Ecol. Model.* **207**(2-4): 171-188.

- Humez, P., Mayer, B., Ing, J., Nightingale, M., Becker, V., Kingston, A., Akbilgic, O., and Taylor, S. 2016. Occurrence and origin of methane in groundwater in Alberta (Canada): Gas geochemical and isotopic approaches. *Sci. Total Environ.* **541**: 1253-1268.
- Jasechko, S., Wassenaar, L.I., and Mayer, B. 2017. Isotopic evidence for widespread cold-season-biased groundwater recharge and young streamflow across central Canada. *Hydrol. Process.* **31**(12): 2196-2209.
- Laliberte, J.J., Post, J.R., and Rosenfeld, J.S. 2014. Hydraulic geometry and longitudinal patterns of habitat quantity and quality for rainbow trout (*Oncorhynchus mykiss*). *River Research and Applications* **30**(5): 593-601.
- Laliberte, J.J., Post, J.R., Rosenfeld, J.S., and Mee, J.A. 2016. Modelling temperature, body size, prey density, and stream gradient impact on longitudinal patterns of potential production of drift-feeding trout. *River Res. Appl.* **32**(10): 2045-2055.
- Mee, J.A., Robins, G.L., and Post, J.R. in prep. Predicted spatial distribution of fish species in the South Saskatchewan River Basin main stem rivers following climate change.
- Mee, J.A., Robins, G., and Post, J.R. 2016. Patterns of fish species assemblage replicated across three parallel rivers suggest biotic zonation in response to a longitudinal temperature gradient. *Ecol. Freshwat. Fish* DOI: **10.1111/eff.12322**.
- Nehring, R.B., and Walker, P.G. 1996. Whirling disease in the wild: The new reality in the intermountain west. *Fisheries* **21**: 28-30.
- Poff, N.L., and Zimmerman, J.K.H. 2010. Ecological responses to altered flow regimes: a literature review to inform the science and management of environmental flows. *Freshwat. Biol.* **55**(1): 194-205.
- Poff, N.L., Tharme, R.E., and Arthington, A.H. 2017. Evolution of environmental flows assessment science, principles, and methodologies. *In* *Water for the environment: from policy and science to implementation and management*. Edited by A.C. Horne, J.A. Webb, M.J. Stewardson, B.D. Richter and M. Acreman. Academic Press is an imprint of Elsevier, London, United Kingdom. pp. 203-236.
- Post, J.R., Mushens, C., Paul, A., and Sullivan, M. 2003. Assessment of alternative harvest regulations for sustaining recreational fisheries: Model development and application to bull trout. *N. Am. J. Fish. Manage.* **23**(1): 22-34.
- Post, J.R., van Poorten, B.T., Rhodes, T., Askey, P., and Paul, A. 2006. Fish entrainment into irrigation canals: An analytical approach and application to the Bow River, Alberta, Canada. *N. Am. J. Fish. Manage.* **26**(4): 875-887.
- Rahel, F.J., and Hubert, W.A. 1991. Fish assemblages and habitat gradients in a Rocky Mountain Great Plains stream - Biotic zonation and additive patterns of community change. *Trans. Am. Fish. Soc.* **120**(3): 319-332.

- Rhodes, T.R. 2005. The immediate and short-term impacts of catch-and-release angling on migrating and pre-spawning condition rainbow trout (*Oncorhynchus mykiss*) in the Bow River, Alberta. University of Calgary, Calgary, Alberta.
- Ripley, T.D., and Council, T. 2006. Bow River Sport Fish Angler Survey. Alberta Conservation Association, Alberta.
- Rood, S.B., Foster, S.G., Hillman, E.J., Luek, A., and Zanewich, K.P. 2016. Flood moderation: Declining, peak flows along some Rocky Mountain rivers and the underlying mechanism. *Journal of Hydrology* **536**: 174-182.
- Rosenfeld, J.S. 2003. Assessing the habitat requirements of stream fishes: An overview and evaluation of different approaches. *Trans. Am. Fish. Soc.* **132**(5): 953-968.
- Rosenfeld, J.S., Post, J.R., Robins, G., and Hatfield, T. 2007. Hydraulic geometry as a physical template for the River Continuum: application to optimal flows and longitudinal trends in salmonid habitat. *Can. J. Fish. Aquat. Sci.* **64**(5): 755-767.
- Sinnatamby, R.N., Mayer, B., Rood, S.B., Farineau, A., and Post, J.R. in prep. From glaciers to prairie: Temporal and spatial variation in ecological processes in a large riverine ecosystem.
- Sosiak, A. 2003. Long-term response of periphyton and macrophytes to reduced municipal nutrient loading to the Bow River (Alberta, Canada). *Can. J. Fish. Aquat. Sci.* **59**(6): 987-1001.
- Sosiak, A. 1987. A fisheries survey on the Bow River from Bearspaw Dam to Carseland, Alberta, in 1985. Fish and Wildlife Division, Alberta Forestry, Lands and Wildlife, Calgary, AB.
- Taube, N., He, J., Ryan, M.C., and Valeo, C. 2016. Relative importance of P and N in macrophyte and epilithic algae biomass in a wastewater-impacted oligotrophic river. *Environ. Monit. Assess.* **188**(8): 494.
- Tharme, R.E. 2003. A global perspective on environmental flow assessment: Emerging trends in the development and application of environmental flow methodologies for rivers. *River Research and Applications* **19**(5-6): 397-441.
- Veiga, V.B., Hassan, Q.K., and He, J. 2015. Development of flow forecasting models in the Bow River at Calgary, Alberta, Canada. *Water* **7**(1): 99-115.
- Vincent, E.R. 1996. Whirling disease and the wild trout: The Montana experience. *Fisheries* **21**: 32-33.
- Wall, C.E., Bouwes, N., Wheaton, J.M., Saunders, W.C., and Bennett, S.N. 2016. Net rate of energy intake predicts reach-level steelhead (*Oncorhynchus mykiss*) densities in diverse basins from a large monitoring program. *Can. J. Fish. Aquat. Sci.* **73**(7): 1081-1091.

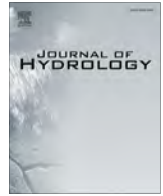
Table of Contents

RIVERS FOR LIFE: SYNTHESIS PROJECT	1
EXECUTIVE SUMMARY.....	3
REFERENCES.....	11
DISSEMINATION OF INFORMATION.....	15
CONTRIBUTED PAPERS	16
Rood et al. 2016.....	17
Jasechko et al. 2017	26
Humez et al. 2016	40
Chao et al. In Revision	56
Laliberte et al. 2016	104
Cahill et al. Submitted	115
Mee et al. 2016	159
Mee et al. in prep.	177
Sinnatamby et al. in prep.	188

DISSEMINATION OF INFORMATION

- Sinnatamby, R.N. & J.R. Post. Responses of ecological processes to variability in water quantity and quality. Bow River Basin Council Science Forum, Calgary AB. May 2, 2018.
- Sinnatamby R.N. & J.R. Post. Responses of ecological processes to variability in water quantity and quality. Canadian Conference For Fisheries Research, Edmonton AB. January 4-7, 2018.
- Sinnatamby, R.N. Responses of ecological processes to variability in water quantity and quality: Case studies from the Bow River. Ecology and Evolutionary Biology Series Seminar, University of Calgary, Calgary AB. November 3, 2017.
- Sinnatamby, R.N. & J.R. Post. Variations in ecological processes along the Bow River. Alberta Innovates – Water Innovation Program Forum, Edmonton AB. May 24-25, 2017.
- Cahill, C.L., S.M. Mogensen, K.L. Wilson, A. Cantin, R.N. Sinnatamby & J.R. Post. Multiple challenges confront a high-effort recreational fishery in decline. Bow River Basin Council Science Forum, Calgary AB. May 2, 2018.
- Cahill, C.L., S.M. Mogensen, K.L. Wilson, A. Cantin, R.N. Sinnatamby & J.R. Post. Paradoxically high mortality in a catch-and-release fishery. Canadian Conference For Fisheries Research, Montreal QC. January 5-8, 2017.
- Mayer, B., Kruk, M., Chao, J., Fau, V., Nightingale, & M., Wieser, M. (2017): Multi-Isotope tracing (N, O, S, B) of sources and fate of nutrients in riverine systems of Western Canada. – 9th International Symposium on Ecosystem Behavior, Biogemon 2017, Litomyšl, Czech Republic, August 20-24, 2017.
- Mayer, B., Kruk, M., Fau, V., Nightingale, M. & Wieser, M. (2017): Tracing sources and fluxes of nitrate and phosphate in riverine systems of Western Canada using chemical and multi-isotope (N, O, B) tracer approaches. Goldschmidt 2017, Paris, France, August 13-18, 2017.

CONTRIBUTED PAPERS



Flood moderation: Declining peak flows along some Rocky Mountain rivers and the underlying mechanism



Stewart B. Rood*, Stephen G. Foster, Evan J. Hillman, Andreas Luek, Karen P. Zanewich

Environmental Science Program, University of Lethbridge, Alberta T1K 3M4, Canada

ARTICLE INFO

Article history:

Received 22 November 2015
 Received in revised form 12 February 2016
 Accepted 23 February 2016
 Available online 2 March 2016
 This manuscript was handled by Andras Bardossy, Editor-in-Chief, with the assistance of Bruno Merz, Associate Editor

Keywords:

Climate change
 River floods
 Historic hydrology
 Hydrographic apex
 North America

SUMMARY

It has been proposed that global warming will amplify the water cycle and intensify river floods. We tested this hypothesis by investigating historic trends in magnitudes, durations and timing of the annual peak flows of rivers that drain the Rocky Mountains around the North American hydrographic apex, the source for rivers flowing to the Pacific, Arctic (including Hudson Bay) and Atlantic Oceans. We sought century-long records and to reduce influences from land-use we assessed drainages from parks and protected areas. Of 30 rivers and reaches that were free-flowing or slightly regulated, seven displayed declining peak flows (7 $p < 0.1$, 4 $p < 0.05$), and one showed increase ($p < 0.05$); three of five moderately regulated rivers displayed decline ($p < 0.05$). Substantial floods, exceeding the 1-in-5 year recurrence (Q_5), were more common in the early versus latter halves of the records for some Arctic drainages and were more common during the Pacific Decadal Oscillation negative phase for all regions. The timing of peak flows was relatively unchanged and Q_5 flood durations declined for a few rivers. These results indicate flood moderation rather than flood intensification, particularly for Arctic Ocean drainages. This could reflect regional hydrological consequences from climate change including: (1) declining overall annual river flows; (2) winter warming that would increase the rain versus snow proportion, thus reducing snow accumulation and melt; and (3) spring warming that advances snow melt, lengthening the melt interval before peak flows. These changes would shift the seasonality of river flows and reduce annual peaks. We might expect continuing moderation of peak flows but there will probably still be occasional major floods from exceptional rain events such as occurred in northern Montana in 1964 and in southern Alberta in 2013.

© 2016 Elsevier B.V. All rights reserved.

1. Introduction

While there is growing concern related to global warming, in many regions an even greater challenge from climate change relates to impacts on water resources (Bates et al., 2008). There has been a common view that atmospheric warming will accelerate or intensify the global water cycle (Durack et al., 2012) and that this could result in heavier rain events that would produce more severe river floods (Huntington, 2006). As summarized by Karl and Melillo (2009), 'Floods ... are likely to be amplified in most regions.'

Supporting this view, Milly et al. (2002) reported that there had been more major floods in recent versus prior decades, and that this was consistent with some hydroclimatic projections based on impacts from greenhouse gases and aerosols. However, those data were very limited (only 21 flood events) and confounding

the influences from climate change, land-use alterations would increase rates of surface run-off, thereby worsening river floods (Wheater and Evans, 2009). In particular, forest harvesting, woodland clearing for crops or pasture, wetland drainage and infilling, and the construction of roadways, buildings and other impermeable surfaces can increase and accelerate run-off, thus increasing flood peaks. Conversely, dams create reservoirs that can attenuate flows and flood-control is a primary objective of many projects. Due to these and other human impacts, it is difficult to assess flood histories and resolve the impacts of climate change versus other human influences.

In considering the literature, the International Panel on Climate Change (IPCC) technical group concluded that it is likely that since about 1950 the number of heavy precipitation events over land has generally increased and that this conclusion is more confident for North America (Stocker, 2013). However, the transition from heavy rains to intense floods has been less certain. In reviewing the broader literature, including papers assessed by the IPCC report, Kundzewicz et al. (2014) suggested that there is low confidence

* Corresponding author.

E-mail address: rood@uleth.ca (S.B. Rood).

in the conclusion that anthropogenic climate change has resulted in increased magnitude or frequency of global river floods over recent decades. This uncertainty partly reflects the confounding complexities from land-use impacts, the natural variability in river flows and limited intervals of flood flow records for most river systems.

To investigate changes in river regimes associated with climate change, we analyzed a study system that straddles the east–west and north–south Continental Divides of North America (Rood et al., 2005, 2008). This study system reflects influences from weather systems from the Pacific Ocean, Gulf of Mexico and Arctic Ocean, and includes the hydrographic apex of North America, the headwater source for some of the major North American river systems that drain to the Pacific, Arctic and Atlantic Oceans. This zone includes the transboundary Rocky Mountain region around the Canada–United States border, which provides a global focus for parks and protected areas, with Jasper, Banff, Kootenay and Waterton Lakes National Parks, Canada; and Glacier, Yellowstone and Grand Teton National Parks, USA (Fig. 1). With substantial landscape protection that extended back to the nineteenth century, this zone includes relatively pristine Rocky Mountain watersheds, thus reducing the confounding influences from human developments.

There has been some river damming and flow regulation within these protected areas and this influence must be recognized in analyses of historic flow patterns (Tables 1a–c).

Consequently, we assessed the records of historic peak flows for rivers that drain this transboundary conservation corridor, and these analyses follow from our prior analyses of the historic annual and seasonal river flow patterns of these rivers (Rood et al., 2005, 2008). We investigated records for individual rivers, and then for the three major drainage regions, and the prospective correspondence with the Pacific (multi) Decadal Oscillation (PDO). Following the principles of water cycle amplification and flood intensification, our primary expectation was that there would have been increasing flood severity, with higher peak magnitudes and longer flood-durations over the past century. As a secondary prediction, following winter warming and earlier snow melt (Barnett et al., 2005; Cunderlik and Ouarda, 2009; Shepherd et al., 2010), we also anticipated that annual flow peaks would occur earlier.

2. Methods

We selected rivers and gauging locations with criteria that extended from our prior studies of annual and seasonal flow



Fig. 1. Map of western North America with the locations of the studied 30 hydrologic gauging stations, sequenced by major watersheds as listed in Tables 1a–c. For the region east of the Continental Divide, the American/Canadian border approximates the north–south Hudson Bay Divide. The triangle orientation indicates the direction of apparent change (Δ upright = increasing, with positive regression slope; inverted = decreasing); the size represents the statistical effect (small = not statistically significant; medium = statistical trend, $p < 0.1$; and large = statistically significant, $p < 0.05$); and the fill indicates the extent of regulation (open = free-flowing or slight regulation, gray = moderate regulation).

Table 1a

Study gauges for rivers flowing to the Hudson Bay and Arctic Ocean, with correlation analyses of flow characteristics and trends ($p < 0.1$) underlined and significant patterns ($p < 0.05$) in bold. The rivers are generally sequenced from north-to-south, west-to-east and upstream to downstream. Status refers to the extent of damming and reservoir storage.

River and gauge	Period of record	Years	Status	Pearson r ;	Kendall τ			
				p value	p value	Q_5 Duration	Q_{max} Date	
				Log Q_{max}	Q_{max}			
<i>Arctic Ocean – Mackenzie River Basin</i>								
1	Smoky R. at Watino, AB (07GJ001)	1916–1921; 1955–2013	65	Free-flowing	–.131 .299	–.129 .131	.026 .795	–.014 .865
2	Athabasca R., Hinton & Entrance, AB (07AD001 & 07AD002)	1915–1939; 1955–2011	82	Free-flowing	–.373 <.001	–.268 .001	–.133 .131	.089 .240
<i>Hudson Bay – Nelson River Basin</i>								
3	North Saskatchewan at Edmonton, AB (05DF001)	1911–2013	103	Moderate Regulation	–.285 .004	–.189 .005	–.070 .370	.038 .572
4	Red Deer River at Red Deer, AB (05CC002)	1913–1932; 1935–2013	100	Slight regulation	–.171 <u>.088</u>	–.109 .108	–.179 .023	.040 .557
5	Bow River at Banff, AB (05BB001)	1909–2012	104	Free-flowing	–.244 .013	–.170 .011	–.130 <u>.093</u>	–.050 .460
6	Bow River at Calgary, AB (05BH004)	1911–1950; 1952–2013	102	Moderate regulation	–.206 .037	–.331 <.001	–.230 .004	.008 .910
7	Elbow River at Bragg Creek, AB (05BJ004)	1935–2012	78	Free-flowing	.071 .539	.047 .540	.029 .747	.016 .832
8	Highwood R., Diebel's Ranch, AB (05BL019)	1951–2012	62	Free-flowing	–.078 .546	–.059 .500	–.092 .363	–.019 .831
9	Oldman R., Waldron's Corner, AB (05AA023)	1950–2008	59	Free-flowing	–.042 .753	–.040 .652	.094 .365;	.073 .417
10	Castle R. near Beaver Mines, AB(05AA022)	1945–2011	67	Free-flowing	–.104 .404	–.120 .153	–.038 .697	.166 .049
11	Waterton R. near Waterton Park, AB (05AD003)	1908–1930; 1948–2012	88	Free-flowing	–.116 .283	–.137 <u>.060</u>	–.072 .401	–.015 .837
12	Belly R. at Mountain View, AB (05AD005)	1912–2012	101	Almost free-flowing	.106 .292	.074 .274	.082 .300	.011 .876
13	St Mary R. Int'l Boundary, AB (05AE027)	1903–2014	112	Slight regulation	–.110; .249	–.084 .188	–.045 .548	.026 .691
14	South Saskatchewan at Medicine Hat, AB (05AJ001)	1911–2013	102	Moderate regulation	–.134 .178	–.068 .310	–.014 .861	.080 .237

Table 1b

Study gauges and rivers flowing to the Pacific Ocean, presentation as in Table 1a.

River and gauge	Period of record	Years	Status	Pearson r ;	Kendall τ			
				p value	p value	Q_5 Duration	Q_{max} Date	
				Log Q_{max}	Q_{max}			
<i>Pacific Ocean – Fraser River Basin</i>								
15	Fraser River at Hansard, BC (08KA004)	1953–2010	58	Free-flowing	–.213 .108	–.162 <u>.073</u>	.055 .601	–.100 .271
16	Fraser River at Hope, BC (08MF005)	1912–2012	101	Moderate regulation	–.068 .502	–.085 .211	.066 .402	.006 .930
<i>Pacific Ocean – Columbia River Basin</i>								
17	Columbia R. at Nicholson, BC (08NA002)	1903–2013	109	Free-flowing	–.014 .882	–.029 .654	–.016 .834	–.103 .117
18	Kootenay R. at Kootenay Crossing, BC (08NF001)	1939–1941; 1945–1946; 1948–2013	71	Free-flowing	.064 .596	.039 .634	.006 .947	.012 .881
19	Bull River near Wardner, BC (08NG002)	1914–1915; 1919–1922; 1928–2013	94	Slight regulation	.131 .208	.084 .233	<u>.140</u> <u>.089</u>	–.026 .717
20	Elk River at Phillips Bridge, BC (08NK005)	1925–1996; 1997–2013	89	Almost free-flowing	–.022 .838	–.051 .483	–.102 .224	<u>.129</u> <u>.076</u>
21	North Fork of Flathead R. near Columbia Falls, MT (USGS 12355500)	1912–1917; 1929–2013	92	Free-flowing	.068 .518	.011 .879	–.040 .632	–.029 .685
22	Middle Fork Flathead R. near West Glacier, MT (USGS 12358500)	1940–2013	74	Free-flowing	–.058 .626	–.052 .516	–.024 .799	–.021 .790

regimes (Rood et al., 2005, 2008). We investigated rivers that drained the central Rocky Mountains region and favored rivers that drained relatively pristine watersheds (Fig. 1). We required peak flow records of more than 50 years and sought century-long records to increase statistical confidence and to dampen influences

from climate oscillations, especially the PDO (Whitfield et al., 2010; Rood et al., 2015).

While free-flowing rivers were favored, these were limited and we also included regional rivers with some damming and regulation. We assessed the extent of regulation based on the storage

Table 1c
Study gauges and rivers flowing to the Gulf of Mexico, presentation as in Table 1a.

River and gauge	Period of record	Years	Status	Pearson <i>r</i> ; <i>p</i> value Log Q_{max}	Kendall τ <i>p</i> value			
					Q_{max}	Q_5 Duration	Q_{max} Date	
<i>Gulf of Mexico – Missouri Sub-basin of Mississippi River Basin</i>								
23	Milk R. at the Western Crossing of International Boundary, AB (11AA025)	1931–1985; 1987–2014	83	Slight regulation	.146 .187	.116 .120	.111 .204	.200 .008
24	Marias R. near Shelby, MT (USGS 06099500)	1904–1907; 1911–2013	109	Slight regulation	–.090 .352	–.079 .223	.036 .636	.055 .400
25	Teton R. near Dutton, MT (USGS 06108000)	1955–2013	59	Almost free-flowing	–.361 .005	–.236 .008	<u>–.170</u> <u>.103</u>	–.021 .814
26	Sun R. near Vaughn, MT (USGS 06089000)	1934–2013	80	Extensive diversions	–.174 .123	–.165 .031	–.104 .249	.047 .541
27	Missouri R. at Toston, MT (USGS 06054500)	1890; 1911–1916; 1941–2013	80	Moderate regulation	–.225 .045	<u>–.125</u> <u>.100</u>	–.094 .287	–.046 .549
28	Gallatin R. near Gallatin Gateway, MT (USGS 06043500)	1890–1894; 1930–1969; 1972–1981; 1985–2013	84	Free-flowing	.093 .401	.104 .163	–.023 .791	–.066 .378
29	Madison R. near West Yellowstone, MT (USGS 06037500)	1915–1917; 1919–1973 1983–1986 1989–2013	85	Free-flowing	.264 .015	.190 .010	.126 .141	–.148 .047
30	Yellowstone R. near Livingstone, MT (USGS 06192500)	1897–1905; 1928–1932; 1937–2013	90	Free-flowing	.042 .697	.038 .601	.029 .724	–.164 .024

index, the total storage capacity of the onstream reservoirs along the river and its tributaries upstream from the gauging location (based on websites of the respective agencies) as a percentage proportion of the average total annual flow. This provided four status categories: free-flowing (unregulated), or slight (up to 15%), moderate (16–30%) or extensive (>30%) regulation. We subsequently rejected the regional rivers with extensive regulation and, along with our requirements for relatively intact watersheds and a minimum half-century time series, this resulted in 30 study rivers and reaches (Table 1a–c).

Discharge (*Q*) records were obtained from the online ‘HYDAT’ data set of the Water Survey of Canada for Canadian rivers (<http://www.wsc.ec.gc.ca/applications/H2O/index-eng.cfm>) and the United States Geological Survey website for American rivers (<http://waterdata.usgs.gov/nwis>, both accessed to January 2015). We assessed peak flows as the maximum mean daily discharges (Q_{max}), since the instantaneous peak (Q_{max-i}) records are often incomplete for the early intervals. Either approach would be almost identical, since very tight associations exist between Q_{max} and Q_{max-i} for these medium to large rivers (e.g. Bow River at Banff (#5); $Q_{max-i} = 1.037 \times Q_{max}$; $r^2 = 0.993$). These Rocky Mountain river systems consistently display ‘nival patterns’ with maximum annual flows in the open water interval (Burn and Whitfield, 2015) and we included only peaks from May through October to avoid localized winter floods from ice jam events. For the Elk River, we coordinated peak discharge data from sequential gauges that displayed 95% correspondence (Fig. 2).

We developed spreadsheets with five river discharge parameters for the interannual time series for each river (Table 1, Fig. 3). These included (1) the Q_{max} and to normalize the distribution for the parametric Pearson correlation the Q_{max} values were also log-transformed (2). We assessed the occurrences of moderate to major floods, considering peaks exceeding the 1-in-5 year recurrence (Q_5). These substantial floods would considerably exceed the bank-full discharge for these cool-region rivers where ice formation and break-up can widen the channels (Smith, 1979; Polzin and Rood, 2006). The Q_5 thresholds were calculated with the log Pearson Type III distribution that closely fit the data series

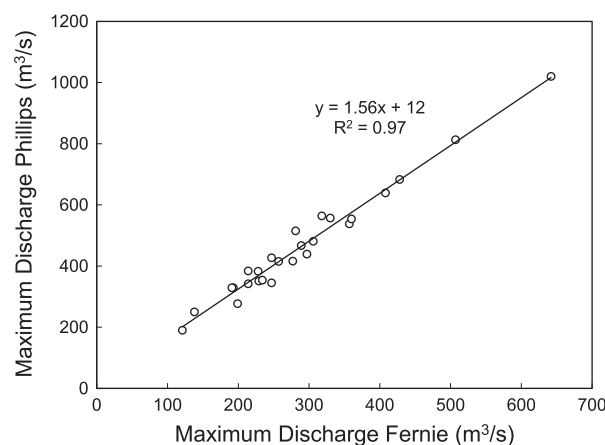


Fig. 2. The maximum discharge of the Elk River at Fernie, BC versus at Phillips Bridge, BC (#20) for the overlapping historic record. This illustrates the coordination of discharge data across sequential gauges enabling extension of the time series.

through the Q_5 range. We investigated the occurrences of these substantial floods over the historic intervals (3) and assessed whether there were more in the recent versus prior halves of the time series, with the χ^2 (chi-square) test and an expected equal split for the two half-series. We also assessed the durations of moderate to major floods as the numbers of days (including 0) that the flow exceeded the Q_5 (4) and investigated trends in these flood durations. The final parameter was the Julian date of the peak flow (5), allowing investigation of changes in peak timing.

Statistical analyses investigated trends for each parameter over the interval of record, with the parametric Pearson *r* and the non-parametric rank-order tests, Kendall τ *b*, and Spearman’s ρ , using SPSS19 (IBM, Armonk, NY). The Kendall and Spearman’s tests provided very similar outcomes and we only present the Kendall results. The Pearson test results were also generally consistent with the non-parametric tests and to streamline the Results tables

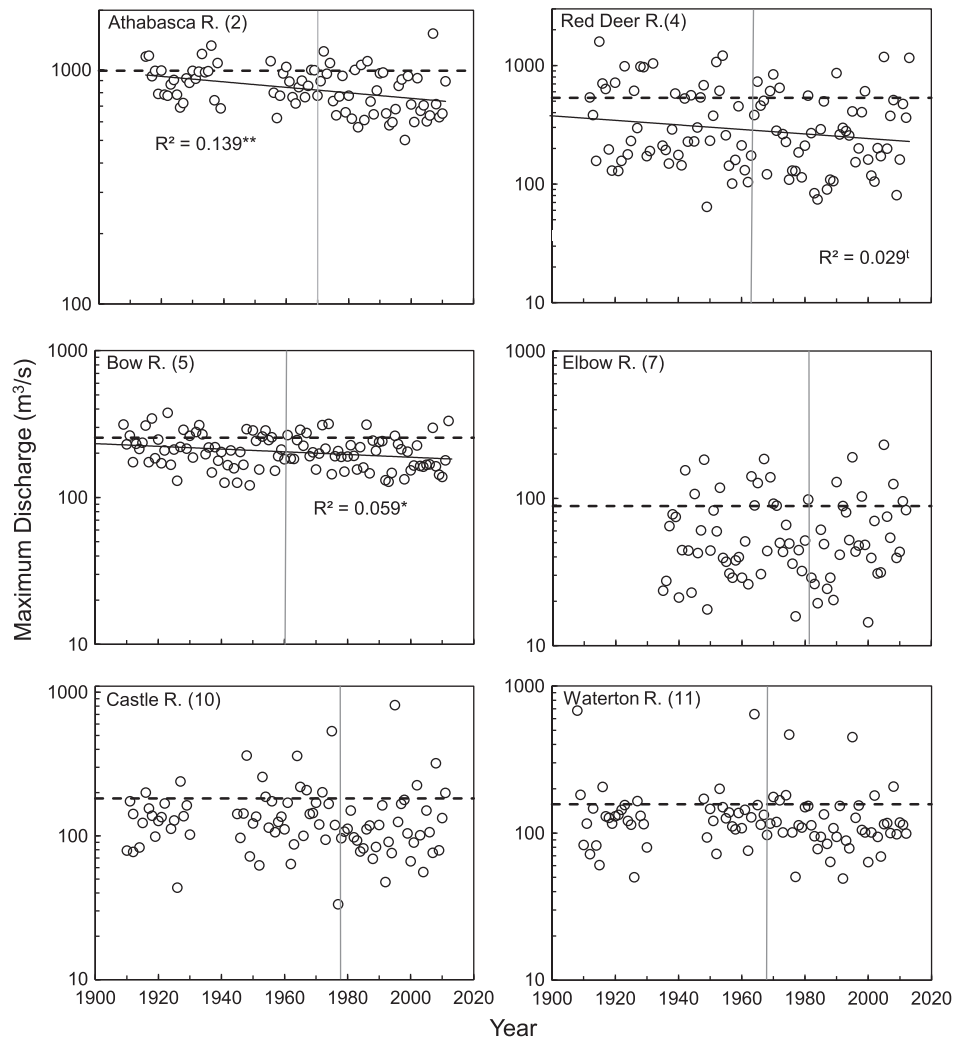


Fig. 3. The mean annual discharge for five free-flowing rivers and the slightly regulated Red Deer River that all flow to the Hudson Bay. Regression lines are plotted for significant ($p < 0.05$) declines and the Kendall τ test indicated a declining trend for the Waterton River ($p = 0.06$). The horizontal dashed line represents the Q_5 value for the data set and the vertical gray line represents the midpoint of the time series for each river.

we present the Kendall test results for all parameters and the Pearson test results only for the annual maxima (Tables 1a–c).

To investigate regional trends in the peak flows, we applied the regional Kendall test (RKT) (Helsel and Frans, 2006) using the library rkt (Marchetto, 2015) in the programming language R. The RKT is a non-parametric rank-order test that performs a standard Mann–Kendall test on all individual rivers within a specified grouping separately, and then evaluates their results for an overall trend. Since each river had more than 15 data points, we corrected for inter-block covariance by calculating p -values for significance with the original Regional Kendall test as well as with the test modified to account for serial dependence (Helsel and Frans, 2006). We grouped the data into the Arctic, Pacific, and Gulf of Mexico drainages but excluded the four moderately regulated rivers.

To investigate possible correspondence with the PDO, yearly PDO conditions were categorized as either positive or negative based on values from the University of Washington (<http://iisao.washington.edu/pdo/PDO.latest>). Positive intervals, which are often characterized by warmer and drier conditions in western North America (Whitfield et al., 2010), were assigned to the periods 1934–1943, 1957–1960, 1976–1988, 1992–1998 and 2002–2006. Conversely, negative phase intervals, frequently associated with cooler and wetter conditions were assigned to 1916–1922,

1944–1956, 1961–1975, 1989–1991, 1999–2001 and 2007–2013. Years in which Q_5 values were exceeded were assessed as either PDO positive or PDO negative and the distribution across these two groups was assessed using a χ^2 analysis with the expected values reflecting the number of record years with the alternate PDO phases for each river's peak flow time series. This was undertaken for each drainage region and for the collective data set.

3. Results

3.1. Historic trends in annual peak flows

From the 30 rivers and reaches that were free-flowing or slightly to moderately regulated, eleven displayed statistical patterns (11 $p < 0.1$; 8 $p < 0.05$; Tables 1a–c). Ten of these displayed declining peaks, a proportion significantly different from a random distribution (10 of 11 $\chi^2 = 7.36$, $p = 0.007$ for all χ^2 presented, $df = 1$). For the full set of rivers and reaches, 21 of 30 displayed negative correlation coefficients, further indicating an overall pattern of declining annual peaks ($\chi^2 = 4.80$, $p = 0.029$).

There were apparent differences across the three watersheds. For the rivers flowing north or northeast to the Arctic Ocean or Hudson Bay, 12 of 14 displayed negative correlation coefficients, strongly indicating regional peak flow decline ($\chi^2 = 7.14$,

$p = 0.008$; Table 1a). This conclusion was also supported with the significant regional Kendall test (RKT) result (Table 2).

Conversely, there was no consistent pattern for annual peaks of the Pacific drainages (5 of 8 with negative coefficients, $p = 0.405$; Table 1b), and this conclusion was supported by the non-significant RKT result (Table 2). There was no overall pattern for the Gulf of Mexico drainages (4 of 8 negative, $p = 1.00$; and non-significant RKT result, Table 2), but apparent regional variation (Table 1c). The Madison River near West Yellowstone, MT was the single river that displayed a significant increasing trend, and the adjacent Yellowstone and Gallatin Rivers also displayed positive but not significant trends (Table 1c). Conversely, three of the more northerly rivers in the Missouri River basin displayed declining trends (Table 1c). This suggested variation within this watershed and patterns for the northern drainages were more similar to the nearby Hudson Bay drainages.

3.2. Substantial floods

Our next consideration assessed peak flows that exceeded the Q_5 , indicating substantial overbank flood events. Similar to Milly et al. (2002), we investigated whether these substantial floods were more prevalent in the recent versus earlier half of each time series. Specific intervals varied across the rivers since the commencement years varied and there were gaps in some historic records (Tables 1a–c).

Historic patterns are plotted for the rivers that drain the Canadian east-slope national parks since this region provided the strongest pattern in the annual peak flow series (Table 1a). In Fig. 3, the dashed lines indicate the Q_5 thresholds and for each plot, the vertical line splits the time series in half. For the rivers that drain to the Arctic Ocean and Hudson Bay, in 10 of the 14 cases there were more floods in the earlier than later half-series ($\chi^2 = 2.57$, $p = 0.109$), also opposing flood intensification over the past century. The collective record for the moderate floods in this region supported that analysis, with 99 peaks exceeding the Q_5 in the early half-series versus 73 in the recent half-series, differing from a random 1:1 ratio ($\chi^2 = 3.93$, $p = 0.048$).

Of the 30 study rivers and reaches, only the Red Deer River displayed a significant declining trend in the flows greater than the Q_5 over the record (Table 1a). Both the Teton River (Table 1c) and Bow River at Banff (Table 1a) showed a tendency for a decrease in Q_5 duration, while there was a tendency for increase along the slightly regulated Bull River (Table 1b). Eighteen of these 30 provided a negative correlation coefficient for flood duration, and this was not statistically different from a random split.

Our investigation of peak flow timing was uncertain relative to our prediction that annual peaks would be occurring earlier within the year. Overall, 14 of the 30 rivers and reaches displayed apparent negative correlation coefficients (Tables 1a–c), indicating little effect ($\chi^2 = 0.133$, $p = 0.715$). There were significantly earlier peaks along the Yellowstone and nearby Madison Rivers (Table 1c) but

there were apparently later peaks along the Castle, Milk and Elk Rivers (Tables 1a–c), suggesting some regional differentiation in the hydrologic patterns. Overall, these results indicate that the timing of flow peaks has not changed as substantially as the advancement of the spring peak along these same rivers (Rood et al., 2008). While there were uncertain trends in peak timing, a spatial pattern was clear, with later peaks occurring at higher latitude (Fig. 4).

The investigations demonstrated significant coordination between the Q_5 flood flows and the phase of the Pacific Decadal Oscillation (PDO, Table 3). For all three drainage regions, Q_5 peaks were apparently more common during the PDO negative phase and less common during the PDO positive phase. For the overall assessment, the Q_5 peaks were about one-third more common (31%) during the PDO negative phase.

4. Discussion

Following from the anticipated amplification of the water cycle, the flood intensification hypothesis predicts that floods would become more severe with climate change and particularly global warming (Huntington, 2006; Karl and Melillo, 2009; Durack et al., 2012). We tested this prediction by analyzing the historic

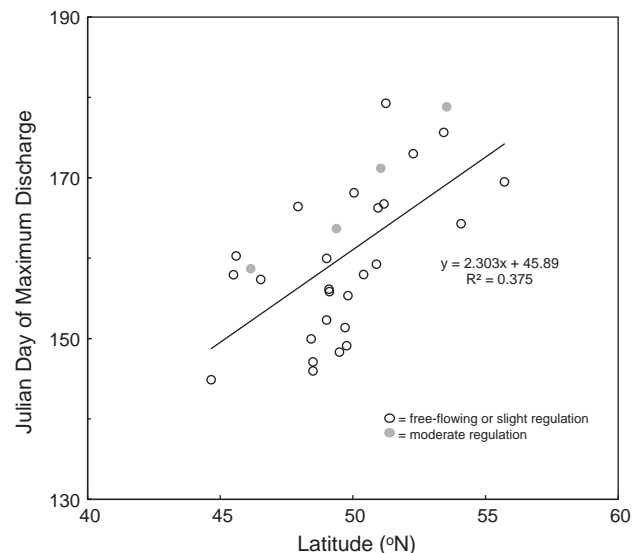


Fig. 4. The mean Julian day of the maximum flow versus the latitude of the gauging station for the study rivers.

Table 3

The interannual coordination between the Pacific Decadal Oscillation (PDO) phase and flood events ($>Q_5$) for the 30 study rivers ($df = 1$ for χ^2). The expected value reflects the proportion of years in the particular records with negative (–) versus positive (+) PDO phases.

Drainage Region	PDO Phase	Observed	Expected
Arctic Ocean and Hudson Bay $\chi^2 = 27.1, p < .001$	–	146	109.5
	+	53	89.6
Pacific Ocean $\chi^2 = 19.1, p < .001$	–	95	70.4
	+	33	57.6
Gulf of Mexico $\chi^2 = 5.9, p < .02$	–	78	64.9
	+	40	53.1
All Rivers and Reaches $\chi^2 = 50.1, p < .001$	–	319	244.75
	+	126	200.25

Table 2

Results from the regional Kendall test (RKT) that investigates interannual trends in annual peak flows for multiple rivers, with watershed groupings. Rivers with moderate regulation were excluded (Table 1).

Watershed	Standard model		Corrected for covariance		Slope
	Variance	p	Variance	p	
Arctic Ocean and Hudson Bay	818,392	0.000	3,528,379	0.050	–.238
Pacific Ocean	515,727	0.718	2,097,867	0.858	–.037
Gulf of Mexico, Atlantic Ocean	566,122	0.719	2,448,509	0.863	–.054

records for the annual peak flows along 30 rivers and reaches draining relatively pristine headwaters in the North American central Rocky Mountains. Our study outcome clearly opposed the flood intensification prediction. Instead, we found that annual flow peaks had declined along a number of the rivers. Thus, peak flows did not increase but instead there were trends of flood moderation over the past century.

There was regionalization of this response and the strongest patterns were observed for the rivers draining the Canadian Rockies to the northeast (Table 1a). There were negative coefficients for twelve of these fourteen reaches, with statistical differences or trends for six, and four more with tendencies ($p < 0.2$). However, while peak flows have thus historically been declining, major floods still persist, including the 2013 flood of the Bow River Basin and through Calgary, Alberta, which may have provided the most costly natural disaster in Canadian history.

There was uncertainty in the historic patterns of peak flows for the drainages to the Gulf of Mexico, and especially the Pacific Ocean (Table 1b). There were significant declines for some rivers in the Missouri River system and probably more so for the northern rivers closer to the Hudson Bay Divide. The Pacific drainages showed little evidence for changes in peak flows, even though some of these records exceeded a century and should thus have been sufficient to dampen the influence of the Pacific Decadal Oscillation and reveal progressive trends (Whitfield et al., 2010).

Other researchers have also investigated trends in peak flows for North American rivers with relative unaltered sites. Lins and Slack (1999) and McCabe and Wolock (2002) assessed locations within the American Hydro Climatic Data Network (HCDN) and found few statistically significant patterns in peak flows from 1941 to 1999. Villarini et al. (2009) reviewed American studies of the early 2000s, and undertook further analyses to reach the same conclusion, that there had not been substantial changes in annual peak flows of the American rivers in our study region.

Prior studies have generally assessed common time series but this reduces the record durations and the prospects for detecting statistical trends that are superimposed on the naturally variable patterns (Merz et al., 2012). This strategy was applied for Canadian rivers by Cunderlik and Ouarda (2009) who found declining annual peak flows for some rivers over the short interval from 1974 to 2003. Some of the rivers in our study were included in that study but there were no statistically significant trends for these rivers over the shorter interval. Subsequent analyses by Burn and Whitfield (2015) investigated patterns from 1961 to 2010 and found some declines in peak flows in the Canadian Rocky Mountain rivers draining to Hudson Bay and the Arctic Ocean, consistent with our findings. In contrast to our findings for Pacific drainages, Burn and Whitfield (2015) reported some declines but their analysis included rivers with greater variation in land-use development and regulation, thus confounding the prospective influence from climate change.

For American rivers, Hirsch and Ryberg (2012) sought to maximize the historic intervals for each river, investigating records with 85–127 years duration, and found statistically significant trends for some American rivers and particularly declining peak flows in the interior region of the American southwest. For their northwest region that included parts of the Rocky Mountain corridor that we investigated, slight patterns suggested declining peak flows for their study intervals up to 2008.

Like Hirsch and Ryberg (2012) we have sought the longest available records in our studies (Rood et al., 2005, 2008). We have even extended the data series by coordination across sequential hydro-metric gauges and by interpolation for short data gaps. With the lengthening data series and the consideration of rivers in both Canada and the United States, our study provides a fairly confident outcome, which is generally consistent with the prior reports. This

rejects the hypothesis that peaks are increasing. Instead, our longer term analyses complement the Hirsch and Ryberg (2012) and Burn and Whitfield (2015) studies, indicating the opposing response, with declining peak flows along some Rocky Mountain rivers.

A complexity with these trend analyses is contributed by the PDO. As expected, we found coordination, whereby substantial Q_5 floods were more likely to occur during the negative phase of the PDO. We had previously found even stronger correspondence between the PDO and annual flows of these rivers (Rood et al., 2005). The partial correspondence between Q_5 floods and the PDO was observed for all three drainage regions and is relevant for studies of trend detection associated with climate change, and also provides a prospective management measure. Dam and reservoir management could increase consideration for flood prospects when the PDO phase is negative, and conversely, there is reduced flood risk when the PDO phase is positive.

4.1. Flood moderation: the underlying mechanism

With the conclusion that annual peak flows have been declining for some Rocky Mountain rivers, we may consider the underlying processes. While there was the proposal that global warming would amplify the water cycle and thus intensify floods (Huntington, 2006; Karl and Melillo, 2009; Durack et al., 2012), an alternate outcome would be reduced flooding with warming conditions. This might match the seasonal pattern in which weather conditions in many regions of North America involve spring seasons that are cool and wet and produce river floods, while the warmer summer is characterized by lower precipitation and fewer floods. This correspondence between cooler and wetter conditions, and major floods also apparently matches the 7,000 year geologic record for the Mississippi River system (Knox, 1993).

To analyze the underlying mechanism of the decline in peak flows from some rivers in this Rocky Mountain region, we considered the regional hydrological consequences of climate change. This present study of historic peak flows followed two studies of the same rivers in which we first investigated patterns in overall annual flows over the past century (Rood et al., 2005), and subsequently investigated changes in the seasonal patterns of those river flows (Rood et al., 2008). The results from those prior studies are combined with the current results to develop a likely mechanism for the moderation of peak flows, as displayed in Fig. 5. Our first finding (Fig. 5, '1') was declining annual flows over past century (Rood et al., 2005), with typical decline rates of ~2% per decade. Associated with this reduction in the overall river flows, there would be a corresponding reduction in the general contributions to peak flows. The lower overall flows would probably also reflect correspondingly dryer watersheds and this would increase the availability for infiltration of some of the precipitation from heavy rain events that are associated with peak flows (Whitfield et al., 2010).

In this Rocky Mountain region the river flow seasonality has also been changing over the past century (Regonda et al., 2005; Rood et al., 2008). Regional warming has been greatest during the cool, winter interval (Akinremi et al., 1999; Cayan et al., 2001) and winter warming will increase the rain versus snow proportions and elevational transitions (Knowles et al., 2006). This results in increased winter flows (Fig. 5, '2') and declining mountain snow packs (Lapp et al., 2005; Mote et al., 2005; Rood et al., 2008). This would reduce snow melt that represents winter precipitation that was temporarily stored as snowpack. Regional warming extends from the winter into the spring, and particularly producing warmer nights. The interval of rapid snow melt relies on night temperatures remaining above freezing and with the night-time warming the commencement of the major snow melt

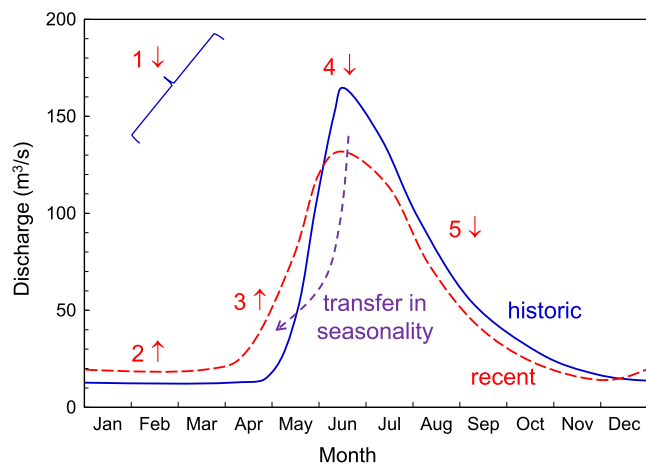


Fig. 5. The prospective hydrological mechanism for flood moderation with climate change, with scaling based on the Bow River at Banff, Alberta (#5). The numbers represent the relevant changes: (1) declining overall annual flows over the past century; (2) with winter warming there is an increase in the proportion of rain versus snow and this increases winter river flows and decreases snow packs; (3) with spring warming there is an advancement in the period of snowmelt, (4) the timing of peak flows is relatively unchanged and there is consequently a longer interval after snowmelt commences. These (3 & 4) reduce the snowmelt contribution to the peak and also reduce the extent of watershed saturation, decreasing runoff from rain. The consequence of (1) through (4) is the reduction in annual peak flows and there is also the subsequent decline in summer flows (5).

interval has become progressively earlier (Fig. 5, '3'), becoming two to four weeks earlier for some regional rivers (Whitfield, 2001; Regonda et al., 2005; Rood et al., 2008; Cunderlik and Ouarda, 2009). Daylength and solar insolation are not altered by climate change, and with the shorter days and less intense sunshine in early spring, the earlier snow melt would be slower, producing a more gradual rise of the spring peak, as we observed (Rood et al., 2008, Fig. 5 '3'). While the period of major snow melt is commencing earlier (Rood et al., 2008), in this study we observed that the timing of the flow peaks was relatively unchanged. There would consequently be a longer snow melt interval prior to the annual peak, leaving less snow melt to contribute to that peak (Fig. 5, '4').

In this region, major river flow peaks and especially flood flows result from the combination of snow melt and heavy rain on a saturated watershed (Shook, 2015). The hydrological alterations accompanying climate change would reduce two of these three factors, with less snow melt contribution due to the transfer in flow seasonality (Fig. 5, following '2' and '3'), and lower watershed saturation (Fig. 5, '1') that would increase infiltration with a heavy rain event. These changes would contribute toward the decline in peak flows (Fig. 5, '4'), which we observed in this study. Following the reduced peak flows, there subsequently be lower summer flows (Fig. 5, '5'), as we previously reported (Rood et al., 2008).

Finally, these analyses emphasize annual flow peaks but there could be somewhat different patterns for extreme flood events (Merz et al., 2012; Shook, 2015). As displayed for the Castle and Waterton rivers (Fig. 3), the historic series apparently includes two separate distributions of peak flows. Modest peaks occur most years providing the common contribution to the peak flow record. Occasional, extreme floods are much higher than would be anticipated from a single, normal distribution, suggesting different hydroclimatic influences. The extreme floods might thus follow from a rare combination of weather events (Shook, 2015) and as these events are more fully investigated, there could be a better understanding of the influences from climate change on extreme floods. Thus, while our study demonstrates that annual flow peaks are declining along some Rocky Mountain rivers, an understanding

of the possible pattern for extreme floods will require a longer time series.

Acknowledgements

Project funding was provided by the Alberta Water Research Institute, Alberta Innovates – Energy and Environment Solutions (AI-EES), and the Natural Sciences and Engineering Research Council (NSERC) of Canada. We extend thanks to John Mahoney, Alberta Environment and Parks, and Karen Gill for assistance and to the journal editors and three reviewers for many helpful recommendations.

References

- Akinremi, O.O., McGinn, S.M., Cutforth, H.W., 1999. Precipitation trends on the Canadian Prairies. *J. Clim.* 12, 2996–3003. [http://dx.doi.org/10.1175/1520-0442\(1999\)012<2996:PTOTCP>2.0.CO;2](http://dx.doi.org/10.1175/1520-0442(1999)012<2996:PTOTCP>2.0.CO;2).
- Barnett, T.P., Adam, J.C., Lettenmaier, D.P., 2005. Potential impacts of a warming climate on water availability in snow-dominated regions. *Nature* 438, 303–309. <http://dx.doi.org/10.1038/nature04141>.
- Bates, B., Kundzewicz, Z.W., Wu, S., Palutikof, J., 2008. *Climate change and water. Technical Paper of the Intergovernmental Panel on Climate Change. IPCC Secretariat, Geneva, 210 pp.*
- Burn, D.H., Whitfield, P.H., 2015. Changes in floods and flood regimes in Canada. *Can. Water Resour. J.* <http://dx.doi.org/10.1080/07011784.2015.1026844>.
- Cayan, D.R., Dettinger, M.D., Kammerdiener, S.A., Caprio, J.M., Peterson, D.H., 2001. Changes in the onset of spring in the western United States. *Bull. Am. Meteorol. Soc.* 82, 399–415. [http://dx.doi.org/10.1175/1520-0477\(2001\)082<0399:CITOO>2.3.CO;2](http://dx.doi.org/10.1175/1520-0477(2001)082<0399:CITOO>2.3.CO;2).
- Cunderlik, J.M., Ouarda, T.B., 2009. Trends in the timing and magnitude of floods in Canada. *J. Hydrol.* 375, 471–480. <http://dx.doi.org/10.1016/j.jhydrol.2009.06.050>.
- Durack, P.J., Wijffels, S.E., Matear, R.J., 2012. Ocean salinities reveal strong global water cycle intensification during 1950 to 2000. *Science* 336, 455–458. <http://dx.doi.org/10.1126/science.1212222>.
- Helsel, D.R., Frans, L.M., 2006. Regional Kendall test for trend. *Environ. Sci. Technol.* 40, 4066–4073. <http://dx.doi.org/10.1021/es051650b>.
- Hirsch, R.M., Ryberg, K.R., 2012. Has the magnitude of floods across the USA changed with global CO₂ levels? *Hydrol. Sci. J.* 57, 1–9. <http://dx.doi.org/10.1080/02626667.2011.621895>.
- Huntington, T.G., 2006. Evidence for intensification of the global water cycle: review and synthesis. *J. Hydrol.* 319, 83–95. <http://dx.doi.org/10.1016/j.jhydrol.2005.07.003>.
- Karl, T.R., Melillo, J.M. (Eds.), 2009. *Global Climate Change Impacts in the United States. Cambridge University Press.*
- Knox, J.C., 1993. Large increases in flood magnitude in response to modest changes in climate. *Nature* 361, 430–432. <http://dx.doi.org/10.1038/36140a0>.
- Knowles, N., Dettinger, M.D., Cayan, D.R., 2006. Trends in snowfall versus rainfall in the western United States. *J. Clim.* 19, 4545–4559. <http://dx.doi.org/10.1175/JCLI3850.1>.
- Kundzewicz, Z.W., Kanae, S., Seneviratne, S.I., Handmer, J., Nicholls, N., Peduzzi, P., Mechler, R., Bouwer, L.M., Arnell, N., Mach, K., Muir-Wood, R., Brakenridge, G.R., Kron, W., Benito, G., Honda, Y., Takahashi, K., Sherstyukov, B., 2014. Flood risk and climate change: global and regional perspectives. *Hydrol. Sci. J.* 59, 1–28. <http://dx.doi.org/10.1080/02626667.2013.857411>.
- Lapp, S., Byrne, J., Townshend, I., Kienzie, S., 2005. Climate warming impacts on snowpack accumulation in an alpine watershed. *Int. J. Climatol.* 25, 521–536. <http://dx.doi.org/10.1002/joc.1140>.
- Lins, H.F., Slack, J.R., 1999. Streamflow trends in the United States. *Geophys. Res. Lett.* 26, 227–230.
- Marchetto, A., 2015. Package 'rkt'. <http://cran.r-project.org/web/packages/rkt/rkt.pdf> (accessed Oct. 2015).
- McCabe, G.J., Wolock, D.M., 2002. A step increase in streamflow in the conterminous United States. *Geophys. Res. Lett.* 29, 2185. <http://dx.doi.org/10.1029/2002GLO15999>.
- Merz, B., Vorogushyn, S., Uhlemann, S., Delgado, J., Hunechea, Y., 2012. More efforts and scientific rigour are needed to attribute trends in flood time series. *HESS Opinions. Hydrol. Earth Syst. Sci.* 16, 1379–1387. <http://dx.doi.org/10.5194/hess-16-1379-2012>.
- Milly, P.C., Wetherald, R.T., Dunne, K.A., Delworth, T.L., 2002. Increasing risk of great floods in a changing climate. *Nature* 415, 514–517. <http://dx.doi.org/10.1038/415514a>.
- Mote, P.W., Hamlet, A.F., Clark, M.P., Lettenmaier, D.P., 2005. Declining mountain snowpack in western North America. *Bull. Am. Meteorol. Soc.* 86, 39–49. <http://dx.doi.org/10.1175/BAMS-86-1-39>.
- Polzin, M.L., Rood, S.B., 2006. Effective disturbance: seedling safe sites and patch recruitment of riparian cottonwoods after a major flood of a mountain river. *Wetlands* 26, 965–980. [http://dx.doi.org/10.1672/0277-5212\(2006\)26\[965:EDSSAJ\]2.0.CO;2](http://dx.doi.org/10.1672/0277-5212(2006)26[965:EDSSAJ]2.0.CO;2).

- Regonda, S.K., Rajagopalan, B., Clark, M., Pitlick, J., 2005. Seasonal cycle shifts in hydroclimatology over the Western United States. *J. Clim.* 18, 372–384. <http://dx.doi.org/10.1175/JCLI-3272.1>.
- Rood, S.B., Samuelson, G.M., Weber, J.K., Wywrot, K.A., 2005. Twentieth-century decline in streamflows from the hydrographic apex of North America. *J. Hydrol.* 306, 215–233. <http://dx.doi.org/10.1016/j.jhydrol.2004.09.010>.
- Rood, S.B., Pan, J., Gill, K.M., Franks, C.G., Samuelson, G.M., Shepherd, A., 2008. Declining summer flows of Rocky Mountain rivers: changing seasonal hydrology and probable impacts on floodplain forests. *J. Hydrol.* 349, 397–410. <http://dx.doi.org/10.1016/j.jhydrol.2007.11.012>.
- Rood, S.B., Stuppel, G.W., Gill, K.M., 2015. Century-long records reveal slight, ecoregion-localized changes in Athabasca River flows. *Hydrol. Process.* 29, 805–816. <http://dx.doi.org/10.1002/hyp.10194>.
- Shepherd, A., Gill, K.M., Rood, S.B., 2010. Climate change and future flows of Rocky Mountain rivers: converging forecasts from empirical trend projection and down-scaled global circulation modelling. *Hydrol. Process.* 24, 3864–3877. <http://dx.doi.org/10.1002/hyp.7818>.
- Shook, K., 2015. The 2005 flood events in the Saskatchewan River Basin: causes, assessment and damages. *Can. Water Resour. J.* <http://dx.doi.org/10.1080/07011784.2014.1001439>.
- Smith, D.G., 1979. Effects of channel enlargement by river ice processes on bankfull discharge in Alberta, Canada. *Water Resour. Res.* 15, 469–475.
- Stocker, T.F., 2013. The closing door of climate targets. *Science* 339, 280–282. <http://dx.doi.org/10.1126/science.1232468>.
- Villarini, G., Serinaldi, F., Smith, J.A., Krajewski, W.F., 2009. On the stationarity of annual flood peaks in the continental United States during the 20th century. *Water Resour. Res.* 45, W08417. <http://dx.doi.org/10.1029/2008WR007645>.
- Wheater, H., Evans, E., 2009. Land use, water management and future flood risk. *Land Use Policy* 26, S251–S264. <http://dx.doi.org/10.1016/j.landusepol.2009.08.019>.
- Whitfield, P.H., 2001. Linked hydrologic and climate variations in British Columbia and Yukon. *Environ. Monit. Assess.* 67, 217–238. <http://dx.doi.org/10.1023/A:1006438723879>.
- Whitfield, P.H., Moore, R.D., Fleming, S.W., Zawadzki, A., 2010. Pacific decadal oscillation and the hydroclimatology of western Canada – Review and prospects. *Can. Water. Res. J.* 35, 1–18. <http://dx.doi.org/10.4296/cwrj3501001>.

RESEARCH ARTICLE

Isotopic evidence for widespread cold-season-biased groundwater recharge and young streamflow across central Canada

Scott Jasechko¹  | Leonard I. Wassenaar² | Bernhard Mayer³

¹Department of Geography, University of Calgary, 2500 University Drive NW, Calgary, AB T2N 1N4, Canada

²Isotope Hydrology Section, International Atomic Energy Agency, Vienna International Center, Vienna A-1400, Austria

³Department of Geoscience, University of Calgary, 2500 University Drive NW, Calgary, AB T2N 1N4, Canada

Correspondence

Scott Jasechko, Department of Geography, University of Calgary, 2500 University Drive NW, Calgary, Alberta T2N 1N4, Canada.
Email: sjasechk@ucalgary.ca

Funding Information

Natural Sciences and Engineering Research Council of Canada, Grant/Award Number: 5668

Abstract

Transformations of precipitation into groundwater and streamflow are fundamental hydrological processes, critical to irrigated agriculture, hydroelectric power generation, and ecosystem health. Our understanding of the timing of groundwater recharge and streamflow generation remains incomplete, limiting our ability to predict fresh water, nutrient, and contaminant fluxes, especially in large basins. Here, we analyze thousands of rain, snow, groundwater, and streamflow $\delta^{18}\text{O}$ and $\delta^2\text{H}$ values in the Nelson River basin, which covers 1.2 million km^2 of central Canada. We show that the fraction of precipitation that recharges aquifers is ~ 1.3 – 5 times higher for precipitation falling during cold months with subzero mean monthly temperatures than for precipitation falling during warmer months. The near-ubiquity of cold-season-biased groundwater recharge implies that changes to winter water balances may have disproportionate impacts on annual groundwater recharge rates. We also show that young streamflow—defined as precipitation that enters a river in less than ~ 2.3 months—comprises $\sim 27\%$ of annual streamflow but varies widely among tributaries in the Nelson River basin (1–59%). Young streamflow fractions are lower in steep catchments and higher in flatter catchments such as the transboundary Red River basin. Our findings imply that flat, lower permeability, heavily tiled landscapes favor more rapid transmission of precipitation into rivers, possibly mobilizing excess soluble fertilizers and exacerbating eutrophication events in Lake Winnipeg.

KEYWORDS

deuterium, groundwater, isotope hydrology, oxygen-18, recharge, transit time

1 | INTRODUCTION

Secure groundwater and surface water supplies are critical for agriculture, hydro-electric energy production, and municipal water supplies in the 1.2 million km^2 , semiarid, Nelson River basin of west-central Canada. Despite the critical importance of groundwater and rivers in this prairie region, the passage of precipitation into aquifers and rivers is not fully understood. There are numerous features of prairie hydrology that remain poorly understood, two of which we investigate in this study.

First, we test for seasonal differences in the groundwater recharge ratio—defined as the fraction of precipitation recharging the aquifer. Recharge ratios are often biased to the colder months (e.g., spring snowmelt) or when rainfall is most intense (Dripps & Bradbury, 2010; Earman, Campbell, Phillips, & Newman, 2006; Florea, 2013; Grasby,

Osborn, Chen, & Wozniak, 2010; Jasechko & Taylor, 2015; Jones & Banner, 2003; O'Driscoll, DeWalle, McGuire, & Gburek, 2005; Rose, 2003; Simpson, Thorud, & Friedman, 1972; Vogel, Ehalt, & Roether, 1963). However, few studies have explicitly quantified seasonal groundwater recharge ratio biases, and fewer still have quantified large-scale spatial distributions of recharge-seasonality biases (e.g., Sánchez-Murillo & Birkel, 2016). Understanding the spatial patterns and variability of recharge ratios is important in order to help predict how groundwater recharge may respond to climatic shifts or to decadal-scale changes to seasonal water balances, and to interpret the many isotope-based records of quaternary climate such as speleothems and fossil groundwater (e.g., Bertrand et al., 2017; Chen et al., 2003; Clark, Stute, Schlosser, Drenkard, & Bonani, 1997; Darling, Edmunds, & Smedley, 1997; Edmunds & Wright, 1979; Jasechko et al., 2015; Phillips, Peeters, Tansey, & Davis,

1986; Plummer, 1993; Wagner et al., 2010; Wang et al., 2001; Wang et al., 2017).

Second, the proportion of central Canadian river flows derived from recently fallen rain or snow remains largely unknown. Although numerous hydrometric-based studies have evaluated how river discharges respond to rain or snowmelt pulses, most of these studies evaluate propagations of pressure (celerity) rather than movements of water molecules (velocity; McDonnell & Beven, 2014). Stable isotopes of water (^{16}O , ^{18}O , ^1H , ^2H) are intrinsic tracers of water movement and can help to constrain the time lags required for precipitation to move into streams—that is, the velocity at which precipitation traverses landscapes and enters rivers (DeWalle, Edwards, Swistock, Aravena, & Drimmie, 1997; Klaus & McDonnell, 2013; Małoszewski & Zuber, 1982; McGuire et al., 2005; McGuire & McDonnell, 2006; Morgenstern, Stewart, & Stenger, 2010; Sánchez-Murillo, Brooks, Elliot, & Boll, 2015; Sklash & Farvolden, 1979; Tetzlaff et al., 2009). Evaluating the time that precipitation takes to flush through a landscape and enter the river network is important in order to better (a) quantify chemical weathering rates (e.g., Maher, 2010), (b) understand and predict riverine nutrient concentrations (Hornberger, Bencala, & McKnight, 1994), (c) evaluate how rapidly catchments can convey surficial pollutants into rivers (Kirchner, Feng, & Neal, 2000; McDonnell et al., 2010), and (d) test how well hydrologic models simulate the ways that actual catchments store and release water (Kirchner, 2006). However, there are no isotope-based studies that evaluate water transit times in rivers spanning central Canada. Hence, our understanding of the time that water spends in these catchments remains unclear, especially at large spatial scales extending beyond small experimental catchments ($<10^3$ km²). Expansive (10^3 – 10^7 km²) isotope-based investigations of hydrological processes and river and groundwater connectivity remain relatively rare, and therefore, the broader relevance and applicability of some small-catchment-scale findings remains uncertain.

The objectives of this study are to map across the 1.2 million km² Nelson River basin (a) seasonal biases in the fraction of precipitation that recharges aquifers and (b) fractions of river discharges derived from precipitation that fell within the past ~2.3 months (denoted “young streamflow”). Quantifying the seasonality and time lags of aquifer recharge and streamflow generation across this expansive Canadian watershed is important not only to improve how we conceptualize cold-region hydrological processes but also to help better manage water quality under changing environmental and land-use conditions.

2 | THE NELSON RIVER BASIN

The Nelson River watershed is comprised of several large subbasins including the Winnipeg River, the Red River, the Assiniboine River, and the North and South Saskatchewan River subwatersheds. The Nelson River watershed discharges northeastward into the Arctic Ocean at Hudson Bay. Basin geology is characterized by sedimentary rocks that are typically covered with Pleistocene-aged low-permeability glacial-clay-containing tills or glacio-lacustrine sediments. The Nelson basin includes several medium-sized population centers (~0.5 to ~1 million persons), where rivers supply the primary drinking water

source for most inhabitants (~92%; Statistics Canada, 2013). In rural areas, free-flowing and impounded rivers often provide water for irrigated agriculture. About 80% of rural populations rely, at least partially, on groundwater for water supply (Statistics Canada, 2012).

The Nelson River's long-term (years: 1964–2000) average discharge to the Hudson's Bay is ~100 km³/year (equating to ~85 mm/year mean annual runoff), ranking its discharge ~32nd among rivers flowing into the oceans (Dai & Trenberth, 2002; Déry, Stadnyk, MacDonald, & Gaudi-Sharma, 2016). The basin is characterized by a wide range of landscapes, ecozones, topographies, geologic substrates, and climatic conditions. Natural ecoregions include alpine forests in the western headwaters, grasslands throughout the southern and central plains, and boreal plains and forests in the northern and the eastern regions. In the western part of the basin, the headwaters of the North and the South Saskatchewan Rivers drain eastern Rocky Mountain slopes towards the boreal and prairie plains. To the southeast, the Red River drains much of the clay-rich, low-relief area of former glacial Lake Agassiz. In the eastern portion, the Winnipeg River mostly drains boreal forest regions (St. George, 2007). Lakes, rivers, or wetlands cover ~9% of the Nelson River basin, with the largest open surface water areas in the low-relief eastern portions of the basin (~15% of the landscape; data from Lehner & Döll, 2004). A few large natural lakes and reservoirs store river water for multiyear timespans (Donald, Parker, Davies, & Leavitt, 2015) and are used for water supply, irrigation, and hydroelectric power generation (e.g., Lake Diefenbaker in south-central Saskatchewan and Lake Winnipeg in central Manitoba).

Nelson subbasins have average slopes that range from a high of ~8% in the Rocky Mountain headwater areas to ~0.1% in the Red River valley of south-central Manitoba (Figure 1b). Mean annual temperatures are highest along the basin's southern boundary (2–6 °C) and lowest at the Nelson River outlet at Hudson Bay (–5 °C; data from New, Lister, Hulme, & Makin, 2002). Mean monthly maximum and minimum basin temperatures are –14 °C in February and +17 °C in August (New et al., 2002). Annual precipitation rates are highest in the Rocky Mountain headwaters (700–1000 mm/year) and lowest in the semiarid central portion of the basin (300–400 mm/year), with an overall basin-wide average of ~500 mm/year (New et al., 2002). Most of annual precipitation inputs occur between late spring and late summer (~April–September), summing to about two thirds of total basin-wide annual precipitation. Agriculture is the primary land use, and cultivated areas cover ~45% of the basin (~33% cropland, ~11% pasture; Ramankutty, Evan, Monfreda, & Foley, 2008). Croplands cover ~90% of the western and southern parts of the basin where the growing season is longer (cultivated land data from Ramankutty et al., 2008).

Large intra-annual temperature variations drive a highly seasonal hydrologic regime. Subdrainages of the Nelson basin store seasonal snowpacks that melt and result in peak discharges between late spring and midsummer in some drainage systems. On the plains, some rain and snowmelt is stored in closed-basin perennial or ephemeral topographic depressions. A large proportion of these (semi) enclosed evaporative water bodies are considered to be noncontributing, although some may recharge local aquifers or “fill-and-spill” into downstream depressions or streams (Ehsanzadeh, van der Kamp, & Spence, 2012; Hayashi, van der Kamp, & Schmidt, 2003; Leibowitz & Vining, 2003; van der Kamp & Hayashi, 2009). The Nelson watershed also

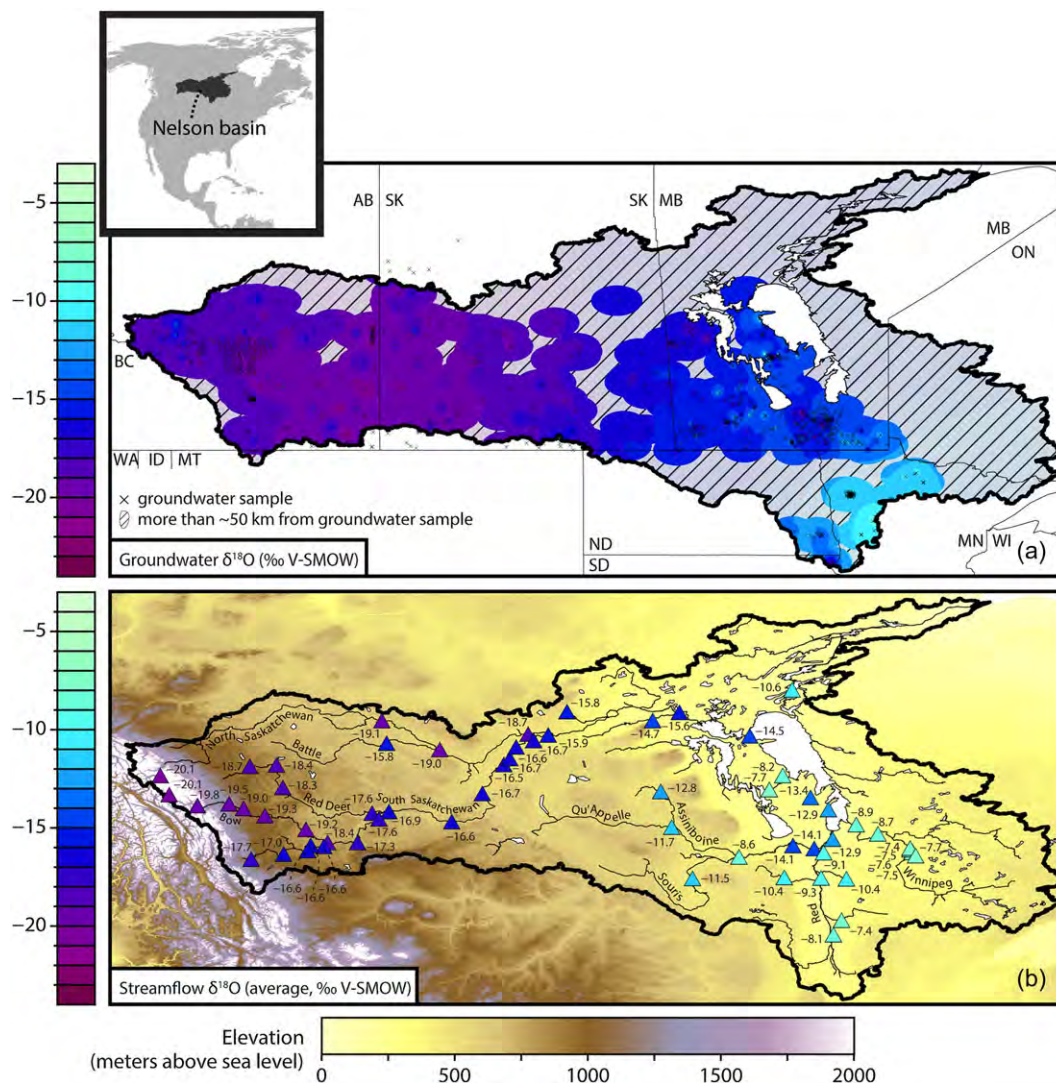


FIGURE 1 $\delta^{18}\text{O}$ values of (a) groundwater and (b) rivers across the Nelson River basin (see Figure 2 for a zoomed-out view of the location of the watershed). In panel (a), groundwater samples are denoted by \times symbols. The $\delta^{18}\text{O}$ data are interpolated across the basin (inverse distance weighted). Areas >50 km from a groundwater sample are greyed out by diagonal lines. Groundwater $\delta^{18}\text{O}$ values are highest in the east and lowest in the west. Black lines denote Canadian provinces (British Columbia [BC], Alberta [AB], Saskatchewan [SK], Manitoba [MB], and Ontario [ON]) and US state borders (Washington [WA], Idaho [ID], Montana [MT], North Dakota [ND], South Dakota [SD], Minnesota [MN], and Wisconsin [WI]). In panel (b), average streamflow $\delta^{18}\text{O}$ values are depicted for all stations where at least five monthly samples were collected. Like the groundwater data, streamflow $\delta^{18}\text{O}$ values are highest in the east, ranging from -7% to -14% . Average streamflow $\delta^{18}\text{O}$ values were lowest in rivers draining high-elevation Rocky Mountain catchments in the west (average $\delta^{18}\text{O}$ values ranging from -20% to -16%)

contains small terminal lakes where the residual water is lost only to evaporation and transpiration, as evidenced by the high salinity of these (semi) closed hydrologic systems.

3 | ISOTOPIC DATA

Over ~ 20 years (1991–2012), several thousand water samples were collected from rivers ($n = 1,604$), groundwater wells ($n = 1,188$), and precipitation events ($n = 615$) and analyzed for their stable oxygen and hydrogen isotope compositions by L. I. W. (e.g., Northern River Basin Study Lake Winnipeg Research Initiative; Saskatchewan Research Council Groundwater Network) and B. M. (Alberta Groundwater Observation Network). Surface water samples were collected close to the surface of these water bodies. The groundwater samples

were collected from boreholes screened within 200 m of the land surface. For samples collected before 2009, hydrogen and oxygen stable isotope compositions were measured by $\text{CO}_2\text{-H}_2\text{O}$ equilibration for $^{18}\text{O}/^{16}\text{O}$ and $\text{H}_2\text{-H}_2\text{O}$ equilibration or by Zn or Cr reduction for $^2\text{H}/^1\text{H}$ analyses. Stable isotope analyses were conducted at Environment Canada (Saskatoon, Saskatchewan, Canada) or the University of Calgary (Calgary, Alberta, Canada). Since 2009, isotope compositions were measured by laser spectrometry using Los Gatos Research or Picarro water isotope analyzers (Lis, Wassenaar, & Hendry, 2008). The hydrogen and oxygen isotope compositions of water samples are denoted $\delta^2\text{H}_{\text{sample}}$ and $\delta^{18}\text{O}_{\text{sample}}$ and defined by

$$\delta^2\text{H}_{\text{V-SMOW}} = \frac{\left(\frac{^2\text{H}}{^1\text{H}}\right)_{\text{sample}} - \left(\frac{^2\text{H}}{^1\text{H}}\right)_{\text{V-SMOW}}}{\left(\frac{^2\text{H}}{^1\text{H}}\right)_{\text{V-SMOW}}} \times 1000 \quad (1)$$

$$\delta^{18}\text{O}_{\text{V-SMOW}} = \frac{\left(\frac{^{18}\text{O}/^{16}\text{O}}{\text{sample}} - \left(\frac{^{18}\text{O}/^{16}\text{O}}{\text{V-SMOW}} \right) \right)}{\left(\frac{^{18}\text{O}/^{16}\text{O}}{\text{V-SMOW}} \right)} \times 1000. \quad (2)$$

The stable isotope data were normalized to the VSMOW-SLAP scales, where the assigned $\delta^2\text{H}$ and $\delta^{18}\text{O}$ values of SMOW/SLAP reference water were 0/−428‰ and 0/−55.5‰, respectively, through the use of two carefully calibrated Environment Canada laboratory water standards (INV1; −28.4/−219.0‰, ROD3; −1.4/−5.1‰ for $\delta^{18}\text{O}$ and $\delta^2\text{H}$, respectively).

Additional precipitation $\delta^2\text{H}$ and $\delta^{18}\text{O}$ values for the Nelson watershed were obtained from the United States and Canadian Network(s) for Isotopes in Precipitation (e.g., Birks & Edwards, 2009; Welker, 2000). Additional shallow groundwater isotope data were provided by the Manitoba Water Stewardship and the University of Manitoba (G. Phillips, Manitoba Water Stewardship, personal communication) and Alberta's Groundwater Observation Well Network. Precipitation isotope data were obtained from the International Atomic Energy Agency's Global Network of Isotopes in Precipitation (www.iaea.org/water). Groundwater isotope data from the US part of the Nelson basin was obtained from the Water Quality Portal administered by the United States Geological Survey, the Environmental Protection Agency, and the National Water Quality Monitoring Council (waterqualitydata.us). Additional groundwater isotope data were obtained from the primary literature sources: Baker, 2009; Cheung & Mayer, 2009; Ferguson, Betcher, & Grasby, 2007; Ferguson, Weinrauch, Wassenaar, Mayer, & Veizer, 2007; Fortin, van der Kamp, & Cherry, 1991; Grasby et al., 2010; Huff, Woods, Moktan, & Jean, 2012; Lanza, 2009; Leybourne, Betcher, McRitchie, Kaszycki, & Boyle, 2009; Maulé, Chanasyk, & Muehlenbachs, 1994; Rock & Mayer, 2009; Wallick, 1981; and Wassenaar, Van Wilgenburg, Larson, & Hobson, 2009.

4 | METHODS

Precipitation, groundwater, and river isotope data were compared in order to determine (a) the seasonal bias in the fraction of precipitation that infiltrates near surface aquifers (recharge ratio seasonality methods—see Section 4.1; Jasechko et al., 2014), and (b) the fractions of streamflow generated by precipitation that reached the stream in less than 2.3 ± 0.8 months (young streamflow methods—see Section 4.2; Kirchner, 2016a, b).

4.1 | Seasonality of groundwater recharge ratios

We compared groundwater and precipitation stable isotope compositions to quantify seasonal bias in the groundwater recharge ratio. First, we calculated the precipitation amount-weighted isotope composition of (a) long-term annual precipitation ($\delta_{\text{P(annual)}}$), (b) the isotopic composition of precipitation falling during any month where the mean temperature was $<0^\circ\text{C}$ ($\delta_{\text{P(cold)}}$), and (c) the isotopic composition of precipitation falling during any month where the mean temperature was $>0^\circ\text{C}$ ($\delta_{\text{P(warm)}}$) following

$$\delta_p = \frac{\sum_{i=1}^{12} \delta_{\text{P}(i)} P_i}{\sum_{i=1}^{12} P_i}, \quad (3)$$

where i represents any month where one of the following conditions was met: (a) all months: $\delta_{\text{P(annual)}}$, (b) months where the mean temperature $<0^\circ\text{C}$: $\delta_{\text{P(cold)}}$, and (c) months where the mean temperature was $>0^\circ\text{C}$: $\delta_{\text{P(warm)}}$. For our comparison of groundwater and measured precipitation isotope compositions (Table 1), we used precipitation isotope and mean monthly temperature measurements reported in precipitation isotope databases (e.g., Canadian Network for Isotopes in Precipitation; Birks & Edwards, 2009). For our pan-basin geospatial analysis (Figure 4), owing to the fact that there are few precipitation isotope stations, we used gridded monthly precipitation isotope (Terzer, Wassenaar, Araguás-Araguás, & Aggarwal, 2013) and mean monthly surface temperature data (New et al., 2002).

We prescreened the groundwater isotope data and discarded 3% of our groundwater isotope data ($n = 40$ out of $n = 1,188$) with deuterium excess values of less than −10‰ (deuterium excess = $\delta^2\text{H} - 8 \times \delta^{18}\text{O}$; Dansgaard, 1964). Groundwater with such low deuterium excess values may have been compromised by evaporation during storage, which would bias our comparison of groundwater and precipitation isotope compositions. Annual precipitation deuterium excess values range from +1.5‰ to +8.8‰ at six Canadian locations (Figure 2).

After screening the groundwater isotope data for quality, the isotopic compositions of precipitation ($\delta_{\text{P(cold)}}$, $\delta_{\text{P(warm)}}$, $\delta_{\text{P(annual)}}$) and groundwater (δ_{GW}) were used to approximate differences in the groundwater recharge ratio (recharge/precipitation, denoted R/P) of precipitation falling during cold ($<0^\circ\text{C}$) versus warm ($>0^\circ\text{C}$) months (Jasechko et al., 2014):

$$\frac{(R/P)_{\text{cold}}}{(R/P)_{\text{warm}}} = \frac{\left(\frac{\delta_{\text{GW}} - \delta_{\text{P(warm)}}}{\delta_{\text{P(annual)}} - \delta_{\text{P(warm)}}} \right)}{\left(\frac{\delta_{\text{GW}} - \delta_{\text{P(cold)}}}{\delta_{\text{P(annual)}} - \delta_{\text{P(cold)}}} \right)}. \quad (4)$$

The unitless term $(R/P)_{\text{cold}}/(R/P)_{\text{warm}}$ describes seasonal biases in the groundwater recharge ratio, where values of less than one imply that summer recharge ratios exceed winter recharge ratios, and values of greater than one imply that winter recharge ratios exceed summer recharge ratios.

4.2 | Young streamflow

For river stations, we compared seasonal $\delta^{18}\text{O}$ variations of river waters against seasonal $\delta^{18}\text{O}$ variations in the rivers' upstream catchment precipitation inputs in order to estimate the fraction of young streamflow flowing in the river (Kirchner, 2016a, b). First, we prescreened the river isotope dataset for data quality. We removed river stations having fewer than 10 $\delta^{18}\text{O}$ and $\delta^2\text{H}$ measurements or with fewer than eight unique months during which a sample was collected and analyzed for its isotope content (Jasechko, Kirchner, Welker, & McDonnell, 2016). We analyzed the annual $\delta^{18}\text{O}$ cycle using samples that were collected during different years, with sampling dates spanning two decades in some cases. Our combining multiple years of data are necessary because precipitation isotope data are not available

TABLE 1 Shallow groundwater recharge ratios (recharge/precipitation) for colder (<0 °C) versus warmer (>0 °C) months

Station	Lat. (°)	Lon. (°)	Annual precipitation		Precipitation when mean monthly temperature < 0 °C		Precipitation when mean monthly temperature > 0 °C		Groundwater ^b		$\frac{(\text{Recharge/Precipitation})_{>0^\circ\text{C}}}{(\text{Recharge/Precipitation})_{<0^\circ\text{C}}}$	
			$\delta^{18}\text{O}$ (‰)	$\delta^2\text{H}$ (‰)	$\delta^{18}\text{O}$ (‰)	$\delta^2\text{H}$ (‰)	$\delta^{18}\text{O}$ (‰)	$\delta^2\text{H}$ (‰)	$\delta^{18}\text{O}$ (‰)	$\delta^2\text{H}$ (‰)	$\delta^{18}\text{O}$ -based	$\delta^2\text{H}$ -based
Calgary	51	-114	-17.9	-137	-23.9	-187	-16.5	-126	-18.3	-144	1.4	1.9
Edmonton	54	-114	-17.1	-131	-26.2	-201	-14.8	-114	-18.3	-144	1.8	2.2
Saskatoon	52	-106	-14.5	-111	-21.7	-171	-13.3	-102	-18.6	-149	10.3	14.2
Wynyard	52	-104	-15.6	-120	-24.4	-187	-13.6	-102	-18.1	-141	3.1	3.2
The Pas	54	-101	-16.5	-126	-23.0	-172	-14.1	-108	-17.1	-136	1.4	2.0
Gimli	51	-97	-14.2	-104	-23.1	-175	-11.1	-81	-16.0	-119	2.0	2.1

^aAll precipitation $\delta^{18}\text{O}$ and $\delta^2\text{H}$ values were amount weighted to account for intra-annual variations in precipitation rates.

^bAverage of samples within 100 km of a precipitation monitoring station.

during some years that river isotope samples were collected. Therefore, our combining samples across multiple years add an unquantified source of uncertainty to our results. These steps excluded those river stations deemed to have insufficient data to evaluate intra-annual streamflow isotope variability (Jasechko et al., 2016). In total, for our analysis, we retained 34 of 84 river sampling stations that met our ascribed minimum sampling frequency thresholds. River isotope data are available in the Table S1.

The seasonal variability in the precipitation isotope input was quantified by fitting cycle (sine and cosine) functions to the precipitation isotope time series. Interpolated vector coefficients and their uncertainties (standard errors) were used to estimate precipitation input cycle coefficients only for the catchment area upstream of each river isotope sampling station (Jasechko et al., 2016). Noncontributing portions of the watershed were excluded from this geospatial analysis. The precipitation-isotope-cycle amplitude was weighted by the spatial distribution of the inverse of the standard error of the precipitation cycle amplitude. The latter step ensured that we down weighted those precipitation stations where seasonal $\delta^{18}\text{O}$ cycle coefficients were poorly characterized.

Once the seasonal precipitation-isotope cycle was determined for each upstream catchment for a single river station, we calculated similar annual cycle coefficients for the individual river isotope time series. The young streamflow fraction was then estimated straightforwardly by comparing the intra-annual cycle amplitudes of catchment precipitation isotope compositions ($A_{\text{precipitation}}$) and river isotope compositions (A_{river} ; Kirchner, 2016a, 2016b; Jasechko et al., 2016):

$$(\text{Young streamflow}) = \frac{A_{\text{river}}}{A_{\text{precipitation}}}, \quad (5)$$

where $A_{\text{precipitation}}$ and A_{river} represent the square root of the sum of the squares of the cosine and sine coefficients (i.e., $A = [\text{cosine coefficient}^2 + \text{sine coefficient}^2]^{1/2}$) for catchment precipitation and streamflow, respectively. Uncertainties were obtained following Gaussian error propagation.

5 | RESULTS AND DISCUSSION

5.1 | Groundwater isotope compositions

Groundwater $\delta^{18}\text{O}$ and $\delta^2\text{H}$ values across the Nelson watershed range from -24.1‰ to -3.1‰ ($\delta^{18}\text{O}$) and -184‰ to -54‰ ($\delta^2\text{H}$), respectively. Groundwater $\delta^{18}\text{O}$ values are lowest along the Alberta-Saskatchewan border and highest in the eastern portion of the basin (Figure 1a). Groundwater $\delta^{18}\text{O}$ patterns are broadly consistent with river and precipitation $\delta^{18}\text{O}$ patterns across North America (e.g., Kendall & Coplen, 2001). Some groundwater $\delta^{18}\text{O}$ values vary substantially over short distances, particularly sites located at the southeast of Lake Winnipeg, where groundwater $\delta^{18}\text{O}$ values are substantially ^{18}O -depleted relative to both modern amount-weighted annual precipitation $\delta^{18}\text{O}$ and nearby groundwater $\delta^{18}\text{O}$

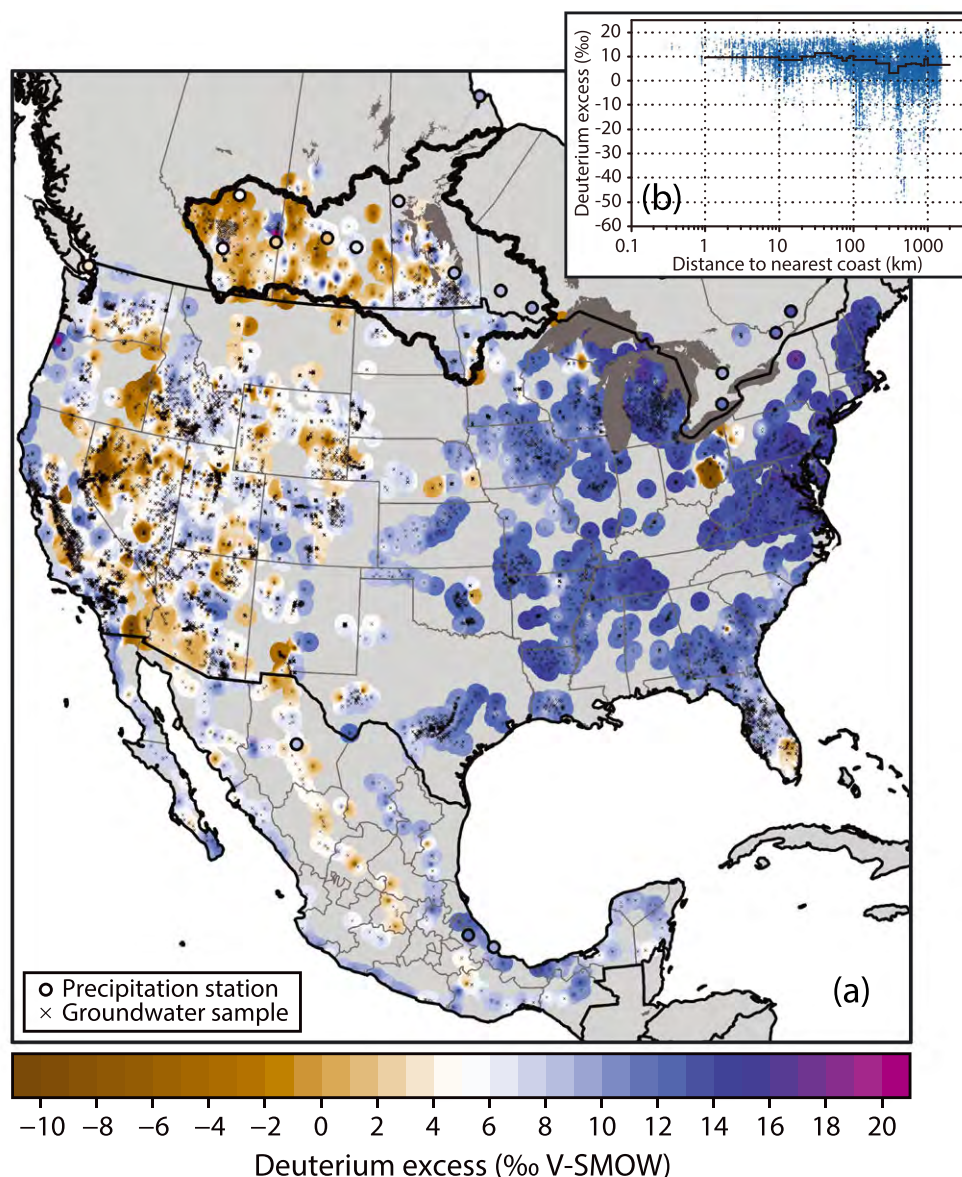


FIGURE 2 Deuterium excess values of precipitation (large circles, only in Canada) and groundwater (small \times symbols and interpolated surface) across the USA and in the Nelson River basin (outlined with black line; panel a). Deuterium excess values are higher in the eastern portions of the Nelson River basin (and continental USA) than in the west. Areas more than 50 km from the nearest groundwater isotope measurement are greyed out. Black lines are boundaries for States (Mexico, USA) and provinces (Canada). The plot in the top right (panel b) relates groundwater deuterium excess and distance to the nearest coast for all groundwater isotope values shown in the figure. The median groundwater deuterium excess is lower for inland locations, which generally have lower annual precipitation amounts than locations closer to coasts. Relatively high deuterium excess values ($>10\text{‰}$) are found in the Laurentian Great Lakes region, where lake evaporate is known to contribute to local precipitation downwind of the lakes. Mexico groundwater deuterium excess values are from Wassenaar et al. (2009)

values. Here, it is well known that former lake-bottom clays retain paleowaters recharged by subglacial meltwaters from the late Pleistocene (Ferguson & Jasechko, 2015; Ferguson, Betcher, et al., 2007; Jasechko, 2016; Remenda, Cherry, & Edwards, 1994); thus, the ^{18}O -depleted samples observed here may contain some late-Pleistocene fossil groundwater, introducing a source of uncertainty into recharge ratio seasonality results in this region.

Nelson basin groundwater deuterium excess values have a 10th–90th percentile range of -3.8‰ to $+10.4\text{‰}$, similar to the long-term average deuterium excess of precipitation measured at the Canadian prairie precipitation isotope stations (range of $+1.5\text{‰}$ to $+8.8\text{‰}$; Figure 2). Groundwater deuterium excess values are lowest

in the west and increase eastward across the Nelson River basin, in a similar pattern to that of precipitation. The broad-scale, west-to-east increase in Nelson basin deuterium excess is consistent with groundwater and precipitation deuterium excess patterns observed throughout North America, where deuterium excess values are lower in most of the (semi) arid west and increase eastwards (Figure 2).

Some of the processes known to impact continental-scale groundwater deuterium excess patterns include spatial variations in primary oceanic moisture sources, air mass mixing, ice-liquid-vapor exchanges and phase changes under nonequilibrium conditions, partial evaporation of falling raindrops, moisture recycling via terrestrial evaporation and transpiration, postdepositional evaporation, and water mixing

within the soil or aquifer (Dansgaard, 1964; Gat, Bowser, & Kendall, 1994; Merlivat & Jouzel, 1979; Salati, Dall'Olio, Matsui, & Gat, 1979; Stewart, 1975; Tian, Masson-Delmotte, Stievenard, Yao, & Jouzel, 2001). The continental-scale east-to-west pattern in groundwater deuterium excess in the Nelson basin and across the United States corresponds, broadly, to patterns of the boundaries of major moisture sources to each region. Locations farther inland tend to have lower deuterium excess values (Figure 2b), possibly indicative of variations moisture sources, upwind evaporation–transpiration balances, or partial evaporation of falling raindrops in these inland regions.

5.2 | River isotope compositions

River $\delta^{18}\text{O}$ values in the Nelson basin are low in the northwest and generally increase eastwards (Figure 1b). Relatively high $\delta^{18}\text{O}$ values

of streamflow (-7‰ to -14‰) characterize eastern drainages including tributaries of the Assiniboine, Winnipeg, and Red Rivers. Lower river $\delta^{18}\text{O}$ values in western drainages (-21‰ to -16‰) have relatively large fractions of their drainage basins in high-elevation Rocky Mountain landscapes (>2000 m above sea level), and may receive larger proportions Pacific-sourced precipitation that has undergone greater upwind rainout leading to lower precipitation $\delta^{18}\text{O}$ values.

Seasonal river $\delta^{18}\text{O}$ variations are smallest in the western headwaters (annual amplitudes of less than $\sim 0.5\text{‰}$; Figure 3a and 3b), more moderate in west-central drainages (annual amplitudes of $\sim 1\text{‰}$; Figure 3c and 3d), and highest in the Red River and its tributaries in the southeast portion of the Nelson basin (annual amplitudes of $\sim 3\text{‰}$; Figure 3e and 3f). Different intra-annual $\delta^{18}\text{O}$ patterns were observed in the western (Figures 3a–d) and southern (Figures 3e and 3f) rivers. Seasonal river $\delta^{18}\text{O}$ variations in westernmost drainages are closely

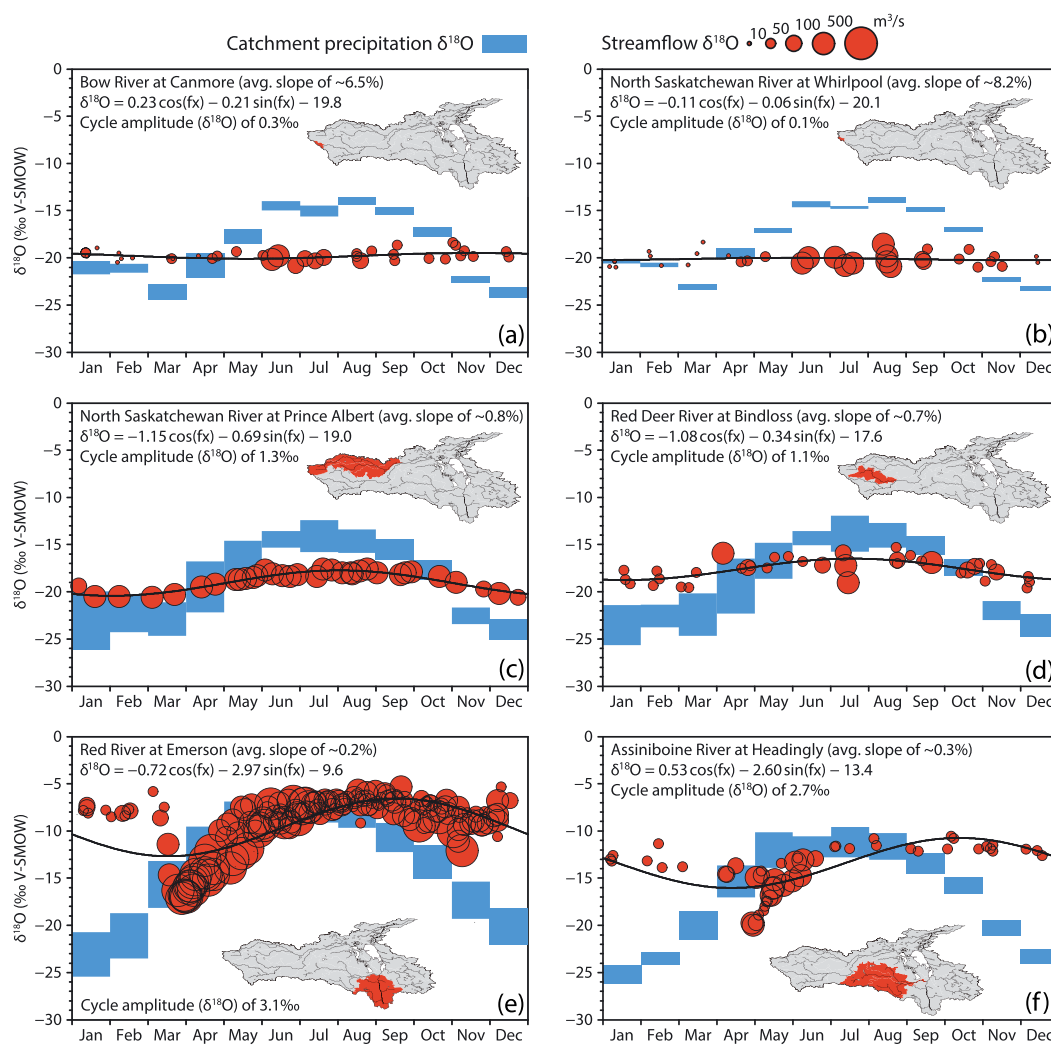


FIGURE 3 Intra-annual streamflow $\delta^{18}\text{O}$ variations in Nelson River subcatchments (red circles). The size of the circle corresponds to river discharge when the isotope sample was collected (see legend at the top). Blue ranges show the estimated range of precipitation $\delta^{18}\text{O}$ values within the subbasins for each month (i.e., the range of precipitation gridded monthly precipitation $\delta^{18}\text{O}$; Terzer et al., 2013). The black line shows the cycle regression fitted to the streamflow data (equation is described in the top left of each panel). Insets show the approximate drainage area for each study catchment. Panels (a) and (b) show data from two headwater rivers draining steep slopes ($>5\%$ grades) of the Rocky Mountains; they show little variation in $\delta^{18}\text{O}$ ($\delta^{18}\text{O}$ cycle amplitudes of 0.3‰ and 0.1‰). Panels (c) and (d) show data for rivers draining moderate slopes ($\sim 0.7\%$ and $\sim 0.8\%$ grades) of the boreal plains, and show detectable $\delta^{18}\text{O}$ variability (cycle amplitudes of 1.3‰ and 1.0‰). Panels (e) and (f) show data for rivers draining very low-relief prairie landscapes ($\sim 0.2\%$ and $\sim 0.3\%$ grades), and show relatively large seasonal variability in riverine $\delta^{18}\text{O}$ (cycle amplitudes of 3.1‰ and 2.7‰)

captured by fitted sine and cosine cycles. Conversely, river $\delta^{18}\text{O}$ variations in more southerly systems (e.g., Red River) show more abrupt $\delta^{18}\text{O}$ declines during the spring freshet, likely resulting from more rapid shunting of spring snowmelt into river channels.

5.3 | Groundwater recharge biased to cold-season precipitation

By comparing groundwater isotope compositions to annual amount-weighted precipitation isotope compositions, we show groundwater recharge to be biased to precipitation falling during colder months ($<0^\circ\text{C}$) relative to precipitation falling during warmer months ($>0^\circ\text{C}$) at all locations where there was sufficient precipitation isotope data (Table 1). A geospatial analysis across the Nelson River basin reveals widespread cold-season biased recharge in the Nelson River basin, with 82% of groundwater measurement sites indicating higher cold-season recharge ratios than warm-season recharge ratios (Figure 4a). Across all of the groundwater sample collection sites, the median $(R/P)_{\text{cold}}/(R/P)_{\text{warm}}$ value is 2.8, and the upper-lower quartile range is 1.3–5.1 (Figure 4). The distinctive cold-season bias in shallow groundwater recharge is near-uniform across the central portion of the Nelson River basin (Figure 4b).

Our finding groundwater recharge to be biased to winter precipitation is consistent with small-scale studies completed in the Canadian prairies (e.g., Grasby et al., 2010; Maulé et al., 1994) and with global-scale point data (Jasechko et al., 2014). Our results build upon these and other previous studies by quantifying and showing the near-ubiquity of cold-season bias in groundwater recharge across a large (~ 1 million km^2) extratropical river basin. It is possible that snowpacks that accumulate during months with subzero temperatures do not recharge until it melts later, potentially during a subsequent month with a mean temperature exceeding 0°C . The fact that groundwater recharge in the Nelson basin derives disproportionately from cold-season precipitation suggests that a unit change to winter water balances, through climatic or stochastic changes in the hydrologic cycle, may have a greater impact on annual groundwater replenishment rates in central Canada than the same unit change to summer water balances.

Critically, however, we note that only about one quarter ($\sim 23\%$) of annual precipitation falls during months with subzero temperatures (New et al., 2002). Our results therefore suggest that changes to winter precipitation may have a disproportionate impact on annual recharge; however, because warmer season rainfall comprises the majority of annual precipitation, potential changes to summer water balances may also be of key importance to annual recharge rates.

Our recharge ratio seasonality results are complicated by two implicit assumptions: (a) that the isotope composition of the snowpack remains unaltered until it melts, and (b) that a two-component mixing model can be used to approximate recharge seasonality. First, snowpack isotope compositions tend to evolve towards higher $\delta^{18}\text{O}$ and $\delta^2\text{H}$ values over time (Earman et al., 2006; Rose, 2003), meaning that our analysis could underestimate the actual $\delta^{18}\text{O}$ and $\delta^2\text{H}$ values of the snowmelt. Hence, our estimated percentage of recharge derived from cold-season precipitation may be an underestimate, strengthening our finding that cold-season precipitation contributes disproportionately to groundwater recharge. Second, our calculation implicitly assumes that the recharge ratio for each of the two binned seasons (cold versus warm) is consistent over each individual season, which is an oversimplification. This assumption, however, is highly unlikely to alter our main finding (cold season precipitation contributes disproportionately to groundwater recharge) but does imply that our results are approximations of true $(R/P)_{\text{cold}}/(R/P)_{\text{warm}}$ values.

5.4 | Young streamflow in Canadian rivers

Across the Nelson drainage basin, young streamflow fractions range between $\sim 1\%$ and 59% of annual river discharge (Figures 5 and 6; Table 2). Low young streamflow fractions are also found in rivers draining Rocky Mountain headwater catchments ($n = 3$; range of 2% to 9%). Low young streamflow fractions exist, unsurprisingly, in rivers directly downstream of large lakes or reservoirs (median of 4% ; range of 1% to 14% ; $n = 10$; Figure 6). Wetland-rich drainages such as the Winnipeg River system discharge little young streamflow, possibly because precipitation is attenuated and mixed in fens and lakes prior to entering main channels. The highest young streamflow fractions among our study rivers exist in tributaries and the main stem of the

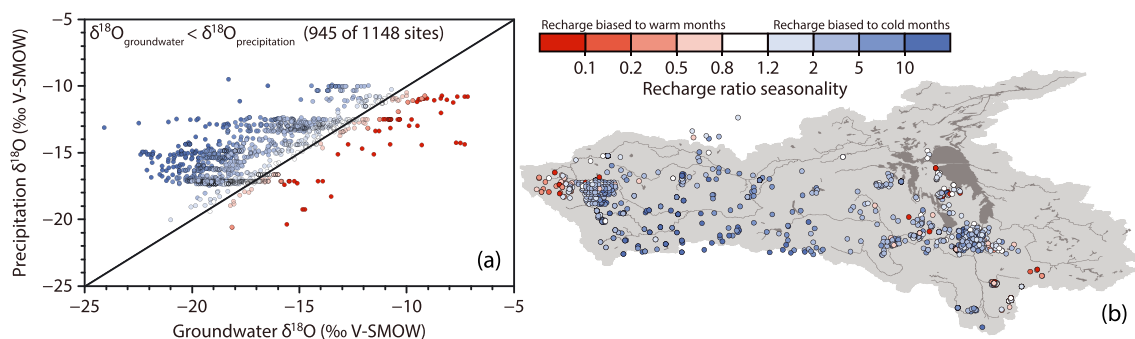


FIGURE 4 Seasonal bias in the Nelson basin groundwater recharge ratio, defined as the proportion of seasonal precipitation that recharges the aquifer. Panel (a) compares measured groundwater $\delta^{18}\text{O}$ values to estimated amount-weighted annual precipitation $\delta^{18}\text{O}$ values. The majority (82%) of groundwater have lower groundwater $\delta^{18}\text{O}$ values than amount-weighted annual precipitation $\delta^{18}\text{O}$ values at the same location, revealing a bias in groundwater recharge ratios toward colder months relative to warmer months. The seasonal bias in the groundwater recharge ratio is shown in panel (b), where the axis “recharge ratio seasonality” refers to the term $(R/P)_{\text{cold}}/(R/P)_{\text{warm}}$ (where R and P refer to groundwater recharge, and to precipitation, respectively)

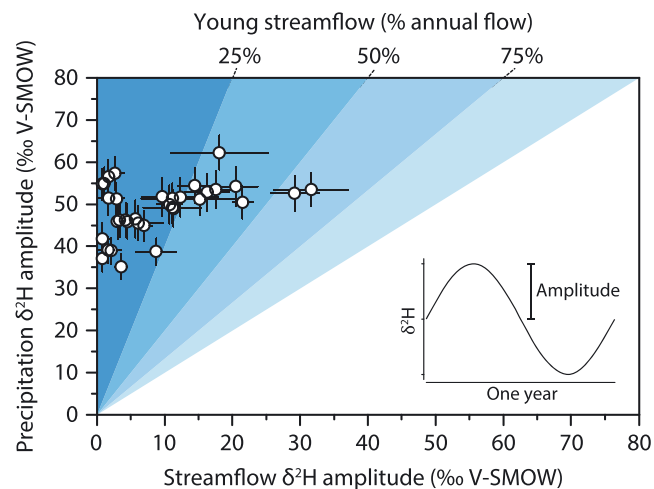


FIGURE 5 Young streamflow fractions calculated on the basis of the intra-annual cycles of precipitation and streamflow $\delta^2\text{H}$ for 34 rivers in the Nelson basin. Each point represents one watershed in central Canada. The intra-annual variability of streamflow $\delta^2\text{H}$ and catchment precipitation $\delta^2\text{H}$ are related on the x and y axes, respectively; the blue shades delineate estimated fractions of young streamflow. Many catchments have a precipitation $\delta^2\text{H}$ cycle amplitude close to ~ 50 per mille. River $\delta^2\text{H}$ cycle amplitudes vary between near zero to ~ 30 per mille

Red River, which drains the Agassiz clay plains from Minnesota (USA) into south-central Canada (median of 30%; range of 18% to 59%; $n = 11$; Figure 6).

Young streamflow fractions are inversely correlated with the negative logarithm of the average topographic slope of the subbasin (Figure 7), that is, steep watersheds tend to discharge lower young streamflow fractions than flatter watersheds. Catchments with mean slopes exceeding 5% all have relatively small young streamflow fractions ($<10\%$ of annual streamflow). By contrast, the young streamflow

fraction exceeds 15% in the majority ($>90\%$) of flatter study catchments with average slopes of less than 1%. High young streamflow fractions in flat landscapes, and lower young streamflow fractions in steep regions, further support the global-scale negative correlation between young streamflow fractions and the logarithm of the average topographic slope (Jasechko et al., 2016).

Our data for the Nelson basin rivers, along with the recent global-scale analyses of rivers, reveal that the majority of river discharge from mountainous catchments is derived from rain and snow that took more than ~ 2.3 months to enter the river, whereas proportionally more discharge from flat-lying landscapes reaches rivers relatively quickly (i.e., within ~ 2.3 months). Unlike the recent assessment of young streamflow in global rivers (Jasechko et al., 2016), here we were able to screen river data to consider only drainage basins that did not have major reservoirs or natural lakes directly upstream. The negative correlation between the young streamflow fraction and the logarithm of topographic relief demonstrated here is substantially stronger than the relationship presented for global rivers, likely because we include fewer drainage systems regulated by dams in this analysis.

The climate and catchment characteristics that lead to the negative correlation between catchment slopes and young streamflow fractions remain unclear and could be a focus for further study. Differences in the architectures of drainage networks among Rocky Mountain versus prairie plain catchments (e.g., McGuire et al., 2005) likely impact these proportions of young streamflow in discharge. Steep Rocky Mountain catchments are often characterized by regosols, highly fractured bedrock, large clastic sedimentary valley fills, and relatively deep water tables. Each of these mountain landscape characteristics plausibly favor vertical infiltration of precipitation into aquifers where the stored groundwater mixes before discharging at springs to sustain river flows distinguished by delayed transit times exceeding ~ 2.3 months. By contrast, the flat Red River subcatchments are covered by low-permeability glacial tills and anisotropic clay soils

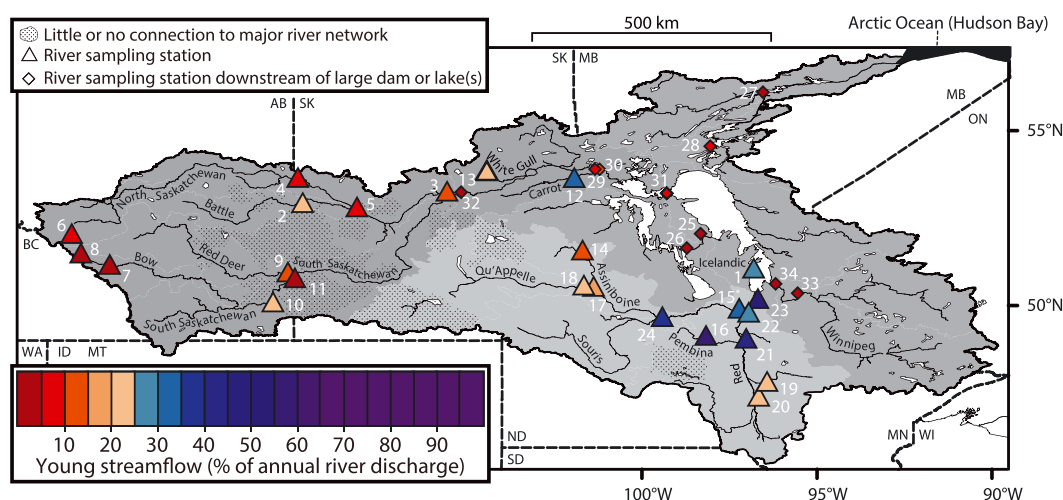


FIGURE 6 Young streamflow fractions in rivers of the Nelson basin ($\delta^2\text{H}$ -based results). Triangles mark sampling stations on rivers that do not have lakes or reservoirs directly upstream, and diamonds mark sampling stations downstream of lakes or reservoirs (numbers refer to site IDs in Table 2). The median young streamflow fraction for rivers in the basin without regulation was 27% ($\delta^2\text{H}$ -based calculations), similar to that of global rivers (Jasechko et al., 2016). Rivers with lower young streamflow fractions than the median are shown as red-orange shades, and higher young streamflow fractions than the median are shown as blue-purple shades. Rivers in the Red River watershed (lightest grey) had the highest fractions of young streamflow (18% to 59%) and rivers draining the steep slopes of the Rocky Mountains had the lowest fractions. River sampling stations downstream of large lakes and dammed reservoirs have young streamflow fractions of less than 15% (marked as diamonds)

TABLE 2 Young streamflow fractions in 34 rivers in the Nelson basin

ID	River	Basin	Lat. (°)	Lon. (°)	Alt. (m)	Drainage (km ²)	N ^o δ ² H (‰)	N ^o δ ¹⁸ O (‰)	Slope (%)	A ^{precipitation} ^a (‰, SMOW)	A ^{river} ^a (‰, SMOW)	Young streamflow ^a (%)
1	Icelandic River	—	51.0	-97.0	220	1,200	14	14	0.1	62 ± 4/8.2 ± 0.5	18 ± 7/2.5 ± 1.0	29 ± 12/30 ± 12
2	Battle River at Unwin	N. Sask. R.	52.9	-109.9	540	23,000	47	32	0.3	49 ± 4/6.4 ± 0.6	11 ± 3/1.9 ± 0.4	23 ± 6/30 ± 7
3	North Sask. River at Prince Albert	N. Sask. R.	53.2	-105.8	430	131,000	46	34	0.9	46 ± 4/6.1 ± 0.6	6 ± 1/1.3 ± 0.1	12 ± 3/22 ± 3
4	North Sask. River at Hwy 17	N. Sask. R.	53.6	-110.0	500	48,000	32	32	1.5	46 ± 4/6.0 ± 0.5	3 ± 1/0.3 ± 0.2	7 ± 3/5 ± 3
5	North Sask. River at North Battleford	N. Sask. R.	52.8	-108.3	460	69,000	18	17	1.3	46 ± 4/6.0 ± 0.5	4 ± 2/0.7 ± 0.2	9 ± 5/11 ± 4
6	North Sask. River at Whirlpool	N. Sask. R.	52.0	-116.5	1,360	1,900	34	34	7.8	35 ± 3/4.6 ± 0.4	3 ± 1/0.1 ± 0.2	10 ± 3/3 ± 4
7	Bow River at Canmore	S. Sask. R.	51.1	-115.4	1,410	3,800	38	38	6.6	39 ± 3/5.0 ± 0.4	2 ± 1/0.3 ± 0.1	5 ± 2/6 ± 2
8	Bow River at Lake Louise	S. Sask. R.	51.4	-116.2	1,560	420	41	41	6.5	37 ± 3/4.8 ± 0.4	1 ± 1/0.1 ± 0.2	2 ± 2/3 ± 3
9	Red Deer River at Bindloss	S. Sask. R.	50.9	-110.3	590	42,000	37	37	0.7	45 ± 4/5.7 ± 0.5	7 ± 1/1.1 ± 0.2	15 ± 3/20 ± 4
10	South Sask. River at Medicine Hat	S. Sask. R.	50.0	-110.7	660	54,000	21	5	1.8	39 ± 3/5.0 ± 0.4	9 ± 3/2.0 ± 1.3	22 ± 8/39 ± 26
11	South Sask. River at Hwy 41	S. Sask. R.	50.7	-110.1	590	62,000	32	32	1.8	39 ± 3/5.1 ± 0.4	2 ± 2/0.2 ± 0.3	4 ± 5/4 ± 6
12	Carrot River at Turnberry	Sask. R.	53.6	-102.1	270	13,000	27	27	0.4	53 ± 4/6.9 ± 0.6	16 ± 3/2.1 ± 0.5	31 ± 7/30 ± 8
13	White Gull Creek	Sask. R.	53.9	-104.6	480	630	20	20	0.4	50 ± 5/6.5 ± 0.6	11 ± 2/1.5 ± 0.2	21 ± 4/23 ± 4
14	Assiniboine River at Hwy 8	Red R.	51.5	-101.9	430	4,300	31	31	0.2	54 ± 4/7.1 ± 0.5	14 ± 3/2.2 ± 0.4	26 ± 5/31 ± 6
15	Assiniboine River Headingly	Red R.	49.9	-97.4	230	160,000	52	52	0.3	53 ± 5/6.8 ± 0.5	17 ± 3/2.7 ± 0.4	33 ± 6/39 ± 6
16	Pembina River at Darlingford	Red R.	49.1	-98.4	350	4,500	12	0	0.3	53 ± 4/6.7 ± 0.4	32 ± 6/—	59 ± 11/—
17	Qu'Appelle River	Red R.	50.5	-101.6	400	17,000	26	26	0.3	52 ± 5/6.7 ± 0.6	10 ± 3/1.3 ± 0.4	18 ± 6/20 ± 6
18	Qu'Appelle River at Tantallon	Red R.	50.5	-101.8	410	16,000	12	0	0.3	52 ± 5/6.7 ± 0.6	12 ± 6/—	24 ± 11/—
19	Red Lake River at Crookston	Red R.	47.8	-96.6	240	14,000	16	16	0.1	51 ± 4/6.6 ± 0.4	11 ± 5/1.7 ± 0.7	22 ± 9/27 ± 11
20	Red River at Halstad	Red R.	47.4	-96.8	250	56,000	14	14	0.2	49 ± 4/6.2 ± 0.4	11 ± 4/1.7 ± 0.7	22 ± 9/27 ± 12
21	Red River at Emerson	Red R.	49.0	-97.2	240	102,000	187	187	0.2	50 ± 4/6.4 ± 0.4	21 ± 2/3.1 ± 0.2	43 ± 5/48 ± 5
22	Red River at Floodway	Red R.	49.8	-97.1	230	120,000	11	11	0.2	51 ± 4/6.4 ± 0.4	15 ± 6/2.1 ± 1.0	30 ± 12/32 ± 16
23	Red River at Selkirk	Red R.	50.1	-96.9	220	287,000	86	72	0.2	53 ± 4/6.7 ± 0.5	29 ± 4/4.3 ± 0.5	55 ± 8/64 ± 9
24	Souris River at Treesbank	Red R.	49.6	-99.6	380	61,000	17	17	0.2	54 ± 5/6.8 ± 0.5	20 ± 3/3.8 ± 0.7	38 ± 7/56 ± 11
25	Dauphin River	Large lake	52.0	-98.3	240	82,000	14	14	n/a ^b	57 ± 4/7.3 ± 0.5	2 ± 1/0.2 ± 0.1	3 ± 1/3 ± 2
26	Lake Manitoba at Fairford	Large lake	51.6	-98.7	250	80,000	22	8	n/a ^b	57 ± 4/7.5 ± 0.5	3 ± 1/0.4 ± 0.3	4 ± 2/6 ± 5
27	Nelson River at Kelsey	Large lake	56.0	-96.5	170	1,050,000	12	0	n/a ^b	51 ± 4/6.7 ± 0.5	2 ± 2/—	3 ± 5/—
28	Nelson River at Jenpeg	Large lake	54.5	-98.0	220	990,000	35	35	n/a ^b	51 ± 4/6.7 ± 0.5	3 ± 1/0.3 ± 0.1	6 ± 2/4 ± 1
29	Saskatchewan River above Carrot	Large lake	53.8	-101.3	270	370,000	29	30	n/a ^b	46 ± 4/5.9 ± 0.5	4 ± 2/0.4 ± 0.3	10 ± 5/7 ± 6
30	Saskatchewan River at The Pas	Large lake	53.8	-101.2	260	390,000	14	0	n/a ^b	45 ± 4/5.9 ± 0.5	6 ± 4/—	13 ± 8/—
31	Saskatchewan River at Grand Rapids	Large lake	53.2	-99.3	260	410,000	49	49	n/a ^b	46 ± 4/6.0 ± 0.5	3 ± 1/0.6 ± 0.1	6 ± 2/10 ± 2
32	South Sask. River at Saskatoon	Large lake	53.2	-105.2	470	141,000	76	64	n/a ^b	42 ± 4/5.4 ± 0.5	1 ± 1/0.5 ± 0.1	2 ± 3/10 ± 2
33	Winnipeg River at PDB	Large lake	50.3	-95.5	290	130,000	63	50	n/a ^b	55 ± 4/7.1 ± 0.5	1 ± 1/0.2 ± 0.1	1 ± 2/3 ± 2
34	Winnipeg River at Pine Falls	Large lake	50.6	-96.2	230	140,000	27	27	n/a ^b	55 ± 4/7.1 ± 0.5	1 ± 1/0.2 ± 0.1	2 ± 1/3 ± 2

^aResults tabulated as δ²H-based calculation/δ¹⁸O-based calculation, units are expressed as a percentage of annual discharge (non-flow-weighted).

^bSlopes are not displayed for watersheds containing large lakes upstream of the sampling point.

^cNumber of unique water samples analyzed for their isotope composition.

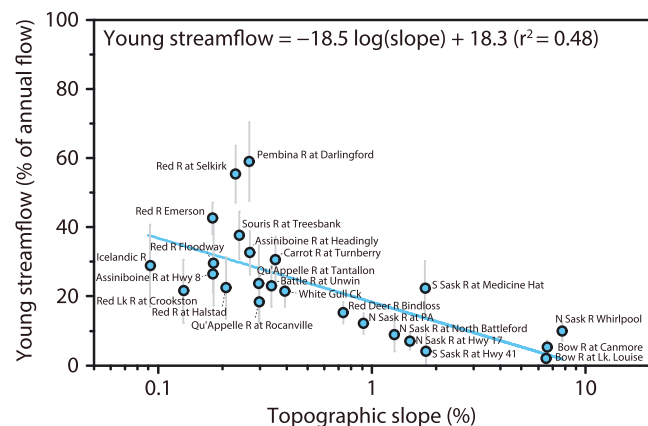


FIGURE 7 Young streamflow as a function of topographic slope in the Nelson River basin ($\delta^2\text{H}$ -based results; error bars mark one standard error). Rivers depicted here are not regulated directly upstream of the sampling site. Rivers in steep regions (slopes of $>5\%$) had little young streamflow ($<10\%$ of annual streamflow), whereas the majority (90%) of rivers draining low-relief watersheds (slopes of $<1\%$) had young streamflow fractions of greater than 15%. The correlation between young streamflow (in units of percent of annual flow) and topographic slope (in units of percent) is shown at the top of the figure panel and marked by the light blue line.

with shallow water tables. Each of these flat landscape characteristics plausibly favor shallow and fast overland flows, especially during snowmelt (water table maps from Fan, Li, & Miguez-Macho, 2013; Miguez-Macho, Li, & Fan, 2008). We also highlight that artificial drainage and surface diversion systems are widespread among the flatter study catchments, meaning our results are likely impacted by land use and hydraulic engineering practices. Recent geophysical investigations have highlighted that stress fields in flat topographical landscapes do not favor the development of deep vertically oriented bedrock fractures (St. Clair et al., 2015). Reduced potential for vertical fracture development in flat landscapes may lead to lower macropore abundances and, consequently, lower bulk near-surface permeability. One plausible implication of such topography–fracture relationships may be more rapid horizontal movements of rain and snowmelt via shallower near-surface flow paths in flatter catchments. The inverse relationship between young streamflow and slope that was observed here is conceptually consistent with recent geophysical findings (e.g., St. Clair et al., 2015), but more research is required to confirm these potential large-scale hydro-geophysical relationships.

Our general finding that rivers draining flatter catchments have higher young streamflow fractions has important implications for diffuse and point source nutrient and contaminant transport. Here, we show that the Red River subbasin discharges high fractions of young streamflow (18–59%). The Red River has total phosphorous concentrations exceeding most Nelson River subbasins by about an order of magnitude. Red River inputs comprise the largest source of nutrients to Lake Winnipeg, where nutrient exceedances have led to major eutrophication events (Bunting et al., 2016; Donald et al., 2015; Schindler, Hecky, & McCullough, 2012). The large nutrient loading of the Red River may be partially related to the drainage basin's ability to quickly deliver snowmelt and precipitation to streams and

rivers within few months, although the importance of high young streamflow fractions is almost certainly secondary to other factors (i.e., land use). The widespread tile drainage systems in the Red River basin may be artificially enhancing young streamflow fractions in the Red River and, consequently, the ability of its subwatersheds to quickly transmit excess nutrients to rivers. The relatively short time lag between precipitation and runoff in the Red River subcatchment leaves little time for biogeochemical reactions that may otherwise partially immobilize or metabolize entrained nutrients before they enter the Red River.

6 | CONCLUDING REMARKS

On the basis of an extensive spatio-temporal dataset of stable isotope tracers obtained over 20 years in the Nelson River basin of central Canada, we demonstrate that (a) cold-season recharge ratios (recharge/precipitation) are ~ 1.3 – 5 times greater than warmer season recharge ratios, (b) recent precipitation that fell within the past ~ 2.3 months comprises about one quarter of river discharge, and (c) that flatter low-relief catchments discharge relatively high-proportions young streamflow compared to steeper catchments. The implications are that hydrologic or climate changes affecting winter processes (e.g., conversion from snow-dominated to rain-dominated precipitation) may have a disproportionate impact on future groundwater recharge fluxes, and that flatter catchments may favor faster shunting of soluble pollutants to streams relative to steeper catchments.

ACKNOWLEDGMENTS

S. J. and B. M. were supported by NSERC Discovery Grants. Groundwater, river, and precipitation isotope data were funded by Environment Canada projects (L. I. W.). We thank S. Terzer (IAEA) for providing monthly precipitation isotope data. G. Koehler (Environment Canada) assisted with sampling and stable isotope analyses. J. M. Welker (U. Alaska Anchorage) provided isotope data for the Icelandic State Park precipitation station. H. Mattheus provided groundwater samples in Saskatchewan. G. Phillips (Manitoba Water Stewardship) provided ground water stable isotope data for Manitoba. The data presented in this manuscript are available for download in tabular format in the Table S2.

REFERENCES

- Baker, J. L. (2009). Groundwater contribution to Sylvan Lake, Alberta, Canada. PhD Thesis, University of Calgary, 112 pp.
- Bertrand, G., Hirata, R., Auler, A., Cruz, F., Cary, L., Petelet-Giraud, E., ... Millo, C. (2017). Groundwater isotopic data as potential proxy for Holocene paleohydroclimatic and paleoecological models in NE Brazil. *Palaeogeography, Palaeoclimatology, Palaeoecology*, 469, 92–103.
- Birks, S. J., & Edwards, T. W. D. (2009). Atmospheric circulation controls on precipitation isotope-climate relations in western Canada. *Tellus*, 61, 566–576.
- Bunting, L., Leavitt, P. R., Simpson, G. L., Wissel, B., Laird, K. R., Cumming, B. F., ... Engstrom, D. R. (2016). Increased variability and sudden ecosystem state change in Lake Winnipeg, Canada, caused by 20th century agriculture. *Limnology and Oceanography*. <https://doi.org/10.1002/lno.10355>
- Chen, Z., Jixiang, Q., Jianming, X., Jiaming, X., Hao, Y., & Yunju, N. (2003). Paleoclimatic interpretation of the past 30 ka from isotopic studies of

- the deep confined aquifer of the North China plain. *Applied Geochemistry*, 18, 997–1009.
- Cheung, K., & Mayer, B. (2009). *Chemical and isotopic characterization of shallow groundwater from selected monitoring wells in Alberta: 2006–2007*. (pp. 88). Alberta Environment Report
- Clair, J. S., Moon, S., Holbrook, W. S., Perron, J. T., Riebe, C. S., Martel, S. J., ... Singha, K. (2015). Geophysical imaging reveals topographic stress control of bedrock weathering. *Science*, 350, 534–538.
- Clark, J. F., Stute, M., Schlosser, P., Drenkard, S., & Bonani, G. (1997). A tracer study of the Floridan aquifer in southeastern Georgia: Implications for groundwater flow and paleoclimate. *Water Resources Research*, 33, 281–289.
- Dai, A., & Trenberth, K. E. (2002). Estimates of freshwater discharge from continents: Latitudinal and seasonal variations. *Journal of Hydrometeorology*, 3, 660–687.
- Dansgaard, W. (1964). Stable isotopes in precipitation. *Tellus*, 16, 436–468.
- Darling, W. G., Edmunds, W. M., & Smedley, P. L. (1997). Isotopic evidence for palaeowaters in the British Isles. *Applied Geochemistry*, 12, 813–829.
- Déry, S. J., Stadnyk, T. A., MacDonald, M. K., & Gauli-Sharma, B. (2016). Recent trends and variability in river discharge across northern Canada. *Hydrology and Earth System Sciences*, 20, 4801–4818.
- DeWalle, D. R., Edwards, P. J., Swistock, B. R., Aravena, R., & Drimmie, R. J. (1997). Seasonal isotope hydrology of three Appalachian forest catchments. *Hydrological Processes*, 11, 1895–1906.
- Donald, D. B., Parker, B. R., Davies, J. M., & Leavitt, P. R. (2015). Nutrient sequestration in the Lake Winnipeg watershed. *Journal of Great Lakes Research*, 41, 630–642.
- Dripps, W. R., & Bradbury, K. R. (2010). The spatial and temporal variability of groundwater recharge in a forested basin in northern Wisconsin. *Hydrological Processes*, 24, 383–392. <https://doi.org/10.1002/hyp.7497>
- Earman, S., Campbell, A. R., Phillips, F. M., & Newman, B. D. (2006). Isotopic exchange between snow and atmospheric water vapor: Estimation of the snowmelt component of groundwater recharge in the southwestern United States. *Journal of Geophysical Research*, 111, D09302.
- Edmunds, W. M., & Wright, E. P. (1979). Groundwater recharge and palaeoclimate in the Sirte and Kufra basins, Libya. *Journal of Hydrology*, 40, 215–241.
- Ehsanzadeh, E., van der Kamp, G., & Spence, C. (2012). The impact of climatic variability and change in the hydroclimatology of Lake Winnipeg watershed. *Hydrological Processes*, 26, 2802–2813. <https://doi.org/10.1002/hyp.8327>
- Fan, Y., Li, H., & Miguez-Macho, G. (2013). Global patterns of groundwater table depth. *Science*, 339(6122), 940–943.
- Ferguson, G., Betcher, R. N., & Grasby, S. E. (2007). Hydrogeology of the Winnipeg formation in Manitoba, Canada. *Hydrogeology Journal*, 15, 573–587.
- Ferguson, G., & Jasechko, S. (2015). The isotopic composition of the Laurentide ice sheet and fossil groundwater. *Geophysical Research Letters*, 42, 4856–4861.
- Ferguson, P. R., Weinrauch, N., Wassenaar, L. I., Mayer, B., & Veizer, J. (2007). Isotope constraints on water, carbon, and heat fluxes from the northern Great Plains region of North America. *Global Biogeochemical Cycles*, 21, GB2023.
- Florea, L. J. (2013). Selective recharge and isotopic composition of shallow groundwater within temperate, epigenic carbonate aquifers. *Journal of Hydrology*, 489, 201–213.
- Fortin, G., van der Kamp, G., & Cherry, J. A. (1991). Hydrogeology and hydrochemistry of an aquifer-aquitard system within glacial deposits, Saskatchewan, Canada. *Journal of Hydrology*, 126, 265–292.
- Gat, J. R., Bowser, C. J., & Kendall, C. (1994). The contribution of evaporation from the Great Lakes to the continental atmosphere: Estimate based on stable isotope data. *Geophysical Research Letters*, 21, 557–560.
- Grasby, S. E., Osborn, J., Chen, Z., & Wozniak, P. R. J. (2010). Influence of till provenance on regional groundwater geochemistry. *Chemical Geology*, 273, 225–237.
- Hayashi, M., van der Kamp, G., & Schmidt, R. (2003). Focused infiltration of snowmelt water in partially frozen soil under small depressions. *Journal of Hydrology*, 270, 214–229.
- Hornberger, G. M., Bencala, K. E., & McKnight, D. M. (1994). Hydrological controls on dissolved organic carbon during snowmelt in the Snake River near Montezuma, Colorado. *Biogeochemistry*, 25, 147–165.
- Huff, G. F., Woods, L., Moktan, H., Jean, G. (2012). Geochemistry of groundwater and springwater in the Paskapoo formation and overlying glacial drift, south-central Alberta. ERCB/AGS Open File Report 2012-05, 66 pp.
- Jasechko, S. (2016). Late-Pleistocene precipitation $\delta^{18}\text{O}$ interpolated across the global landmass. *Geochemistry, Geophysics, Geosystems*, 17, 3274–3288.
- Jasechko, S., Birks, S. J., Gleeson, T., Wada, Y., Fawcett, P. J., Sharp, Z. D., ... Welker, J. M. (2014). The pronounced seasonality of global groundwater recharge. *Water Resources Research*, 50, 8845–8867.
- Jasechko, S., Kirchner, J. W., Welker, J. M., & McDonnell, J. J. (2016). Substantial proportion of global streamflow less than three months old. *Nature Geoscience*, 8, 126–129.
- Jasechko, S., Lechler, A., Pausata, F. S. R., Fawcett, P. J., Gleeson, T., Cendón, D. I., ... Yoshimura, K. (2015). Late-glacial to late-Holocene shifts in global precipitation $\delta^{18}\text{O}$. *Climate of the Past*, 11, 1375–1393.
- Jasechko, S., & Taylor, R. G. (2015). Intensive rainfall recharges tropical groundwaters. *Environmental Research Letters*, 10, 124015.
- Jones, I. C., & Banner, J. L. (2003). Estimating recharge thresholds in tropical karst island aquifers: Barbados, Puerto Rico and Guam. *Journal of Hydrology*, 278, 131–143.
- van der Kamp, G., & Hayashi, M. (2009). Groundwater-wetland ecosystem interaction in the semiarid glaciated plains of North America. *Hydrogeology Journal*, 17, 203–214.
- Kendall, C., & Coplen, T. B. (2001). Distribution of oxygen-18 and deuterium in river waters across the United States. *Hydrological Processes*, 15(7), 1363–1393.
- Kirchner, J. W. (2006). Getting the right answers for the right reasons: Linking measurements, analyses, and models to advance the science of hydrology. *Water Resources Research*, 42, W03S04.
- Kirchner, J. W. (2016a). Aggregation in environmental systems—Part 1: Seasonal tracer cycles quantify young water fractions, but not mean transit times, in spatially heterogeneous catchments. *Hydrology and Earth System Sciences*, 20, 279–297.
- Kirchner, J. W. (2016b). Aggregation in environmental systems—Part 2: Catchment mean transit times and young water fractions under hydrologic nonstationarity. *Hydrology and Earth System Sciences*, 20, 299–328.
- Kirchner, J. W., Feng, X., & Neal, C. (2000). Fractal stream chemistry and its implications for contaminant transport in catchments. *Nature*, 403, 524–527.
- Klaus, J., & McDonnell, J. J. (2013). Hydrograph separation using stable isotopes: Review and evaluation. *Journal of Hydrology*, 505, 47–64.
- Lanza, S. (2009). Groundwater anammox at an industrial site in Calgary. MSc Thesis, University of Calgary, 96 pp.
- Lehner, B., & Döll, P. (2004). Development and validation of a global database of lakes, reservoirs and wetlands. *Journal of Hydrology*, 296, 1–22.
- Leibowitz, S. G., & Vining, K. C. (2003). Temporal connectivity in a prairie pothole complex. *Wetlands*, 23, 13–25.
- Leybourne, M. I., Betcher, R. N., McRitchie, W. D., Kaszycki, C. A., & Boyle, D. R. (2009). Geochemistry and stable isotopic composition of tufa

- waters and precipitates from the Interlake region, Manitoba, Canada: Constraints on groundwater origin, calcitization, and tufa formation. *Chemical Geology*, 260, 221–233.
- Lis, G., Wassenaar, L. I., & Hendry, M. J. (2008). High-precision laser spectroscopy D/H and $^{18}\text{O}/^{16}\text{O}$ measurements of microliter natural water samples. *Analytical Chemistry*, 80, 287–293.
- Maher, K. (2010). The dependence of chemical weathering rates on fluid residence time. *Earth and Planetary Science Letters*, 294, 101–110.
- Małozzewski, P., & Zuber, A. (1982). Determining the turnover time of groundwater systems with the aid of environmental tracers: 1. Models and their applicability. *Journal of Hydrology*, 57, 207–231.
- Maulé, C. P., Chanasyk, D. S., & Muehlenbachs, K. (1994). Isotopic determination of snow-water contribution to soil water and groundwater. *Journal of Hydrology*, 155, 73–91.
- McDonnell, J. J., & Beven, K. (2014). Debates—The future of hydrological sciences: A (common) path forward? A call to action aimed at understanding velocities, celerities and residence time distributions of the headwater hydrograph. *Water Resources Research*, 50, 5342–5350.
- McDonnell, J. J., McGuire, K., Aggarwal, P., Beven, K. J., Biondi, D., Destouni, G., ... Lyon, S. (2010). How old is streamwater? Open questions in catchment transit time conceptualization, modelling and analysis. *Hydrological Processes*, 24, 1745–1754.
- McGuire, K. J., & McDonnell, J. J. (2006). A review and evaluation of catchment transit time modeling. *Journal of Hydrology*, 330, 543–563.
- McGuire, K. J., McDonnell, J. J., Weiler, M., Kendall, C., McGlynn, B. L., Welker, J. M., & Seibert, J. (2005). The role of topography on catchment-scale water residence time. *Water Resources Research*, 41, W05002.
- Merlivat, L., & Jouzel, J. (1979). Global climatic interpretation of the deuterium-oxygen 18 relationship for precipitation. *Journal of Geophysical Research, Oceans*, 84, 5029–5033.
- Miguez-Macho, G., Li, H., & Fan, Y. (2008). Simulated water table and soil moisture climatology over North America. *Bulletin of the American Meteorological Society*, 89, 663.
- Morgenstern, U., Stewart, M. K., & Stenger, R. (2010). Dating of streamwater using tritium in a post nuclear bomb pulse world: Continuous variation of mean transit time with streamflow. *Hydrology and Earth System Sciences*, 14, 2289–2301.
- New, M., Lister, D., Hulme, M., & Makin, I. (2002). A high-resolution data set of surface climate over global land areas. *Climate Research*, 21, 1–25.
- O'Driscoll, M. A., DeWalle, D. R., McGuire, K. J., & Gburek, W. J. (2005). Seasonal ^{18}O variations and groundwater recharge for three landscape types in central Pennsylvania, USA. *Journal of Hydrology*, 303, 108–124.
- Phillips, F. M., Peeters, L. A., Tansey, M. K., & Davis, S. N. (1986). Paleoclimatic inferences from an isotopic investigation of groundwater in the central San Juan Basin, New Mexico. *Quaternary Research*, 26, 179–193.
- Plummer, L. N. (1993). Stable isotope enrichment in paleowaters of the southeast Atlantic Coastal Plain, United States. *Science*, 262, 2016–2020.
- Ramankutty, N., Evan, A. T., Monfreda, C., & Foley, J. A. (2008). Farming the planet: 1. Geographic distribution of global agricultural lands in the year 2000. *Global Biogeochemical Cycles*, 22, GB1003.
- Remenda, V. H., Cherry, J. A., & Edwards, T. W. D. (1994). Isotopic composition of old ground water from Lake Agassiz: Implications for late Pleistocene climate. *Science*, 266, 1975.
- Rock, L., & Mayer, B. (2009). Identifying the influence of geology, land use, and anthropogenic activities on riverine sulfate on a watershed scale by combining hydrometric, chemical and isotopic approaches. *Chemical Geology*, 262, 121–130.
- Rose, T. P. (2003). Stable isotope investigation of precipitation and recharge processes in central Nevada, in Hydrologic Resources Management Program and Underground Test Area Project FY2001–2002 Progress Report, Rep. UCRL-ID-154357
- Salati, E., Dall'Olio, A., Matsui, E., & Gat, J. R. (1979). Recycling of water in the Amazon basin: An isotopic study. *Water Resources Research*, 15, 1250–1258.
- Sánchez-Murillo, R., & Birkel, C. (2016). Groundwater recharge mechanisms inferred from isoscapes in a complex tropical mountainous region. *Geophysical Research Letters*, 43, 5060–5069.
- Sánchez-Murillo, R., Brooks, E. S., Elliot, W. J., & Boll, J. (2015). Isotope hydrology and baseflow geochemistry in natural and human-altered watersheds in the Inland Pacific Northwest, USA. *Isotopes in Environmental and Health Studies*, 51, 231–254.
- Schindler, D. W., Hecky, R. E., & McCullough, G. K. (2012). The rapid eutrophication of Lake Winnipeg: Greening under global change. *Journal of Great Lakes Research*, 38, 6–13.
- Simpson, E. S., Thorud, D. B., & Friedman, I. (1972). Distinguishing seasonal recharge to groundwater by deuterium analysis in southern Arizona. In *Proc. Reeding Symposium International Association of Scientific Hydrology* (pp. 623–633). Gentbrugge, Belgium: UNESCO-WMO.
- Sklash, M. G., & Farvolden, R. N. (1979). The role of groundwater in storm runoff. In: Back, W. and D. A. Stephenson (eds.), *Contemporary Hydrogeology—The George Burke Maxey Memorial Volume. Developments in Water Science*, 43, 45–65.
- St. George, S. (2007). Streamflow in the Winnipeg River basin, Canada: Trends, extremes and climate linkages. *Journal of Hydrology*, 332, 396–411.
- Statistics Canada (2012), Agricultural water use in Canada. Report 16–402-X, 37 pp. Accessed May-2016 from <http://www.statcan.gc.ca/pub/16-402-x/16-402-x2013001-eng.pdf>.
- Statistics Canada (2013), Survey of drinking water plants. Report 16–403-X, 55 pp. Accessed May-2016 from www.statcan.gc.ca/pub/16-403-x/16-403-x2013001-eng.pdf.
- Stewart, M. K. (1975). Stable isotope fractionation due to evaporation and isotopic exchange of falling waterdrops: Applications to atmospheric processes and evaporation of lakes. *Journal of Geophysical Research*, 80, 1133–1146.
- Terzer, S., Wassenaar, L. I., Araguás-Araguás, L. J., & Aggarwal, P. K. (2013). Global isoscapes for $\delta^{18}\text{O}$ and $\delta^2\text{H}$ in precipitation: Improved prediction using regionalized climatic regression models. *Hydrology and Earth System Sciences*, 17, 4713–4728.
- Tetzlaff, D., Seibert, J., McGuire, K. J., Laudon, H., Burns, D. A., Dunn, S. M., & Soulsby, C. (2009). How does landscape structure influence catchment transit time across different geomorphic provinces? *Hydrological Processes*, 23, 945–953.
- Tian, L., Masson-Delmotte, V., Stievenard, M., Yao, T., & Jouzel, J. (2001). Tibetan plateau summer monsoon northward extent revealed by measurements of water stable isotopes. *Journal of Geophysical Research-Atmospheres*, 106, 28081–28088.
- Vogel, J. C., Ehler, D., Roether, W. (1963), A survey of the natural isotopes of water in South Africa, Proceedings of Tokyo Conference on Radioisotopes in Hydrology, 407–416.
- Wagner, J. D. M., Cole, J. E., Beck, J. W., Patchett, P. J., Henderson, G. M., & Barnett, H. R. (2010). Moisture variability in the southwestern United States linked to abrupt glacial climate change. *Nature Geoscience*, 3, 110–113.
- Wallick, E. I. (1981). Chemical evolution of groundwater in a drainage basin of Holocene age, east-central Alberta, Canada. *Journal of Hydrology*, 54, 245–283.
- Wang, X., Edwards, R. L., Auler, A. S., Cheng, H., Kong, X., Wang, Y., ... Chiang, H. W. (2017). Hydroclimate changes across the Amazon lowlands over the past 45,000 years. *Nature*, 541, 204–207.
- Wang, Y. J., Cheng, H., Edwards, R. L., An, Z. S., Wu, J. Y., Shen, C.-C., & Dorale, J. A. (2001). A high-resolution absolute-dated late Pleistocene monsoon record from Hulu Cave, China. *Science*, 294, 2345–2348.
- Wassenaar, L. I., Van Wilgenburg, S. L., Larson, K., & Hobson, K. A. (2009). A groundwater isotope (δD , $\delta^{18}\text{O}$) for Mexico. *Journal of Geochemical Exploration*, 102, 123–136.

Welker, J. M. (2000). Isotopic ($\delta^{18}\text{O}$) characteristics of weekly precipitation collected across the USA: An initial analysis with application to water source studies. *Hydrological Processes*, 14, 1449–1464.

SUPPORTING INFORMATION

Additional Supporting Information may be found online in the supporting information tab for this article.

How to cite this article: Jasechko S, Wassenaar LI, Mayer B. Isotopic evidence for widespread cold-season-biased groundwater recharge and young streamflow across central Canada. *Hydrological Processes*. 2017;31:2196–2209. <https://doi.org/10.1002/hyp.11175>



Occurrence and origin of methane in groundwater in Alberta (Canada): Gas geochemical and isotopic approaches



P. Humez^{a,*}, B. Mayer^a, J. Ing^a, M. Nightingale^a, V. Becker^a, A. Kingston^a, O. Akbilgic^{a,b}, S. Taylor^a

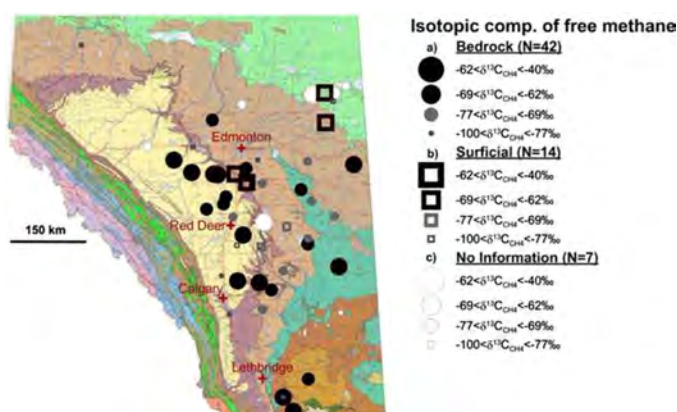
^a Department of Geoscience, University of Calgary, 2500 University Drive NW, Calgary, Alberta T2N 1N4, Canada

^b UTHSC-ORNL Center for Biomedical Informatics, 910 Madison Avenue, Memphis, TN, 38104, USA

HIGHLIGHTS

- Analysis of gas geochemical data from 186 monitoring wells in Alberta revealed that methane is ubiquitous;
- Methane concentrations increased with depth and were elevated in aquifers containing coals and shales;
- A multi-isotope approach revealed that methane is of biogenic origin formed predominantly via CO₂ reduction;
- Comparison of free and dissolved gas sampling approaches for baseline groundwater monitoring yielded similar results;

GRAPHICAL ABSTRACT



ARTICLE INFO

Article history:

Received 27 July 2015

Received in revised form 11 September 2015

Accepted 12 September 2015

Available online xxxx

Editor: D. Barcelo

Keywords:

Groundwater monitoring

Methane

Stable isotopes

Statistical analysis

Gas geochemistry

Alberta

ABSTRACT

To assess potential future impacts on shallow aquifers by leakage of natural gas from unconventional energy resource development it is essential to establish a reliable baseline. Occurrence of methane in shallow groundwater in Alberta between 2006 and 2014 was assessed and was ubiquitous in 186 sampled monitoring wells. Free and dissolved gas sampling and measurement approaches yielded comparable results with low methane concentrations in shallow groundwater, but in 28 samples from 21 wells methane exceeded 10 mg/L in dissolved gas and 300,000 ppmv in free gas. Methane concentrations in free and dissolved gas samples were found to increase with well depth and were especially elevated in groundwater obtained from aquifers containing coal seams and shale units. Carbon isotope ratios of methane averaged $-69.7 \pm 11.1\text{‰}$ ($n = 63$) in free gas and $-65.6 \pm 8.9\text{‰}$ ($n = 26$) in dissolved gas. $\delta^{13}C$ values were not found to vary with well depth or lithology indicating that methane in Alberta groundwater was derived from a similar source. The low $\delta^{13}C$ values in concert with average $\delta^2H_{CH_4}$ values of $-289 \pm 44\text{‰}$ ($n = 45$) suggest that most methane was of biogenic origin predominantly generated via CO₂ reduction. This interpretation is confirmed by dryness parameters typically >500 due to only small amounts of ethane and a lack of propane in most samples. Comparison with mud gas profile carbon isotope data revealed that methane in the investigated shallow groundwater in Alberta is isotopically similar to hydrocarbon gases found in 100–250 meter depths in the WCSB and is currently not sourced from thermogenic

* Corresponding author.

E-mail address: phumez@ucalgary.ca (P. Humez).

hydrocarbon occurrences in deeper portions of the basin. The chemical and isotopic data for methane gas samples obtained from Alberta groundwater provide an excellent baseline against which potential future impact of deeper stray gases on shallow aquifers can be assessed.

© 2015 Elsevier B.V. All rights reserved.

1. Introduction

The recent expansion of shale gas and shale oil exploitation from unconventional energy resources in North America facilitated by horizontal drilling and hydraulic fracturing has had a profound impact on global fossil fuel supplies and costs (US Energy Information Administration, 2014; Mason et al., 2014). The rapid expansion of this industry in North America has, however, also generated public concern regarding the potential contamination of shallow groundwater, for example via leakage of stray gas from deeper strata (CCA, Council of Canadian Academies, 2014). Several peer-reviewed manuscripts have been published demonstrating conclusively the impacts of stray gas from unconventional natural gas or oil reservoirs on shallow aquifers (e.g. Osborn et al., 2011a,b; Jackson et al., 2013a,b; Darrah et al., 2014; and references therein). A key pre-requisite for assessing current or potential future impacts of stray gas leakage from unconventional energy resource development on shallow aquifers is the establishment of a scientifically defensible groundwater baseline that includes an understanding of the occurrence and the origin of naturally occurring methane in shallow aquifers (CCA, Council of Canadian Academies, 2014; The Royal Society and Royal Academy of Engineering, 2012; ACOA, 2013).

The ownership of energy resources in North America is typically private (USA) and the regulators are the states (in the USA), while the ownership in Canada is provincial. Different requirements for baseline groundwater monitoring are typically developed by individual jurisdictions. For instance, the province of Alberta (Canada) introduced baseline well water testing requirements for coalbed methane development in May 2006. This program requests that energy companies arrange for sampling of groundwater from landowner wells in 600 m radius from a planned energy well. The obtained water is analyzed for water quality parameters including major ionic constituents (e.g. Ca, Na, K, Cl, F, SO₄, pH, alkalinity, and TDS), and free gas samples are obtained where possible for subsequent gas composition analyses and carbon isotope ratio measurements on methane, ethane and CO₂ (AER Directive 35). In contrast, regulations in Colorado and Wyoming require groundwater sampling in a radius of half a mile around a new energy well and analysis of dissolved gas composition and isotope ratios (e.g. Colorado Oil and Gas Conservation Commission COGCC Rules 609 and 318.e; Wyoming Oil and Gas conservation commission, WOGCC). Other US states have other regulations (e.g. New York State Department of Environmental Conservation DEC; Pennsylvania Department of Environmental Protection, Office of Oil and Gas management). To the best of our knowledge, there has been no systematic comparison of free gas and dissolved gas sampling approaches for assessing the occurrence and the origin of methane during shallow groundwater baseline sampling programs because most studies focus only on dissolved methane. Also, the variabilities of chemical and isotopic parameters associated with different free and dissolved gas samplings and analytical approaches, the extent of natural variability in baseline gas compositions and isotopic fingerprints, and the related question of the desirable frequency of groundwater baseline sampling have not been fully investigated yet. Furthermore, guidelines for methane concentration alert thresholds are not identical in the different jurisdictions where they exist. For instance, the Quebec Ministry of Environment and the Pennsylvania Department of Environment Protection have set a threshold value of 7 mg/L for dissolved methane in groundwater. Above this level, well owners have to take measures to avoid the accumulation of gaseous methane in water pipes and distribution systems. In contrast, the U.S. Department of Energy recommends that “action is required” when dissolved methane

concentrations exceed 10 mg/L, since outgassing of methane and its accumulation may result in explosions.

Occurrence and origin of methane in shallow aquifers have been investigated in several natural gas and oil producing US states including Pennsylvania (Osborn et al., 2011a,b; Warner et al., 2012, 2013a; Darrah et al., 2012, 2014; Jackson et al., 2013a,b; Molofsky et al., 2013; Siegel et al., 2015; Vengosh et al., 2013; Brantley et al., 2014; Baldassare et al., 2014), Arkansas (Kresse et al., 2012; Warner et al., 2013b), Colorado (Li and Carlson, 2014), Texas (Zhang et al., 1998), and New York (McPhillips et al., 2014), among others. In Canada, similar studies have been reported for part of Ontario (Aravena et al., 1995; McIntosh et al., 2014), Quebec (Moritz et al., 2015) and Alberta (Cheung et al., 2010; Van Stempvoort et al., 2005; Humez et al., 2015; Rowe and Muehlenbachs, 1999; Tilley and Muehlenbachs, 2011). Several of these studies have tested correlations between methane occurrence in groundwater and distance to oil or gas wells, density of energy wells, geological settings and hydrogeochemical conditions. Detection of markedly elevated methane concentrations in groundwater may indicate stray gas migration from deeper formations. However, sampling of landowner wells with long screen intervals and often unknown well completion and lacking maintenance records may not always provide conclusive results often triggering controversial debates about the correct interpretation of the data (e.g. Jackson et al., 2013a, b; Vengosh et al., 2014; Baldassare et al., 2014; Molofsky et al., 2013). Where the occurrence of thermogenic methane in shallow groundwater was detected, further questions arise on whether fugitive gas migration occurs due to previous conventional oil and gas activities, due to anthropogenic causes associated with development of unconventional energy resources either via induced fractures or leaky well casings, or naturally (Vidic et al., 2013). Nevertheless, these studies revealed that geochemical and isotopic approaches are highly suitable to differentiate between shallow biogenic methane and deep mature thermogenic gas sources, and are potentially capable of identifying the depth from which contaminating stray gases originate (e.g. Tilley & Muehlenbachs, 2011). Therefore, establishing reliable and tested approaches comprised of effective sampling strategies and accurate and reproducible analytical methods for obtaining reliable information on the occurrence and sources of methane in shallow groundwater using chemical and isotopic techniques is of utmost importance for assessing future anthropogenic impacts from unconventional oil and natural gas development.

The objective of this study was to assess the occurrence of methane in shallow aquifers of the province of Alberta (Canada) and to use geochemical and isotopic characteristics of dissolved and free gas phases to determine the origin of methane. To achieve this, the variabilities of methane concentrations and C isotope ratios due to sampling and analytical uncertainties, geographical distribution, well depth, and geological formations in which the groundwater well is completed, were evaluated. Another goal was to compare free gas and dissolved gas sampling approaches to generate groundwater baseline data for samples obtained from dedicated monitoring wells to facilitate the future detection of potential environmental impacts of oil and gas development on shallow aquifers.

2. Background

2.1. Study site

The study was conducted in Alberta, Canada, a province with a long history of conventional and unconventional energy exploitation.

Conventional oil and natural gas have been produced from numerous reservoirs in the province after a first natural gas find in 1883 and more than 400,000 oil and natural gas wells have been drilled. More recently, unconventional natural gas has been exploited from rather shallow coalbed deposits (200–800 m below ground) predominantly in the Horseshoe Canyon Formation in and east of the Edmonton to Calgary corridor (ECC) in the southeastern part of the province with a maximum activity between 2006 and 2010. Shale gas exploration and exploitation have also commenced in the last decade focusing on the Triassic Montney and the Devonian Duvernay Formations. These unconventional energy resources are located in the northwestern part of the province typically at depths exceeding 1.5 km.

The provincial Groundwater Observation Well Network (GOWN) in Alberta is a network of groundwater monitoring wells completed in various shallow aquifers throughout the province. The associated monitoring program collects water level information together with geochemical and isotopic data in order to record natural and human-induced fluctuations of groundwater quantity and quality at sites identified as representative of the various hydrogeological environments found in Alberta. Today the GOWN consists of over 250 active observation wells in Alberta with many wells located in coalbed methane (CBM)

production areas in the southeastern part of the province, but very few wells exist in the shale gas development regions in the northwest. Since 2006, dissolved gas and free gas samples (where possible) from GOWN wells have been routinely obtained for chemical and isotopic analyses.

2.2. Climate and hydrogeological characteristics of selected aquifers in Alberta

The locations of GOWN water wells are presented in Fig. 1. The spatial distribution of GOWN wells throughout Alberta is unequal with the majority of water wells located within the Beaver River (East-central Alberta), North-Saskatchewan River (South-central Alberta), and South-Saskatchewan River (Southern Alberta) drainage basins. Only a small number of water wells are located in the Hay River, Peace River (Northern Alberta) and Milk River (Southern Alberta) basins. The Province of Alberta has a wide range of hydrological conditions related to variations in climatic and geological aquifer conditions. The average annual precipitation reported in the Edmonton–Calgary corridor (ECC), where the density of water wells is the highest, ranges from 360 to 630 mm (Riddell et al., 2014) with less precipitation in the southeastern portion

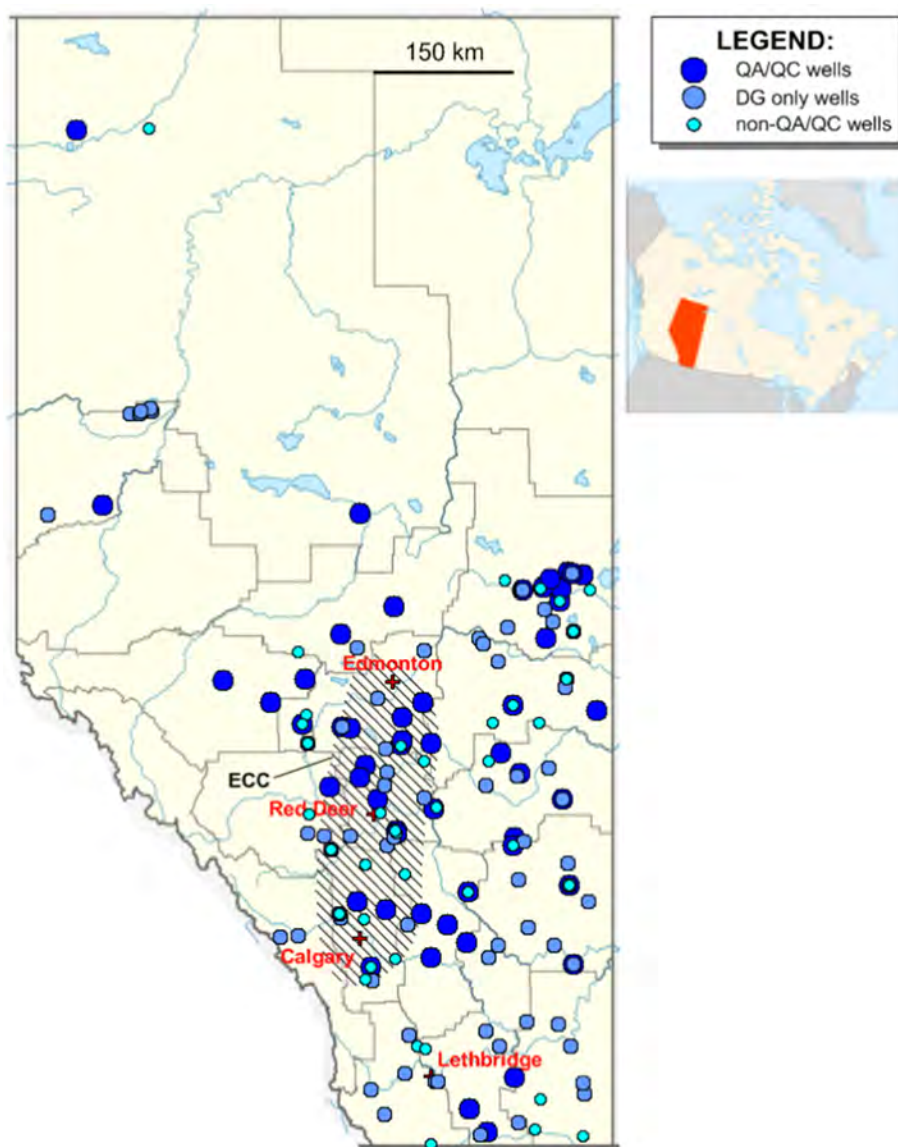


Fig. 1. Location of 186 GOWN wells sampled for this study in the province of Alberta. There are “QA/QC wells” ($n = 66$), “DG only wells” ($n = 74$), and “non-QA/QC wells” ($n = 46$): see Section 3.3 for further explanations of these well classifications.

of the ECC area relative to the northwest. Topography is highly variable with: (i) the Rocky Mountains and the Foothills region along the western border of the province with the highest elevations > 1000 m above sea level (asl), (ii) the edge of the Canadian Shield in the northeast with elevations < 300 m asl, and (iii) the Interior Plains in the remaining portion of the province with intermediate elevations.

GOWN wells are completed in aquifers either composed of surficial deposits resulting from the last major glaciation or reach the bedrock. The depth of the GOWN wells varies from 26 m to 250 m below ground surface (bgs) accessing groundwaters from different shallow aquifers. The aquifer lithologies vary considerably comprising fractured mudstone, sandstone and siltstone beds or lenses, pre-glacial sand, surficial sandy and gravelly lacustrine or moraine deposits. The regional Upper Cretaceous-Tertiary stratigraphy, differentiates many sandy clastic depositions including the (i) Lower Campanian Milk River formation (and equivalents), (ii) Middle to Upper Campanian Belly River (Judith River) Group (and equivalents), (iii) Upper Campanian to Lower Maastrichtian Horseshoe Canyon Formation (and equivalents), (iv) Upper Maastrichtian to Lower Paleocene Scollard Formation (and equivalents), and (v) the Middle to Upper Paleocene Paskapoo formation (and equivalents). Four intervals of limited coarse-grained deposition can be found in the stratigraphy: (i) the Lower Campanian Pakowki formation, (ii) the Middle Campanian Bearpaw shales, (iii) the Maastrichtian Battle Shales formation, and (iv) the upper part of the Scollard formation (Dawson et al., 1994a,b).

Milk River sandstones consist of one or several sandstone beds interbedded with shale (Meyboom, 1960) within shallow marine and shoreline or minor fluvial deposits. Fine-grained sediments of marine strata of the Lea Park and Pakowki Formations consist of mudstone and siltstone (Rosenthal et al., 1984). The overlying continental strata of the Belly River Group are subdivided into the upper Oldman Formation and the stratigraphically lower Foremost Formation. The Belly River Group formations consist of fluvial sandstone and siltstone with minor mudstone and coal. The marine Bearpaw formation consists of shale and siltstone with some sand layers (Hamblin, 1998). The Horseshoe Canyon Formation was deposited in a marine to terrestrial fluvial setting and is subdivided into Lower, Middle and Upper portions. Both the Upper and Lower Horseshoe Canyon consist primarily of sand and coal, whereas the Middle Horseshoe Canyon consists predominantly of shale with bentonite and little sandstone or coal (Dawson et al., 1994b). The Scollard and Willow Creek formations consist of sandstone and siltstone units interbedded with mudstone beds and coal. The Paskapoo and Porcupine Hills Formations were deposited in a terrestrial fluvial environment and consist of sequences of thick tabular sandstones overlain by interbedded siltstone and mudstone (Lyster and Andriashek, 2012; Dawson et al., 1994a; Hamblin, 2004) and these formations constitute heavily used aquifers in the prairies region of Alberta (Grasby et al., 2008). The Paskapoo formation grades into the equivalent Porcupine Hills Formation south of Calgary (Prior et al., 2013). The lithology descriptions revealed that the groundwater samples were predominantly collected from the sandstone, sandstone & shale, and sandstone & shale & coal layers of these formations. The quaternary deposits include the Muriel Lake Formation that is composed of silt, sand and gravel of glacio-fluvial origin. 77% of the wells are completed in confined aquifers, whereas 23% of the wells accessed semi-confined or unconfined aquifers.

3. Sampling and analytical methods

3.1. Sampling of groundwater and its dissolved and free gases

Groundwater samples and free gas and dissolved gas samples were repeatedly obtained from GOWN wells accessing various aquifers between 2006 and 2014. Before collecting groundwater and gas samples, the groundwater wells were purged until field parameters including pH, redox, dissolved oxygen, temperature, and electrical conductivity

stabilized to collect samples representative of aquifer conditions. Groundwater samples were collected in glass or plastic containers and preserved as necessary. Free gas samples were collected in Summa canisters or flexfoil bags through a PVC gas separator described in Humez et al. (2015). Time, pump flow rate, pressure in the gas separator and water level fluctuations were recorded during each sampling event. Dissolved gas samples for concentration analyses were collected in 40 ml vials with Teflon lined septa caps. The inverted vials were submerged into a bucket filled with sample water as a seal to prevent atmospheric contamination. Dissolved gas samples for isotope analysis were subsequently taken by filling a 250 ml amber glass bottle with a Teflon septa cap using the same approach. A detailed description of the sampling equipment and procedures is given in Humez et al. (2015).

3.2. Laboratory analyses

3.2.1. Gas composition

The composition of free and dissolved gas samples was determined in the laboratory by gas chromatography yielding concentrations for nitrogen, oxygen, carbon dioxide, methane and higher alkane chain compounds such as ethane and propane with measurements conducted by Alberta Innovates Technology Futures (AITF) with uncertainties of $\pm 5\%$ of the analyte. Gas composition data for free gas samples is reported in parts per million by volume (ppmv) and for dissolved gases in $\mu\text{g/L}$ or mg/L . These units were chosen to facilitate comparisons with results in numerous other studies reporting dissolved methane concentrations data.

3.2.2. Isotopic analyses

The carbon and hydrogen isotope ratios of methane and ethane, the hydrogen isotope ratios of water, and the carbon isotope ratios of carbon dioxide were analyzed in the Isotope Science Laboratory at the University of Calgary. All gas isotope analyses were conducted on a ThermoFisher MAT 253 isotope ratio mass spectrometer (IRMS) coupled to Trace GC Ultra + GC Isolink (ThermoFisher). Stable isotope ratios are reported in the standard delta notation (‰) relative to VPDB for $\delta^{13}\text{C}$ values and VSMOW for $\delta^2\text{H}$. The precision for carbon isotope analyses was better than $\pm 0.5\text{‰}$ for hydrocarbons and better than $\pm 0.2\text{‰}$ for carbon dioxide. Hydrogen isotope analyses on methane were conducted with uncertainties better than $\pm 3\text{‰}$. Water isotope analysis was performed by Off-axis Cavity Ringdown Spectroscopy using a Los Gatos Water Isotope Analyzer (DLT-100). Precision was better than $\pm 2\text{‰}$ for $\delta^2\text{H}$.

3.3. QA/QC criteria and number of samples obtained

Quality assurance and quality control (QA/QC) criteria were applied based on mass balance and methane concentration considerations. For the free gas samples, the sum of the determined partial pressures of all analyzed gas components was required to be within $\pm 10\%$ of the total pressure at 1 atm. A cutoff of 1500 ppmv or 0.15% for methane concentrations in free gas was chosen to minimize measurement uncertainties (Jones et al., 2009). The mass balance consideration and the methane concentration cutoff resulted in 40% of the free gas samples passing the QA/QC criteria. For free gas samples passing the QA/QC criteria, an air correction approach was used. The approach consists of three steps: 1) to calculate the oxygen concentration in free gas in equilibrium with the measured field dissolved oxygen concentrations; 2) to calculate the corrected nitrogen concentration based on the atmospheric N_2/O_2 ratio of 3.72 and corrected oxygen-free gas concentrations; and 3) to correct the concentrations of free gas compounds, to achieve a balance of 100% (Humez et al., 2015).

A total of 377 free and dissolved gas samples from 186 wells were collected in this study. These 186 wells are subdivided into "QA/QC wells", "DG (Dissolved Gas) only wells" and "non-QA/QC wells" defined as follows: QA/QC wells refers to 66 wells that yielded free gas samples

passing the QA/QC criteria. 74 wells yielded no free gas samples, but did yield dissolved gas concentrations data, and these sites are identified as “DG only wells”. Forty-six wells yielded free gas samples that did not pass the QA/QC criteria having either methane concentration in free gas <1500 ppmv ($n = 41$) or free methane concentration >1500 ppmv but with a gas composition not adding up to $100 \pm 10\%$ ($n = 5$). These wells are classified as ‘non-QA/QC wells’ (Fig. 1).

For the category of 66 “QA/QC wells”, 36 wells were sampled once, while 30 wells were sampled on 2 to 11 occasions during the observation period. Ten triplicate samples obtained on the same day from the same well for free gas analyses, and 9 triplicate samples for dissolved gas analyses were collected to assess combined sampling and analytical uncertainties. Additionally, one well had an 8-year record with 11 samples collected and three triplicates for both free and dissolved methane concentrations (Humez et al., 2015). This resulted in a dataset of 124 free and dissolved gas samples from the 66 “QA/QC wells” category throughout the observation period. Chemical and isotopic data obtained for these samples were correlated with geological formations, lithology, and completion depths of the water wells. The mean water well depth is 86 ± 47 m, the median, minimum and maximum depths are 76, 26 and 250 m, respectively. The mid-production depths for wells where the information is available are on average 79 ± 42 m with a minimum of 22 and a maximum of 207 m ($n = 61$).

3.4. Statistical data analyses

Descriptive statistics, such as minimum, maximum, mean, median, and standard deviation (SD or σ), are used to provide a summary of the data. Median and mean values are both used since they differ due to the asymmetric distribution of some variables in the dataset (Table 1). SPSS 22 was used for statistical treatment of the data. For statistical analysis, variables with values below the method detection limit (10% of overall data) were treated as being equal to the detection limit. Shapiro–Wilk’s test is used to test normality of each variable in datasets where p-values are presented in Table 1. The results reveal that only 10 of 18 variables follow a normal distribution ($p > 0.05$) even after log-transformation (Reimann and Filzmoser, 2000). The outliers of the gas geochemical dataset are included in the statistical analysis because they contain important information. Pearson correlation analysis was conducted to determine which variables are most closely correlated. Non-parametric tests were also used such as Spearman’s rho and Kendall’s tau tests, to capture outliers and non-linear dependencies between variables (Siegel et al., 2015). Correlation coefficients range from -1 indicating a perfect negative correlation, 0 indicating no correlation,

to $+1$ revealing a perfect positive correlation. Although Spearman’s rho and Kendall’s tau tests usually yield similar conclusions, both were calculated and reported. Significant correlation is assumed for p-values lower than 0.05. Different scenarios are reported in Table 3: i) significance of the Pearson’s R coefficient indicating a linear correlation between two variables ii) non-significance of Pearson’s R coefficient but significance of Spearman’s rho/Kendall’s tau coefficients indicating non-linear dependency between two variables, and iii) non-significance of the Pearson’s R, Spearman’s rho and Kendall’s tau coefficients indicating no significant correlation between two variables.

The (Student) t-test was used for comparing normally distributed parameters between two groups of variables. For other parameters with skewed data distributions, the non-parametric Mann–Whitney and Kruskal–Wallis tests were implemented to estimate the significance difference between two or more groups of variables. All hypotheses were tested at the significance level α of 0.05.

4. Results and discussion

Methane is ubiquitous in shallow groundwater of Alberta accessed by the GOWN wells. In groundwater from 179 of 186 GOWN wells methane was observed in dissolved form. Groundwater from 74 GOWN wells yielded methane only in dissolved gas samples, but not in free gas samples. In 112 GOWN wells, methane was observed in both dissolved form and in free gas samples. In 66 of these 112 GOWN wells, methane was observed in free gas samples after applying the QA/QC criteria (see Section 3.3) with chemical and isotopic compositions of free gas samples presented in Table 1.

4.1. Quantification of sampling and analytical uncertainties

The sampling and analytical uncertainties for concentration measurements on methane were assessed based on triplicate samples taken successively from the same well on the same day during a sampling event. Ten triplicate samples for free methane concentrations and 9 triplicate samples for dissolved methane concentrations from the same sampling date were measured and results are summarized in Table 2. The average coefficient of variation (μ) is 5% for methane concentrations in free gas and 12% for dissolved gas samples. We defined the cumulative sampling and analytical uncertainty as $\mu + 1\sigma$ resulting in threshold values of 13% for methane concentrations in free gas samples and 20% for methane concentrations in dissolved gas samples. Hence, temporal variabilities in methane concentrations for groundwater from the same well exceeding these calculated sampling and

Table 1

Descriptive statistics of the gas geochemical dataset for dissolved (DG) and free gas (FG) of the 66 “QA/QC wells” category (Section 3.3).

	Unit	N	Min	Max	Mean	Med	SD	p*	p-lg10*
Methane	ppmv	66	1668	986,142	399,687	232,462	406,922	<0.001	<0.001
Ethane	ppmv	66	0.05	3369.84	302.66	25.15	685.81	<0.001	<0.001
Carb diox.	ppmv	66	78	40,812	6934	1798	9869	<0.001	0.053
Propane	ppmv	66	0.05	226.29	4.00	0.06	27.82	<0.001	<0.001
Nitrogen	ppmv	66	11,199	997,453	594,590	766,010	402,139	<0.001	<0.001
Oxygen	ppmv	58	17	708	109	73	123	<0.001	<0.001
$\delta^{13}\text{C}_{\text{CH}_4}$ (FG)	‰	63	-95.8	-50.6	-69.7	-69.3	11.3	0.264	
$\delta^{13}\text{C}_{\text{CO}_2}$ (FG)	‰	54	-40.5	+14.3	-16.4	-19.7	10.5	≤ 0.001	0.889
$\delta^{13}\text{C}_{\text{C}_2\text{H}_6}$ (FG)	‰	16	-65.9	-36.1	-51.8	-51.6	7.7	0.983	
$\delta^2\text{H}_{\text{CH}_4}$ (FG)	‰	45	-437.1	-202.0	-289.4	-288.0	43.7	≤ 0.001	–
$\delta^{13}\text{C}_{\text{CH}_4}$ (DG)	‰	26	-85.5	-46.6	-65.6	-65.8	8.9	1	
$\delta^{13}\text{C}_{\text{CO}_2}$ (DG)	‰	19	-34.3	-12.9	-14.6	-18.2	12.1	0.363	
$\delta^2\text{H}_{\text{H}_2\text{O}}$	‰	60	-176.5	-95.2	-141.2	-141.4	13.6	0.234	
Ethane	µg/L	54	0.0	225.5	37.4	2.6	37.4	<0.001	<0.001
Methane	µg/L	61	0.1	42,900	12,416	5830	14,920	<0.001	<0.001
Carb diox.	mg/L	62	0.01	204	16.3	5.3	29.3	<0.001	0.311
Nitrogen	mg/L	60	2.4	33.0	19.7	20.1	7.4	0.116	
Oxygen	mg/L	58	0.1	4.0	0.5	0.4	0.2	<0.001	0.115

Numbers of wells (N), Minimum (Min), Maximum (Max), Mean (Mean), Median (Med), Standard Deviation (SD).

* p-Values of Shapiro–Wilk test for normality of the original and log-transformed (p-lg10) data.

analytical uncertainties indicate natural or anthropogenic variations (see Section 4.5).

4.2. Distribution of methane and other components in free gas in Alberta groundwater

A histogram of methane concentration distribution from all 112 wells yielding free gas ('QA/QC' wells and 'non-QA/QC wells') is shown in Fig. 2A. The calculated mean methane concentration was 225,535 ppmv ($n = 112$). A highly asymmetric distribution of the free gas methane concentrations was observed with 71 wells or 63% having concentrations less than 66,667 ppmv (Fig. 2A). Free gas samples from ten wells or 9% had methane concentrations $>933,333$ ppmv.

For free gas samples from the 66 QA/QC wells, the mean methane concentration was 399,687 ppmv and the median was 232,462 ppmv with a range of 984,473 ppmv (Fig. 2A) and hence the coefficient of variation is higher than 100% (Table 1). Fig. 3A illustrates the high spatial variability of the methane concentrations in free gas from these 66 GOWN wells. The highest free methane concentrations were observed in the ECC with $>300,000$ ppmv. Such high methane concentrations are not found anywhere else in the GOWN data set of the province of Alberta.

Other hydrocarbon compounds were only observed occasionally in low concentrations in free gas samples. Ethane had a median concentration of 25 ppmv with 53 samples having concentrations above the detection limit of 0.05 ppmv. The mean ethane concentration is 303 ppmv (Table 1). Only 26 samples had propane concentrations above the detection limit of 0.05 ppmv with a maximum of 226 ppmv (Table 1). Hence the dryness parameter, i.e. the ratio of methane to higher alkane concentrations varied from 66 to $>10,000$. This indicates that most of the gas samples are dry containing mainly methane except for free gas from one GOWN well located east of Calgary with the lowest dryness parameter value of 66. The dryness parameter is one of the indicators often used to define the origin of gas in groundwater. Ethane and propane are generally not coproduced during microbial methanogenesis and therefore the presence of higher-chain hydrocarbons at relatively low methane to ethane ratios (<100) is often used as an indicator of the occurrence of deeper thermogenic gas (Barker and Fritz, 1981a,b).

The major complementary gas compound in addition to methane was N_2 with a median concentration of 766,010 ppmv and a mean value of $594,590 \pm 402,139$ ppmv. Methane and N_2 typically represented $>93\%$ (minimum value) of the sampled free gases and an inverse correlation between these parameters was observed based on Pearson, Kendall and Spearman correlation coefficients (Table 3). Oxygen concentrations calculated after air correction approaches (see Section 3.3)

Table 2

Average concentrations and $\delta^{13}C$ values with standard deviations (SD) and coefficient of variation (CV) for triplicate samples obtained from the same well on the same day.

Wells	Dissolved methane concentration			Free methane conc. & isotope ratios				
	Avg ($\mu\text{g/L}$)	SD ($\mu\text{g/L}$)	CV (%)	Avg (ppmv)	SD (ppmv)	CV (%)	Avg (‰)	SD (‰)
Clu-t	9036	473	5	346,091	11,326	3	-77	0.5
Cross-t	9703	795	8	305,176	9984	3	-93	0.3
Mana-t	885	56	6	39,688	2347	6	-58	0.1
Min-m-t-a	1175	303	26	265,712	15,196	6	-79	0.4
Min-m-t-b	4006	833	21	215,711	5614	3	-77	1.0
Min-m-t-c	6220	545	9	220,006	58,255	26	-78	0.1
Red-t	27,467	5847	21	965,748	26,091	3	-68	2.8
Ros-t	34,566	3534	10	948,411	2053	0	-64	0.4
Wet-t	221	11	5	8926	287	3	-60	0.1
ForC-t				813,746	12,507	1		
Average (μ)	10,364	1378	12	412,921	14,366	5	-73	0.6
σ	12,325	1986	8	381,967	17,215	8	11	1

had a median value of 73 ppmv with a minimum concentration of 17 ppmv, a maximum value of 708 ppmv, and a mean value of 109 ppmv ($n = 58$). Carbon dioxide concentrations had a median value of 1798 ppmv and a mean value of 6934 ppmv ($n = 66$) (Table 1).

4.3. Distribution of dissolved methane and other components in Alberta groundwater

A histogram of methane concentration distribution for 179 GOWN wells yielding dissolved gas is shown in Fig. 2B. A highly asymmetric distribution of the dissolved methane concentration was observed with 138 wells (77%) having dissolved methane concentrations noted as $[CH_4]_{\text{diss}}$ of less than 3333 $\mu\text{g/L}$ and a mean value of 5232 $\mu\text{g/L}$ ($n = 179$). The highest $[CH_4]_{\text{diss}}$ observed was 42,900 $\mu\text{g/L}$ and 28 of 179 samples (16%) had an average $[CH_4]_{\text{diss}}$ higher than the 10 mg/L safety threshold value of the Office of Surface Mining, U.S. Department of the Interior (Eltschlager et al., 2001). Fourteen of 179 samples had methane concentrations higher than 31 mg/L, which corresponds to the maximum solubility of methane in water at 1 atm and 10 °C, which is the average groundwater temperature. These waters are oversaturated with methane at surface (atmospheric) pressures and were obtained from wells located mainly between Edmonton and Lethbridge.

Of the 66 QA/QC wells, 61 groundwater samples yielded $[CH_4]_{\text{diss}}$ concentrations with an average of 12,416 $\mu\text{g/L}$ and a median value of 5830 $\mu\text{g/L}$ with a range of 42,899 $\mu\text{g/L}$. Groundwater from 21 wells had average $[CH_4]_{\text{diss}}$ higher than the 10 mg/L safety threshold value. There is a high spatial variability of $[CH_4]_{\text{diss}}$ from these 61 GOWN wells (Fig. 3B). The highest $[CH_4]_{\text{diss}}$ (e.g. $>10,000$ $\mu\text{g/L}$) were mainly observed between Calgary and Edmonton and such high dissolved methane concentrations in groundwater are not found anywhere else in the province. The spatial distribution of free and dissolved methane concentrations in groundwater shown in Fig. 3 displays a similar pattern that is further discussed in Section 4.4.

In the dissolved gas samples other n-alkanes were only detected occasionally in low concentrations. Ethane had a median value of 2.6 $\mu\text{g/L}$ and 36 samples had a concentration higher than 0.01 $\mu\text{g/L}$. The mean ethane concentration was 37 ± 2 $\mu\text{g/L}$ (Table 1). Groundwater from 15 of 66 wells had propane concentrations above the detection limit varying from 0.01 to 0.38 $\mu\text{g/L}$.

The remainder of the dissolved gas was predominantly composed of N_2 with a median and mean value of 20 mg/L (Table 1). Oxygen concentrations based on the field data had a median value of 0.4 mg/L with a minimum concentration of 0.1 mg/L, maximum values of 4.0 mg/L, and a mean value of 0.5 ± 0.5 mg/L ($n = 58$). Carbon dioxide concentrations had a median value of 5.3 mg/L and a mean value of 16 mg/L ($n = 62$).

4.4. Comparison of methane concentrations in free and dissolved gas samples

Both free and dissolved methane concentrations in groundwater from different wells throughout Alberta revealed extremely high variabilities ($CV > 100\%$). Table 3 summarizes the correlation analyses that evaluated which variables are most closely correlated. Pearson, Kendall and Spearman approaches revealed that methane concentrations in free and dissolved gas samples are significantly correlated (Pearson $R = 0.93$, Kendall's tau = 0.79, Spearman's rho = .93 with $p < 0.05$, Table 3) and plot close to the equilibrium state with saturation coefficients calculated for 0 to 10 °C (Fig. 4) based on the Lawrence Livermore National Laboratory database (Parkhurst and Appelo, 1999). Fig. 3 revealed similar spatial distributions of free and dissolved methane concentrations in Alberta groundwater. Fig. 4 confirms this observation with a strong positive correlation between methane concentrations in free and dissolved gas samples consistent with water-gas interaction and Henry's law. This

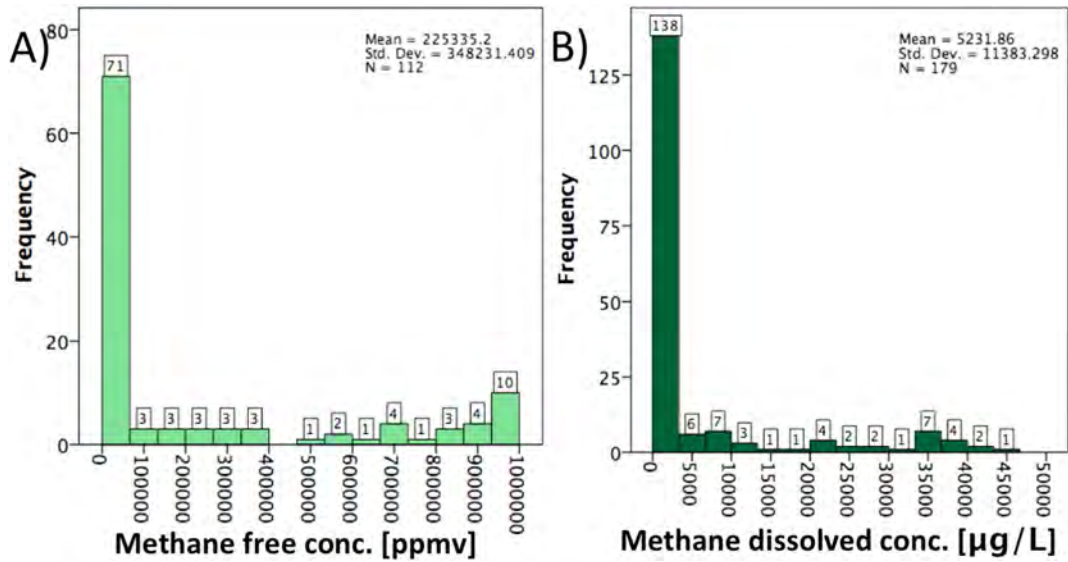


Fig. 2. Histograms of frequency for A) methane concentrations in free gas samples, and B) dissolved methane concentrations in Alberta groundwater. The number of samples in each concentration category is displayed above each bar.

indicates that dissolved gas and free gas sampling approaches lead to comparable results. Only few samples seem to be undersaturated with respect to methane (i.e. they plot below the equilibrium state lines). In general, the correlation between similar variables in free and dissolved gas samples such as C₂H₆, C₃H₈, CO₂, N₂, O₂ concentrations is strong and significant (Table 3, orange shading) confirming that both sampling approaches yield comparable results.

4.5. Temporal variabilities in methane concentrations

Temporal variabilities in methane concentrations were evaluated by comparing repeat analyses of free and dissolved gas samples obtained from the same wells. Temporal variabilities occur when resulting

dispersion values are higher than the sampling and analytical uncertainties defined in Section 4.1. Groundwater from 11 of 26 wells for dissolved methane concentration, and from 9 of 25 wells for methane concentrations in free gas samples resulted in CV values higher than the combined analytical and sampling uncertainties. This suggests either (i) that less than 50% of the repeatedly sampled wells displayed temporal variabilities in methane concentrations or (ii), as the majority of the samples are saturated with methane (Fig. 4), that gas slugs may be arriving at the well and are dissipating between sampling events (Gorody, 2012). The sampling may be too infrequent to pick up gases arriving occasionally as slugs leading to saturation of groundwater with methane.

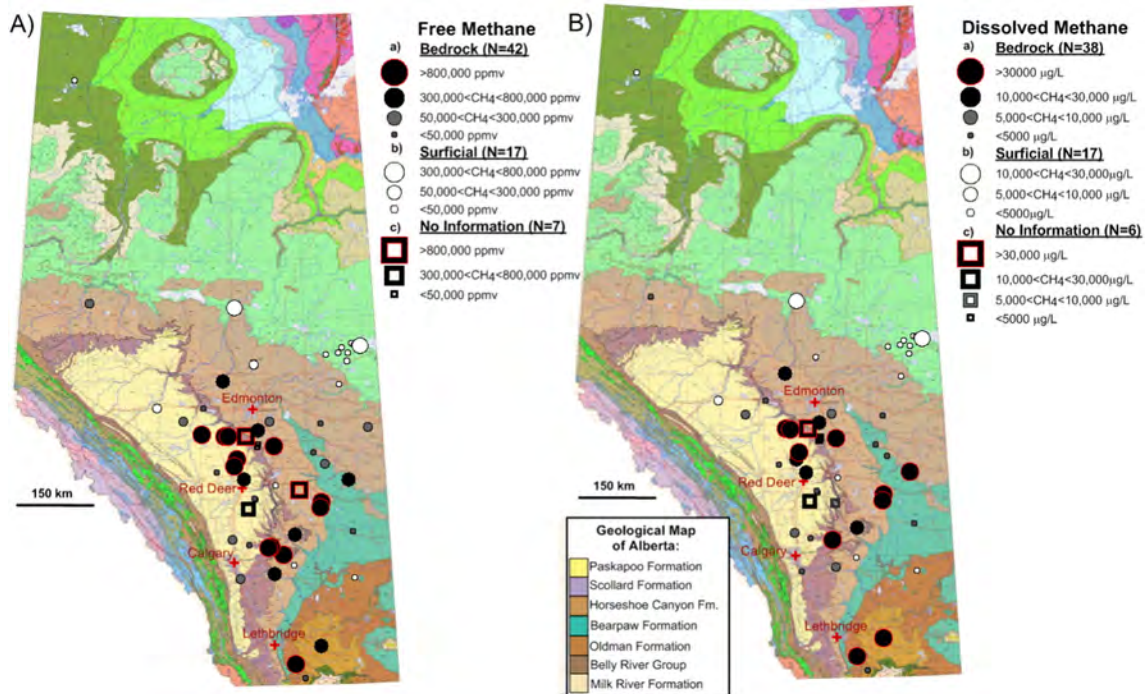


Fig. 3. Spatial variation of A) average methane concentrations (ppmv) for free gas from 66 wells passing the QA/QC criteria throughout the province of Alberta, and B) associated average dissolved methane concentrations (µg/L) for groundwater from 61 wells. Modified maps from AGS of bedrock geology beneath the Quaternary cover.

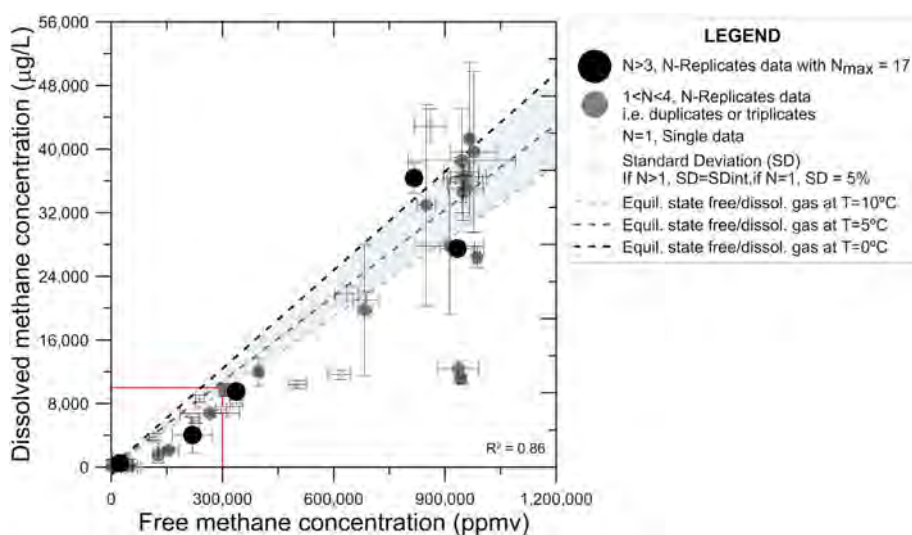


Fig. 4. Comparison of methane concentrations for free gas and dissolved gas samples from the same GOWN wells for all samples passing the QA/QC criteria. Average groundwater temperatures were around 8 °C. Error bars for n-replicates are based on internal standard deviation (SDint). Error bars are calculated either by standard analytical uncertainties provided by the laboratories when there is only one sample per well, or are calculated based on data from replicate samples per wells (same sampling date, Sections 4.1 and 4.5). The horizontal red line represents the regulation threshold for dissolved methane of 10 mg/L (U.S. Department of Energy), corresponding with a methane concentration of 300,000 ppmv in free gas samples at 10 °C. (For interpretation of the references to color in this figure legend, the reader is referred to the web version of this article.)

On average, methane concentration variabilities in samples from these wells were three times higher than the sampling and analytical uncertainties defined for both free and dissolved methane concentrations. Also, temporal variability for methane concentrations in free and dissolved gas samples from these wells was comparable as shown in Fig. 4. The temporal variability of methane concentration at some wells may be in part explained by variable sampling conditions (extent of water level drawdown, pumping speed) as shown by Humez et al. (2015), but other natural or anthropogenic causes can not be excluded as potential explanations.

4.6. Isotopic fingerprints to delineate sources and formation pathways for methane

The sampling and analytical uncertainties for carbon isotope measurements on methane were assessed based on triplicate samples taken from the same well on the same day. $\delta^{13}\text{C}$ values of triplicate samples obtained from nine wells revealed that the standard deviation of three measurements was typically $\leq \pm 1.0\%$ with only one triplicate sample exceeding this value (Table 2). The average standard deviation (σ) of the mean $\delta^{13}\text{C}$ values for triplicate samples obtained on the same day was $\pm 0.6\%$. We defined the sampling and analytical uncertainty as $\mu + 1\sigma$ resulting in 1.0% for $\delta^{13}\text{C}$ of methane indicating an excellent sampling and analytical reproducibility compared to only the analytical uncertainty usually reported for carbon isotope ratios of methane in free gas of $\pm 0.5\%$.

Carbon isotope ratios ($\delta^{13}\text{C}$) of methane in free gas samples from 106 wells are summarized in Fig. 5 and show a symmetric distribution. It is interesting to note that $\delta^{13}\text{C}$ values of methane in free gas samples passing the QA/QC tests varied between -95 and -50% with an average value of $-69.7 \pm 11.1\%$ ($n = 63$). In contrast, the $\delta^{13}\text{C}$ values of methane in free gas samples not passing the QA/QC test varied between -85 and -20% . $\delta^{13}\text{C}$ values of methane $> -50\%$ were only observed in free gas samples with methane concentrations of < 1500 ppmv. It is possible that these high $\delta^{13}\text{C}$ values at relatively low methane concentrations are caused by bacterial methane oxidation in the aquifer or the sampling containers, a process during which residual methane is enriched in ^{13}C (Barker and Fritz, 1981a,b).

For free gas from groundwater of shallow aquifers passing the QA/QC criteria there was a considerable variability of $\delta^{13}\text{C}$ values of methane from -95.8 to -50.6% for samples with CH_4 concentrations

$< 100,000$ ppmv (Fig. 6). It is possible that methane oxidation in the aquifers is responsible for some of the $\delta^{13}\text{C}$ values $> -55\%$ at low methane concentrations resulting in enrichment of ^{13}C and ^2H in the remaining methane, resulting also in a decreasing dryness parameters suggesting falsely a thermogenic fingerprint. However, preferential oxidation of ethane or propane may also occur resulting in an increase of the dryness parameter suggesting falsely a more biogenic signature (Aharon et al., 1992; Kessler et al., 2006; Pape et al., 2010; Darrah et al., 2015). For free gas samples with methane concentrations between 100,000 and 650,000 ppmv, the $\delta^{13}\text{C}$ values of methane were generally below -69.7% with one exception of a sample with a $\delta^{13}\text{C}_{\text{CH}_4}$ value of -63.3% (average of -75.2% ; minimum of -92.6% ; maximum of -63.3%). In contrast, free gas samples with the highest methane concentrations ($> 680,000$ ppmv) had again higher $\delta^{13}\text{C}$ values between -73.5 and -55.9% (Fig. 6). Such free gas samples were exclusively observed in a corridor between Edmonton and Lethbridge (Fig. 6) in groundwater wells perforated mostly in the Horseshoe Canyon and Paskapoo

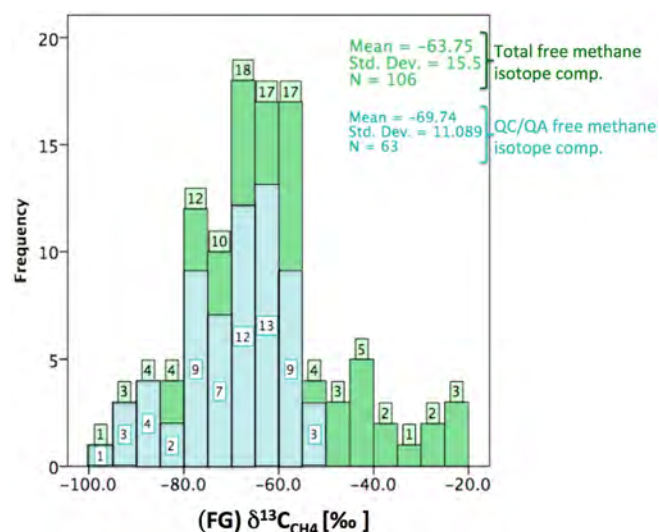


Fig. 5. Histogram of frequency for $\delta^{13}\text{C}$ values of methane in all free gas samples ($n = 106$). Samples passing the QA/QC criteria are shown in blue. Numbers of samples belonging to isotope ratio intervals are indicated above each bar. (For interpretation of the references to color in this figure legend, the reader is referred to the web version of this article.)

Formations and in a few cases in the Milk River and Bearpaw Formations, some of which contain coal seams.

When assessing the temporal variabilities of $\delta^{13}\text{C}$ values of methane in free gas samples from the same groundwater well sampled on different occasions between 2006 and 2014, 14 of 23 GOWN wells with duplicate analyses had $\delta^{13}\text{C}$ values of methane with a standard deviation of 1.0‰ or less. For five samples the standard deviation varied between 1 and 2‰, and only in five cases did the $\delta^{13}\text{C}$ value of methane for free gas samples obtained in different years from the same groundwater well deviate by more than 2‰ (Table 4). This indicates little temporal variability in the $\delta^{13}\text{C}$ values of methane of free gas with only a few exceptions thus indicating a unique and constant gas source signature.

The carbon isotope values of dissolved methane in groundwater from QA/QC wells had a mean value of $-65.6 \pm 8.9\%$ ($n = 26$), with a minimum value of -85.5% and a maximum of -46.6% . Fig. 7 shows a cross-plot of $\delta^{13}\text{C}$ values of methane in free gas samples and dissolved gas samples obtained from the same wells ($n = 26$) indicating that most samples plot close to the 1:1 line. Moreover, Table 3 reveals a strong and significant correlation between the $\delta^{13}\text{C}$ values of methane in free gas samples and dissolved gas samples (Pearson $R = 0.79$, Kendall's tau = 0.73, Spearman's rho = 0.84 with $p < 0.05$). The difference (Δ) between $\delta^{13}\text{C}$ values of methane in free gas and dissolved gas samples was $< 1\%$ in 13 cases. Δ ranged between 1 and 2‰ in samples from four wells, varied between 2 and 5‰ for 5 wells, and exceeded 5‰ on 4 occasions. This indicates, for the most part, good agreement between carbon isotope measurements on methane in free and dissolved gas further supported by an insignificant t-test ($p > 0.05$).

The hydrogen isotope ratios ($\delta^2\text{H}$) of methane in free gas samples had a mean value of $-289.4 \pm 43.7\%$ ($n = 45$). The minimum $\delta^2\text{H}_{\text{CH}_4}$ value was -437% and the maximum value was -202% . Together with $\delta^{13}\text{C}$ values of methane of $< -55\%$ this suggests a predominantly biogenic origin of methane in groundwater. $\delta^{13}\text{C}_{\text{CH}_4}$ values $> -50\%$ are indicative of deeper thermogenic methane whereas values $< -60\%$ are strongly indicative of microbial methane (Bernard et al. 1976; Schoell, 1980). Likewise, $\delta^2\text{H}_{\text{CH}_4}$ values lower than -175% particularly when combined with low $\delta^{13}\text{C}_{\text{CH}_4}$ values often indicate a pure biogenic methane origin.

Fig. 8 shows that the majority of samples from QA/QC wells have a $\delta^{13}\text{C}$ value of methane $< -58\%$ and dryness parameters of > 177 . Therefore, joint evaluation of gas compositions, dryness parameters, $\delta^{13}\text{C}_{\text{CH}_4}$ and $\delta^2\text{H}_{\text{CH}_4}$ values of methane indicate that the majority of the baseline groundwater samples contained methane of biogenic origin (Fig. 8). Only one sample obtained from a well located east of Calgary was characterized by a dryness parameter of 66 due to a methane concentration of 2543 ppmv and an ethane content of 26 ppmv. Methane in this

sample had a $\delta^{13}\text{C}$ value of -55.8% . Hence, this sample plots in the mixed gas zone on Fig. 8. The chemical and isotopic composition of this sample could result from bacterial methane oxidation or partial impact of immature thermogenic gas (Rowe and Muehlenbachs, 1999) on the shallow aquifer. Only in a small subset of samples was a minor thermogenic gas admixture or the microbial oxidation of methane potentially required to explain slightly elevated $\delta^{13}\text{C}$ values of methane and/or low dryness values shown in Fig. 8.

Chemical and isotopic approaches are not only useful for constraining methane sources but can also be used to identify the formation pathway of bacterially generated methane gas. The two major metabolic pathways are acetate fermentation and CO_2 reduction (Whiticar et al., 1986) that use several possible substrates. The difference between carbon isotope ratios of methane and CO_2 can assist in identifying the predominant reaction pathways.

The average $\delta^{13}\text{C}$ value of carbon dioxide in free gas samples was $-16.4 \pm 10.5\%$ ($n = 54$) indicating that the CO_2 was predominantly derived from organic carbon oxidation and to a lesser extent impacted by carbonate dissolution (Mook, 2000). $\delta^{13}\text{C}$ of dissolved carbon dioxide had a similar mean value of $-14.6 \pm 12.1\%$ ($n = 19$). The carbon isotopic data of methane and carbon dioxide are plotted in Fig. 9A. The isotopic fractionation between the coexisting CO_2 and CH_4 has a mean value of 1.05 defined by $\alpha_c = \frac{\delta^{13}\text{C}_{\text{CO}_2} + 1000}{\delta^{13}\text{C}_{\text{CH}_4} + 1000}$ (Whiticar et al., 1986) and α_c values of up to 1.08 were observed. α values from 1.06 to 1.09 are characteristic of CO_2 reduction, whereas acetate and methyl-type fermentation result in α values from 1.03 to 1.06. The values obtained in this case study plot predominantly in the CO_2 reduction field and to a lesser extent in the methyl-fermentation boundaries according to Fig. 9A.

The comparison of $\delta^2\text{H}$ values of methane and formation water (Fig. 9B) is another indicator of biogenic methane formation processes, because the relationship of hydrogen isotopes between methane and water is dependent on the methanogenic pathway. During CO_2 reduction, all of the methane hydrogen is derived from coexisting H_2O with a H isotope fractionation of $-160 \pm 10\%$ (Schoell, 1980) resulting in a slope of 1 in Fig. 9B. In contrast, during acetate fermentation, only one of the four hydrogen atoms in methane is derived from water resulting in a much lower slope of 0.25 (Whiticar et al., 1986). Most of the samples in Fig. 9B plot close to the range predicted for CO_2 reduction suggesting that it is the predominant biogenic methane formation pathway according to Figs. 9A and 9B. Hence, it is important to measure not only the carbon isotope ratios of methane and CO_2 , but also the hydrogen isotope ratios for methane and water to identify the predominant methanogenic pathways in the groundwater environment.

Bacterially mediated methane oxidation processes, mixing with gases from other biogeochemical pathways, or with gases of thermogenic origin could influence the apparent carbon isotope fractionation factors α_c (Whiticar et al., 1986). Microbial oxidation of methane will also affect the $\delta^{13}\text{C}$ values of the remaining methane (Barker and Fritz, 1981a,b), with the measurability of this effect being dependent on the mass balance of the residual CH_4 and the formed CO_2 . These reactions, together with other isotope fractionating processes such as diffusion must be taken into account while using stable isotope data for identification of depths of stray gas leakage (e.g., Schloemer and Krooss, 2004; Prinzhofer and Perneton 1997).

The average $\delta^{13}\text{C}$ values of ethane in free gas samples from QA/QC wells was $-51.9 \pm 7.8\%$ ($n = 16$) with values ranging from -65.9 to -36.1% . Only one sample had an ethane $\delta^{13}\text{C}$ value of $> -40\%$ while no other indicators for this sample (e.g. $\delta^{13}\text{C}_{\text{CH}_4}$ of -77.7% , $\delta^2\text{H}_{\text{CH}_4}$ of -296% , dryness parameter of 1476) hinted towards a thermogenic gas origin. Some studies have revealed that ethane can be produced through microbially mediated pathways (Taylor et al., 2000; Hinrichs et al., 2006). Others have suggested that ethane and propane with rather negative $\delta^{13}\text{C}$ values may be formed during thermogenic gas generation at low temperatures (Rowe and Muehlenbachs, 1999).

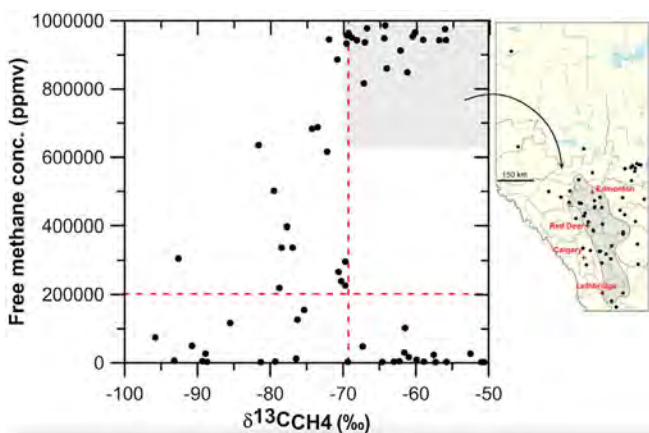


Fig. 6. Concentrations versus carbon isotope ratios of methane in free gas samples from QA/QC wells (median values are represented by red dotted lines). (For interpretation of the references to color in this figure legend, the reader is referred to the web version of this article.)

Table 4

Variabilities of methane concentrations and carbon isotope ratios for dissolved gas and free gas samples obtained from the same well in different years.

Wells	Time	Dissol. methane conc.			Free methane conc. & carbon isotope ratios				
		Avg (µg/L)	SD (µg/L)	CV (%)	Avg (ppmv)	SD (ppmv)	CV (%)	Avg (‰)	SD (‰)
Clu-yr	2006; 2011	9508	667	7	336,973	12,894	4	-77	0.0
Barr-yr	2008; 2013	27,800	8626	31	912,599	91,536	10	-62	0.2
Mana-yr	2008; 2012	494	554	112	23,034	235,532	102	-57	0.9
Min-yr	2006; 2013	573	382	67	189,391	75,691	40	-79	1.3
Red-yr	2007; 2013	27,483	23	0	933,176	46,064	5	-69	1.8
Bot-yr	2006; 2011	19,750	8273	41	683,099	18,820	3	-74	0.6
Wet-yr	2007; 2011	72	6	9	3194	251	8	-63	0.3
Cres-yr	2007; 2011	39,650	10,111	25	952,500	64,346	7	-67	0.1
Flag-yr	2008; 2012	83	5	6	4343	2243	52	-62	2.7
For-yr	2008; 2012	113	86	76	49,780	9106	18	-91	0.2
ForC-yr	2009; 2013	36,350	1909	5	816,362	3706	0	-67	9.3
Gul-yr	2006; 2011	12,400	989	8	936,465	5460	6	-67	0.1
Har-yr	2007; 2011	2135	304	14	154,716	27,033	17		
Inni-yr	2007; 2011	58	8	14	2553	1037	41	-69	1.2
Met-yr	2007; 2011	38,550	6576	17	945,267	144,554	15	-72	0.5
Mil-yr	2009;2013:2014	573	382	67	16,781	970	6	-61	14
Oko-yr	2007; 2011	3810	438	11					
Rol-yr	2007; 2011	26,400	1272	5	986,142	8140	1	-64	1.0
Taw-yr	2008; 2012	1522	1000	66	126,141	13,144	10	-76	0.4
War310-yr	2008; 2013	63,200	424	1					
War311-yr	2008; 2013				943,139	8938	1	-56	6.4
War316-yr	2006; 2011	32,950	12,657	38	848,941	24,707	3	-61	0.2
War-yr	2006; 2012	41,250	9687	23	965,935	4634	0		
War125-yr	2006; 2012	12,000	1697	14	397,471	8486	2		
Wol-yr	2008; 2012	424	535	126	4543	3493	77	-89	2.0
Kir-yr	2007; 2012	36,550	1343	4	950,628	20,363	2	-69	0.0
Pri-yr	2007; 2008	3765	898	13	265,954	80,091	30	-71	1.1

A third potential pathway explaining the occurrence of low concentrations of ethane and traces of propane in shallow groundwater could be secondary biogenic gas generation associated with the biodegradation of crude oils in parts of the Western Canadian Sedimentary Basin (WCSB) e.g. Osadetz et al. (1994); Larter et al. (2003). While we are currently not able to assess which of the above processes best explains the occurrence of low concentrations of ethane in most samples and traces of propane in some samples, the carbon isotope fingerprints of ethane and the dryness parameters are not consistent with leakage of mature

thermogenic gases from deep unconventional reservoirs (Tilley and Muehlenbachs, 2013), where $\delta^{13}\text{C}$ of ethane is typically $> -40\%$.

4.7. Influence of well depth and bedrock on methane occurrences

Finally, we investigated to which extent well depth and aquifer lithology influence the occurrence of methane in Alberta groundwater. The correlation analysis (Table 3) shows that there is a moderate positive correlation between methane concentrations in free gas (Pearson's $R = 0.46$, Kendall's tau = 0.22, Spearman's rho = 0.32 with $p < 0.05$) and dissolved gas samples (Pearson's $R = 0.42$, Kendall's tau = 0.22, Spearman's rho = 0.32 with $p < 0.05$) with water well depth, suggesting a moderate trend of increasing methane concentrations with increasing well depth. An inverse moderate correlation was observed between nitrogen concentration for both free and dissolved gas samples and well depth (Pearson $R = -0.47$, Kendall's tau = -0.26 , Spearman's rho = -0.38 with $p < 0.05$ for nitrogen in free gas samples and Pearson $R = -0.26$, Kendall's tau = -0.22 , Spearman's rho = -0.31 with $p < 0.05$ for nitrogen in dissolved gas samples, Table 3). The statistical results for nitrogen concentrations described in Sections 4.2 and 4.3 indicate various potential explanations for this observation including excess air, gas-water partitioning, some fractionation during gas extraction for dissolved gas analysis, and due to the correlation with depth, a source of excess N_2 possibly linked to nitrate reduction (e.g. denitrification). Underestimation of air contamination may also explain some of the elevated nitrogen concentrations. No significant correlations were found between well depth and $\delta^{13}\text{C}$ values of methane in free gas.

The impact of aquifer lithology on methane concentrations in shallow groundwater is illustrated in Fig. 10. The boxplots show that higher methane concentrations in both free (Fig. 10A) and dissolved gas samples (Fig. 10B) occurred in formations containing coal and clastic fine-grained rocks (e.g. shale), while aquifers composed of siliciclastic coarse-grained rocks (e.g. sandstones, sands) and gravel contained little methane. In contrast, $\delta^{13}\text{C}$ values of methane display no correlation with lithology (Fig. 10C), whereas $\delta^{13}\text{C}_{\text{C}_2\text{H}_6}$ values are slightly lower in groundwater from aquifers composed of coarser rocks (Fig. 10D). No

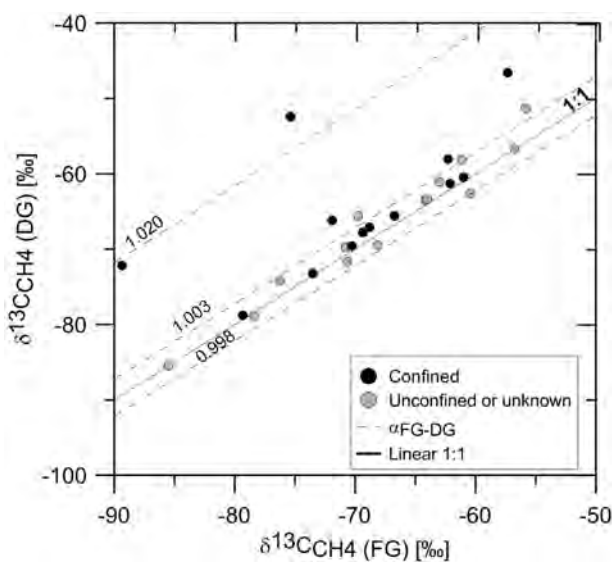


Fig. 7. Cross plot between C isotope ratios of methane in free and dissolved gas. Dotted lines indicate differences of $\delta^{13}\text{C}$ values of -2 , $+3$ and $+20\%$ using the isotope fractionation factor $\alpha_{\text{FG-DG}} = 0.998$, 1.003 and 1.020 fitting the isotopic data set defined by

$$\alpha_{\text{FG-DG}} = \frac{\delta^{13}\text{C}_{\text{CH}_4\text{DG}} + 1000}{\delta^{13}\text{C}_{\text{CH}_4\text{FG}} + 1000}$$

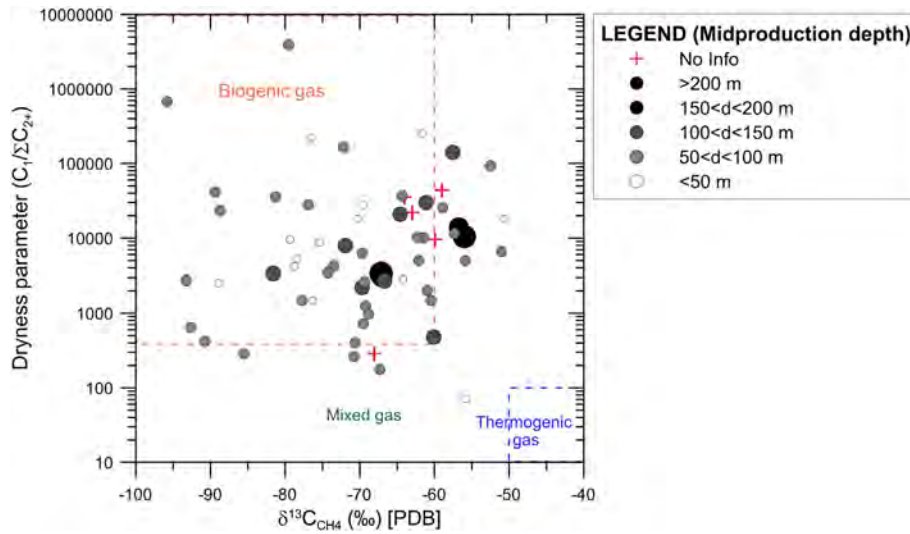


Fig. 8. Dryness parameter versus $\delta^{13}\text{C}$ of methane in free gas obtained from QA/QC wells and boundaries for gases of thermogenic and biogenic origin based on data from Whiticar (1999).

significant lithology-dependent differences were found in either methane ($p = 0.857$) or ethane ($p = 0.115$) carbon isotope ratios by statistical tests.

Groundwater wells were completed in seven geological formations: Paskapoo, Horseshoe Canyon (HSC), Belly River, Porcupine, Milk River, Muriel Lake, Judith River formations. Markedly elevated methane concentrations in both free and dissolved gas samples were observed in the Horseshoe Canyon (HSC) formation. A Mann–Whitney test revealed a significant difference in methane concentrations only between HSC and surficial formations with higher concentrations in groundwater from the HSC ($p < 0.005$). The majority of samples with the highest methane concentrations in free gas and $\delta^{13}\text{C}$ values between -70.8 and -56.0% were obtained from wells completed in aquifers of the Horseshoe Canyon and the Paskapoo formations (Fig. 6). It is likely that coal-bearing units impact the geochemical and isotopic composition of gas present in shallow aquifers because coal constitutes the major reservoir of organic matter potentially available for methanogenic microbial communities in the subsurface.

5. Summary and implications

The gas geochemical dataset of this study illustrates that methane is ubiquitous in the groundwater of the province of Alberta based on the monitoring of 186 GOWN wells. Comparison of methane concentrations for free gas and dissolved gas samples obtained from the same wells yielded comparable results (Pearson $R = 0.93$, Kendall's tau = 0.79, Spearman's rho = 0.93 with $p < 0.05$). Twenty-eight samples from 21 wells had dissolved methane concentrations higher than 10 mg/L associated with a free methane concentration higher than 300,000 ppmv. These samples were obtained from wells located in the ECC and elevated methane concentrations were typically correlated with increasing well depth and with aquifer bedrock units containing coals and shale. Assessment of temporal variabilities of methane concentrations in free and dissolved gas samples taken from the same wells several years apart revealed that in 40% of the cases the temporal variability of methane concentrations was higher than the calculated sampling and analytical uncertainties, in some cases by a factor of 6. Further investigations with higher temporal sampling resolution are required to distinguish extrinsic (e.g. pumping operation) from anthropogenic or natural causes of methane concentration variations in aquifers potentially

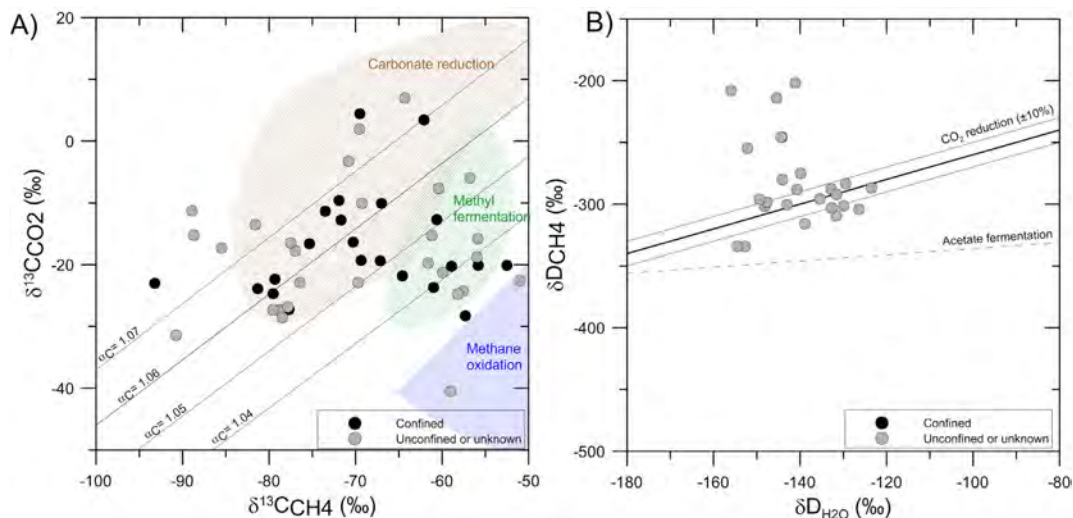


Fig. 9. Cross plots of A) $\delta^{13}\text{C}$ values of methane and carbon dioxide for confined, unconfined and unknown aquifer types; B) $\delta^2\text{H}$ values of methane and formation water. The trends of methanogenesis via CO_2 reduction and acetate fermentation are displayed based on information provided by Whiticar et al. (1986) and Whiticar (1999).

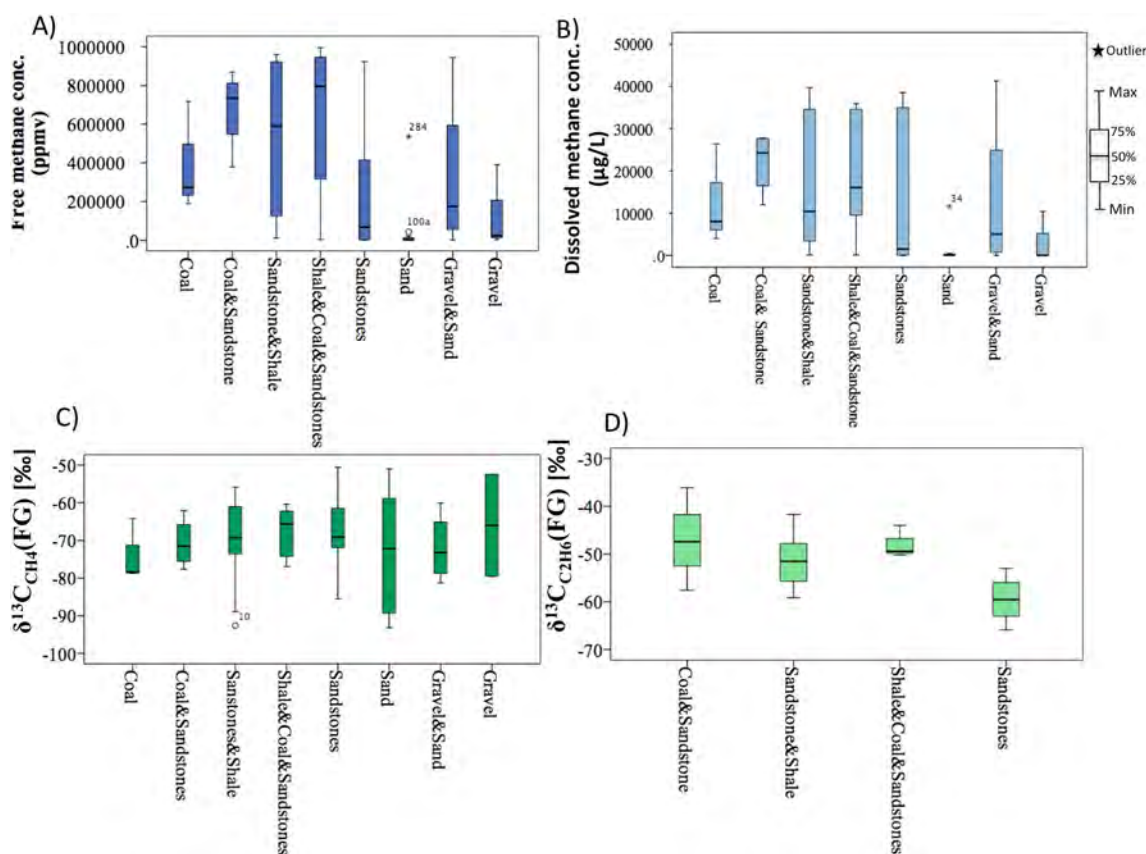


Fig. 10. Impact of lithology on A) methane concentrations in free gas, and B) dissolved methane concentrations, C) $\delta^{13}\text{C}$ values of methane, and D) $\delta^{13}\text{C}$ values of ethane in free gas samples from 66 QA/QC wells.

caused by varying groundwater flows, residence times, seasonal water table fluctuations, recharge, and mixing, among others.

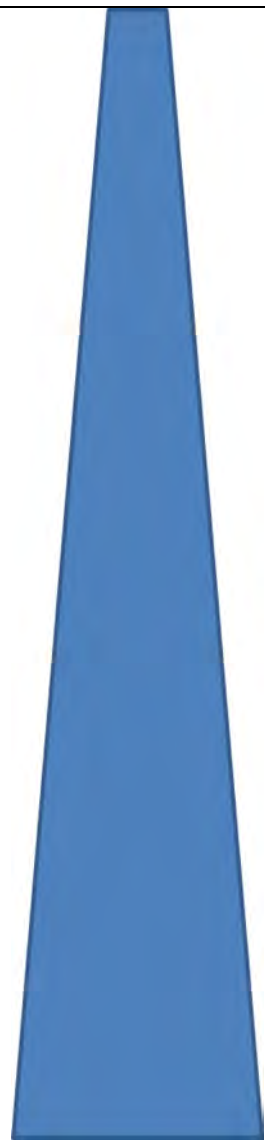
In addition to the gas concentration measurements, a multi-isotope approach analyzing $\delta^{13}\text{C}_{\text{CH}_4}$, $\delta^2\text{H}_{\text{CH}_4}$, $\delta^{13}\text{C}_{\text{C}_2\text{H}_6}$, $\delta^{13}\text{C}_{\text{CO}_2}$, and $\delta^2\text{H}_{\text{H}_2\text{O}}$ values was used to identify methane sources and formation processes. Chemical and isotopic data revealed that methane in shallow groundwater is mainly biogenic (dryness parameter >500 , $\delta^{13}\text{C}_{\text{CH}_4} < -55\%$, $\delta^2\text{H}_{\text{CH}_4} < -175\%$) and is predominantly generated via CO_2 -reduction. A marked contrast of isotope signatures of predominantly biogenic methane in baseline groundwater samples and potential thermogenic stray gas leakage from hydraulic fracturing operations in deep shale formations is therefore highly likely where such leakage occurs. Only minor temporal variation of carbon isotope ratios of methane in baseline groundwater samples was observed indicating that methane in Alberta groundwater was derived from a similar source. The mean $\delta^{13}\text{C}_{\text{CH}_4}$ and $\delta^{13}\text{C}_{\text{C}_2\text{H}_6}$ values of $-69.7 \pm 11.3\%$ and $-51.9 \pm 7.7\%$ respectively in free gas samples of shallow groundwater from wells that are on average <100 m bgs deep are consistent with the upper portion of an isotopic mud gas profile obtained for methane and ethane in east-central Alberta by Tilley and Muelhenbachs (2011). This agreement suggests that methane and ethane in shallow groundwater accessed via GOWN wells are isotopically similar to hydrocarbon gases found in 100 to 250 meter depths in the Western Canadian Sedimentary Basin and are not sourced from deeper thermogenic hydrocarbon occurrences deep in the basin. This comparison is based on a very limited mud gas data set due to lack of published mud gas data for Alberta. It indicates that the future compilation of mud gas depth profiles for chemical and isotopic compositions is of critical importance for estimating depths of potential stray gas leakage.

Based on the geochemical and isotopic datasets for free and dissolved gas from this study conducted in Alberta (Canada) we evaluated the added values and relative complexity of two different sampling

approaches for baseline groundwater monitoring programs (Table 5). Obtaining dissolved gas samples is technically easy in the field with combined sampling and analytical uncertainties of $<20\%$ for methane concentration analyses readily achievable. Using this approach, we found dissolved methane concentrations in shallow groundwater in a similar range as was observed in other regions of North America (e.g. Li and Carlson, 2014; Moritz et al., 2015). Adequate containers and chemical preservatives must be used to prevent or minimize any gas loss or post-sampling alterations (Eby et al., 2015). Obtaining free gas samples is technically more demanding and the design of the free gas samplers as well as sampling conditions such as pumping rates may impact results (e.g. Humez et al., 2015). Combined sampling and analytical uncertainties for methane concentration analyses are $<13\%$ and hence similar or slightly better than those of dissolved gas analyses. The Province of Alberta through the Alberta Energy Regulator (AER) Directive 035 introduced in May 2006 a requirement to test baseline well water including the collection of free gas samples when it is possible. Our results show that free gas and dissolved gas sampling approaches yielded comparable methane concentration results for shallow groundwater. However, to our best knowledge no other jurisdiction recommends the free gas sampling approach for baseline groundwater sampling and hence the inter-comparison of results with data from other studies is difficult. Methane concentrations in both free and dissolved gas samples are susceptible to alterations by different factors during the various steps from sampling to analysis, e.g. by air contamination, methane oxidation, or water level fluctuations during pumping causing degassing (Humez et al., 2015). These factors can either result in under- or over-estimation of methane concentrations and therefore should be carefully considered and evaluated.

The carbon isotope ratios of methane displayed excellent reproducibility for free gas samples and rather consistent results between free and dissolved gas samples from the same well. Obtaining reliable

Table 5
Analysis of the sampling approaches and monitoring approaches used in this study for both free and dissolved gas components. The width of the blue bar indicates the complexity and costs of the respective approaches.

Approach	Information obtained/added value	Complexity/costs
Dissolved methane concentration analysis	Baseline/contamination level of methane, comparison to legal thresholds	
Dissolved + free methane concentration analysis	Check of inconsistencies related to degassing, oxidation, leakage etc. (upon sampling, transport, analysis)	
Dissolved/free gas analysis for methane, other alkanes, CO ₂ , other gases	Correction of air contamination, detection of oxidative processes, dryness parameter → indicator of origin and transport pathways (e.g. diffusive vs. advective transport)	
C-isotope analyses of dissolved/free methane	Indicator of CH ₄ -source (biogenic vs. thermogenic), mixing of different sources (including stray gas)	
C-isotope analyses of dissolved/free CO ₂ , alkanes	Detection of sources/formation mechanisms and secondary processes, e.g. oxidation (e.g. Chung et al., 1988)	
C and H-isotope analyses of CH ₄ and H ₂ O	Further discrimination of reactive mechanisms within the main gas types : identification of biogeochemical processes, e.g. CO ₂ reduction, acetate fermentation...	
Statistical data analysis (chemical and isotopic larger data sets)	<ul style="list-style-type: none"> - Geostatistical analysis (not applied in our study): spatial variability of baseline, identification of anomalies, contamination pathways... - Triplicate sampling: assessment of realistic combined sampling analytical uncertainties - Periodic sampling on same well: assessment of baseline variations/contamination events - Continuous sampling for varying operating conditions: assessment of the impact of sampling conditions, e.g. pumping rates - Descriptive statistics: significance of differences between data subsets (e.g. lithological, depth-dependences), significance of multi-parameter correlations 	

carbon isotope ratios of methane in dissolved gas may be more challenging for samples with very low methane concentrations. Methane oxidation could occur in the sampling containers in cases of inadequate preservation resulting in an increase in the $\delta^{13}\text{C}$ values of the remaining methane. In contrast, free gas samples contain larger quantities of gas and methane in suitable water-free containers minimizing the risk of methane oxidation and facilitating not only accurate measurement of $\delta^{13}\text{C}$ values of methane, but also of $\delta^2\text{H}$ values of methane and $\delta^{13}\text{C}$ values of ethane and higher alkanes when present. The identification of gas origin and formation pathway is further improved by hydrogen isotope ratio data for methane and carbon isotope ratios of higher alkanes. The appropriate choice of sampling containers, avoidance of gas losses during transport, and strict adherence to storage times is important for high quality isotope analyses on dissolved and free gas samples (Eby et al., 2015). To achieve comparable and reproducible isotope compositions for methane and higher alkanes, our analysis suggests that free gas sampling is preferable.

An analysis of the utilized sampling approaches and monitoring tools in this study is shown in Table 5 outlining the hierarchic steps

for baseline shallow groundwater assessment from concentration measurements, isotope analyses, to statistical analysis of the compiled data, supplemented by remarks on their added values and a complexity evaluation. This study demonstrated that the obtained dissolved methane concentration data for shallow groundwater are comparable to those of other studies. Across North America, dissolved gas sampling has been the preferred approach, which allows comparison of results between different studies and with legal thresholds where they exist. However, gas concentration analyses alone are insufficient to assess the potential impact of stray gases on shallow groundwater impacting baseline conditions. Analysis of the stable isotope composition of methane in shallow groundwater, from mud gas profiles, and from production formations of unconventional gas reservoirs are excellent complementary fingerprinting tools that are capable and usually highly sensitive to indicate stray gas influence on shallow aquifers if sufficient baseline data exist. To achieve comparable and reproducible isotope composition data for methane and higher alkanes, our analysis suggests that free gas sampling is preferable. A multi-isotope approach determining C isotope ratios of methane, ethane, and CO₂ and $\delta^2\text{H}$ values of

methane and water can yield unique insights into methane sources, formation pathways of methane, and secondary transformation processes affecting the concentration and isotopic fingerprint of methane. This is most effectively achieved if both dissolved and free gas samples are obtained. If only dissolved gas sampling is conducted carefully, it can also yield reliable isotope ratio data for methane. Careful data assessment and evaluation using field blanks, triplicate sampling, and blind sample ring tests are also recommended to ensure the utmost integrity and accuracy of the obtained data sets. Finally, adequate statistical analyses of the compiled data sets (Table 5) are a highly valuable part of the data analysis that should be included in any groundwater baseline assessment.

Acknowledgments

Financial support for this project was provided by the Natural Sciences and Engineering Research Council of Canada (NSERC), Alberta Innovates Energy & Environment Solutions (AI-EES), Alberta Environment, and the University of Calgary's Eyes High postdoctoral fellow program. We thank Steve Wallace and Guy Bayegnak (formerly with Alberta Environment) for their continued support and encouragement since 2006. We also thank Dr. Wolfram Kloppmann for his constructive review that resulted in a significant improvement of this manuscript. The final year of sampling and part of the data evaluation were supported by a NSERC strategic project grant (SPG) and by the French Agence Nationale de la Recherche (ANR) in support of the bilateral project entitled environmental baseline conditions for impact assessment of unconventional gas exploitation: advancing geochemical tracer and monitoring techniques. We also thank three anonymous reviewers for their constructive comments and suggestions, which greatly improved this manuscript.

References

- ACOLA (Australian Council of Learned Academies), 2013. *Engineering Energy: Unconventional Gas Production*. Melbourne. ACOLA, Australia.
- Aharon, P., Graber, E.R., Roberts, H.H., 1992. Dissolved carbon and delta-C-13 anomalies in the water column caused by hydrocarbon seeps on the northwestern Gulf of Mexico slope. *Geo-Marine Letters* 12, 33–40.
- Aravena, R., Wassenaar, L.I., Barkera, J.F., 1995. Distribution and isotopic characterization of methane in a confined aquifer in southern Ontario, Canada [J]. *J. Hydrol.* 173, 51–70.
- Baldassare, F.J., McCaffrey, M.A., Harper, J.A., 2014. A geochemical context for stray gas investigations in the northern Appalachian Basin: implications of analyses of natural gases from Neogene-through Devonian-age strata. *AAPG Bull.* 98 (2), 341–372.
- Barker, J.F., Fritz, P., 1981a. The occurrence and origin of methane in some groundwater-flow systems. *Can. J. Earth Sci.* 18 (12), 1802–1816.
- Barker, J.F., Fritz, P., 1981b. Carbon isotope fractionation during microbial methane oxidation. *Nature* (293), 289–291.
- Bernard, B.B., Brook, J.M., Sackett, W.M., 1976. Natural gas seepage in the Gulf of Mexico. *Earth Planet. Sci. Lett.* 31, 48–54.
- Brantley, S.L., Yoxtheimer, D., Arjmand, S., Grieve, P., Vidic, R., Pollak, J., Llewellyn, G.T., Abad, J., Simon, C., 2014. Water resource impacts during unconventional shale gas development: The Pennsylvania experience. *Int. J. Coal Geol.* 126, 140–156.
- CCA (Council of Canadian Academies), 2014. *Environmental impacts of shale gas extraction in Canada*. The Expert Panel on Harnessing Science and Technology to Understand the Environmental Impacts of Shale Gas Extraction, CCA, Ottawa (ON).
- Cheung, K., Klassen, P., Mayer, B., Goodarzi, F., Aravena, R., 2010. Major ion and isotope geochemistry of fluids and gases from coalbed methane and shallow groundwater wells in Alberta, Canada. *Appl. Geochem.* 25, 1307–1329.
- Darrah, T., Vengosh, A., Jackson, R.B., Warner, N., 2012. Constraining the source and migration of natural gas in shallow aquifers within active shale gas production zone: insights from integrating noble gas and hydrocarbon isotope geochemistry. Paper Presented at the Geological Society of America Annual Meeting, 2012, Charlotte (NC).
- Darrah, T.H., Vengosh, A., Jackson, R.B., Warner, N.R., Poreda, R.J., 2014. Noble gases identify the mechanism of fugitive gas contamination in drinking-water wells overlying the Marcellus and Barnett Shales. *Proc. Natl. Acad. Sci.* 111 (39), 14076–14081. <http://dx.doi.org/10.1073/pnas.1322107111>.
- Darrah, T.H., Jackson, R.B., Vengosh, A., Warner, N.R., Whyte, C.J., Walsh, T.B., Kondash, A.J., Poreda, R.J., 2015. The evolution of Devonian hydrocarbon gases in shallow aquifers of the northern Appalachian Basin: insights from integrating noble gas and hydrocarbon geochemistry. *Geochim. Cosmochim. Acta* 170 (1).
- Dawson, F., Kalkreuth, W., Sweet, A.R., 1994a. Stratigraphy and coal resource potential of the Upper Cretaceous to Tertiary strata of northwestern Alberta. *Geological Survey of Canada, Bulletin.* 466 (60 pp.).
- Dawson, F.M., Evans, C.G., Marsh, R. and Richardson, R. (1994b): Uppermost Cretaceous and Tertiary strata of the Western Canada sedimentary basin; in *Geological Atlas of the Western Canada Sedimentary Basin*, G. Mossop and I. Shetsen (comp.), Canadian Society of Petroleum Geologists and Alberta Research Council, Special Report 4, p. 387–406, (URL <http://www.ags.gov.ab.ca/publications/wcsb_atlas/atlas.html> [April 2011]).
- Eby, P., Gibson, J.J., Yi, Y., 2015. Suitability of selected free-gas and dissolved-gas sampling containers for carbon isotopic analysis. *Rapid Commun. Mass Spectrom.* 29 (13), 1215–1226.
- Eltischlager, K.K., Hawkins, J.W., Ehler, W.C., Baldassare, F., 2001. *Technical Measures for the Investigation and Mitigation of Fugitive Methane Hazards in Areas of Coal Mining 2001*. Department of Interior Office of Surface Mining (124 pp.).
- Gorody, A., 2012. Factors affecting the variability of stray gas concentration and composition in groundwater. *Environ. Geosci.* 19, 17–31.
- Grasby, S.E., Zhuoheng, C., Hamblin, A.P., Wozniak, P.R.J., Sweet, A.R., 2008. Regional characterization of the Paskapoo bedrock aquifer system, southern Alberta. *Can. J. Earth Sci.* 45 (12), 1501–1516.
- Hamblin, A.P., 1998. Detailed outcrop measured section of the St. Mary River Formation, Oldman River, west of Monarch, southern Alberta. *Geological Survey of Canada, Open File* 3613 (12 pp.).
- Hamblin, A.P., 2004. The Horseshoe Canyon Formation in southern Alberta: surface and subsurface stratigraphic architecture, sedimentology, and resource potential. *Geological Survey of Canada, Bulletin.* 578 (180 pp.).
- Hinrichs, K.-U., Hayes, J.M., Bach, W., Spivack, A.J., Hmelo, L.R., Holm, N.G., Johnson, C.G., Sylva, S.P., 2006. Biological formation of ethane and propane in the deep marine subsurface. *Proc. Natl. Acad. Sci. U. S. A.* 103, 14684–14689.
- Humez, P., Mayer, B., Nightingale, M., Ing, J., Becker, V., Jones, D., Lam, V., 2015. An 8-year record of gas geochemistry and isotopic composition of methane during baseline sampling at a groundwater observation well in Alberta (Canada). *Hydrogeology J.* <http://dx.doi.org/10.1007/s10040-015-1319-1>.
- Jackson, R.E., Gorody, A.W., Mayer, B., Roy, J.W., Ryan, M.C., Van Stempvoort, D.R., 2013a. Groundwater protection and unconventional gas extraction: the critical need for field-based hydrogeological research. *Groundwater* 51 (4), 488–510. <http://dx.doi.org/10.1111/gwat.12074>.
- Jackson, R.B., Vengosh, A., Darrah, T.H., Warner, N.R., Down, A., Poreda, R.J., Osborn, S.G., Zhao, K., Karr, J.D., 2013b. Increased stray gas abundance in a subset of drinking water wells near Marcellus shale gas extraction. *Proc. Natl. Acad. Sci.* 110 (28), 11250–11255. <http://dx.doi.org/10.1073/pnas.1221635110>.
- Jones, D., Gordon, S., Mayer, B., Hiltz, M., Blyth, A., 2009. *The Free Gas Sampling Standard Operating Procedure for Baseline Water Well Testing*. Alberta Research Council Inc. (13 pp.).
- Kessler, J.D., Reeburgh, W.S., Tyler, S.C., 2006. Controls on methane concentration and stable isotope (δ -H-2-CH₄ and δ -C-13-CH₄) distributions in the water columns of the Black Sea and Cariaco Basin. *Global Biogeochem. Cycles* 20 (4).
- Kresse, T.M., Warner, N.R., Hays, P.D., Down, A., Vengosh, A., Jackson, R.B., 2012. Shallow groundwater quality and geochemistry in the Fayetteville shale gas-production area, north-central Arkansas, 2011. *U.S. Geological Survey Scientific Investigations Report* 2012, pp. 2012–5273.
- Larter, S., Wilhelm, A., Head, I., Koopmans, M., Aplin, A., Di Primio, R., Zwach, C., Erdmann, M., Telnæs, N., 2003. The controls on the composition of biodegraded oils in the deep subsurface—part 1: biodegradation rates in petroleum reservoirs. *Org. Geochem.* 34 (4), 601–613.
- Li, H., Carlson, K.H., 2014. Distribution and origin of groundwater methane in the Wattenberg oil and gas field of Northern Colorado. *Environ. Sci. Technol.* 48 (3), 1484–1491. <http://dx.doi.org/10.1021/es404668b>.
- Lyster, S., Andriashek, L., 2012. Geostatistical rendering of the architecture of hydrostratigraphic units within the Paskapoo Formation, Alberta. *Energy Research Conservation Board, ERCB/AGS Bulletin.* 66.
- Mason, C.F., Muehlenbachs, L.A., Olmstead, S.M., 2014. The economics of shale gas development. *Ann. Rev. Resour. Econ.* 7. <http://dx.doi.org/10.1146/annurev-resource-100814-125023> (Submitted).
- McIntosh, J.C., Grasby, S.E., Hamilton, S.M., Osborne, S.G., 2014. Origin, distribution and hydrogeochemical controls on methane occurrences in shallow aquifers, southwestern Ontario. *Canada. Appl. Geochem.* 50, 37–52.
- McPhillips, L.E., Creamer, A.E., Rahm, B.G., Walter, M.T., 2014. Assessing dissolved methane patterns in central New York groundwater. *J. Hydrol. Reg. Stud.* 1 (0), 57–73. <http://dx.doi.org/10.1016/j.ejrh.2014.06.002>.
- Meyboom, P., 1960. *Geology and Groundwater Resources of the Milk River Sandstone in Southern Alberta*. Alberta Research Council, Edmonton, Alberta.
- Molofsky, L.J., Connor, J.A., Wylie, A.S., Wagner, T., Farhat, S.K., 2013. Evaluation of methane sources in groundwater in northeastern Pennsylvania. *Groundwater* 51 (3), 333–349. <http://dx.doi.org/10.1111/gwat.12056>.
- Mook, W.G., 2000. *Environmental Isotopes in the Hydrological Cycle: Principles and Applications*. International Atomic Energy Agency, Vienna.
- Moritz, A., Hélie, J.-F., Pinti, D.L., Larocque, M., Barnette, D., Retailleau, S., Lefebvre, R., Gélinas, Y., 2015. Methane baseline concentrations and sources in shallow aquifers from the shale gas-prone region of the St. Lawrence Lowlands (Quebec, Canada). *Environ. Sci. Technol.* 49 (7), 4765–4771.
- Osadetz, K.G., Snowdon, L.R., Brooks, P.W., 1994. Oil families in the Canadian Williston Basin (SW Saskatchewan). *Bull. Cdn. Pet. Geol.* 42, 155–177.
- Osborn, S.G., Vengosh, A., Warner, N.R., Jackson, R.B., 2011a. Methane contamination of drinking water accompanying gas-well drilling and hydraulic fracturing. *Proc. Natl. Acad. Sci.* 108, 8172–8176. <http://dx.doi.org/10.1073/pnas.1100682108>.
- Osborn, S.G., Vengosh, A., Warner, N.R., Jackson, R.B., 2011b. Reply to Saba and Orzechowski and Schon: Methane contamination of drinking water accompanying gas-well drilling and hydraulic fracturing. *Proc. Natl. Acad. Sci.* 108 (37), E665–E666. <http://dx.doi.org/10.1073/pnas.1109270108>.

- Pape, T., Bahr, A., Rethemeyer, J., Kessler, J.D., Sahling, H., Hinrichs, K.U., Klapp, S.A., Reeburgh, W.S., Bohrmann, G., 2010. Molecular and isotopic partitioning of low-molecular-weight hydrocarbons during migration and gas hydrate precipitation in deposits of a high-flux seepage site. *Chem. Geol.* 269 (3–4), 350–363.
- Parkhurst, D.L., Appelo, C.A.J., 1999. User's guide to PHREEQC (version 2) - a computer program for speciation, reaction-path, 1D-transport, and inverse geochemical calculations. *US Geol. Surv. Water Resour. Inv. Rep.* 99–4259, 312.
- Prinzhofer, A., Pematón, É., 1997. Isotopically light methane in natural gas: bacterial imprint or diffusive fractionation? *Chem. Geol.* 142, 193–200.
- Prior, G.J., Hathaway, B., Glombick, P.M., Pana, D.L., Banks, C.J., Hay, D.C., Schneider, C.L., Grobe, M., Elgr, R., Weiss, J.A., 2013. *Bedrock Geology of Alberta*. Alberta Geological Survey, Map 600 (Retrieved 2013-0813).
- Reimann, C., Filzmoser, P., 2000. Normal and lognormal data distribution in geochemistry: death of a myth. Consequences for the statistical treatment of geochemical and environmental data. *Environ. Geol.* 39 (9), 1001–1014.
- Riddell, J.T.F., Moktan, H., Jean, G., 2014. Regional hydrology of the Edmonton–Calgary Corridor. Alberta Energy Regulator, AER/AGS Open File Report 2014-02 (URL <http://www.ags.gov.ab.ca/publications/abstracts/OFR_2014_02.html> [September 2012]).
- Rosenthal, L., Leckie, D.A., Nadon, G.C., 1984. Depositional cycles and facies relationships within the Upper Cretaceous Wapiabi and Belly River formations of west central Alberta. Summer Field Trip Guidebook. Canadian Society of Petroleum Geologists (54 pp.).
- Rowe, D., Muehlenbachs, A., 1999. Low-temperature thermal generation of hydrocarbon gases in shallow shales. *Nature* 398 (6722), 61–63.
- Schloemer, S., Krooss, B.M., 2004. Molecular transport of methane, ethane and nitrogen and the influence of diffusion on the chemical and isotopic composition of natural gas accumulations. *Geofluids* 4, 81–108.
- Schoell, M., 1980. The hydrogen and carbon isotopic composition of methane from natural gases of various origins. *Geochim. Cosmochim. Acta* 44, 649–661.
- Siegel, D.I., Azzolina, N.A., Smith, B.J., Perry, A.E., Bothun, R.L., 2015. Methane concentrations in water wells unrelated to proximity to existing oil and gas wells in Northeastern Pennsylvania. *Environ. Sci. Technol.* 49 (7), 4106–4112.
- Taylor, S.W., Sherwood Lollar, B., Wassenaar, L.I., 2000. Bacteriogenic ethane in near-surface aquifers: implications for leaking hydrocarbon well bores. *Environ. Sci. Technol.* 34 (22), 4727–4732.
- The Royal Society and Royal Academy of Engineering, 2012. *Shale Gas Extraction in the U.K.: A Review of Hydraulic Fracturing*. London, United Kingdom. The Royal Society and The Royal Academy of Engineering.
- Tilley, B., Muehlenbachs, K., 2013. Isotope reversals and universal stages and trends of gas maturation in sealed, self-contained petroleum systems. *Chem. Geol.* 339, 194–204. <http://dx.doi.org/10.1016/j.chemgeo.2012.08.002>.
- Tilley, B., Muehlenbachs, K., 2011. Fingerprinting of gas contaminating groundwater and soil in a pretoliferous region, Alberta, Canada. Presented at Proceedings from International Network of Environmental Forensics Conference, 2011, Cambridge (UK).
- US Energy Information Administration, 2014. *Annual Energy Outlook 2014, With Projections to 2040*. EIA. Rep. US Energy Information Administration, Washington, DC <http://www.eia.gov/forecasts/aeo>.
- Van Stempvoort, D., Maathuis, H., Aworski, E., Mayer, B., Rich, K., 2005. Oxidation of fugitive methane in ground water linked to bacterial sulfate reduction. *Groundwater* 43 (2), 187–199. <http://dx.doi.org/10.1111/j.1745-6584.2005.0005.x>.
- Vengosh, A., Warner, N., Jackson, R., Darrah, T., 2013. The effects of shale gas exploration and hydraulic fracturing on the quality of water resources in the United States. *Procedia Earth Planetary Sci.* 7, 863–866. <http://dx.doi.org/10.1016/j.proeps.2013.03.213>.
- Vengosh, A., Jackson, R.B., Warner, N., Darrah, T.H., Kondash, A., 2014. A critical review of the risks to water resources from unconventional shale gas development and hydraulic fracturing in the United States. *Environ. Sci. Technol.* 48 (15), 8334–8348. <http://dx.doi.org/10.1021/es405118y>.
- Vidic, R.D., Brantley, S.L., Vandenbossche, J.M., Yoxheimer, D., Abad, J.D., 2013. Impact of shale gas development on regional water quality. *Science* 340 (6134). <http://dx.doi.org/10.1126/science.1235009>.
- Warner, N.R., Jackson, R.B., Darrah, T.H., Osborn, S.G., Down, A., Zhao, K., White, A., Vengosh, A., 2012. Geochemical evidence for possible natural migration of Marcellus Formation brine to shallow aquifers in Pennsylvania. *Proceedings of the National Academy of Sciences USA* 109 (30), 11961–11966.
- Warner, N.R., Christie, C.A., Jackson, R.B., Vengosh, A., 2013a. Impacts of Shale Gas Waste-water Disposal on Water Quality in Western Pennsylvania. *Environ. Sci. Technol.* 47, 11849–11857.
- Warner, N.R., Kresse, T.M., Hays, P.D., Down, A., Karr, J.D., Jackson, R.B., Vengosh, A., 2013b. Geochemical and isotopic variations in shallow groundwater in areas of the Fayetteville Shale development, north-central Arkansas. *Appl. Geochem.* 35, 207–220.
- Whiticar, M.J., 1999. Carbon and hydrogen isotope systematics of bacterial formation and oxidation of methane. *Chem. Geol.* 161, 291–314.
- Whiticar, M.J., Faber, E., Schoell, M., 1986. Biogenic methane formation in marine and freshwater environments: CO₂ reduction vs. acetate fermentation—isotope evidence. *Geochim. Cosmochim. Acta* 50 (5), 693–709.
- Zhang, C., Grossman, E.L., Ammerman, J.W., 1998. Factors influencing methane distribution in Texas ground water. *Ground Water* 36 (1), 58–66. <http://dx.doi.org/10.1111/j.1745-6584.1998.tb01065.x>.

1
2
3
4 **Isotopic Apportionment of Nitrate Sources in the Bow River, Alberta, Canada**
5
6
7

8
9
10
11 June Chao, Bernhard Mayer* and M. Cathryn Ryan
12
13
14
15
16
17

18
19 Department of Geoscience, University of Calgary, 2500 University Drive NW,
20
21 Calgary, Alberta, Canada T2N 1N4
22
23
24
25
26
27
28
29
30
31
32
33
34
35
36
37
38
39
40
41
42

43
44 *Corresponding author: tel: 403-220-5389; e-mail: bmayer@ucalgary.ca
45
46
47
48
49
50
51
52
53
54
55
56
57
58
59
60
61
62
63
64
65

1
2
3
4 **Abstract**
5

6 Elevated nitrate (NO₃) loadings to streams and rivers from urban wastewater and
7
8 agricultural return flows can cause eutrophication of surface waters as urbanization and
9
10 industrial and agricultural activities intensify in many watersheds worldwide. We have
11
12 integrated physical, chemical and isotopic approaches to identify and quantify sources of
13
14 riverine nitrate in the Bow River (southern Alberta, Canada), which flows 645 km from
15
16 rather pristine alpine-montane regions in the Rocky Mountains to grassland prairies,
17
18 passing through one major urban centre, the city of Calgary. Nitrate concentrations in a
19
20 year-long, monthly sampling program were low, <0.4 mg/L, at the headwater sampling
21
22 sites, but increased to up to 8 mg/L below Calgary. The $\delta^{15}\text{N}$ and $\delta^{18}\text{O}$ of riverine nitrate
23
24 changed from values consistent with dominantly forest soil-derived nitrate in the
25
26 headwaters ($\delta^{15}\text{N}_{\text{NO}_3} = 1.1 \pm 0.5 \text{‰}$, $\delta^{18}\text{O}_{\text{NO}_3} = 8.4 \pm 0.7 \text{‰}$) to values indicating urban
27
28 wastewater effluents below Calgary ($\delta^{15}\text{N}_{\text{NO}_3} > 7\text{‰}$; $\delta^{18}\text{O}_{\text{NO}_3} < 3\text{‰}$). The $\delta^{15}\text{N}$ and $\delta^{18}\text{O}$
29
30 values of riverine nitrate from eight sampling sites were consistent with a two end-
31
32 member mixing trend between nitrate derived from nitrification in forest soils and nitrate
33
34 from urban wastewater. Although nitrate concentrations were consistently low upstream
35
36 of Calgary's WWTPs (<0.4 mg/L), the isotopic composition at three sampling sites
37
38 indicated that up to 50% of the nitrate load was wastewater-derived presumably from
39
40 smaller villages and towns upstream of Calgary. Below Calgary the riverine nitrate load
41
42 increased significantly from 1.4 to 8.9 kt/year, an estimated 84-92% of which was
43
44 wastewater-derived. Combined mass load, NO₃/Cl ratio, and isotopic parameters showed
45
46 no significant nitrate contributions from dominantly agricultural activities downstream of
47
48 Calgary nor significant nitrate removal via denitrification. This study demonstrates that
49
50
51
52
53
54
55
56
57
58
59
60
61
62
63
64
65

1
2
3
4 riverine nitrate derived from sources with distinct isotopic compositions can be
5
6 effectively differentiated, traced and apportioned using a combination of physical,
7
8 chemical and isotopic approaches.
9

10
11
12
13
14 Keywords: nitrate, stable isotopes, wastewater effluents, nitrification, Bow River, Alberta,
15
16 Canada;
17
18
19
20

21 **1. Introduction**

22
23 The rate of nitrogen (N) fixation has been greatly altered by human activities in the past
24
25 50 years through fertilizer production, widespread cultivation of leguminous crops, and
26
27 fossil fuel combustion (Townsend and Davidson, 2006). Human perturbation of the N
28
29 cycle is expected to have continued long-term consequences on the environment
30
31 (Galloway, 2003, 2004; Gruber and Galloway, 2008). One of the manifestations of the
32
33 environmental effect of the altered nitrogen cycle are the steadily increasing nitrate
34
35 concentrations in many river networks and freshwater systems worldwide (e.g. Vitousek
36
37 et al., 1997; Goolsby 2000; Galloway et al., 2004).
38
39
40
41
42
43
44

45 The nitrogen pollution of water resources and aquatic ecosystems especially in populated
46
47 watersheds is a growing problem that can cause eutrophication, hypoxia and loss of
48
49 biodiversity in many freshwaters and coastal marine waters (NRC 2000; Howarth et al.,
50
51 2002; Paerl et al., 2002; Rabalais et al., 2001; Rabalais 2002; Galloway et al., 2004). An
52
53 estimated 70% of the anthropogenic nitrogen input to large watersheds is stored,
54
55 denitrified, or volatilized in the catchments, but delineating the origin of nitrogen species
56
57
58
59
60
61
62
63
64
65

1
2
3
4 exported from these catchments by rivers has remained difficult on a basin scale
5
6 (Howarth et al., 1996, 2002). Although there have been numerous model estimates of the
7
8 nitrogen budget regionally and globally, balancing the nitrogen cycle with limited
9
10 quantitative knowledge of denitrification rates and of major nitrogen sources and removal
11
12 pathways is problematic (Davidson and Seitzinger, 2006; Boyer et al., 2006; Groffman et
13
14 al., 2006; Burgin and Hamilton, 2007). Hence, uncertainties of model estimates and
15
16 predictions are inherently large.
17
18
19
20
21
22

23
24 Obtaining quantitative details of nitrogen budgets of rivers can be difficult due to
25
26 multiple nitrogen sources and transformations within rivers (e.g. denitrification; Böttcher
27
28 et al., 1990). The use of isotope ratio measurements to complement surface water
29
30 concentration data has proven useful for identifying sources and processes governing the
31
32 nitrogen cycle in riverine systems (Mayer et al., 2002; Kendall et al., 2007). Different
33
34 sources of N species often have distinct isotopic signatures. For example, atmospheric
35
36 nitrate is characterized by high $\delta^{18}\text{O}_{\text{NO}_3}$ values usually $>60\text{‰}$ while synthetic nitrate
37
38 fertilizers produced from atmospheric O_2 and N_2 are characterized by $\delta^{18}\text{O}_{\text{NO}_3}$ values
39
40 between $+18$ and $+22\text{‰}$ and by $\delta^{15}\text{N}_{\text{NO}_3}$ values between -5 and $+5\text{‰}$ (Kendall et al.,
41
42 2007). In addition, nitrate derived from nitrification of ammonium (NH_4) in fertilizers,
43
44 soil and manure typically have similar $\delta^{18}\text{O}_{\text{NO}_3}$ values between -15 and $+15\text{‰}$, but a
45
46 different range of $\delta^{15}\text{N}_{\text{NO}_3}$ values (between -10 and $+25\text{‰}$; Kendall et al., 2007). Nitrate
47
48 derived from manure and septic systems has typically higher $\delta^{15}\text{N}$ values than nitrate
49
50 derived from soil, precipitation and fertilizers. Another benefit of isotopic approaches is
51
52 the predictable isotopic fractionation that occurs during some biogeochemical processes
53
54
55
56
57
58
59
60
61
62
63
64
65

1
2
3
4 (e.g. denitrification), which can be used in tandem with concentration changes as a tool to
5
6
7 identify whether these process affect riverine nitrate loads (e.g. Mayer et al., 2002; Sebilo
8
9 et al., 2003; Mulholland et al., 2008). In addition to denitrification, other nitrogen
10
11 transformation processes such as anammox and dissimilatory nitrate reduction to
12
13 ammonium have recently been identified as potentially important nitrate removal
14
15
16 pathways of aquatic systems (Burgin and Hamilton, 2007).
17
18
19
20

21 Since tracing nitrate sources and sinks using stable isotopes can be difficult in watersheds
22
23 with multiple nitrogen sources (e.g. Gravotta, 1997, Mayer et al., 2002), a study in a
24
25 watershed with relatively few spatially separated land use activities is desirable for
26
27 testing how isotopic techniques can be effectively applied in nitrate source identification,
28
29 tracing, and apportionment in riverine systems. The Bow River in Alberta (Canada)
30
31 provides an excellent opportunity for testing the effectiveness of isotopic techniques in
32
33 source apportionment of riverine nitrate on a basin scale since it flows through three
34
35 distinct land use regions (Figure 1). This river originates in rather pristine forested
36
37 headwater catchments in the Rocky Mountains. Subsequently, the river flows eastwards
38
39 through the foothills and through the major urban center Calgary with a population
40
41 exceeding one million (Statistics Canada 2011). Downstream of Calgary, the river
42
43 meanders through agricultural land that is partially irrigated. Therefore, the two major
44
45 anthropogenic nitrate sources, urban wastewaters from the city of Calgary and
46
47 agricultural return flows, are spatially separate in the Bow River Basin.
48
49
50
51
52
53
54
55
56
57
58
59
60
61
62
63
64
65

1
2
3
4 Continued urban expansion and population growth in southern Alberta make nutrient
5 loading management in the Bow River increasingly challenging. Low dissolved oxygen
6 levels (< 5 mg/L) have been observed in spring and fall in the Bow River downstream of
7 Calgary (e.g. Iwanyshyn et al., 2008; Robinson et al., 2009) indicating a deteriorating
8 water quality. Intensified diel cycles are attributed to macrophyte and periphyton
9 photosynthesis and respiration that is driven in significant part by wastewater loading
10 (Iwanyshyn et al., 2008). An inverse correlation between macrophyte growth and
11 wastewater nitrogen loading observed on a decadal scale (Sosiak, 2002) suggests riverine
12 nitrogen plays an important role in causing low pre-dawn dissolved oxygen levels.
13
14 Improved understanding of nitrogen sources is therefore an important component for
15 managing riverine aquatic ecosystems and for ensuring that urban and agricultural
16 activities can continue to develop sustainably without exacerbating the nutrient loading of
17 the Bow River.
18
19
20
21
22
23
24
25
26
27
28
29
30
31
32
33
34
35
36
37

38 The objective of this study was to combine physical, chemical and isotopic approaches to
39 identify and apportion nitrate sources in the Bow River along its flow path through
40 regions with markedly different land use. It was anticipated that the application of stable
41 isotope techniques would reveal unique information about nitrate sources that may be
42 beneficial for improving watershed management practices.
43
44
45
46
47
48
49
50
51
52

53 **2. Study Area**

54
55 The Bow River flows for 645 km through southern Alberta, Canada, with an annual
56 discharge between 3 and 4 x10⁹ m³/yr. The Rocky Mountain catchments constitute 30%
57
58
59
60
61
62
63
64
65

1
2
3
4 (7714km²) of the total basin drainage area and the prairies account for the remaining 70%
5
6
7 (Grasby et al., 2000). The Rocky Mountains receive between 500 and >800 mm of
8
9 precipitation annually in a cold and humid climatic regime whereas the prairies are semi-
10
11 arid, receiving only 300-400 mm of precipitation annually (Atlas of Canada 2009).
12
13
14 Meltwaters from snowpack and to a lesser degree, melting of glacial ice, in the Rocky
15
16 Mountains are important sources of headwater flow for the Bow River (Bow River Basin
17
18 Council, 2005) resulting in seasonally highly variable discharge, with peakflow typically
19
20 occurring between late May and July. Flow recession typically starts in July followed by
21
22 transition into baseflow periods, which usually last from August until early spring
23
24 snowmelt in April. Relatively little flow contribution is thought to come from the prairies,
25
26 which have a net evapotranspirative deficit with dominantly non-flow contributing and
27
28 internally isolated drainage systems that become often endorheic in the lower watershed
29
30
31 (Agriculture and Agri-Food Canada 2008; Last and Ginn, 2005).
32
33
34
35
36
37

38 The majority (>85%) of the watershed population lives in the City of Calgary (Pernitsky
39
40 and Guy, 2010), which consequently has the largest contribution of treated wastewater
41
42 effluent. In Calgary, the Bonnybrook Wastewater Treatment Plant (BBWWTP) treats the
43
44 largest fraction of wastewater with a designed capacity of up to 500 x 10⁶ L/day followed
45
46 by the Fish Creek Wastewater Treatment Plant (FCWWTP) with a capacity of only 72 x
47
48 10⁶ L/day (City of Calgary 2009). The Pine Creek Wastewater Treatment Plant became
49
50 operational in May 2009 after the field work for this study was completed. Three small
51
52 towns upstream of Calgary with wastewater effluent discharge licenses (for a combined
53
54 total of up to 40 x 10⁶/day) are located within the upper 150 km of the watershed. Two
55
56
57
58
59
60
61
62
63
64
65

1
2
3
4 small licensed treated effluent discharges occur downstream of Calgary: Strathmore
5
6 releasing $\sim 3.6 \times 10^6$ L/day (Pernitsky and Guy, 2010) into the Bow River about 40km
7
8 east of Calgary, and Okotoks with a 5.1×10^6 L/day license with discharge to a tributary
9
10 of the Highwood River.
11
12
13
14

15
16 In the late 1970s, biomass blooms driven by wastewater nutrients in the Bow River
17
18 (Ongley and Blachford, 1982; Hamilton, 1982) prompted the city of Calgary to upgrade
19
20 its wastewater treatment facilities. Currently, all wastewater treatment facilities located
21
22 within the Bow River Basin are tertiary wastewater treatment plants (City of Calgary
23
24 2009; Epcor Utilities 2010). The wastewater treatment plant (WWTP) upgrades have
25
26 improved the water quality in the Bow River. A correlation between decreasing
27
28 occurrences of aquatic macrophytes and reduced nitrogen load suggests that the Bow
29
30 River may be nitrogen limited (Sosiak 2002).
31
32
33
34
35
36
37

38 The Bow River provides drinking, stock, and irrigation water for many small
39
40 communities scattered on the semi-arid prairies east of Calgary. Agricultural activities
41
42 account for 77% (2.8×10^{12} L) of the annually licensed Bow River water allocation, while
43
44 17% is licensed for municipalities (Bow River Basin Council 2005). Most of the irrigated
45
46 agriculture occurs downstream of Calgary, with agricultural return flows reaching the
47
48 Bow River via the irrigation canal network. Sewage from smaller prairie communities is
49
50 typically treated by lagoons with intermittent discharge to the Bow River via irrigation
51
52 canals and prairie creeks (Bow River Basin Council 2005).
53
54
55
56
57
58
59
60
61
62
63
64
65

1
2
3
4 Although the Bow River has numerous near-pristine tributaries occurring mostly in the
5
6 Rocky Mountains, two large Rocky Mountain tributaries, the Elbow and Highwood
7
8 Rivers, reach the plains. The Elbow River discharges at Calgary, while the Highwood
9
10 River joins the Bow River circa 80 km below Calgary. Of these two tributaries, only the
11
12 Highwood River is impacted by a licensed effluent discharge.
13
14
15
16
17
18
19
20

21 **3. Methods**

22 *3.1 Data Collection and Sampling*

23
24 Daily flow data of 16 stations (Figure 1) were obtained from Alberta Environment
25
26 (AENV) and the Water Survey of Canada. Four of the Bow River sampling sites (Site #1,
27
28 3, 7, and 19) correspond to AENV flow stations. Flows at Site #2 were estimated by
29
30 combining the upstream flows at Banff with those of the nearby Spray River. Flow at
31
32 Calgary (Site #4) was approximated by using flow data measured by AENV ~10 km
33
34 downstream. Given the non-flow contributing drainage systems of the prairies, flow at
35
36 Site #11 was assumed constant as that measured by AENV 60 km upstream (below the
37
38 Bassano Dam). Within the irrigation districts on the prairies, AENV monitors the flows
39
40 of three prairie creeks (i.e. Crowfoot Creek, New West Coulee and Twelve Mile Creek)
41
42 corresponding to Sites #9, 16, and 18 on Figure 1. The flows of the three major irrigation
43
44 canals diverted from the Bow River at Calgary, Carseland and the Bassano Dam were
45
46 also obtained.
47
48
49
50
51
52
53
54
55
56
57
58
59
60
61
62
63
64
65

1
2
3
4 River water was sampled monthly along the Bow River at ten locations (numbered
5
6 sequentially with flow distance relative to the town of Lake Louise (0 km); Figure 1) and
7
8 at the Highwood River near the mouth (Site #6) between June 2007 and July 2008. Nine
9
10 prairie creeks draining irrigated agricultural fields were sampled between September
11
12 2007 and July 2008. Fieldwork was paused during winter months (December to March)
13
14 due to ice cover. Treated wastewater effluent samples were obtained from the two
15
16 WWTPs in Calgary in April, May and July of 2008. The mainstem sites at the Bow River
17
18 are referred to by their flow distance (ranging from 0 km at Lake Louise to 571 km at
19
20 Ronalane; Figure 1), while tributary and creek sites are referred to by their site numbers
21
22 (e.g. Site #6 for the Highwood River).
23
24
25
26
27
28
29
30

31 *3.2 Laboratory Analyses*

32
33 Nitrate concentrations (reported here as mg NO₃/L) were determined using an ion
34
35 chromatography system (EPA600/4-87/062) and ammonium (NH₄⁺) was measured by the
36
37 automated Phenate EPA350.1 method with detection limits (MDL) of 0.04 mg/l for NO₃
38
39 and 0.0068 mg/L for NH₄. Chloride (Cl) concentrations were determined using an ICS-
40
41 1000 Dionex Ion Chromatography system. The measurement uncertainty of Cl
42
43 concentrations was <±5% of the reported concentrations.
44
45
46
47
48
49

50
51 The isotopic composition of nitrate was determined by converting NO₃ to N₂O gas using
52
53 the bacterial denitrifier method of Sigman et al. (2001) and Casciotti et al. (2002). The
54
55 N₂O gas was subsequently trapped cryogenically in a Trace Gas Pre-Concentrator,
56
57 purified by gas chromatography, followed by mass spectrometric (Finnigan MAT delta
58
59
60
61
62
63
64
65

1
2
3
4 plus XL) measurements of $^{15}\text{N}/^{14}\text{N}$ and $^{18}\text{O}/^{16}\text{O}$ ratios. Ammonium-nitrogen was
5
6 quantitatively converted to $(\text{NH}_4)_2\text{SO}_4$ using the diffusion method (Sebilo et al., 2004).
7
8 The $(\text{NH}_4)_2\text{SO}_4$ precipitates were then freeze-dried, packed into tin cups and thermally
9
10 decomposed in an elemental analyzer (Fissions NA 1500) to generate N_2 gas for
11
12 subsequent $^{15}\text{N}/^{14}\text{N}$ measurements. Isotope data are reported in the internationally
13
14 accepted delta (δ) notation in per mil (‰):
15
16
17
18
19
20

$$\delta [\text{‰}] = [(R_{\text{sample}} / R_{\text{standard}}) - 1] \times 1000$$

21
22
23
24
25
26 where R denotes the $^{15}\text{N}/^{14}\text{N}$ or $^{18}\text{O}/^{16}\text{O}$ ratios respectively. The $\delta^{15}\text{N}$ values of nitrate
27
28 ($\delta^{15}\text{N}_{\text{NO}_3}$) and NH_4 ($\delta^{15}\text{N}_{\text{NH}_4}$) are reported with respect to air, whereas the $\delta^{18}\text{O}$ values of
29
30 nitrate ($\delta^{18}\text{O}_{\text{NO}_3}$) are reported with respect to Standard Mean Ocean Water (V-SMOW).
31
32 The precision and accuracy were $\pm 0.3\text{‰}$ for $\delta^{15}\text{N}_{\text{NO}_3}$, $\pm 0.5\text{‰}$ for $\delta^{15}\text{N}_{\text{NH}_4}$, and $\pm 0.5\text{‰}$ for
33
34 $\delta^{18}\text{O}_{\text{NO}_3}$.
35
36
37
38
39
40

41 *3.3 Data Management*

42
43 Mole ratios of NO_3/Cl were calculated and used to trace the fate of effluent nitrate in the
44
45 Bow River downstream of WWTPs. Since Cl is conservative, its usefulness is not
46
47 limited to tracing wastewater impact along the river flow path. When combined with
48
49 NO_3 , variation in the NO_3/Cl ratio can help identify potential sources of nitrate other than
50
51 wastewater effluents and possible sinks of nitrate along the river flow path (e.g.
52
53 Vandenberg et al., 2005).
54
55
56
57
58
59
60
61
62
63
64
65

Annual or monthly discharge of the Bow River at each sampling location was estimated by summing average daily flow values. Fluxes of nitrate in the Bow River were estimated by multiplying concentrations with flows. The annual mass loads of nitrate were discharge-weighted averages of the total 2007 and 2008 fluxes. For locations upstream of Calgary (0-212 km), the average nitrate concentrations were used because nitrate concentrations in the upper reaches of the Bow River were low (<0.4 mg/L) and typically did not vary by more than 0.2 mg/L (see section 4.1). For the Bow River downstream of Calgary (302-378 km), the unknown daily nitrate concentrations were extrapolated based on daily flow values using the NO₃-flow relationship discussed in section 4.1.

Mass and isotope balance calculations were carried out with the isotopic composition of the mixture (δ_{final}) being described as follows:

$$d_{\text{final}} = \sum_{i=1}^n (f_i \cdot d_i); \text{ given that } \sum_{i=1}^n f_i = 1$$

where f is the fraction of contributions from source i with an isotopic value of δ_i and n is the total number of sources contributing to the final mixture.

4. Results

4.1 Flow and nitrate concentrations

While peak annual flows in the uppermost part of the watershed (0 km) were below 70 m³/s, flow in the lower reaches of the river reached a maximum of 500-1000 m³/s during

1
2
3
4 the May to June snowmelt and rainfall season (Figure 2). In contrast, Bow River flows
5
6 were lowest in the winter and early spring with values ranging from as low as 1-2 m³/s at
7
8 Lake Louise (0 km) to as high as 40-70 m³/s at 179 km at the downstream edge of
9
10 foothills (Figure 2). Downstream of the Rocky Mountain Foothills, the Bow River did not
11
12 exhibit sustained increase in flow with distance. Rather, flow throughout the prairies after
13
14 the confluence with the Highwood River remained relatively constant and similar to that
15
16 at 302 km (Figure 2). Volumetrically, >95% of the equivalent total discharge of the Bow
17
18 River at its mouth originates in the Rocky Mountain portions of the catchment (Table 1).
19
20 The prairie parts of the catchment are characterized by many non-contributing drainage
21
22 areas (Agriculture and Agri-Food Canada 2008) and make only very small contributions
23
24 to the total discharge of the Bow River Basin (estimated as <0.3%; Table 1).
25
26
27
28
29
30
31
32

33 Bow River nitrate concentrations ranged from 0.10 mg/L in the headwaters at Lake
34
35 Louise (0 km) to 7.89 mg/L at 513 km in the final reach of the river during the fall (Table
36
37 2; Figure 3). Consistently low nitrate concentrations (<0.74 mg/L) were observed
38
39 upstream of the WWTPs in Calgary while up to an order of magnitude increase in nitrate
40
41 concentrations was observed downstream of Calgary (Table 2 and Figure 3). Throughout
42
43 the prairie reaches downstream of Calgary, the mainstem nitrate concentrations of the
44
45 Bow River remained elevated with seasonal variations (Figure 3). Nitrate concentrations
46
47 downstream of Calgary approached 4-8 mg/L during baseflow periods in the fall and
48
49 early spring, were intermediate (between 1 and 4 mg/L) in mid-late summer, and were
50
51 lowest around 1 mg/L in spring and early summer (Figure 3).
52
53
54
55
56
57
58
59
60
61
62
63
64
65

1
2
3
4 Nitrate concentrations in the Highwood River (Site #6) ranged from non-detectable
5 (<0.04 mg/L) to as high as 1.32 mg/L in November (Table 2) and were also variable in
6
7 the prairie creeks. Some creeks had consistently low nitrate concentrations (<1 mg/L or
8
9 not detectable) while some had occasionally higher nitrate concentrations (≥ 1 mg/L).
10
11 During a runoff event in June 2008, nitrate concentrations ten times the detection limit
12
13 (0.04 mg/L) were observed in prairie creeks at Sites #9, 10 and 14 in June 2008 (Table 2).
14
15 Nevertheless, the most notable occurrence of elevated nitrate concentrations were
16
17 sporadic; for example, the April 2008 peak nitrate concentration (5.5 mg/L) in Crowfoot
18
19 Creek (Site #9, Figure1) was more than two orders of magnitude higher than baseflow
20
21 concentrations (<0.04 mg/L; Table 2). Similarly, nitrate concentrations at Site #10
22
23 during baseflow periods (Oct, Nov and Apr) ranged between 3.18 and 6.46 mg/L, which
24
25 were significantly higher than nitrate concentrations (<0.43 mg/L) observed in mid spring
26
27 and summer (May-July) (Table 2).
28
29
30
31
32
33
34
35
36
37

38 Nitrate concentrations in treated wastewater effluent from Calgary's BBWWTP ranged
39
40 between 50 and 66 mg/L (Table 2). Treated wastewater effluent from the FCWWTP in
41
42 Calgary, which does not have biological N removal, had low nitrate concentrations of
43
44 <0.4 mg/L. In contrast NH_4 concentrations were high around 30 mg/L in FCWWTP
45
46 effluent, and low in BBWWTP effluent (<0.5 mg/L; Table 2).
47
48
49
50
51
52

53 A linear relationship between nitrate concentration and flow was observed upstream of
54
55 Calgary (0 – 212 km) during the June-July peakflow period in both 2007 and 2008,
56
57 whereas no apparent relationship to flow was observed during baseflow (August –
58
59
60
61
62
63
64
65

1
2
3
4 November) or early spring runoff season (April – May; Figure 4a). In contrast, an
5
6 inverse hyperbolic concentration-flow relationship was observed at sampling stations
7
8 downstream of Calgary (Figure 4b). This inverse relationship exhibited high nitrate
9
10 concentrations (~ 2 - 8 mg NO₃/L) at low flow below 50 m³/s, and low concentrations (<
11
12 2 mg NO₃/L) at high flow exceeding 100 m³/s. Data points below the hyperbolic curve
13
14 represent the lowest reach of the river (482 to 571 km) during the irrigation season from
15
16 mid May to late September (marked as open symbols in Figure 4b).
17
18
19
20
21
22

23 *4.2 NO₃/Cl ratios*

24
25 Molar equivalent ratios of NO₃/Cl were only considered below Calgary where WWTP-
26
27 released chloride concentrations are significant. The BBWWTP effluent had high
28
29 NO₃/Cl molar equivalent ratios (>0.27) relative to the FCWWTP effluent and the river
30
31 water downstream of Calgary that had NO₃/Cl ratios <0.27 (Figure 5). Decreased NO₃/Cl
32
33 ratios were consistently observed in the 15 km nitrate rich wastewater mixing zone
34
35 between BBWWTP and FCWWTP (231 km – 245 km) and throughout the rest of the
36
37 river downstream of the city (Figure 5).
38
39
40
41
42
43
44

45 *4.3 Isotopic composition of nitrate*

46
47 There is no wastewater release or agricultural influence in the headwaters of the Bow
48
49 River above Lake Louise (0 km). Here, the δ¹⁵N_{NO₃} values varied between -0.1 and +3.5‰
50
51 and δ¹⁸O_{NO₃} values ranged between +6.8 and +11.3 ‰ (Table 2; Figure 6). From the
52
53 headwaters at Lake Louise (0 km) to Calgary downstream of WWTPs, δ¹⁵N_{NO₃} values
54
55 increased from +1‰ to +8‰ while δ¹⁸O_{NO₃} values decreased by about 20‰ approaching
56
57
58
59
60
61
62
63
64
65

1
2
3
4 a value of -8‰ (Figure 7). The isotopic composition of Bow River nitrate remained
5
6 relatively constant at +8‰ and -8‰ for $\delta^{15}\text{N}_{\text{NO}_3}$ and $\delta^{18}\text{O}_{\text{NO}_3}$ respectively downstream of
7
8 Calgary. The isotopic compositions of nitrate in river water samples collected between
9
10 Lake Louise and Calgary's WWTPs (i.e. at 99, 179, and 212 km) were intermediate
11
12 between those samples from up- and down-stream sites with values around +5‰ for
13
14 $\delta^{15}\text{N}_{\text{NO}_3}$ and +2‰ for $\delta^{18}\text{O}_{\text{NO}_3}$ (Figures 6,7).
15
16
17
18
19
20

21 The $\delta^{15}\text{N}_{\text{NO}_3}$ values of the Highwood River varied between +5 and +12‰, with lower
22
23 values (< +7.5‰) during the May to July snowmelt and rainfall season and consistently
24
25 higher values (>10‰) during the November to April baseflow periods (Table 2). Waters
26
27 sampled from prairie creeks had $\delta^{15}\text{N}_{\text{NO}_3}$ values that were similar to those of the lower
28
29 Bow River (between +5 and +12‰), but many had high $\delta^{18}\text{O}_{\text{NO}_3}$ values between +10 and
30
31 +30‰ (Figure 6). Elevated $\delta^{18}\text{O}_{\text{NO}_3}$ values occurred in waters containing low (<0.2 mg/L)
32
33 nitrate concentrations, whereas $\delta^{15}\text{N}_{\text{NO}_3}$ values showed no correlation with nitrate
34
35 concentrations (Table 2). The $\delta^{15}\text{N}_{\text{NO}_3}$ and $\delta^{18}\text{O}_{\text{NO}_3}$ values of baseflow nitrate at prairie
36
37 creek Site #10 were similar (7.9 and 7.0‰ for $\delta^{15}\text{N}_{\text{NO}_3}$, and -10.3 and -10.1 for $\delta^{18}\text{O}_{\text{NO}_3}$)
38
39 to those of wastewater nitrate from the BBWWTP in Calgary (7.7 to 8.3‰ for $\delta^{15}\text{N}_{\text{NO}_3}$,
40
41 and -9.5 to -9.7‰ for $\delta^{18}\text{O}_{\text{NO}_3}$; Tables 1, 3; Figure 6). The $\delta^{15}\text{N}_{\text{NO}_3}$ values of BBWWTP
42
43 effluent were similar to the $\delta^{15}\text{N}_{\text{NH}_4}$ values from the FCWWTP (8.0-9.1‰).
44
45
46
47
48
49
50
51
52

53 **5. Discussion**

54 *5.1 Nitrate concentration-flow relationships*

55
56
57
58
59
60
61
62
63
64
65

1
2
3
4 Nitrate concentrations in the Bow River upstream of Calgary are seasonally and
5
6 hydrologically controlled. The linear relationship showing nitrate concentration increases
7
8 (between 0.20 and 0.80 mg/L) with flow in the upstream reaches (0 to 212 km) during
9
10 peak flow periods (Figure 4a) suggests that nitrate loading from the mountain catchments
11
12 is related to drainage-contributing watershed area. Increased nitrate concentrations in late
13
14 spring and early summer suggest that nitrate from the headwater portions of the
15
16 watershed is exported into the Bow River during snowmelt and rainfall periods.
17
18

19 Although temporally variable, nitrate concentrations are relatively constant with flow
20
21 distance in the upper portions of the Bow River watershed.
22
23
24
25
26
27

28 In contrast to the upstream reaches, Bow River nitrate concentrations below Calgary
29
30 appeared hyperbolically related to flow (Figure 4b). This type of relationship is
31
32 commonly observed in rivers due to contributions from varying sources (Johnson et al.,
33
34 1969, Salmon et al., 2001). The high discharge-end of the curve (Figure 4b) shows the
35
36 effect of increasing dilution of wastewater effluent nitrate with the river's nitrate
37
38 concentrations approaching a minimum value of approximately 1 mg/L, still higher than
39
40 nitrate concentrations in the headwaters. Nitrate concentrations in the low-discharge end
41
42 of Figure 4b approach high values >7 mg/L indicative of wastewater effluent impact.
43
44
45
46
47
48
49

50 *5.2 Nitrate Source Identification*

51

52 In the uppermost headwaters (0 km) where wastewater and agricultural impacts are
53
54 absent, the $\delta^{15}\text{N}_{\text{NO}_3}$ and $\delta^{18}\text{O}_{\text{NO}_3}$ values of the Bow River fell within the characteristic
55
56 range of soil derived nitrate (Table 2; Figure 6). Soil derived nitrate generated by
57
58
59
60
61
62
63
64
65

1
2
3
4 ammonification and nitrification of soil organic N (Mayer et al., 2001) in the forested
5 parts of the Bow River Basin in the Rocky Mountains is thus the dominant source of
6
7 nitrate in the pristine headwaters. The isotopic composition of nitrate between 0 km and
8
9 Calgary WWTPs at 99, 179, and 212 km was intermediate between that typical for soil-
10
11 derived nitrate found at 0 km and that of effluent nitrate from Calgary's WWTPs.
12
13 Although not clearly evident by nitrate concentration values, the change in isotopic
14
15 compositions indicates an influence of wastewater-derived nitrate between Lake Louise
16
17 (0 km) and Calgary WWTPs (231, 245 km). Downstream of Calgary, the isotopic
18
19 composition of nitrate in the Bow River remained relatively constant and similar to the
20
21 isotopic composition of wastewater nitrate from the WWTPs. This suggests that the
22
23 nitrate rich wastewater discharge from Calgary is the dominant source of nitrate
24
25 throughout the lower reaches of the river.
26
27
28
29
30
31
32
33
34
35

36 The $\delta^{15}\text{N}_{\text{NO}_3}$ and $\delta^{18}\text{O}_{\text{NO}_3}$ values of the prairie creeks were more variable, fluctuating
37
38 within 8‰ and by >40‰ respectively (Table 2). The similarity of the prairie creek
39
40 $\delta^{15}\text{N}_{\text{NO}_3}$ values to Calgary wastewater nitrate (within $\pm 4\%$) suggests that nitrogen isotope
41
42 ratios may not be useful for distinguishing agriculturally derived nitrate sources from
43
44 wastewater effluents. The isotopic composition of nitrate at Site #10 (Table 2) is unique
45
46 from other creeks in that high baseflow nitrate had isotopic signatures similar to those of
47
48 WWTP effluent. The water supply for a number of prairie communities is extracted from
49
50 the irrigation canals and reservoirs, and the treated wastewater effluents of local villages
51
52 and towns are returned to the Bow River via some of these canals (Bow River Basin
53
54 Council 2005). The data suggest, but do not confirm, that some prairie creeks may
55
56
57
58
59
60
61
62
63
64
65

1
2
3
4 contain nitrate derived from animal and feedlot manure, and septic and domestic
5
6 wastewater. Similarly, in the Highwood River during irrigation and baseflow periods,
7
8 $\delta^{15}\text{N}_{\text{NO}_3}$ values above +10‰ and $\delta^{18}\text{O}_{\text{NO}_3}$ values near 0‰ (Table 2) suggest admixture of
9
10 anthropogenic nitrate possibly derived from fertilizer, manure, and sewage effluent.
11
12
13
14

15 16 *5.3 $\delta^{15}\text{N}_{\text{NO}_3}$ and $\delta^{18}\text{O}_{\text{NO}_3}$ variations with nitrate concentrations*

17
18 The Bow River $\delta^{15}\text{N}_{\text{NO}_3}$ and $\delta^{18}\text{O}_{\text{NO}_3}$ values showed well defined relationships with
19
20 nitrate concentrations (Figure 8). Riverine nitrate between Lake Louise and Calgary
21
22 WWTPs (0, 99, 179, 212 km) exhibited a change in the $\delta^{15}\text{N}_{\text{NO}_3}$ values of up to 8‰ (to
23
24 values ~ 5-6‰) and a change in the $\delta^{18}\text{O}_{\text{NO}_3}$ values of up to 15‰ (to values ~5-6‰;
25
26 Figure 8), despite a small range of nitrate concentration changes (<0.4 mg/L; Figure 3).
27
28
29
30
31 Much more pronounced changes in nitrate concentrations downstream of Calgary
32
33 (ranging from ~1 to ~8 mg/L) were accompanied by a comparatively small change in the
34
35 isotopic compositions, which remained similar to wastewater values of around +8‰ for
36
37 $\delta^{15}\text{N}_{\text{NO}_3}$ and -10‰ for $\delta^{18}\text{O}_{\text{NO}_3}$ (Figure 8). The pattern of isotopic compositions with
38
39
40 flow distance suggests increasing wastewater contributions to the nitrate load in the upper
41
42 part of the watershed, and a dominant wastewater contribution below Calgary, where
43
44 nitrate concentrations >1 mg/L are persistent. The relationship between the isotopic
45
46 compositions and concentrations of NO_3 is consistent with a two end-member mixing
47
48
49
50
51 model.
52
53
54
55

56 *5.4 Isotope balance estimation*

57
58
59
60
61
62
63
64
65

1
2
3
4 A two-end member isotopic mixing model was used to evaluate mixing between forest
5 soil derived nitrate from the headwaters and nitrate contributed by wastewater effluents.
6
7
8
9 Figure 9 suggests that mixing of different percentages of soil derived nitrate (as
10 represented by the site at 0 km) with wastewater derived nitrate causes the isotopic values
11 of riverine nitrate to fall on a mixing line between the isotopic composition of the two
12 end-members of soil- and wastewater-derived nitrate. However, the contribution of
13
14
15
16
17
18
19 effluent-derived ammonium needs also to be considered. Of the estimated 3.15kt of
20
21
22
23
24
25
26
27
28
29
30
31
32
33
34
35
36
37
38
39
40
41
42
43
44
45
46
47
48
49
50
51
52
53
54
55
56
57
58
59
60
61
62
63
64
65

Dilution-corrected wastewater effluent ammonium concentrations tend to decrease to less than 10% of their initial value after about 10 km flow distance in Bow River (Vandenberg et al., 2005). It is not clear what fraction of the wastewater ammonium is assimilated as opposed to nitrified, however.

Nitrification is a bacterially mediated, multi-step process in which oxygen incorporated into nitrate comes from H₂O and O₂ in a 2:1 ratio (Andersson and Hooper, 1983; Kumar et al., 1983; Hollocher, 1984). The oxygen isotope ratio of nitrate produced by nitrification can be estimated as:

$$\delta^{18}\text{O}_{\text{NO}_3} = 2/3 \delta^{18}\text{O}_{\text{H}_2\text{O}} + 1/3 \delta^{18}\text{O}_{\text{O}_2} \quad (4)$$

1
2
3
4 where $\delta^{18}\text{O}_{\text{H}_2\text{O}}$ and $\delta^{18}\text{O}_{\text{O}_2}$ are the isotopic values of water and atmospheric O_2 ,
5
6
7 respectively (Kendall et al., 1997). An average $\delta^{18}\text{O}$ value for Bow River downstream of
8
9
10 Calgary of -18.7‰ (Katvala 2008; Hogue 2009; Chao 2011) and a $\delta^{18}\text{O}$ value of
11
12 atmospheric O_2 of 23.5‰ (Kroopnick and Craig, 1972) were used to estimate a $\delta^{18}\text{O}_{\text{NO}_3}$
13
14 value for nitrified wastewater ammonium of -4.6‰ (underlined values in Table 3).
15
16 Mixing 34% of nitrification-derived nitrate ($\delta^{18}\text{O}_{\text{NO}_3}$ value of -4.6‰) with 66% of
17
18 effluent-derived nitrate ($\delta^{18}\text{O}_{\text{NO}_3}$ of -10‰) would result in a mixture with a $\delta^{18}\text{O}_{\text{NO}_3}$ value
19
20 of -8‰ (Table 3). Nitrogen isotope fractionation during nitrification is also well
21
22 documented, with enrichment factors that range between -12 and -29‰ (Kendall et al.,
23
24 1997), but the apparent isotope effect becomes small if ammonium conversion to nitrate
25
26 approaches completion. The expected effect of nitrification of all of the effluent
27
28 ammonium would be increased $\delta^{15}\text{N}_{\text{NO}_3}$ and $\delta^{18}\text{O}_{\text{NO}_3}$ values, as indicated with an arrow in
29
30 Figure 9), with predicted values of +9.3‰ for $\delta^{15}\text{N}_{\text{NO}_3}$ and -8‰ for $\delta^{18}\text{O}_{\text{NO}_3}$. The
31
32 observed isotopic composition of nitrate in the Bow River fell slightly above the
33
34 conservative mixing trend (Figure 9), suggesting that in-stream nitrification of
35
36 wastewater ammonium occurred.
37
38
39
40
41
42
43
44

45
46 The estimated contribution of wastewater derived river nitrate is significant below
47
48 Calgary, ranging from 84 to 92% (Figure 9). Despite insignificant nitrate concentration
49
50 changes below Lake Louise and upstream of Calgary, the isotopic values suggest that as
51
52 much as 50% of the river nitrate is wastewater derived (Figure 9). Urban impacts on the
53
54 N budget of the Bow River are thus significant and can be quantitatively estimated.
55
56
57
58
59
60
61
62
63
64
65

1
2
3
4 *5.5 Mass loads of nitrate*
5

6
7 The annual mass load of nitrate to the Bow River upstream of Calgary was less than 1.41
8
9 kt, increasing to 8.92 kt downstream of the city (302 km; Table 1), with an estimated
10
11 Calgary WWTP contribution of about 9.18 kt/yr. Since the prairie contribution of
12
13 discharge to the Bow River flow was small (~0.3%) and the nitrate concentrations from
14
15 sampled prairie creeks were typically low (non-detectable or <1 mg/L), the grossly
16
17 estimated total nitrate flux contribution from prairie creeks was <1 kt/yr, making only a
18
19 minor contribution to the total riverine nitrate load below Calgary.
20
21
22

23
24
25
26 The 13% difference between the estimated (10.59 kt/yr) and the measured (8.92 kt/yr)
27
28 nitrate loads observed between 212 km (Calgary above WWTPs) and 302 km (first Bow
29
30 River site downstream of Calgary; Table 1) suggests nitrate is being consumed with or
31
32 lost from the river. Elevated nitrate concentrations downstream of Calgary were observed
33
34 during low flow periods when the river's dilution capacity was low. The reduction in
35
36 mass flux observed at 302 km can be largely attributed to upstream irrigation withdrawals
37
38 (WID and BRID removed an estimated total of 0.69 kt NO₃/yr; Table 1) from the Bow
39
40 River, and in-stream biological assimilation as observed in reduced NO₃/Cl ratios.
41
42
43

44
45 Although the total nitrate load to the Bow River from irrigation return flow water and
46
47 other agricultural activities was difficult to estimate based on sampled prairie creek
48
49 waters, the mass balance (Table 1) suggests they are minor in comparison to urban
50
51 discharge of nitrate rich wastewaters.
52
53
54
55
56
57
58
59
60
61
62
63
64
65

6. Summary and Conclusions

Although the annual nitrate mass loads in the Bow River upstream of Calgary's WWTPs were low (~1kt), up to half of the Bow River nitrate mass load at 99 km, 179 km and 212 km was derived from wastewater effluents. Peakflow nitrate concentrations increased linearly with increasing downstream flows in the Rocky Mountains, with $\delta^{15}\text{N}_{\text{NO}_3}$ and $\delta^{18}\text{O}_{\text{NO}_3}$ values between -0.1 and 3.5‰ and +6.8 and +11.3‰ respectively. Non-peakflow nitrate also had an isotopic composition consistent with nitrate derived via nitrification in forest soils, and concentrations that did not vary systematically with flow. This confirms that ammonification and nitrification of soil organic N is a major nitrate source in the forested catchments of the river basin.

In contrast to the headwater reaches, nitrate concentrations downstream of Calgary decreased with increasing flow, showing dilution of nitrate loads during high flow. The similarity between the isotopic compositions of nitrate in the Bow River downstream of Calgary with those of wastewater effluents revealed that nitrate loads to the Bow River on the prairies are dominantly from Calgary's WWTPs, especially BBWWTP. Isotope mass balance estimations showed that wastewater nitrate typically accounted for 84-92% of nitrate load in the Bow River downstream of Calgary. Although concentrations remain relatively low upstream of Calgary, the fraction of wastewater derived riverine nitrate is significant, with stable isotopic compositions at 99 km, 179 km and 212 km indicative of $\leq 50\%$ wastewater.

1
2
3
4 This study provides evidence that nitrate in the Bow River is significantly affected by
5
6 human wastewater effluents at all sampling sites, except the uppermost sampling site
7
8 where urban and agricultural activities are absent. The impact persists throughout the
9
10 entire flow length of the river from the second uppermost sampling site (99 km)
11
12 downstream to the mouth (570 km). Nitrate inputs from creeks draining through
13
14 agricultural fields on the prairies had minimal contribution and insignificant effect on the
15
16 isotopic composition of the Bow River nitrate. Isotope ratio measurements provided
17
18 unique data for discerning sources and processes that cannot be easily detected with only
19
20 chemical and hydrometric analyses. The use of isotopic techniques integrated with
21
22 interpretation of flow and chemical data demonstrated that riverine nitrate source
23
24 apportionment can be highly effective enabling assessment of their relative contributions
25
26 to riverine nitrate fluxes. Such information is of great value for improving watershed
27
28 management practices..
29
30
31
32
33
34
35
36
37

38 **Acknowledgements**

39
40 Financial support from the Natural Sciences and Engineering Research Council of
41
42 Canada (NSERC) and the Alberta Water Research Institute is gratefully acknowledged.
43
44
45
46
47

48 **References**

49
50 Agriculture and Agri-Food Canada, 2008. PFRA Watershed Project - Areas of Non-
51
52 Contributing Drainage. Version 8. <agr.gc.ca>
53

54 Andersson, K.K., Hooper, A.B. 1983. O₂ and H₂O are each the source of one O in NO₂⁻
55
56 produced from NH₃ by Nitrosomonas: ¹⁵N-NMR evidence. FEBS Letters 164, 236-240.
57

58 Atlas of Canada. 2009. Water Balance – Derived Precipitation and Evaporation.
59
60 <nrcan.gc.ca>.
61
62
63
64
65

1
2
3
4
5
6 Böttcher, J., Strebel, O., Voerkelius, S., Schmidt, H.L. 1990. Using isotope
7 fractionation of nitrate-nitrogen and nitrate-oxygen for evaluation of microbial
8 denitrification in a sandy aquifer. *J. Hydrol.* 114, 413-424.
9

10 Bow River Basin Council. 2005. Nurture, Renew, Protect: A Report on the State of the
11 Bow River Basin. Bow River Basin Council, Calgary.
12

13
14 Boyer, E.W., Alexander, R.B., Parton, W.J., Li, C., Butterbach-Bahl, K., Donner, S.D.,
15 Skaggs, R.W., Del Grosso, S.J., 2006. Modeling denitrification in terrestrial and aquatic
16 ecosystems at regional scales. *Ecol. Appl.* 16, 2123-2142.
17

18
19 Burgin, A.J., Hamilton, S.K., 2007. Have we overemphasized the role of
20 denitrification in aquatic ecosystems? A review of nitrate removal pathways. *Front. Ecol.*
21 *Environ.* 5, 89-96.
22

23
24 Casciotti, K.L., Sigman, D.M., Hastings, M.G., Bohlke, J.K., Hilkert, A. 2002.
25 Measurement of the oxygen isotopic composition of nitrate in seawater and freshwater
26 using the denitrifier method. *Anal. Chem.* 74, 4905-4912.
27

28
29 Chao, Y.-J. J., 2010. Major Ion and Stable Isotope Geochemistry of the Bow River,
30 Alberta, Canada HESIS MSc. thesis. Department of Geoscience. University of Calgary,
31 Calgary, Alberta
32

33
34 City of Calgary. 2009. Wastewater Treatment Plants Historical Data. Bonnybrook
35 Wastewater Treatment Plant - City of Calgary Water Services. Calgary, Alberta.
36 <calgary.ca>
37

38
39 Davidson, E.A., Seitzinger, S. 2006. The enigma of progress in denitrification research.
40 *Ecol. Appl.* 16, 2057–2063.
41

42
43 EPCOR Utilities. 2010. Water and Wastewater in Alberta. <epcor.ca>
44

45
46 Galloway, J.N., Aber, J.D., Erisman, J.W., Seitzinger, S.P., Howarth, R.W., Cowling,
47 E.B., Cosby B.J., 2003. The nitrogen cascade. *Biosci.* 53, 341-356.
48

49
50 Galloway, J.N., Dentener, F.J., Capone, D.G., Boyer, E.W., Howarth, R.W., Seitzinger,
51 S.P., Asner, G.P., Cleveland, C.C., Green, P.A., Holland, E.A., Karl, D.M., Michaels,
52 A.F., Porter, J.H., Townsend, A.R., Vorosmarty, C.J., 2004. Nitrogen cycles: past,
53 present, and future. *Biogeochem.* 70, 153-226.
54

55
56 Gruber, N., Galloway, J.N., 2008. An Earth-system perspective of the global nitrogen
57 cycle. *Nature.* 451, 293-296.
58

59
60 Davidson, E.A., Seitzinger, S. 2006. The Enigma of Progress in Denitrification Research.
61 *Ecological Applications* 16 (6), 2057-2063.
62
63
64
65

1
2
3
4
5
6 Goolsby, D. A., 2000. Mississippi Basin nitrogen flux believed to cause Gulf hypoxia.
7 EPS, *Trans. Am. Geophys. Union* 81, 321-327.
8

9
10 Grasby, S.E., Hutcheon, I., 2000. Chemical dynamics and weathering rates of a
11 carbonate basin Bow River, southern Alberta. *Appl. Geochem.* 16, 67-77.
12

13
14 Gravotta, C. 1997. Use of stable isotopes of carbon, nitrogen, and sulfur to identify
15 sources of nitrogen in surface waters in the Lower Susquehanna River Basin,
16 Pennsylvania. U.S. Geological Survey Water-Supply Paper 2497.
17

18
19 Groffman, P.M., Altabet, M.A., Köhlke, J.K., Butterbach-Bahl, K., David, M.B.,
20 Firestone, M.K., Giblin, A.E., Kana, T.M., Nielsen, L.P., Voytek, M.A., 2006. Methods
21 for measuring denitrification: diverse approaches to a difficult problem. *Ecological*
22 *Applications* 16, 2091-2122.
23

24
25 Hamilton, H.R. 1982. Bow River Water Quality 1970-1980. Alberta Environment Water
26 Quality Control Branch. Calgary, Alberta.
27

28
29 Hogue, K.J., 2009. Assessing the Usefulness of Stable Isotope Data for Estimating
30 Snowmelt Contributions to Runoff in the Headwaters of the South Saskatchewan River
31 Basin, Alberta, Canada. MSc. thesis, Department of Geoscience. University of Calgary,
32 Calgary, Alberta.
33

34
35 Hollocher, T.C. 1984. Source of oxygen atoms of nitrate in the oxidation of nitrite by
36 *Nitrobacter agilis* and evidence against a P-O-N anhydride mechanism in oxidative
37 phosphorylation. *Arch. Biochem. Biophys.* 233, 721-727.
38

39
40 Howarth, R.W., Billen G, Swaney D., Townsend A., Jaworksi N., Lajtha K., Downing
41 J.A., Elmgren R., Caraco N., Jordan T., Berendse F., Freney J., Kudeyarov V., Murdoch
42 P., Zhu Zhao-Liang 1996. Regional nitrogen budgets and riverine N and P fluxes for the
43 drainages to the North Atlantic Ocean: Natural and human influences. *Biogeochem.* 35,
44 75-139.
45

46
47 Howarth, R.W., Sharpley A.W., Walker, D. 2002. Sources of nutrient pollution to coastal
48 waters in the United States: Implications for achieving coastal water quality goals.
49 *Estuaries* 25, 656-676.
50

51
52 Iwanyshyn, M., Ryan, M.C., Chu, A. 2008. Separation of physical loading from
53 photosynthesis/respiration processes in rivers by mass balance. *Sci. Total*
54 *Env.* 390, 205-214.
55

56
57 Johnson, N.M., Likens, G.E., Bormann, F.H., Fisher, D.W., Pierce, R.S. 1969. A
58 working model for the variation in stream water chemistry at the Hubbard Brook
59 Experimental Forest, New Hampshire. *Wat. Res. Res.* 5, 1353-1363.
60
61
62
63
64
65

1
2
3
4 Katvala, S.M. 2008. Isotope Hydrology of the Upper Bow River Basin, Alberta, Canada.
5 MSc. thesis. Department of Geoscience. University of Calgary, Calgary, Alberta.
6

7
8 Kendall, C., Elliott, E.M., Wankel, S.D. 2007. Tracing anthropogenic inputs of
9 nitrogen to ecosystems, in: Michener, R., Lajtha, K. (Eds.), *Stable Isotopes in Ecology
10 and Environmental Science*. Blackwell Publishing, Malden, MA. Pp. 375-449.
11

12
13 Kool, D.M., Wrage, N., Oenema, O., Dolfing, J., Van Groenigen, J.W., 2007. Oxygen
14 exchange between (de)nitrification intermediates and H₂O and its implications for source
15 determination of NO₃ and N₂O: a review. *Rapid Commun. Mass Spectrom.* 21, 3569-
16 3578.
17

18
19 Kroopnick, P., Craig, H., 1972. Atmospheric oxygen: isotopic composition and
20 solubility fractionation. *Science* 175, 54-55.
21

22
23 Kumar, S., Nicholas, D.J.D., Williams, E.H., 1983. Definitive ¹⁵N NMR evidence that
24 water serves as a source of 'O' during nitrite oxidation by *Nitrobacter agilis*. *FEBS
25 Letters* 152, 71-74.
26

27
28 Last, W.M., Ginn, F.M., 2005. Saline systems of the Great Plains of western Canada: an
29 overview of the limnogeology and paleolimnology. *Saline Systems*. 1:1-38.
30

31
32 Mayer, B., Boyer, E.W., Goodale, C., Jaworski, N.A., Van Breemen, N., Howarth, R.W.,
33 Seitzinger, S., Billen, G., Lajtha, L.J., Nosal, M., Paustian, K., 2002. Sources of nitrate in
34 rivers draining sixteen watersheds in the northeastern US: Isotopic constraints.
35 *Biogeochem.* 57, 171-197.
36

37
38 Mulholland, P.J., Helton, A.M., Poole, G.C., Hall, R.O., Jr., Hamilton, S.K.,
39 Peterson, B.J., Tank, J.L., Ashkenas, L.R., Cooper, L.W., Dahm, C.N., Dodds, W.K.,
40 Findlay, S.E.G., Gregory, S.V., Grimm, N.B., Johnson, S.L., McDowell, W.H., Meyer,
41 J.L., Valett, H.M., Webster, J.R., Arango, C P., Beaulieu, J.J., Bernot, M.J., Burgin, A.J.,
42 Crenshaw, C.L., Johnson, L.T., O'Brien, J.M., Potter, J.D., Sheibley, R.W., Sobota,
43 D.J., Thomas, S.M., 2008. Stream denitrification across biomes and its response to
44 anthropogenic nitrate loading. *Nature*. 452:202-U46.
45
46

47
48 National Research Council, 2000. *Clean coastal waters: Understanding and reducing the
49 effects of nutrient pollution*. National Academy Press, Washington.

50
51 Ongley, E.D., Blachford, D.P. 1982. *Nutrient and Contaminant Pathways in the bow and
52 Oldman Rivers, Alberta 1980-1981*. Final Report to Environment Canada. Contract
53 OSU80-00056.
54

55
56 Paerl, H.W., Dennis R.L., Whitall, D.R., 2002. Atmospheric deposition of nitrogen:
57 implications for nutrient over-enrichment of coastal waters. *Estuaries*. 25, 677-693.
58
59
60
61
62
63
64
65

- 1
2
3
4 Pernitsky, D.J., Guy, N.D., 2010. Closing the South Saskatchewan River Basin to new
5 water licenses: Effects on municipal water supplies. *Can. Water Res. J.* 35, 79-82.
6
7
8 Rabalais, N.N., Turner, R.E., Wiseman, W.J. 2001. Hypoxia in the Gulf of Mexico. *J.*
9 *Env. Qual.* 30, 320-329.
10
11 Rabalais, N. 2002. Nitrogen in aquatic ecosystems. *Ambio* 31, 102-112.
12
13
14 Robinson, K.L., Valeo, C., Ryan, M.C., Chu, A., Iwanyshyn, M. 2009. Modelling aquatic
15 vegetation and dissolved oxygen after a flood event in the Bow River, Alberta, Canada.
16 *Can. J. Civ. Eng.* 36, 492-503.
17
18
19 Salmon, C.D., Walter, M.T., Hedin, L.O., Brown, M.G., 2001. Hydrological controls on
20 chemical export from an undisturbed old-growth Chilean forest. *J. Hydrol.* 253:68-9-80.
21
22
23 Sebilo, M., Billen, G., Grably, M., Mariotti, A. 2003. Isotopic composition of nitrate-
24 nitrogen as a marker of riparian and benthic denitrification at the scale of the whole Seine
25 River system, *Biogeochem.* 63:35-51.
26
27
28 Sebilo, M., Mayer, B., Grably, M., Billiou, D., Mariotti, A. 2004. The use of the
29 'Ammonium Diffusion' method for $\delta^{15}\text{N-NH}_4^+$ and $\delta^{15}\text{N-NO}_3^+$ measurements:
30 Comparison with other techniques. *Env. Chem.* 1, 99-103.
31
32
33 Sigman, D.M., Casciotti, K.L., Andreani, M., Barford, C., Galanter, M., Bohlke,
34 J.K., 2001. A bacterial method for the nitrogen isotopic analysis of nitrate in seawater and
35 freshwater. *Anal. Chem.* 78, 4145-4153.
36
37
38 Sosiak, A. 2002. Long-term response of periphyton and macrophytes to reduced
39 municipal nutrient loading to the Bow River (Albert, Canada). *Can. J. Fish. Aq. Sci.* 59,
40 987-1001.
41
42
43 Statistics Canada. 2011. Population of Census Metropolitan Areas. <statcan.gc.ca >.
44
45
46 Townsend, A.R., Davidson, E.A., 2006. Denitrification across landscapes and
47 waterscapes. *Ecol. Appl.* 16, 2055-2056.
48
49
50 Vandenberg, J.A., Ryan, M.C., Chu, A., 2005. Field evaluation of mixing length and
51 attenuation of nutrients and fecal coliform in a wastewater effluent plume. *Env. Monit.*
52 *Assess.* 107, 45-57.
53
54
55 Vitousek, P.M., Matson, P.A., Schindler, D.W., Schlesinger, W.H., Tilman, D.G., Aber,
56 J.D., Howarth, R.W., Likens G.E., 1997. Human alteration of the global nitrogen cycle:
57 sources and consequences. *Ecol. Appl.* 7, 737-750.
58
59
60
61
62
63
64
65

1
2
3
4 LIST OF FIGURE CAPTIONS
5
6

7 **Figure 1** Map of the Bow River Basin in southern Alberta, physiographic regions,
8 irrigation districts and sampling sites within the river basin. Flow distances measured in
9 km from Site #1 (Lake Louise) are noted for mainstem sites.
10

11 **Figure 2** Bow River daily flow (m^3/s ; 2007-2008) in the Rocky Mountains (Main
12 Ranges (0 km, black), Front Ranges (99 km; grey), at the downstream edge of the
13 Foothills (179 km; blue), on the prairies (302 km; dotted red) and near the river mouth
14 (571 km; solid red).
15
16

17 **Figure 3** Bow River nitrate concentrations versus flow distance throughout different
18 seasons from June 2007 to July 2008. The grey bar indicates the urban Calgary reach.
19
20

21 **Figure 4** Relationship between nitrate concentration and flow for a) upstream of
22 Calgary's WWTPs (0-212 km) and b) downstream of Calgary from 302-571 km. Linear
23 regressions (a) and hyperbolae (b) were fitted for the peakflow month of June in 2007 and
24 2008 (shown in both plots with filled symbols).
25
26

27 **Figure 5** NO_3/Cl mole equivalent ratios in Calgary's WWTP effluent and in the Bow
28 River downstream of Calgary. The shaded region indicates the urban Calgary reach.
29

30 **Figure 6** a) Dual isotope diagram showing the $\delta^{18}\text{O}_{\text{NO}_3}$ and $\delta^{15}\text{N}_{\text{NO}_3}$ values of samples
31 from the Bow River, its tributaries, wastewater effluents and the typical isotopic ranges of
32 the various nitrate sources in the environment. The arrows indicate changes in isotopic
33 compositions as a result of denitrification (after Kendall et al. 2007; Kool et al. 2007;
34 Böttcher et al. 1990); b) Plot of $\delta^{18}\text{O}_{\text{NO}_3}$ versus $\delta^{15}\text{N}_{\text{NO}_3}$ values for waters of the Bow
35 River from headwater to mouth.
36

37 **Figure 7** Average $\delta^{15}\text{N}_{\text{NO}_3}$ and $\delta^{18}\text{O}_{\text{NO}_3}$ values of the Bow River along its flow path
38 between Site #1 and Site #19.
39

40 **Figure 8** a) $\delta^{15}\text{N}_{\text{NO}_3}$ - NO_3 concentration and b) $\delta^{18}\text{O}_{\text{NO}_3}$ - NO_3 concentration relationships
41 for the Bow River during baseflow periods from August 2007-April 2008.
42

43 **Figure 9** Dual isotope diagram showing $\delta^{18}\text{O}_{\text{NO}_3}$ and $\delta^{15}\text{N}_{\text{NO}_3}$ values produced by
44 mixing variable amounts of wastewater nitrate with the Bow River headwater nitrate
45 from forest soils (0 km). The red arrow shows the extent of isotopic shift in wastewater
46 nitrate under the influence of nitrification of wastewater ammonium (see Table 3 for
47 derivation of the wastewater nitrification trend). The nitrate flux weighted average values
48 for sampling sites upstream (99, 179, and 212km) and downstream (248, 302, 482,
49 571km) are shown.
50
51
52
53
54
55
56
57
58
59
60
61
62
63
64
65

Table 1 Analyses of waters obtained from along the Bow River, selected prairie creeks draining irrigation fields, and treated wastewater effluents from Calgary. Site #'s are indicated in Figure 1.

Bow River Sites at:	Analyses:	Year 2007						Year 2008				
		Jun	Jul	Aug	Sep	Oct	Nov	Feb	Apr	May	Jun	Jul
0 km Site #1		6/22/07	7/16/07	8/29/07	9/26/07	10/24/07	11/28/07		4/4/08	5/10/08	6/13/08	7/23/08
	NO ₃ (mg/L)	0.20	0.18	0.14	0.10	0.21	0.30	-	0.31	0.12	0.41	0.46
	Cl (mg/L)	0.23	0.18	0.16	0.26	0.41	0.35	-	0.38	0.29	0.25	0.22
	δ ¹⁵ N _{NO3} (‰)	2.1	0.6	3.5	0.4	-0.1	1.2	-	0.1	1.8	1.3	0.5
	δ ¹⁸ O _{NO3} (‰)	9.5	11.3	10.0	6.8	8.2	8.8	-	7.7	7.5	8.6	9.7
99 km Site #2		6/22/07	7/16/07	8/29/07	9/26/07	10/24/07	11/28/07		4/4/08	5/10/08	6/13/08	7/23/08
	NO ₃ (mg/L)	0.30	0.20	0.30	0.34	0.31	0.20	-	0.23	0.29	0.56	0.58
	Cl (mg/L)	0.7	0.6	1.0	1.2	1.3	0.9	-	1.1	1.7	0.9	0.7
	δ ¹⁵ N _{NO3} (‰)	4.6	6.3	7.2	5.3	6.2	7.5	-	7.5	8.0	4.8	4.9
	δ ¹⁸ O _{NO3} (‰)	2.5	3.3	-0.7	-3.1	-3.9	-10.2	-	3.9	-0.2	0.8	8.3
179 km Site #3		6/22/07	7/16/07	8/29/07	9/26/07	10/24/07	11/28/07	2/8/08	4/4/08	5/10/08	6/13/08	7/23/08
	NO ₃ (mg/L)	0.40	0.32	0.29	0.28	0.28	0.40	1.24	0.14	0.18	0.65	0.51
	Cl (mg/L)	1.3	1.3	1.3	1.5	1.6	1.5	2.8	1.3	1.6	1.4	1.1
	δ ¹⁵ N _{NO3} (‰)	3.7	4.9	6.2	5.7	5.6	6.4	7.4	7.0	8.1	5.3	3.4
	δ ¹⁸ O _{NO3} (‰)	0.6	-0.4	0.4	-1.7	-0.4	-1.4	-4.6	1.9	4.1	1.4	4.8
212 km Site #4		6/20/07	7/16/07	8/29/07	9/26/07	10/24/07	11/29/07	2/8/08	4/4/08	5/10/08	6/13/08	7/23/08
	NO ₃ (mg/L)	0.38	0.27	0.21	0.25	0.33	0.50	0.48	0.44	0.33	0.74	0.61
	Cl (mg/L)	1.7	1.3	1.6	2.0	2.0	2.0	1.5	1.5	3.0	3.2	1.3
	δ ¹⁵ N _{NO3} (‰)	3.5	6.9	6.6	6.3	5.9	5.8	4.4	7.4	9.5	5.1	5.3
	δ ¹⁸ O _{NO3} (‰)	3.4	2.1	0.6	-0.2	-1.5	-1.4	-1.5	1.1	-0.9	7.7	3.0

571 km	NO ₃ (mg/L)	6/19/07	7/17/07	8/30/07	9/28/07	10/26/07	11/29/07		4/3/08	5/9/08	6/11/08	7/21/08
Site #19	Cl (mg/L)	1.40	0.07	1.35	1.68	3.18	6.66	-	4.75	1.87	1.70	0.64
	δ ¹⁵ N _{NO3} (‰)	4.1	5.0	7.0	7.2	8.2	9.7	-	9.9	13.9	4.8	5.1
	δ ¹⁸ O _{NO3} (‰)	6.4	11.4	9.8	9.1	7.1	7.5	-	8.6	11.0	7.4	9.3
		-8.5	3.3	-5.9	-8.5	-10.7	-10.2	-	-8.7	-2.5	-5.3	0.5
Prairie Sites:												
Highwood R.		6/19/07	7/17/07	8/30/07	9/29/07	10/25/07	11/29/07		4/4/08	5/10/08	6/10/08	7/21/08
272 km	NO ₃ (mg/L)	0.25	<0.04	0.09	<0.04	0.20	1.32	-	1.13	0.40	0.26	0.25
Site #6	Cl (mg/L)	1.5	1.8	2.6	2.4	2.7	7.4	-	5.3	4.9	1.4	1.7
	δ ¹⁵ N _{NO3} (‰)	5.1	6.4	10.3	11.0	10.2	10.4	-	10.3	7.2	7.4	11.2
	δ ¹⁸ O _{NO3} (‰)	-17.8	-18.2	-18.4	-18.0	-18.0	-19.3	-	-18.7	-18.9	-17.9	-18.7
Crowfoot Ck.					9/28/07	10/26/07	11/30/07		4/3/08	5/10/08	6/12/08	7/22/08
406 km	NO ₃ (mg/L)	-	-	-	<0.04	0.04	<0.04	-	5.75	<0.04	0.77	0.29
Site #9	Cl (mg/L)	-	-	-	13.6	16.8	37.9	-	33.9	29.0	32.8	13.9
	δ ¹⁵ N _{NO3} (‰)	-	-	-	3.8	11.9	6.7	-	7.1	6.3	10.6	6.6
	δ ¹⁸ O _{NO3} (‰)	-	-	-	23.0	30.0	24.5	-	23.5	23.5	6.5	25.1
481 km	NO ₃ (mg/L)				9/28/07	10/26/07	11/30/07		4/3/08	5/9/08	6/11/08	7/22/08
Site #10	Cl (mg/L)	-	-	-	<0.04	4.46	6.46	-	3.18	0.11	0.43	0.25
	δ ¹⁵ N _{NO3} (‰)	-	-	-	9.7	9.3	11.3	-	9.2	15.0	6.6	5.8
	δ ¹⁸ O _{NO3} (‰)	-	-	-	10.1	7.9	7.0	-	8.7	12.4	5.2	8.3
		-	-	-	14.4	-10.3	-10.1	-	-6.9	10.6	15.6	20.9
487 km	NO ₃ (mg/L)									5/9/08	6/12/08	7/22/08
Site #12	Cl (mg/L)	-	-	-	-	-	-	-	-	0.06	4.43	0.31
	δ ¹⁵ N _{NO3} (‰)	-	-	-	-	-	-	-	-	19.5	4.5	5.0
	δ ¹⁸ O _{NO3} (‰)	-	-	-	-	-	-	-	-	8.4	11.3	9.0
		-	-	-	-	-	-	-	-	26.3	1.5	3.6

498 km Site #13	NO ₃ (mg/L)	-	-	-	9/28/07	10/26/07	-	-	-	5/9/08	6/12/08	7/22/08
	Cl (mg/L)	-	-	-	<0.04	0.68	-	-	-	1.01	0.46	0.24
	δ ¹⁵ N _{NO3} (‰)	-	-	-	7.6	8.0	-	-	-	17.1	17.4	5.1
	δ ¹⁸ O _{NO3} (‰)	-	-	-	5.0	9.0	-	-	-	10.4	5.5	5.9
503 km Site #14	NO ₃ (mg/L)	-	-	-		10/26/07			4/3/08	5/9/08	6/11/08	7/22/08
	Cl (mg/L)	-	-	-	-	<0.04	-	-	0.04	0.02	0.51	<0.04
	δ ¹⁵ N _{NO3} (‰)	-	-	-	-	8.8	-	-	7.7	9.6	9.3	11.4
	δ ¹⁸ O _{NO3} (‰)	-	-	-	-	7.8	-	-	-2.8	7.2	10.4	n.d.
516 km Site #16	NO ₃ (mg/L)	-	-	-	9/28/07	10/26/07			4/3/08	5/9/08	6/11/08	7/21/08
	Cl (mg/L)	-	-	-	<0.04	0.01	-	-	0.01	<0.04	x	x
	δ ¹⁵ N _{NO3} (‰)	-	-	-	11.6	20.0	-	-	15.5	12.9	12.8	11.1
	δ ¹⁸ O _{NO3} (‰)	-	-	-	n.d.	9.5	-	-	8.0	7.6	n.d.	n.d.
524 km Site #17	NO ₃ (mg/L)	-	-	-	n.d.	28.9	-	-	25.0	24.6	n.d.	n.d.
	NO ₃ (mg/L)	-	-	-	9/28/07	10/26/07			5/9/08	6/11/08	7/21/08	
	Cl (mg/L)	-	-	-	0.04	0.08	-	-	-	0.31	0.48	x
	δ ¹⁵ N _{NO3} (‰)	-	-	-	7.2	10.9	-	-	-	17.8	25.5	4.5
557 km Site #18	NO ₃ (mg/L)	-	-	-	7.9	3.7	-	-	-	6.3	17.8	n.d.
	Cl (mg/L)	-	-	-	1.2	14.6	-	-	-	1.0	4.2	n.d.
	δ ¹⁵ N _{NO3} (‰)	-	-	-	9/28/07	10/26/07			4/3/08	5/9/08	6/11/08	7/21/08
	δ ¹⁸ O _{NO3} (‰)	-	-	-	<0.04	0.08	-	-	0.02	0.19	<0.04	x
557 km Site #18	NO ₃ (mg/L)	-	-	-	8.9	9.2	-	-	10.2	15.0	8.6	8.7
	Cl (mg/L)	-	-	-	5.1	-0.5	-	-	6.5	4.6	15.6	n.d.
	δ ¹⁵ N _{NO3} (‰)	-	-	-	28.8	12.0	-	-	28.8	16.8	24.6	n.d.
	δ ¹⁸ O _{NO3} (‰)	-	-	-								

					9/28/07	10/26/07				5/9/08	6/11/08	7/21/08
572 km	NO ₃ (mg/L)	-	-	-	<0.04	<0.04	-	-	-	0.05	<0.04	<0.04
Site #20	Cl (mg/L)	-	-	-	11.2	15.2	-	-	-	12.2	12.1	11.9
	δ ¹⁵ N _{NO3} (‰)	-	-	-	n.d.	-0.2	-	-	-	6.3	n.d.	n.d.
	δ ¹⁸ O _{NO3} (‰)	-	-	-	n.d.	6.5	-	-	-	14.7	n.d.	n.d.
WWTPs at:												
									4/4/08	5/10/08		7/22/08
231 km	NO ₃ (mg/L)	-	-	-	-	-	-	-	48.81	56.72	-	65.53
(BBWWTP)	NH ₄ (mg/L)	-	-	-	-	-	-	-	0.3	0.4	-	0.2
	Cl (mg/L)	-	-	-	-	-	-	-	98.2	83.8	-	77.2
	δ ¹⁵ N _{NO3} (‰)	-	-	-	-	-	-	-	7.7	8.3	-	7.7
	δ ¹⁵ N _{NH4} (‰)	-	-	-	-	-	-	-	n.d.	21.8	-	13.2
	δ ¹⁸ O _{NO3} (‰)	-	-	-	-	-	-	-	-9.6	-9.5	-	-9.7
									4/4/08	5/10/08		7/23/08
245 km	NO ₃ (mg/L)	-	-	-	-	-	-	-	0.30	0.06	-	0.38
(FCWWTP)	NH ₄ (mg/L)	-	-	-	-	-	-	-	30.4	28.8	-	28.7
	Cl (mg/L)	-	-	-	-	-	-	-	119.7	96.9	-	92.3
	δ ¹⁵ N _{NO3} (‰)	-	-	-	-	-	-	-	10.2	12.7	-	9.2
	δ ¹⁵ N _{NH4} (‰)	-	-	-	-	-	-	-	8.3	9.1	-	8.0
	δ ¹⁸ O _{NO3} (‰)	-	-	-	-	-	-	-	1.8	8.4	-	0.0

- : not sampled

n.d.: not detected

x : data not reported due to possible measurement error

Table 2 Estimates of annual average discharges and NO₃ loads of the Bow River from Lake Louise to Ronalane and unknown sources or sinks along the flow path. Discharge and NO₃ load contributions from the Rocky Mountain headwaters, Calgary's WWTPs and the prairie reaches are given in percentages. Sources include the Elbow and Highwood Rivers, two wastewater treatment plant effluents (BBWWTP and FCWWTP), and three irrigation canals (WID, BRID, and EID).

Site #	Dist. (km)	Total Estimated		Estimated Sources or Sinks between Stations		Estimated Headwater Input		Estimated WWTP Input		Estimated Prairie Input	
		Discharge (x 10 ⁹ L)	NO ₃ Load (kt)	Discharge (x 10 ⁹ L)	NO ₃ Load (kt)	Discharge (%)	NO ₃ Load (%)	Discharge (%)	NO ₃ Load (%)	Discharge (%)	NO ₃ Load (%)
1	0	317	0.09	-	-	100	100	0	0	0	0
2	99	1309	0.34	992	0.25	100	100	0	0	0	0
3	179	3064	1.37	1755	1.03	100	100	0	0	0	0
4	212	3026	1.41	-38	0.04	100	100	0	0	0	0
<i>Elbow R.</i>	<i>~229</i>	<i>+315</i>	<i>+0.07</i>	-	-	-	-	-	-	-	-
<i>WID</i>	<i>~229</i>	<i>-93</i>	<i>-0.04</i>	-	-	-	-	-	-	-	-
<i>BBWWTP</i>	<i>230</i>										
<i>+ FCWWTP</i>	<i>245</i>	<i>+167</i>	<i>+9.18</i>	-	-	-	-	-	-	-	-
<i>Highwood R.</i>	<i>272</i>	<i>+695</i>	<i>+0.19</i>	-	-	-	-	-	-	-	-
<i>BRID</i>	<i>~301</i>	<i>-295</i>	<i>-0.65</i>	-	-	-	-	-	-	-	-
7	302	3687	8.92	-128	-1.24	99.0	17	4.2	96	-3.2	-13
<i>EID</i>	425	-489	-1.98	-	-	-	-	-	-	-	-
11	482	3158	*	-40	*		*	-	*	-	*
19	571	3304	*	146	*	95.7	*	4.1	*	0.3	*

- : not applicable

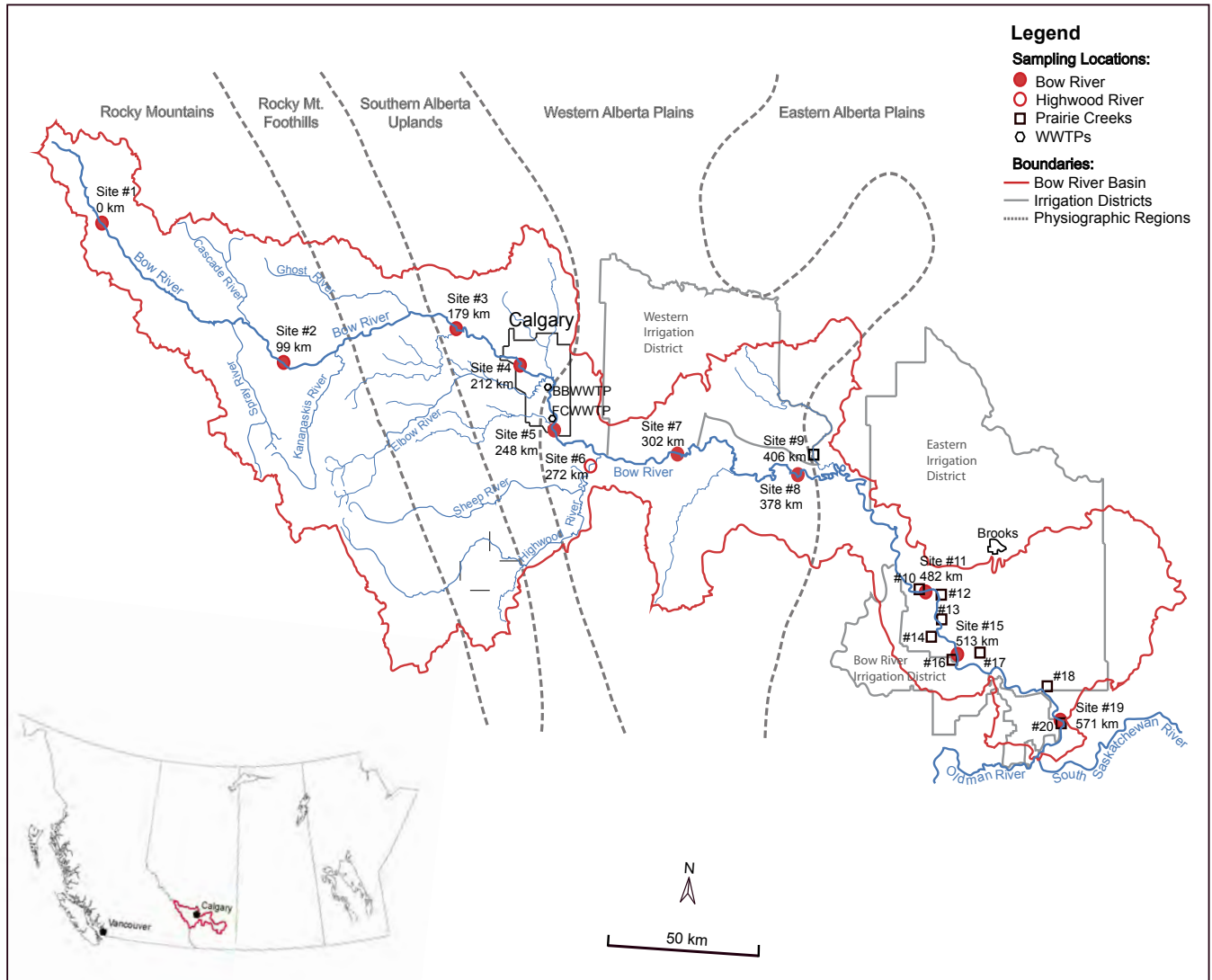
* : nitrate fluxes not reported since a majority of NO₃ concentrations are not correlated with flow (open circles in Figure 4b)

Italic: major sources of input (tributaries and WWTPs) or withdrawal (main irrigation canals) in and downstream of Calgary

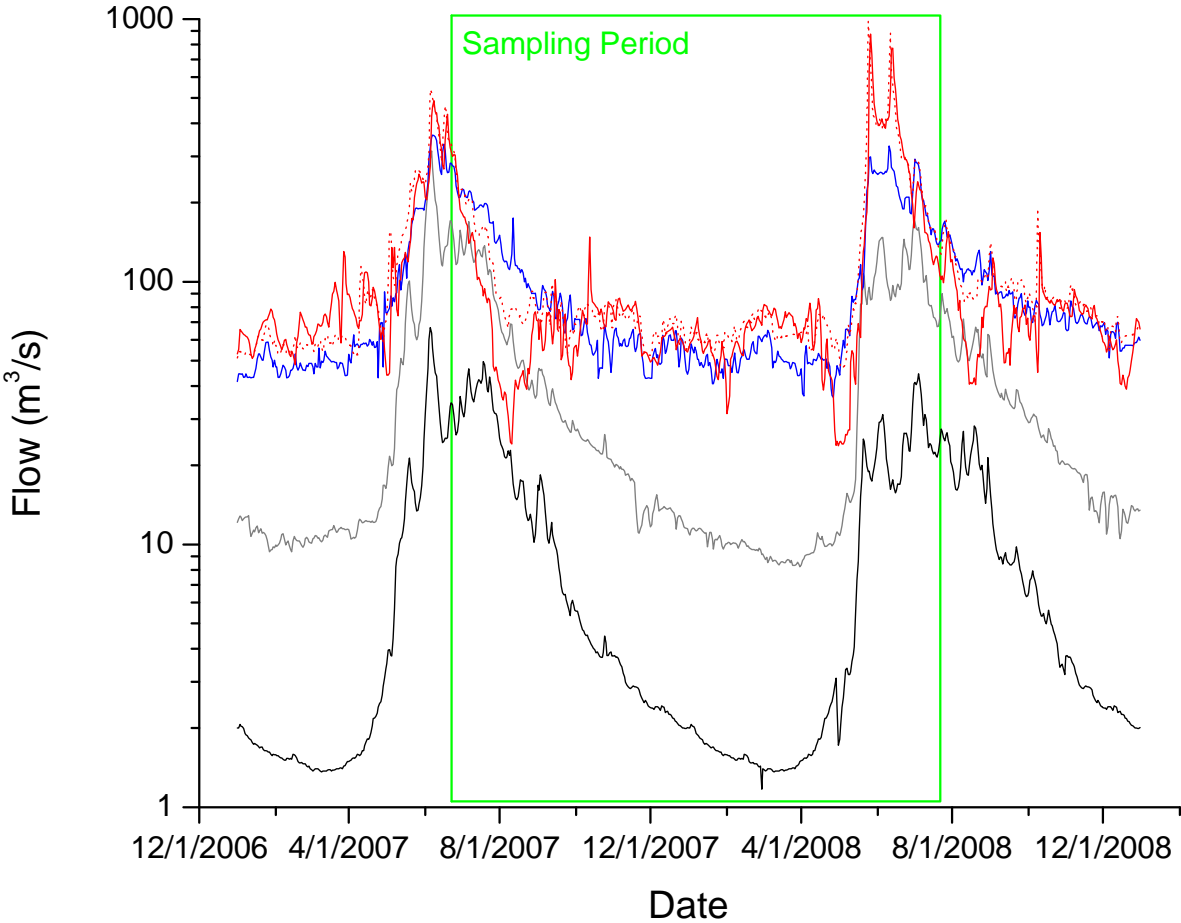
Table 3 Summary of results and the parameters used in the isotope mass balance calculations. The estimated range of isotopic values from conservative mixing of NO_3 and nitrified NH_4 are shown in italics. The $\delta^{18}\text{O}_{\text{NO}_3}$ values (underlined) from presumed nitrification of NH_4 are estimated using isotopic mass balance whereas the rest of the isotopic values are measured.

	BBWWTP		FCWWTP		Total N
	NO ₃ -N	NH ₄ -N	NO ₃ -N	NH ₄ -N	
Flux (kt/yr)	2.07	0.18	0.002	0.88	3.15
Mass Load %	66.0	5.7	0.1	28.2	100
$\delta^{15}\text{N}$ (‰)	7.7 to 8.3	13.2 to 21.8	9.2 to 12.7	8.0 to 9.1	+8.1 to +9.3 (as $\delta^{15}\text{N}_{\text{NO}_3}$)
$\delta^{18}\text{O}$ (‰)	-9.5 to -9.7	<u>-4.6</u>	0.0 to 8.4	<u>-4.6</u>	-7.8 to -8.0 (as $\delta^{18}\text{O}_{\text{NO}_3}$)

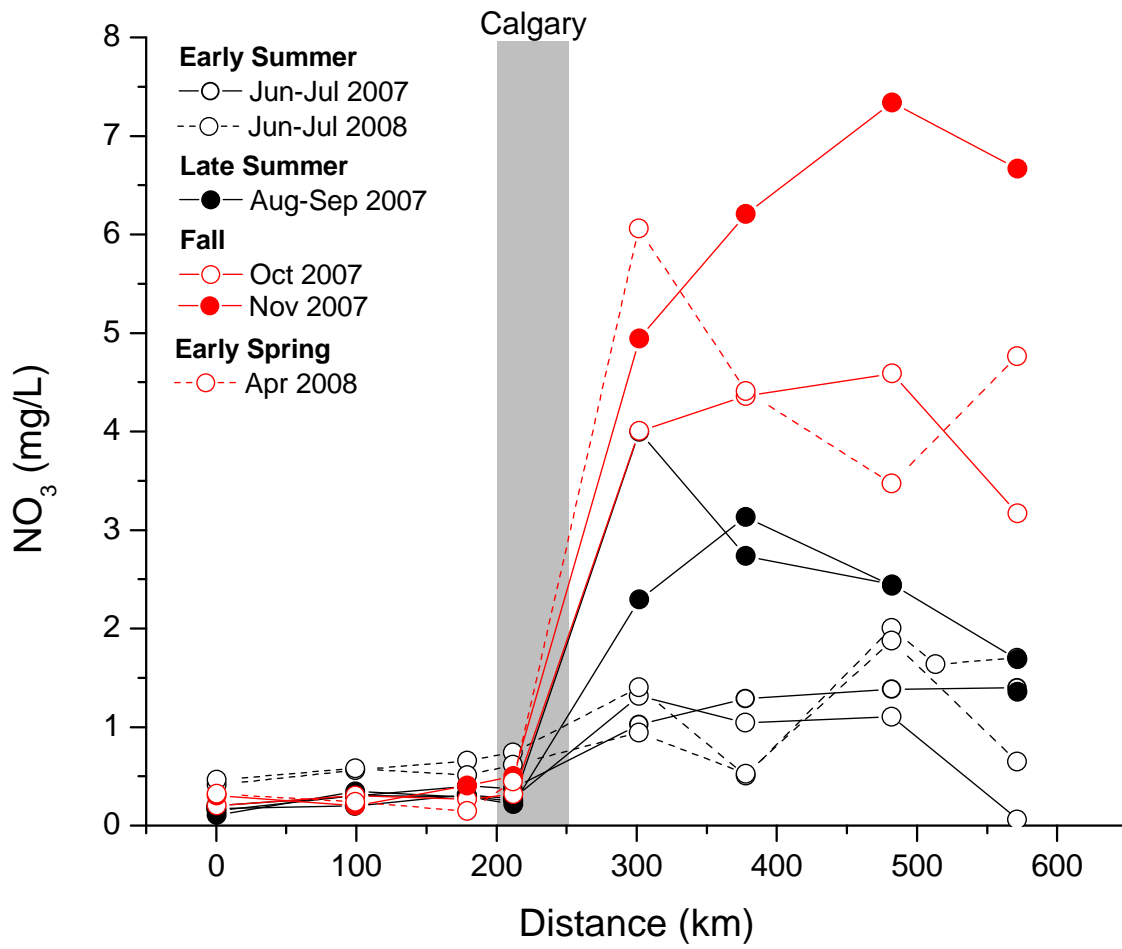
Chao et al. Figure 1



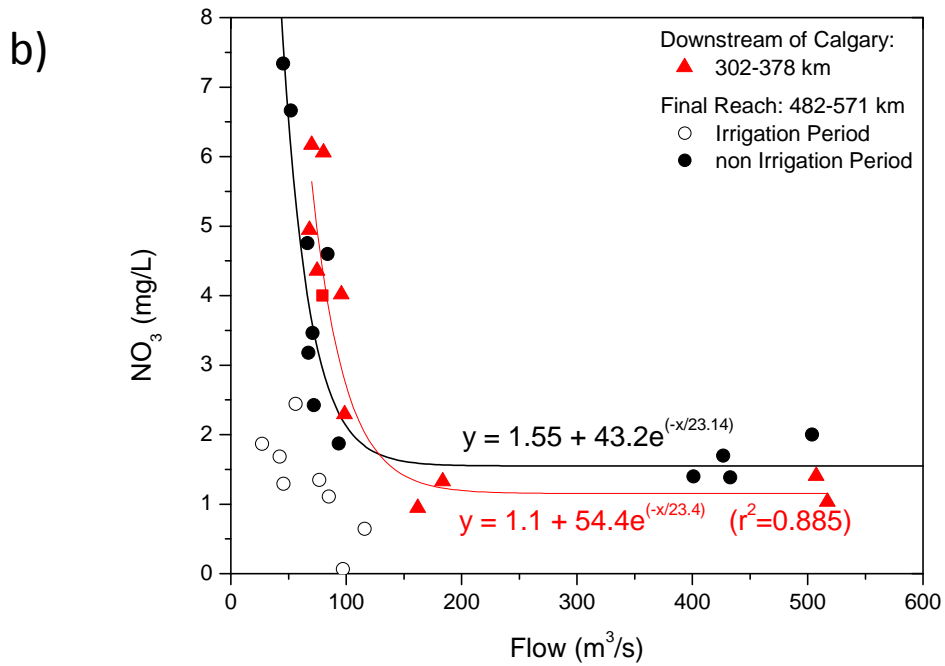
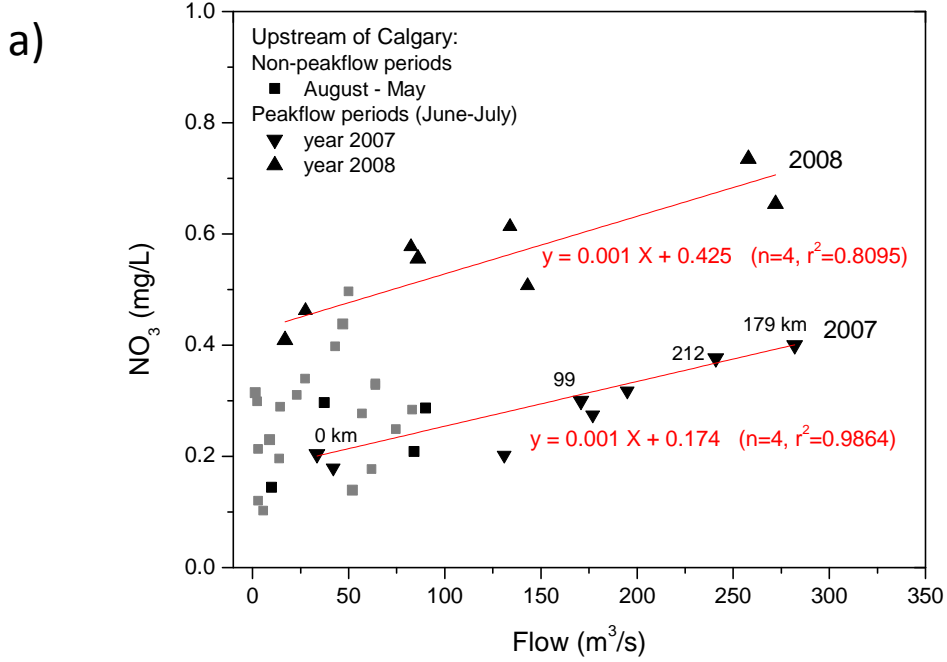
Chao et al. Figure 2



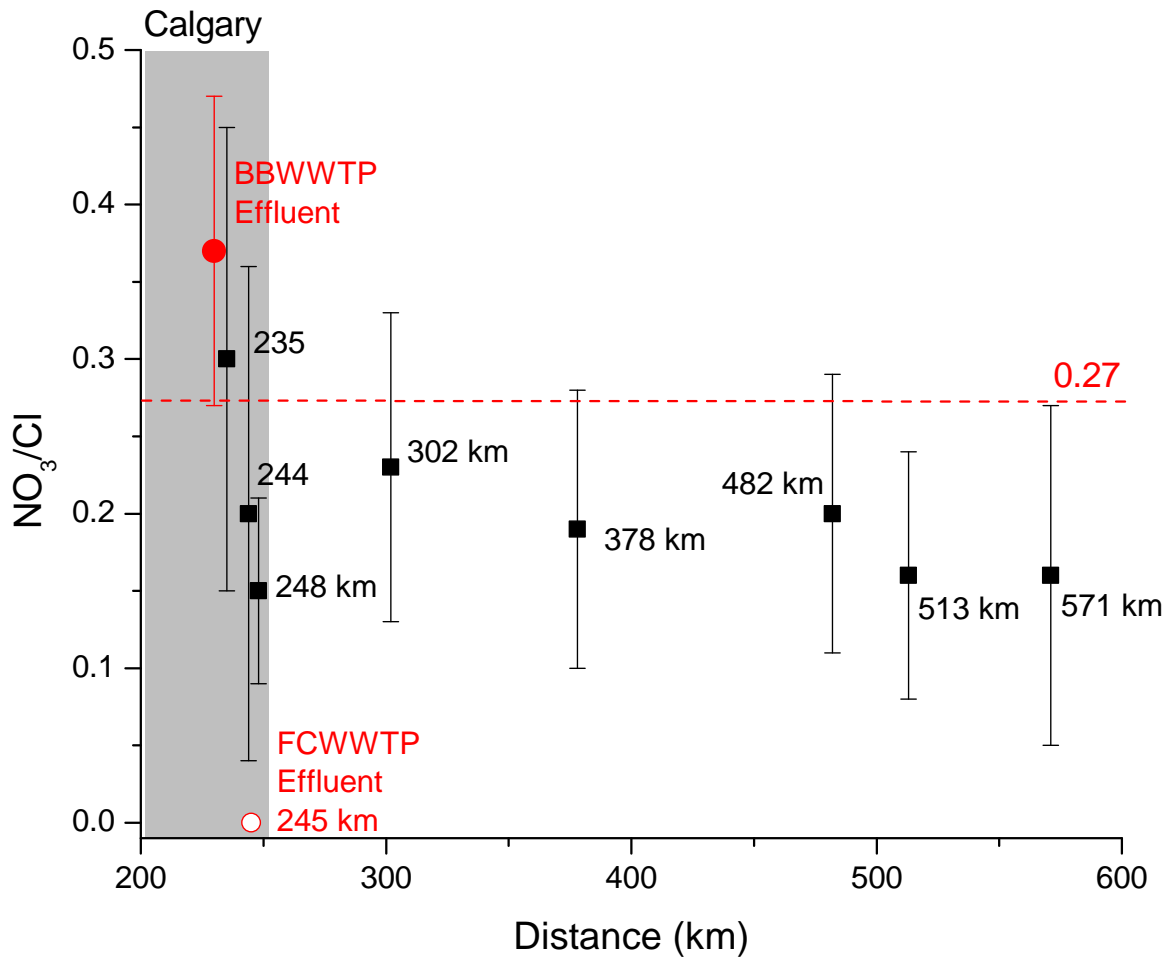
Chao et al. Figure 3



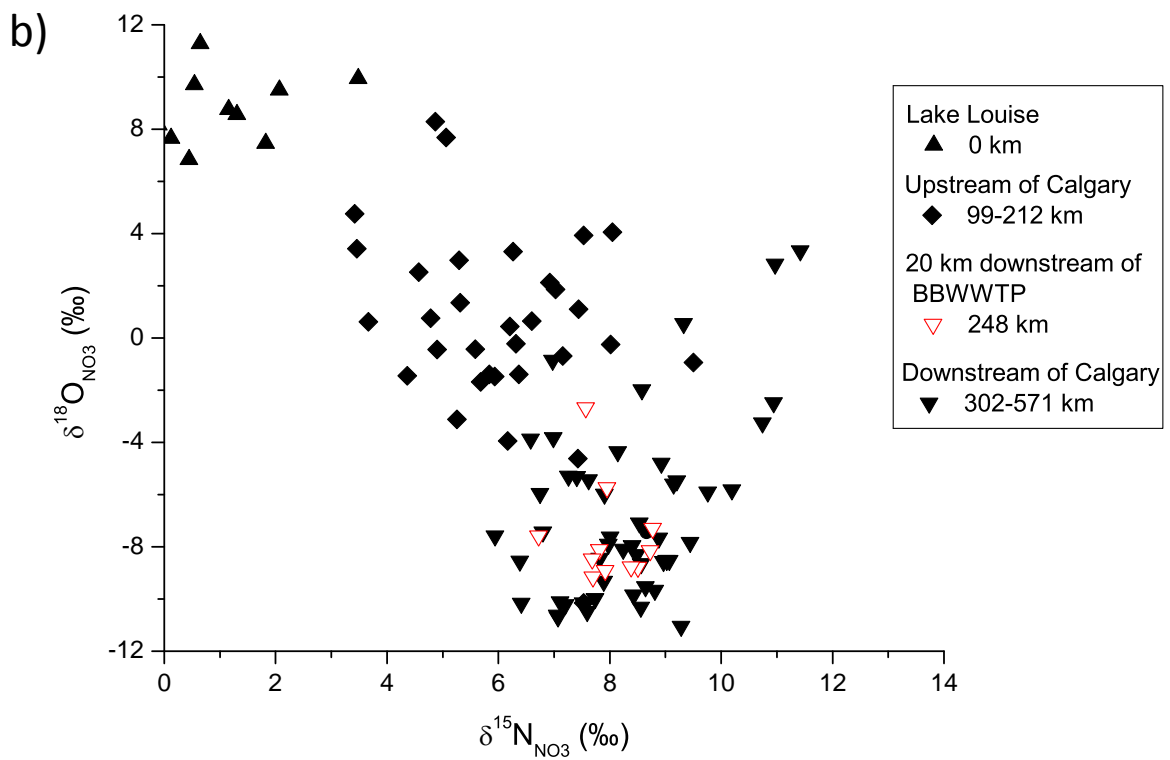
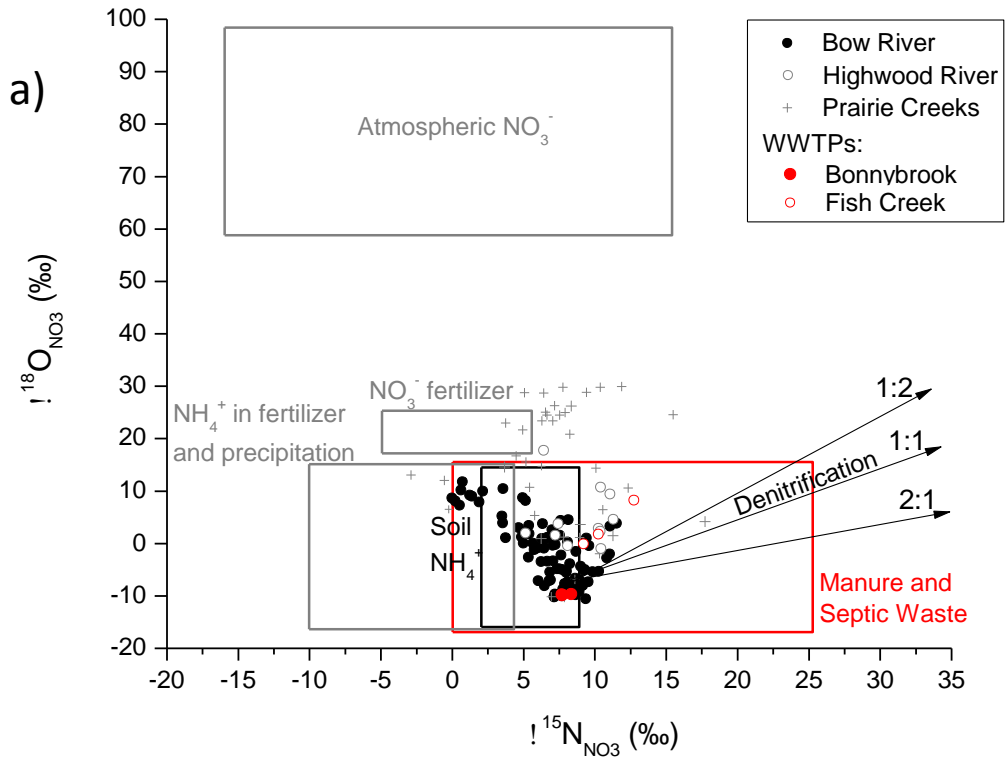
Chao et al. Figure 4a and 4b



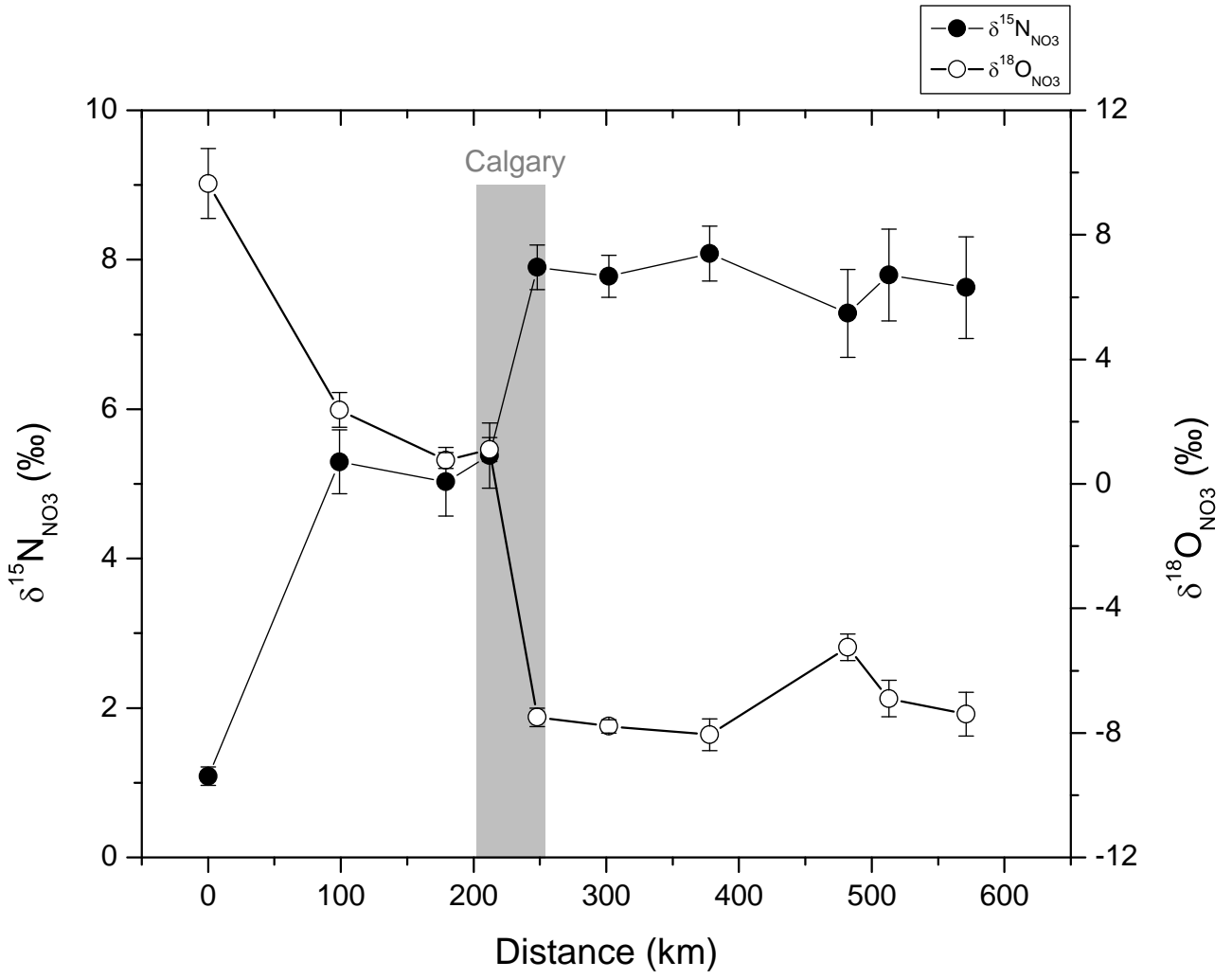
Chao et al. Figure 5



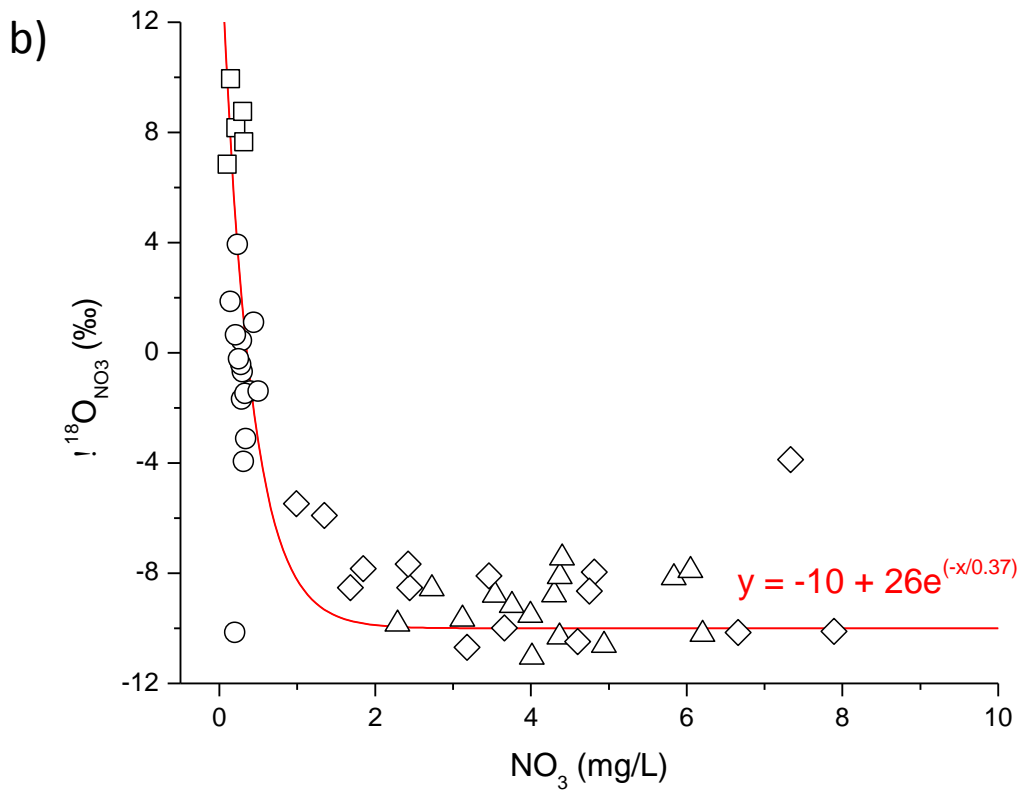
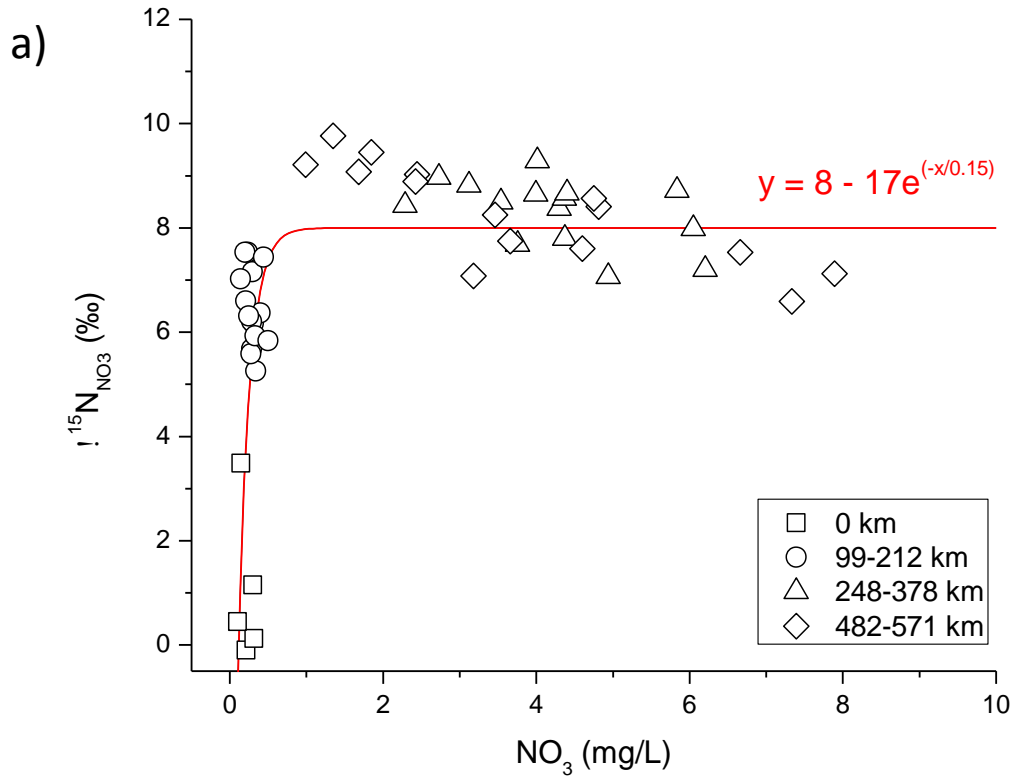
Chao et al. Figure 6a and 6b



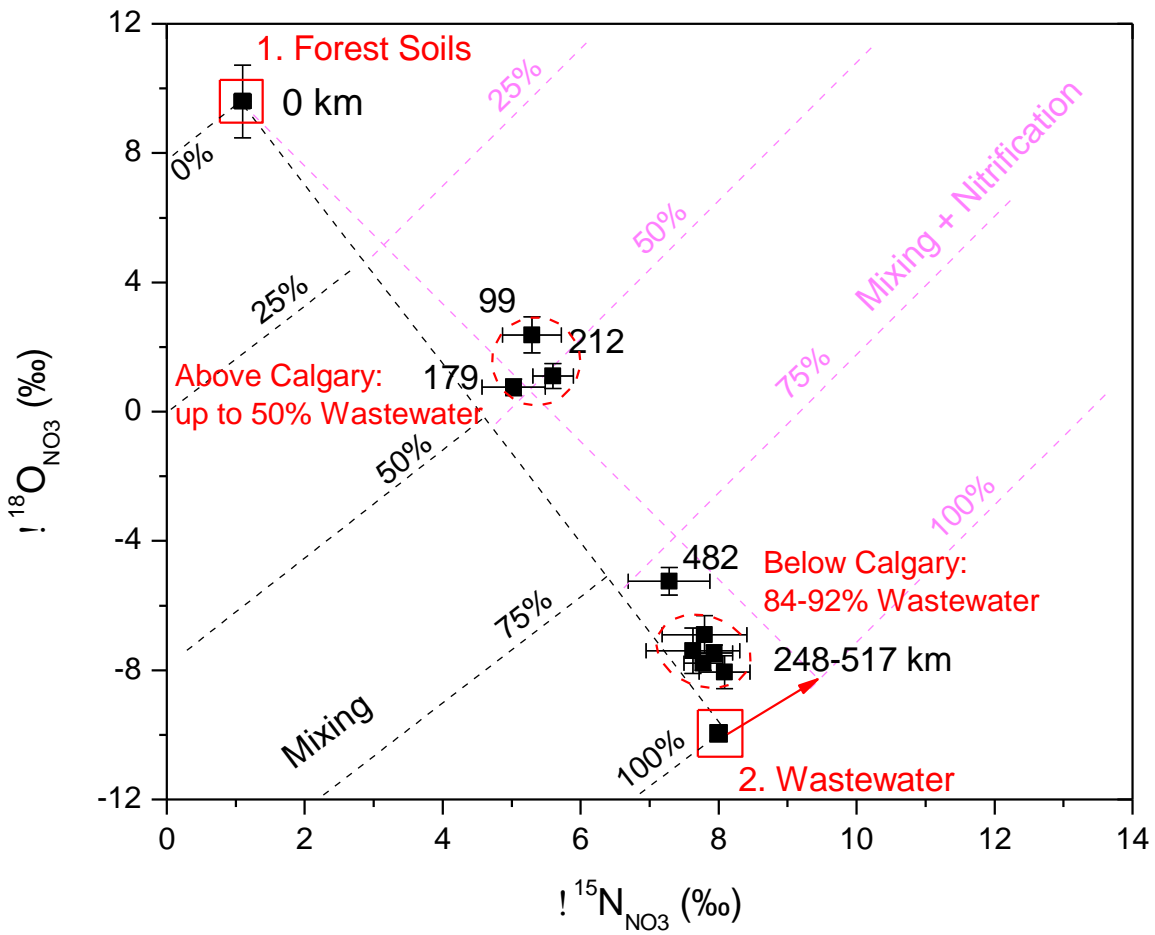
Chao et al. Figure 7



Chao et al. Figure 8a and 8b



Chao et al. Figure 9



MODELLING TEMPERATURE, BODY SIZE, PREY DENSITY, AND STREAM GRADIENT IMPACTS ON LONGITUDINAL PATTERNS OF POTENTIAL PRODUCTION OF DRIFT-FEEDING TROUT

J. J. LALIBERTE^a, J.R. POST^{a*}, J.S. ROSENFELD^b AND J.A. MEE^a

^a *University of Calgary, Department of Biological Sciences, Calgary, Alberta, Canada*

^b *Ministry of the Environment, Province of British Columbia, Vancouver, British Columbia, Canada*

ABSTRACT

In this study, we modelled idealized stream reaches using empirical hydrodynamic and bioenergetic parameters to predict how rainbow trout production depends on physical and biological variations across a downstream gradient, and we compared these downstream effects in a low and high-gradient stream reach. We found that longitudinal production potential (i.e. net rate of energetic intake per 100 m of stream length) generally increased with increasing stream size when stream gradient was low. This was not the case, however, for high-gradient streams, wherein maximum longitudinal production potential was associated with middle or low stream size ($Q_{MAD} = 2.5$ to $25 \text{ m}^3 \text{ s}^{-1}$). Areal production potential (net rate of energetic intake per m^2 of wetted stream bed) reached a maximum at low stream size ($Q_{MAD} = 2.5 \text{ m}^3 \text{ s}^{-1}$) with both high and low gradients. We also showed that high stream temperature and low drift density could potentially cause adult rainbow trout to be excluded from stream reaches with high flow. The models presented here have a stronger mechanistic basis for predicting fish production across heterogeneous stream environments and provide more nuanced predictions in response to variation in environmental features than their physical habitat-based predecessors. Copyright © 2016 John Wiley & Sons, Ltd.

KEY WORDS: hydraulic geometry; river continuum; fish production potential; invertebrate drift; fish bioenergetics; stream size; net rate of energy intake modelling

Received 16 October 2015; Revised 14 April 2016; Accepted 13 May 2016

INTRODUCTION

Stream systems are highly complex and change as they flow downstream (Lotrich, 1973; Naiman *et al.*, 1987). The dominant paradigm for describing the downstream changes in fluvial processes and the resulting changes in instream habitat, biodiversity, and community structure remain the river continuum concept (Vannote *et al.*, 1980) and its derivatives (e.g. the serial discontinuity concept; Ward and Stanford, 1995; Rice *et al.*, 2001; Stanford and Ward, 2001). The mechanistic connection between fluvial processes and biological responses across the river continuum, however, is poorly understood. In particular, the use of physical models of stream flow across a longitudinal gradient to predict and understand changes in fish production and abundance has seen surprisingly limited development (Rosenfeld *et al.*, 2007).

Physical habitat structure (e.g. water depth, water velocity, cover, and substrate composition) is important for determining animal abundance and species composition within a stream (Bovee *et al.*, 1998; Peeters and Gardeniers, 1998;

Vadas and Orth, 2001). Physical habitat (hydraulic) models produce an estimate of habitat quality within a stream reach called weighted useable area (WUA) (Bovee, 1982; Milhous *et al.*, 1989; Jowett, 1998). WUA within a reach is calculated as the sum of the products of the areas and habitat suitability index values for all cells within a reach (Vismara *et al.*, 2001). Physical habitat models are most often used for assessing not only how availability of fish habitat changes with flows (Jowett, 1998) but can also be used to provide a comparison of WUA (i.e. fish habitat quantity and quality) between stream reaches that vary in gradient and stream size (Laliberte *et al.*, 2014). To translate WUA into flow management recommendations for fish production or to understand variation in fish production along a continuum in stream size, it is generally assumed that fish population abundance and/or biomass is linearly related to WUA (Bovee and Milhous, 1978; Anderson *et al.*, 2006). There is, however, very little empirical support for linear WUA–biomass relationships (Scott and Shirvell, 1987; Rosenfeld, 2003). Furthermore, many argue that fish habitat preference is determined by complex processes involving many abiotic and biotic variables, which are all influenced by stream discharge (Railsback and Rose, 1999), many of which are ignored by most physical habitat models (Anderson *et al.*, 2006).

*Correspondence to: J. R. Post, Department of Biological Sciences, University of Calgary, Calgary, Alberta T2N 1N4, Canada.
E-mail: jrpost@ucalgary.ca

Unlike physical habitat models, bioenergetic models consider how fish respond to numerous interacting abiotic and biotic variables. Bioenergetic models accomplish this by combining models of drift transport and drift-foraging behaviour to provide spatially explicit estimates of the net rate of energetic intake (NREI) or production rates as a measure of habitat quality within a study reach (Kelly *et al.*, 2005; Hayes *et al.*, 2007; Piccolo *et al.*, 2014). Production is the rate of somatic and gonadal tissue growth during a given period of time for an individual or entire population (Mahon and Balon, 1985). Bioenergetic models have been shown to generate reasonable predictions of habitat selection (Hughes and Dill, 1990), behaviour (Railsback and Harvey, 2002), and growth (Rosenfeld and Taylor, 2009) in contrast with predictions from physical habitat models (Railsback *et al.*, 2003). As a result, bioenergetic models are emerging as more biologically realistic alternatives to physical habitat models for instream flow management (Anderson *et al.*, 2006; Rosenfeld *et al.*, 2014; Weber *et al.*, 2014; Hayes *et al.*, 2015).

In this study, our objective was to make the mechanistic links between stream characteristics and fish bioenergetics based on empirical species-specific allometric relationships governing bioenergetics and to draw conclusions about how fish production and biomass are expected to vary with respect to stream size [i.e. mean annual discharge (Q_{MAD})], stream gradient, fish size, prey density, and water temperature. We built upon the physical habitat model used to predict longitudinal patterns in habitat quantity and quality (i.e. WUA) for rainbow trout (Laliberte *et al.*, 2014) by incorporating the foraging energetics model framework as developed by Kelly *et al.* (2005). We hypothesized that combining physical and bioenergetic models would provide a more nuanced depiction of the habitat selection and production of drift-feeding trout across heterogeneous stream environments. Based on the longitudinal patterns of WUA modelled by Laliberte *et al.* (2014), we predicted that

the production potential (i.e. NREI) of rainbow trout would increase with increasing stream size (e.g. with increasing stream order) and would be greater in low-gradient stream reaches than in high-gradient stream reaches, as more rapid downstream increases in water velocity at higher gradients would generate less optimal foraging habitat.

MATERIALS AND METHODS

Three-dimensional stream template

To set up the hydraulic model framework, we used the idealized two-dimensional (2D) hydrodynamic models from Laliberte *et al.* (2014) for streams of varying size (i.e. along a river continuum) with high contrasting and low gradients (Table I) based on the hydraulic geometry parameter values from Jowett (1998) and Leopold and Maddock (1953). These were virtual, idealized streams modelled with characteristics based on empirical hydrodynamic parameters and were not based on actual surveyed reaches. The *StreamTubes* modelling program uses river hydraulic information to determine invertebrate drift transport and to predict foraging energetic of drift-feeding salmonids (Kelly *et al.*, 2005). The program converts a 2D hydraulic model into a cross-sectional bundle of hydraulic cells, wherein each cell conveys an equal proportion of the river's total flow. These cells are aligned in a longitudinal array of tubes (i.e. streamtubes) such that, within the modelled reach, the area of each tube can vary with longitudinal position as the 2D distribution of flow rates changes downstream. Calibrated River2D hydraulic models (Steffler and Blackburn, 2002) from Laliberte *et al.* (2014) were used as inputs to the *StreamTubes* modelling program (Kelly *et al.*, 2005) to provide the foraging energetics model with the appropriately formatted hydraulic data for stream reaches. The *StreamTubes* program allowed modelling of vertical and lateral invertebrate drift dispersal (advection/diffusion)

Table I. Hydraulic geometries, bed slopes, and numbers of streamtube divisions for different stream sizes in high-gradient and low-gradient stream reaches

Stream characteristics	High-gradient stream reaches					Low-gradient stream reaches				
	H1	H2	H3	H4	H5	L1	L2	L3	L4	L5
Q_{MAD} ($m^3 s^{-1}$)	1.0	2.5	10.0	25.0	50.0	1.0	2.5	10.0	25.0	50.0
w (m)	7.800	12.333	24.666	39.000	55.154	9.230	14.594	29.188	46.150	65.266
d (m)	0.370	0.465	0.658	0.827	0.984	0.260	0.375	0.653	0.942	1.243
v ($m s^{-1}$)	0.360	0.453	0.640	0.805	0.957	0.420	0.460	0.529	0.579	0.621
Slope	0.0090	0.0063	0.0037	0.0026	0.0020	0.0090	0.0042	0.0013	0.0006	0.0004
Cross-sectional divisions, wherein each division defines a cell with equivalent flow in the StreamTubes model (Kelly <i>et al.</i> , 2005)										
Lateral	10	10	20	40	40	10	10	20	40	40
Vertical	1	3	4	5	5	5	5	5	5	5

The physical stream dimensions of channel width (w), depth (d), and mean velocity (v) are all at mean annual discharge (Q_{MAD}).

across the stream channel. As each streamtube represents a zone of equal discharge, they can vary dramatically in size, depending on the local hydraulic properties of the stream being modelled.

We sampled 2D cross sections of our modelled reach every 0.5 m (longitudinally) to depict a pseudo-three-dimensional (3D) stream reach. The 0.5 m longitudinal spacing was deemed fine enough to ensure a high degree of spatial resolution within reaches and large enough for all fish size classes to fit lengthwise into a given cell. To maintain sufficient lateral spatial resolution, it was necessary to increase the number of lateral streamtubes with increasing stream size (Q_{MAD} , Table I). We specified enough vertical streamtubes to reflect the vertical velocity profiles present in streams in nature. We initially set the number of vertical streamtubes to five, and then adjusted the number of vertical divisions, when necessary, so that overlapping streamtubes (an unforeseen problem in the software) would not occur (Table I). In the high-gradient cases, the number of vertical streamtubes increased from one in the smallest reach to five for stream sizes exceeding $10 \text{ m}^3 \text{ s}^{-1}$. All stream reaches with low gradient were able to accommodate five vertical streamtubes.

Invertebrate drift transport model development

The parameters required to model invertebrate drift are taxa-specific size of drifting invertebrates, dry weight, initial drift density, settling rate, entry rate, and time spent near the bed following a near bed release. We modelled Ephemeroptera larvae with a total length of 6 mm and a dry weight of 0.00115 g, based on the gill raker spacing and gape size (i.e. the edible size range) for Atlantic salmon (*Salmo salar*) between 75 and 500 mm FL (Wankowski, 1979; Hayes *et al.*, 2000; Hughes *et al.*, 2003) and the length–weight relationship from Smock (1980). Parameter values for Ephemeroptera were used primarily because they represent intermediate values compared with other taxa investigated by Smock (1980). Initial drift concentrations for each model run were assumed to be constant for all cells in the first (upstream) cross section. We simulated a range of initial drift concentrations (0.2, 0.4, and 0.8 m^{-3}) based on mean equilibrium values from Hayes *et al.* (2007), and we held these drift concentration values constant at the top of each modelled reach. Settling rate (SR) was set to 0.004 m s^{-1} based on an estimate for a 7.5 mm Ephemeropteran *Deliatidium* sp. (Hayes *et al.*, 2007). The entry rate parameter specifies the rate at which invertebrates enter the water column from the benthos for the bottommost streamtube cells in the modelled reach. Given a lack of empirical data on entry rate (Elliott, 1971; Ciborowski, 1983; Hayes *et al.*, 2007), we approximated entry rate using the following equilibrium relationship: drift concentration = entry rate / settling

rate. Hence, entry rates corresponding to our range of initial drift concentrations were calculated as 0.0008, 0.0016, and $0.0032 \text{ m}^2 \text{ s}^{-1}$. We set the time near bed parameter to 5 s based on estimates for Baetis and Ephemerella larvae (Elliott, 1973 2002).

Foraging energetics model

An estimate of NREI was based on the model developed by Kelly *et al.* (2005), which assimilates outputs from the 3D stream template model (i.e. *StreamTubes*) and the drift transport model with information on fish size for each life history stage (YOY, juveniles, and adults), water temperature, height of the focal point above bed, and probability of prey detection. Fork lengths were set to 0.075, 0.25, and 0.5 m for YOY, juvenile, and adult rainbow trout respectively, which correspond to weights of 8.42, 212.07, and 1359.06 g based on length–weight regression parameter values from previous work on the Bow River, Alberta (RL&L Environmental Services Ltd, 2001). We chose temperatures (8, 12, 16, and 20°C) that cover a suitable range of potential growing season temperatures. We chose a constant height of the focal point above the bed of 0.1 m as per Hayes *et al.* (2007), and we set the probability of prey detection to 0.55 as per Kelly *et al.* (2005) and Hayes *et al.* (2007).

To produce biologically meaningful reach-scale metrics of fish habitat quality based on NREI, we took the sum of positive NREI values across cells, thus representing the total productive potential (J s^{-1}), for each stream reach. We standardized this value per 100 m of stream to give a longitudinal production potential in NREI 100 m^{-1} , which is useful for understanding how total production potential (the product of habitat area and quality) changes along a drainage network. We also estimated the areal production (per wetted area) of the reach in NREI m^{-2} , which controls for longitudinal changes in channel width that affect total available habitat area (i.e. habitat quantity), such that areal production accurately represents habitat quality.

RESULTS

Within-reach patterns of drift density and productivity

Drift concentrations were always highest in streamtubes adjacent to the streambed and declined towards the water surface. The lowest observed drift concentrations occurred in streamtubes near the water surface and, most noticeably, in those streamtubes at the water's edge (Figure 1A). The vertical gradient in drift density was sharpest at the stream margins and most gradual at the stream centre or thalweg. The range of vertical variation was greatest in the larger model reaches. This was partly explained by the greater number of vertical streamtubes in large versus small stream

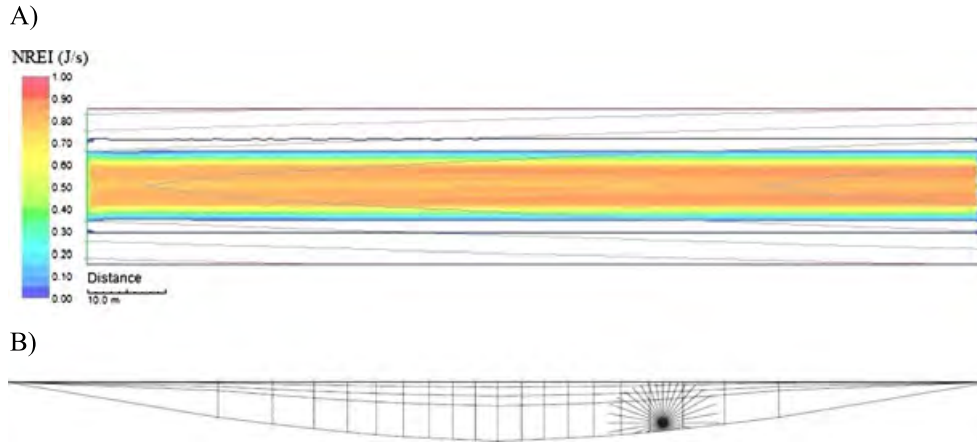


Figure 1. (A) Plan view of the spatial variation in net rate of energetic intake (NREI) ($J s^{-1}$) for adult rainbow trout in stream H3 ($Q_{MAD} = 2.5 m^3 s^{-1}$) with initial drift concentrations of $0.4 m^{-3}$ and a stream temperature of $12 ^\circ C$. (B) Cross-sectional view showing vertical and lateral streamtube divisions and the location of the highest NREI within the reach (black starburst)

when gradient was high, but this pattern was also observed in low-gradient streams where the number of vertical streamtube divisions did not vary with stream size.

In the smallest stream reaches, the NREI was found to be greatest near the centre of the channel and would decline laterally. This was found to be the case in the smallest

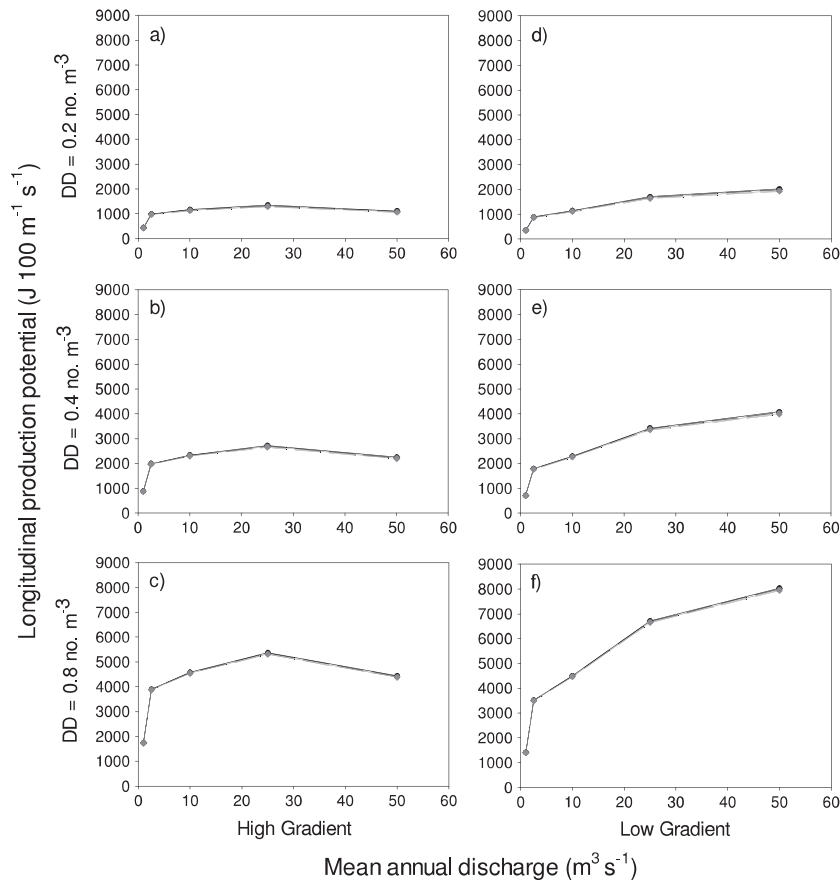


Figure 2. Downstream patterns of longitudinal production potential (NREI, $J 100 m^{-1} s^{-1}$) estimated for YOY rainbow trout in high- (a–c) and low-gradient (d–f) streams. Initial drift concentrations were 0.2 (a, d), 0.4 (b, e), and $0.8 m^{-3}$ (c, f). Note that we did analyse the effects of temperature on these relationships for YOY trout, but the lines for different water temperatures are superimposed in this figure

streams for YOY, juvenile, and adult rainbow trout. As stream size increased, the NREI peaked in longitudinal habitat corridors on either side of the stream centre and extending the length of each reach. For example, the best foraging location for an adult rainbow trout in stream H3 ($Q_{MAD}=2.5\text{ m}^3\text{ s}^{-1}$; initial drift density= 0.4 no. m^{-3} ; 12°C) is located adjacent to the stream centre near the stream bottom (Figure 1B).

Longitudinal patterns of productivity

The NREI was positive (i.e. there was some potential for production) in most scenarios except those with adult trout, low drift density (0.2 items per m^3), and high temperatures (16°C or higher). Longitudinal production potential increased with drift density and decreased at high temperatures (Figures 2–4), although the effects of temperature were very small in YOY trout (i.e. lines overlap in Figure 2). Whereas we predicted that the production potential of rainbow trout would increase with stream size, we found that in high-gradient streams, longitudinal production potential for YOY and juvenile trout plateaued or decreased

slightly beyond a Q_{MAD} of $25\text{ m}^3\text{ s}^{-1}$, regardless of temperature or drift density (Figures 2 and 3). For adult trout in high-gradient streams, the Q_{MAD} that resulted in maximum longitudinal production potential (i.e. the optimal stream size for longitudinal production potential) depended on drift density and temperature, where warmer temperatures and lower drift concentrations gave lower optimal stream sizes (Figure 4). In low-gradient streams, higher Q_{MAD} (e.g. in larger streams or higher-order streams) was always associated with higher longitudinal production potential, except for the simulations with adult trout, low drift concentrations, and high temperatures (Figure 4d).

Areal production potential was always highest when Q_{MAD} was $2.5\text{ m}^3\text{ s}^{-1}$ and declined with increasing Q_{MAD} (Figure 5–7). Areal production potential increased with higher drift density and decreased with higher temperature (Figures 5–7), although the effects of temperature were again very small for YOY trout (Figure 5). Consistent with our prediction that the production potential of rainbow trout would be greater in low-gradient streams than in high-gradient streams, longitudinal (but not areal) production potential reached higher values in low-gradient streams than

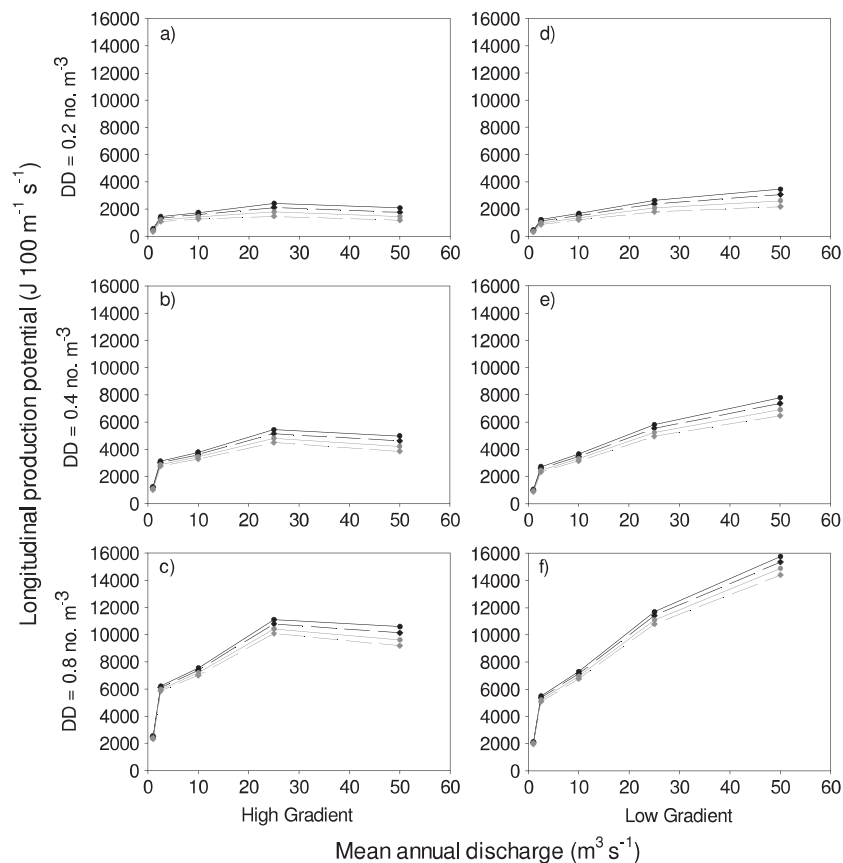


Figure 3. Downstream patterns of longitudinal production potential ($\text{J } 100\text{ m}^{-1}\text{ s}^{-1}$) estimated for juvenile rainbow trout. The effects of water temperature are displayed for 8°C (FX), 12°C (FX), 16°C (FX), and 20°C (FX). Other details as in Figure 2

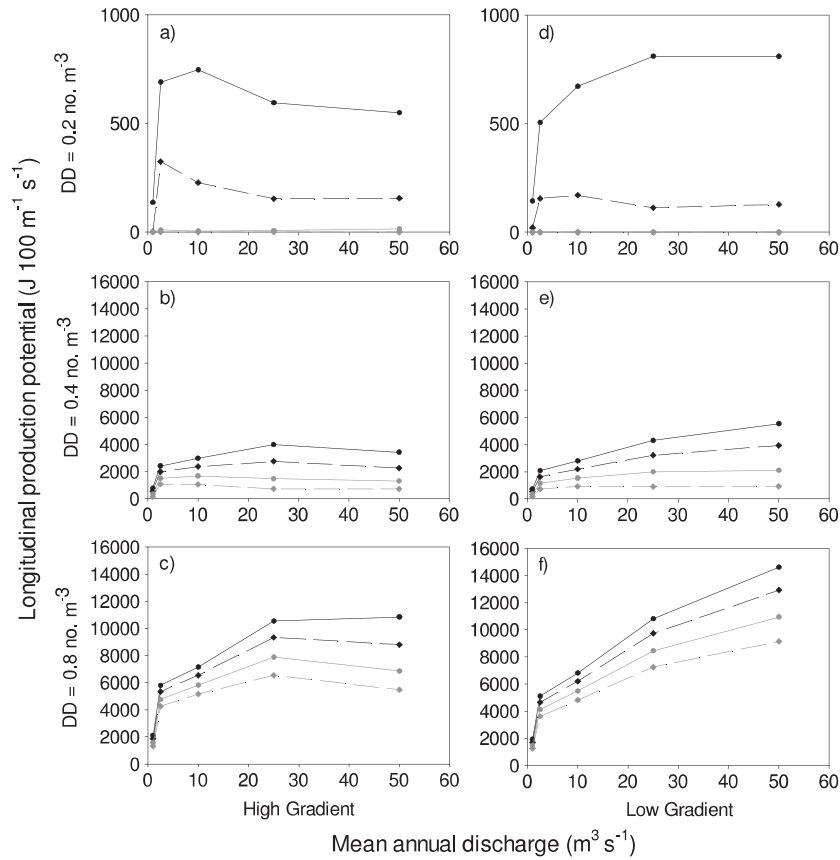


Figure 4. Downstream patterns of longitudinal production potential ($\text{J } 100 \text{ m}^{-1} \text{ s}^{-1}$) estimated for adult rainbow trout. Layout and details as in Figure 3. Note different vertical scale in the top two panels

in high-gradient streams (Figures 2–7). These contrasting trends between longitudinal and area-based measures of NREI occur because low-gradient streams are wider, and consequently, have proportionally less area with high NREI. Hence, high longitudinal measures of productivity in low-gradient streams compared with high-gradient streams are the result of increased stream area rather than higher mean productivity on a per-area basis.

DISCUSSION

We predicted that the NREI of drift-feeding trout would increase with increasing stream size and would be greater in low-gradient stream reaches than in high-gradient stream reaches. We found that similar to the pattern observed for WUA (Laliberte *et al.*, 2014), and consistent with our prediction, longitudinal production potential (i.e. NREI per 100 m of stream) increased with increasing stream size for low-gradient streams. This was not the case, however, for high-gradient streams, where longitudinal production potential plateaued or declined beyond middle or low stream size ($Q_{\text{MAD}} = 2.5$ to $25 \text{ m}^3 \text{ s}^{-1}$). In contrast, areal production

potential (NREI per m^2 of wetted stream bed) reached a maximum at low stream size ($Q_{\text{MAD}} = 2.5 \text{ m}^3 \text{ s}^{-1}$) in both high- and low-gradient streams, indicating that increasing available habitat rather than increasing habitat quality drove downstream increases in longitudinal production potential. Overall, we have demonstrated that combining bioenergetic models with physical models of fish habitat provides a more nuanced, and likely more accurate, prediction of the variability in fish production across variable stream reaches than can be derived from physical or bioenergetic models on their own.

A key assumption of our model was that the capture efficiency of fish for invertebrate prey was fixed at 55% (Kelly *et al.*, 2005; Hayes *et al.*, 2007). However, it has been shown that capture efficiency is sensitive to fish and prey size, water velocity, depth, and distance of prey from the focal point of the fish (Hill and Grossman, 1993; Rosenfeld and Taylor, 2009; Rosenfeld *et al.*, 2014), and most drift-foraging bioenergetic models now incorporate a more dynamic capture success function that accounts for these covariates (Railsback *et al.*, 2009; Rosenfeld *et al.*, 2014). A more recent version of the Kelly *et al.* (2005) model is under development that includes a variable capture success

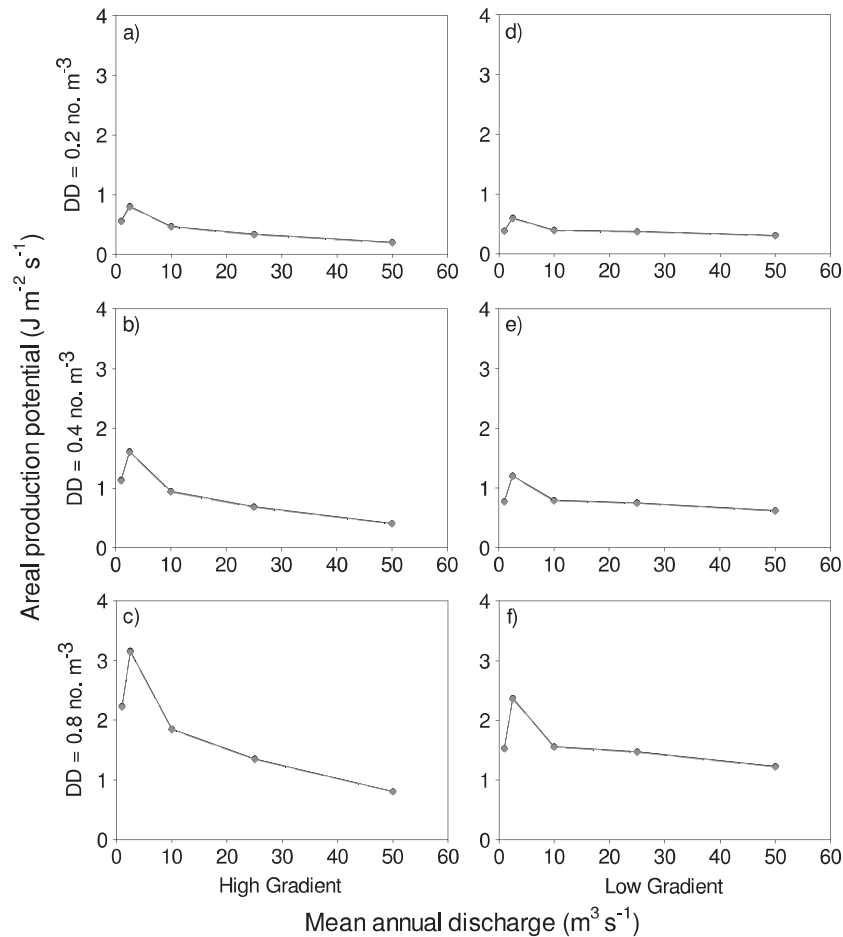


Figure 5. Downstream patterns of areal production potential ($\text{J m}^{-2} \text{s}^{-1}$) estimated for YOY rainbow trout in high- (a–c) and low-gradient (d–f) streams. Initial model drift concentrations were 0.2 (a, d), 0.4 (b, e), and 0.8 m^{-3} (c, f). Note that we did not analyse the effects of temperature on these relationships for YOY trout, but the lines for different water temperatures are superimposed in this figure

function (Hayes *et al.*, 2015), although this was not available during our simulations. However, the overall longitudinal trends that we observe are likely robust to the assumption of constant capture success, even though capture success is sensitive to water velocity (Grossman *et al.*, 2002), because water velocity was lowest at upstream sites and increases longitudinally downstream in our model. Including a variable capture success function would reduce relative NREI at downstream sites, further strengthening the downstream declines in production potential observed in our simulations.

To better isolate the role of longitudinal changes in velocity and depth on productive capacity, we assumed that initial input drift concentrations and temperatures were similar at all sites. Although patterns of invertebrate drift were not the primary focus of this study, the resulting spatial patterns were nonetheless informative. Because of the idealized spatial patterns in the model stream reaches and the constant initial drift concentrations throughout the input

cross section, we expected that a quasi-equilibrium in longitudinal invertebrate drift concentrations might emerge. It was encouraging that longitudinal patterns in drift concentrations appeared to approach an equilibrium. The observation that drifting invertebrates were less concentrated near the stream margins and more concentrated at the stream bottom was expected, given the way that entry, settling, and dispersion were modelled in Kelly *et al.* (2005), and is partly consistent with more recent predictions (Anderson *et al.*, 2013). It could also be reasonably predicted that terrestrial prey inputs would elevate drift concentration at the water surface (Leung *et al.*, 2008), but terrestrial drift generation is not included in the model.

Sensitivity of our predictions to drift concentration indicates that longitudinal changes in productive capacity will depend greatly on actual spatial patterns in drift concentration (which is dependent on benthic biomass and production) along the river continuum, which are currently unclear (Rosenfeld *et al.*, 2014; Naman *et al.*, 2016). Increasing

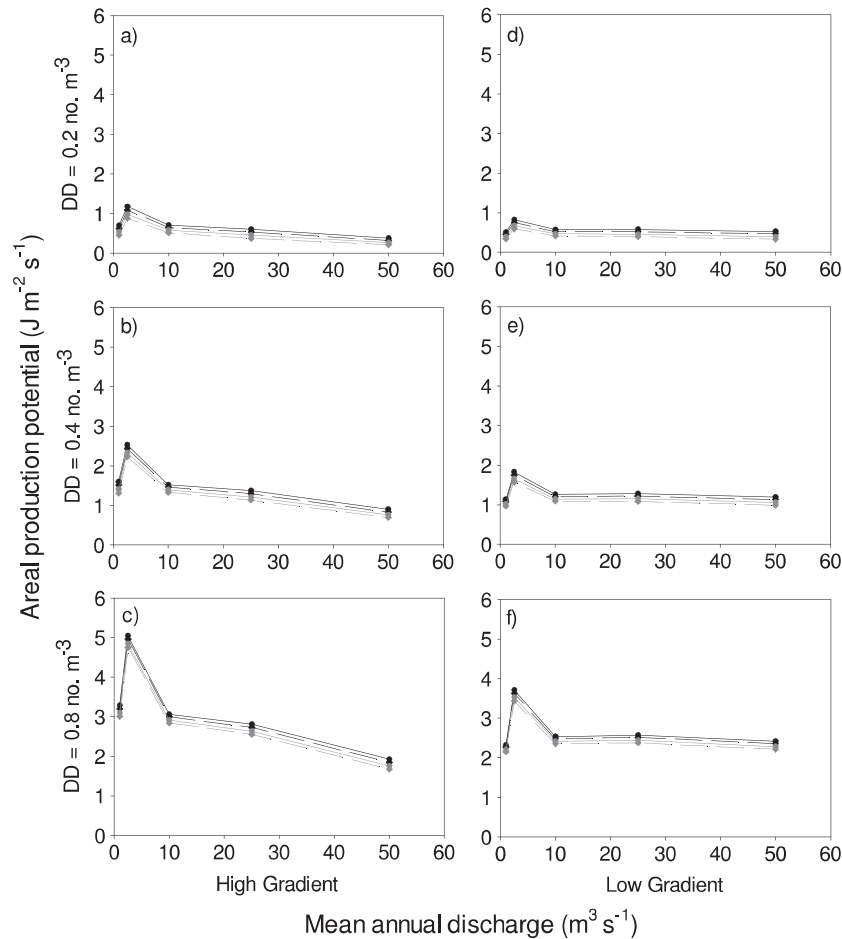


Figure 6. Downstream patterns of areal production potential ($\text{J m}^{-2} \text{s}^{-1}$) estimated for juvenile rainbow trout. The effects of water temperature are displayed for 8 °C (FX), 12 °C (FX), 16 °C (FX), and 20 °C (FX). Other details as in Figure 5

water depth (relative to bed area) may effectively dilute drift concentration (Hayes *et al.*, 2007; Hayes *et al.*, 2015), reducing prey availability to fish; however, increasing downstream turbulence and velocity that reduces settling rates and increases time in suspension may tend to elevate downstream drift concentrations. More than anything, our modelling highlights the importance of better understanding how the prey base of drift-feeding fishes varies along environmental gradients (Piccolo *et al.*, 2014; Rosenfeld *et al.*, 2014).

Under certain model conditions, production potential maxima at intermediate stream sizes were observed for YOY, juveniles, and adult trout. This suggests that trout production attains a maximum at intermediate stream sizes. In the low-gradient system, however, production potential attained a maximum at only intermediate stream sizes for adult rainbow trout under specific conditions, whereas longitudinal production potential (but not areal production) increased continuously with stream size for YOY and juvenile rainbow trout. It is likely that the limited range of the

stream sizes in our modelling may be insufficient to detect the hypothesized maxima in low-gradient systems (i.e. the maximum is achieved at larger stream sizes), and that longitudinal production potential for YOY and juvenile trout did not increase to a maximum in the low-gradient system because velocity fields experienced by trout were not high enough to limit their capture of prey relative to their bioenergetics needs.

Increases in temperature consistently produced declines in longitudinal production potential, rendering many stream reaches unusable for adult rainbow trout as a result of negative NREI, especially for low initial drift concentrations. Growth and survival of adult rainbow trout in such cases may be especially sensitive to changes in food availability. During periods of low food availability or increased competition for limited food resources, fish may decide to migrate to another foraging location either inside or outside the stream reach or wait for prey densities to increase or switch feeding modes in an effort to maintain growth rates and satisfy their metabolic demands (Hayes *et al.*, 2007).

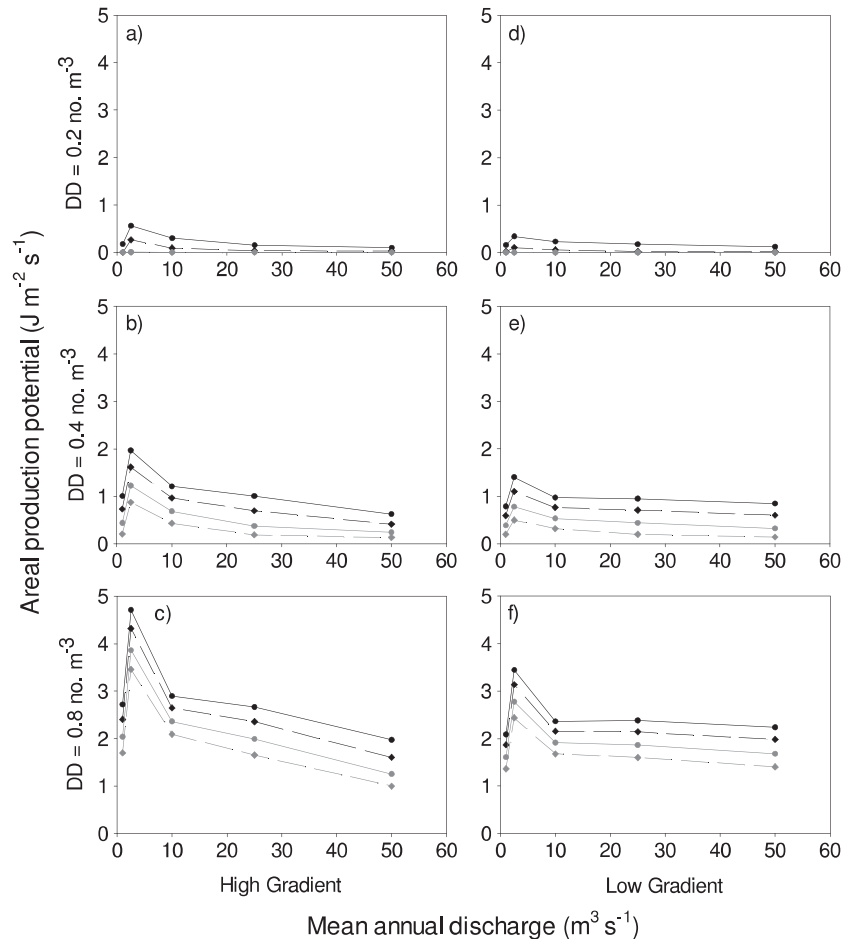


Figure 7. Downstream patterns of areal production potential ($\text{J m}^{-2} \text{s}^{-1}$) estimated for adult rainbow trout. Layout and details as in Figure 6

Sufficiently large trout may also switch from drift to benthic feeding (Harvey and Railsback, 2014) or from insectivory to piscivory because fish are a more energy-rich prey than invertebrates. We did not include these behavioural effects in our predictions of fish production potential. Hence, we expect that our predictions are conservative with regard to instream flow needs (a.k.a. environmental flow needs), given that these behavioural modifications should buffer adult fish against temporary periods of negative NREI. Also, it is plausible that younger trout modelled were not exposed to sufficiently low drift concentrations to produce the decline in production potential predicted for adult trout, although this is difficult to assess in the absence of reliable information on drift concentrations.

Our study represents a novel approach for predicting longitudinal trends in fish production potential based on bioenergetic principles and physical habitat modelling. Although the model provides a snapshot of habitat quality in contrasting reaches rather than integrating the long-term projected effects of habitat on population trajectories (as with individual-based population models; e.g. Harvey and

Railsback, 2009; Ayllón *et al.*, 2016), it provides a relatively effective framework for evaluating anticipated longitudinal contrasts in habitat quality among sites. Previously, physical habitat models have shown that WUA increases with stream size in high- and low-gradient streams when variation in hydraulics across the channel is included in the model (Laliberte *et al.*, 2014), but that WUA declines with stream size in simplified physical habitat models that assume modal transect velocities (Rosenfeld *et al.*, 2007). Our approach was to build upon a physical habitat model (i.e. an idealized stream model) that was based on realistic, empirically based assumptions regarding stream hydraulics (Laliberte *et al.*, 2014) and to incorporate models of invertebrate drift transport and fish bioenergetics. We contend that the longitudinal patterns in fish production potential that we observed in the present study, with longitudinal patterns depending on gradient and fish life stage, represent an improvement in the realism of the predicted effects of variation in flow on drift-feeding trout. There are some clear advantages going forward with a fish habitat quality modelling framework that includes mechanistic models of foraging energetics to

address how alterations to flow regimes and other factors may impact populations of drift-feeding fish. The models presented here have a much stronger mechanistic basis for predicting habitat quality and potential growth rates of fish than their physical habitat based predecessors (Piccolo *et al.*, 2014; Rosenfeld *et al.*, 2014). Critics of physical habitat models have consistently described the need for fish habitat models to be more mechanistic or include more biological realism. Importantly, the bioenergetic models indicate that stream temperature and prey availability can impact the longitudinal habitat allometry expected within a stream system, highlighting the need for better empirical data on how prey abundance changes with stream size. In particular, adult trout are expected to be affected most strongly by high temperatures and low drift concentrations. The next logical step in the development of bioenergetically based habitat quality models is to evaluate their predictions against observed habitat use and growth rates of drift-feeding fish in natural systems (e.g. Rosenfeld *et al.*, 2014; Weber *et al.*, 2014; Hayes *et al.*, 2015).

ACKNOWLEDGEMENTS

We are grateful for the comments from two anonymous reviewers. Funding for this research was provided by Alberta Innovates — Energy and Environmental Solutions (the former Alberta Water Research Institute) and Alberta Environment and Sustainable Resources Development. Discussions with and reviews from Andrew Paul, Allan Locke, Stewart Rood, Ed McCauley, Masaki Hayashi, Yvonne Martin, and Ed Johnson at various stages of the research and manuscript development were greatly appreciated.

REFERENCES

- Anderson KE, Paul AJ, McCauley E, Jackson LJ, Post JR, Nisbet RM. 2006. Instream flow needs in streams and rivers: the importance of understanding ecological dynamics. *Frontiers in Ecology and the Environment* **4**: 309–318.
- Anderson KE, Harrison LR, Nisbet RM, Kolpas A. 2013. Modeling the influence of flow on invertebrate drift across spatial scales using a 2D hydraulic model and a 1D population model. *Ecological Modelling* **265**: 207–220.
- Ayllón D, Railsback SF, Vincenzi S, Groeneveld J, Almodóvar A, Grimm V. 2016. InSTREAM-Gen: modelling eco-evolutionary dynamics of trout populations under anthropogenic environmental change. *Ecological Modelling* **326**: 36–53.
- Bovee K. 1982. A guide to stream habitat analysis using the instream flow incremental methodology. FWS/OBS-82/26, Instream flow information paper 12.
- Bovee KD, Milhous RT. 1978. Hydraulic simulation in instream flow studies: theory and techniques. IFIP No. 5. *FWS/OBS*.
- Bovee K, Lamb B, Barthlow J, Stalnaker C, Taylor J, Henriksen J. 1998. Stream habitat analysis using the instream flow incremental methodology. *Biological Resources Division Information and Technology Report*.
- Ciborowski JJH. 1983. Influence of current velocity, density, and detritus on drift of two mayfly species (Ephemeroptera). *Canadian Journal of Zoology-Revue Canadienne De Zoologie* **61**: 119–125.
- Elliott JM. 1971. Some Methods for the Statistical Analysis of Samples of Benthic Invertebrates. Freshwater Biological Association: Ambleside, Westmorland, U.K..
- Elliott JM. 1973. The food of brown and rainbow trout (*Salmo trutta* and *S. gairdneri*) in relation to the abundance of drifting invertebrates in a mountain stream. *Oecologia* **12**: 329–347.
- Grossman GD, Rincon PA, Farr MD, Ratajczak RE. 2002. A new optimal foraging model predicts habitat use by drift-feeding stream minnows. *Ecology of Freshwater Fish* **11**: 2–10.
- Harvey BC, Railsback SF. 2009. Exploring the persistence of stream-dwelling trout populations under alternative real-world turbidity regimes with an individual-based model. *Transactions of the American Fisheries Society* **138**: 348–360.
- Harvey BC, Railsback SF. 2014. Feeding modes in stream salmonid population models: is drift feeding the whole story? *Environmental Biology of Fishes* **97**: 615–625.
- Hayes JW, Stark JD, Shearer KA. 2000. Development and test of a whole-lifetime foraging and bioenergetics growth model for drift-feeding brown trout. *Transactions of the American Fisheries Society* **129**: 315–332.
- Hayes JW, Hughes NF, Kelly LH. 2007. Process-based modelling of invertebrate drift transport, net energy intake and reach carrying capacity for drift-feeding salmonids. *Ecological Modelling* **207**: 171–188.
- Hayes JW, Shearer KA, Goodwin EO, Hay J, Allen C, Olsen DA, Jowett IG. 2015. Test of a benthic macroinvertebrate habitat flow time series model incorporating disturbance and recovery processes. *River Research and Applications* **31**: 785–797.
- Hill J, Grossman GD. 1993. An energetic model of microhabitat use for rainbow trout and rosyside dace. *Ecology* **74**: 685–698.
- Hughes NF, Dill LM. 1990. Position choice by drift-feeding salmonids — model and test for arctic grayling (*Thymallus arcticus*) in sub-Arctic mountain streams, interior Alaska. *Canadian Journal of Fisheries and Aquatic Sciences* **47**: 2039–2048.
- Hughes NF, Hayes JW, Shearer KA, Young RG. 2003. Testing a model of drift-feeding using three-dimensional videography of wild brown trout, *Salmo trutta*, in a New Zealand river. *Canadian Journal of Fisheries and Aquatic Sciences* **60**: 1462–1476.
- Jowett IG. 1998. Hydraulic geometry of New Zealand rivers and its use as a preliminary method of habitat assessment. *Regulated Rivers-Research & Management* **14**: 451–466.
- Kelly LH, Hay J, Hughes NF, Hayes JW. 2005. Flow related models for simulating river hydraulics, Invertebrate Drift Transport, and Foraging Energetics of Drift-feeding Salmonids: Users Guide (Version 1.0). Cawthron Report No. 922, Prepared in association with the U.S. Bureau of Land Management and University of Alaska Fairbanks.
- Laliberte JJ, Post JR, Rosenfeld JS. 2014. Hydraulic geometry and longitudinal patterns of habitat quantity and quality for rainbow trout (*Oncorhynchus mykiss*). *River Research and Applications* **30**: 593–601.
- Leopold LB, Maddock T. 1953. The hydraulic geometry of stream channels and some physiographic implications. *Geological Survey Professional Paper* 252. Washington: Department of the Interior.
- Leung ES, Rosenfeld JS, Bernhardt JR. 2008. Habitat effects on invertebrate drift in a small trout stream: implications for prey availability to drift-feeding fish. *Hydrobiologia* **623**: 113–125.
- Lotrich VA. 1973. Growth, production, and community composition of fishes inhabiting a first-order, second-order, and third-order stream of eastern Kentucky. *Ecological Monographs* **43**: 377–397.
- Mahon R, Balon EK. 1985. Fish production in warmwater streams in Poland and Ontario. *Canadian Journal of Fisheries and Aquatic Sciences* **42**: 1211–1215.

- Milhous RT, Updike MA, Schneider DM. 1989. Physical habitat simulation system reference manual: version II. *Biological Report*. Washington, D.C.
- Naiman RJ, Melillo JM, Lock MA, Ford TE, Reice SR. 1987. Longitudinal patterns of ecosystem processes and community structure in a sub-Arctic river continuum. *Ecology* **68**: 1139–1156.
- Naman SM, Rosenfeld JS, Richardson JS. 2016. Causes and consequences of invertebrate drift in running waters: from individuals to populations and trophic fluxes. *Canadian Journal of Fisheries and Aquatic Sciences*. DOI: 10.1139/cjfas-2015-0363
- Peeters E, Gardeniers JJP. 1998. Logistic regression as a tool for defining habitat requirements of two common gammarids. *Freshwater Biology* **39**: 605–615.
- Piccolo JJ, Frank BM, Hayes JW. 2014. Food and space revisited: the role of drift-feeding theory in predicting the distribution, growth, and abundance of stream salmonids. *Environmental Biology of Fishes* **97**: 475–488.
- Railsback SF, Harvey BC. 2002. Analysis of habitat-selection rules using an individual-based model. *Ecology* **83**: 1817–1830.
- Railsback SF, Rose KA. 1999. Bioenergetics modeling of stream trout growth: temperature and food consumption effects. *Transactions of the American Fisheries Society* **128**: 241–256.
- Railsback SF, Stauffer HB, Harvey BC. 2003. What can habitat preference models tell us? Tests using a virtual trout population. *Ecological Applications* **13**: 1580–1594.
- Railsback SF, Harvey BC, Jackson SK, Lamberson RH. 2009. InSTREAM: the individual-based stream trout research and environmental assessment model. *Gen. Tech. Rep. PSW-GTR-218*. Albany, CA: U.S. Department of Agriculture, Forest Service, Pacific Southwest Research Station, 254 pp.
- Rice SP, Greenwood MT, Joyce CB. 2001. Tributaries, sediment sources, and the longitudinal organisation of macroinvertebrate fauna along river systems. *Canadian Journal of Fisheries and Aquatic Sciences* **58**: 824–840.
- RL&L Environmental Services Ltd. 2001. Lower Bow River fish population status assessment — August 2000. RL&L Report No. 855F, Prepared for Alberta Environment.
- Rosenfeld J. 2003. Assessing the habitat requirements of stream fishes: an overview and evaluation of different approaches. *Transactions of the American Fisheries Society* **132**: 953–968.
- Rosenfeld JS, Taylor J. 2009. Prey abundance, channel structure and the allometry of growth rate potential for juvenile trout. *Fisheries Management and Ecology* **16**: 202–218.
- Rosenfeld JS, Post J, Robins G, Hatfield T. 2007. Hydraulic geometry as a physical template for the river continuum: application to optimal flows and longitudinal trends in salmonid habitat. *Canadian Journal of Fisheries and Aquatic Sciences* **64**: 755–767.
- Rosenfeld JS, Bouwes N, Wall CE, Naman SM. 2014. Successes, failures, and opportunities in the practical application of drift-foraging models. *Environmental Biology of Fishes* **97**: 551–574.
- Scott D, Shirvell CS. 1987. A critique of the instream flow incremental methodology and observations on flow determination in New Zealand. In *Regulated Streams: Advances in Ecology*, Craig JF, Kemper JB (eds). Plenum Press: New York; 27–43.
- Smock LA. 1980. Relationships between body size and biomass of aquatic insects. *Freshwater Biology* **10**: 375–383.
- Stanford JA, Ward JV. 2001. Revisiting the serial discontinuity concept. *Regulated Rivers-Research & Management* **17**: 303–310.
- Steffler P, Blackburn J. 2002. River2D, two-dimensional depth averaged model of river hydrodynamics and fish habitat, Introduction to Depth Averaged Modeling and User's Manual. Edmonton.
- Vadas RL, Orth DJ. 2001. Formulation of habitat suitability models for stream fish guilds: do the standard methods work? *Transactions of the American Fisheries Society* **130**: 217–235.
- Vannote RL, Minshall GW, Cummins KW, Sedell JR, Cushing CE. 1980. River continuum concept. *Canadian Journal of Fisheries and Aquatic Sciences* **37**: 130–137.
- Vismara R, Azzellino A, Bosi R, Crosa G, Gentili G. 2001. Habitat suitability curves for brown trout (*Salmo trutta fario* L.) in the River Adda, Northern Italy: comparing univariate and multivariate approaches. *Regulated Rivers: Research & Management* **17**: 37–50.
- Wankowski JWJ. 1979. Morphological limitations, prey size selectivity, and growth response of juvenile Atlantic salmon, *Salmo salar*. *Journal of Fish Biology* **14**: 89–100.
- Ward JV, Stanford JA. 1995. The serial discontinuity concept — extending the model to floodplain rivers. *Regulated Rivers-Research & Management* **10**: 159–168.
- Weber N, Bouwes N, Jordan CE. 2014. Estimation of salmonid habitat growth potential through measurements of invertebrate food abundance and temperature. *Canadian Journal of Fisheries and Aquatic Sciences* **71**: 1158–1170.

1 **Multiple Challenges Confront a High-Effort Inland Recreational Fishery in Decline**

2

3

CHRISTOPHER L. CAHILL*¹

4 STEPHANIE MOGENSEN¹, KYLE L. WILSON¹, ARIANE CANTIN¹, R. NILO SINNATAMBY¹, ANDREW J.

5 PAUL², PAUL CHRISTENSEN², JESSICA R. REILLY², LINDA WINKLE², ANNE FARINEAU¹, AND JOHN

6

R. POST¹

7

1. *Department of Biological Sciences, University of Calgary*

8

2500 University Drive NW

9

Calgary, Alberta, T3A 4X5, Canada

10

11

2. *Fish and Wildlife Policy, Alberta Environment and Parks*

12

Provincial Building

13

Cochrane, Alberta, T4C 1A5, Canada

14

15

16

17

18

19

*Corresponding author: christopher.cahill@ucalgary.ca

20

21 *Abstract*—Catch and release regulations designed to protect fisheries may fail to halt
22 population declines, particularly in situations where fishing effort is high and when multiple
23 stressors threaten a population. We demonstrate this claim using Alberta’s Bow River, which
24 supports a high-effort Rainbow Trout *Oncorhynchus mykiss* fishery where anglers voluntarily
25 release rates > 99% of their catch. We examined the population trend of adult trout, which were
26 tagged and recaptured using electrofishing surveys conducted intermittently during 2003-2013.
27 We used multi-session capture-recapture models to obtain abundance estimates for trout, and
28 regressed trend during two periods to account for variation in sampling locations. General
29 patterns from all models indicated the population declined throughout the study. Potential
30 stressors to this system that may have contributed to the decline include Whirling Disease
31 *Myxobolus cerebralis*, which was detected for the first time in 2016, notable floods, and release
32 mortality. Because disease and floods are largely uncontrollable from a management
33 perspective, our findings suggest that stringent tactics such as angler effort restrictions may be
34 necessary to maintain similar fisheries.

35

36 **Introduction**

37 Recreational fisheries can decline and collapse when exploitation rate is high relative to
38 the productivity of the targeted population (Post et al. 2002; Sullivan 2003; Johnston et al. 2007),
39 when environmental conditions are unfavorable (Beamish et al. 1999), or when multiple stressors
40 surpass the compensatory abilities of a given fish population (Hansen et al. 2015). However,
41 declines documented as reductions in catch or abundance are generally multi-faceted and subject
42 to much debate (Hilborn and Walters 1992). Failure to achieve scientific consensus on the
43 cause(s) of a decline stems from the fact that data collected by management agencies are
44 observational in nature (Hilborn 2016), extracted from ecosystems with complex dynamics
45 (Sugihara et al. 2012; Glaser et al. 2014), and often lack the experimental manipulations,
46 controls, and replication necessary for causal inference (Jones and Hansen 2014). Consequently,
47 disentangling key factors responsible for a decline, such as the effects of fishing vs. abiotic or
48 environmental stressors, is often difficult (Walters 1986).

49 Several policy options are available to managers seeking to offset the effects of fishing-
50 related mortality in inland recreational fisheries. Traditionally, fishing mortality has been
51 managed using passive regulations such as bag or length limits (Lester et al. 2003), seasonal or
52 area closures (Welcomme 2008), and gear restrictions (Rahel 2016). Such regulations attempt to
53 manipulate the catchability portion of fishing mortality without directly limiting fishing effort,
54 and thus the ability of passive regulations to offset issues related to high angling effort remains
55 tenuous (Cox et al. 2003; Pereira and Hansen 2003). For example, minimum length limits may
56 fail to prevent recruitment overfishing when angler effort is unresponsive to declines in fishery
57 quality (Allen et al. 2013). Similarly, catch and release regulations may fail to achieve
58 management objectives or maintain fish populations in situations where effort is high or when

59 release mortality is present (Post et al. 2003). Despite the potential for problems in high-effort
60 situations, catch and release regulations are generally the most stringent regulations enacted by
61 inland recreational fisheries managers in North America (Hubert and Quist 2010).

62 Anthropogenic stressors such as fishing-related mortality reduce a population's ability to
63 offset stochastic natural disturbances or disease outbreaks (Holling 1973). For example, severe
64 floods may reduce fish density through direct mortality or downstream displacement (Warren et
65 al. 2009). Pathogens may also alter population dynamics through reductions in growth (Johnson
66 et al. 2004) or competitive ability (Godwin et al. 2015), changes in behavior (Barber et al. 2000),
67 or through direct mortality events (Hatai and Hoshiai 1992). For instance, viral hemorrhagic
68 septicemia virus resulted in mass mortality events in Freshwater Drum *Aplodinotus grunniens*
69 (Lumsden et al. 2007) and Muskellunge *Esox masquinongy* (Elsayed et al. 2006) within the
70 Laurentian Great Lakes. The importance of pathogen-induced mortality was also illustrated
71 throughout the intermountain-west region of the United States, where Whirling Disease
72 *Myxobolus cerebralis* reduced salmonid abundance by up to 90% in some watersheds (Nehring
73 and Walker 1996; Vincent 1996). While stochastic events and disease outbreaks influence fish
74 population dynamics, biologists have few direct tools for managing stressors such as these.

75 A central challenge facing recreational fisheries managers is how to mitigate the
76 combined effects of anthropogenic and stochastic environmental threats, as freshwater systems
77 appear particularly vulnerable to the effects of multiple stressors (Ormerod et al. 2010).
78 Unfortunately, traditional fisheries management approaches rarely incorporate the effects of
79 multiple, potentially changing stressors on population sustainability (Lynch et al. 2016; Paukert
80 et al. 2016). Thus, approaches that explicitly recognize management tradeoffs among key
81 stressors may be useful. For example, Carpenter et al. (2017) developed a multi-dimensional

82 sustainable Safe Operating Space (i.e., “SOS”) that distinguished among stressors that were
83 controllable (e.g., harvest) and largely uncontrollable (e.g., environmental change or disease
84 outbreaks) by fisheries managers. These authors suggested that managers may need to offset the
85 effects of uncontrollable variables with those they can influence to maintain a quality fishery
86 within a particular SOS (Carpenter et al. 2017).

87 The Lower Bow River (LBR) Rainbow Trout *Oncorhynchus mykiss* fishery highlights the
88 challenges of managing inland recreational fisheries in the presence of multiple stressors. The
89 LBR is reputed as a world-class Rainbow Trout fishery (Post et al. 2006; Askey et al. 2007), and
90 experiences high angling effort in part because of its proximity to a large city (Calgary, Alberta,
91 1.2 million people; Rhodes 2005; Statistics Canada 2016). Notable floods occurred in 2005 and
92 2013 (i.e., 1/10 and 1/100-year flood events, respectively; Veiga et al. 2015). Furthermore,
93 Whirling Disease was detected in the LBR for the first time in 2016, although it is unknown
94 when the disease arrived (Canadian Food Inspection Agency 2017). Given that the potential for
95 these threats to impact Rainbow Trout in the LBR appears high, our objectives were to determine
96 (i) abundance of Rainbow Trout ≥ 250 mm fork length (FL), and (ii) assess trends in abundance
97 during 2003-2013. Results from this study are then used to demonstrate the potential importance
98 of effort restrictions as an inland recreational fisheries management tool, particularly when
99 angling effort is high and the remaining stressors are uncontrollable.

100

Methods

101

102

103

104

Study Area—The Bow River originates in the Rocky Mountains of southwestern Alberta,
and is a major tributary of the South Saskatchewan River (Figure 1). Our study occurred in the
Lower Bow River, which designates a 224-km section of the river beginning at the Bearspaw
Dam and flowing eastward through Calgary, Alberta to the Bassano Dam (Figure 1). The LBR

105 receives substantial nutrient inputs from wastewater effluent as it flows through Calgary (Sosiak
106 2002), which increases production of top trophic levels in the system (Askey et al. 2007).

107 Rainbow Trout were introduced into the LBR by stocking between 1933 and 1947
108 (Gilmour 1950) and are now naturalized (Rhodes 2005). Rainbow Trout are the most sought-
109 after species in the LBR fishery, and most fish are caught via fly-fishing during August. This
110 system supports the highest effort fishery in Alberta (average 161 angler hours/ha; Ripley and
111 Council 2006), has been functionally catch and release since at least 2006 (e.g., 0.005% of
112 captured Rainbow Trout were kept by anglers; Ripley and Council 2006), and is worth \$24.5
113 million CAD/year (Crowe-Swords 2016).

114 *Field Sampling*—Alberta Environment and Parks biologists conducted seven multi-day
115 capture-recapture surveys during 2003-2013 to assess trout population trends in the LBR. A
116 contiguous 4.32 km section of the river was sampled in 2003, 2005, 2007, and 2008 (Figure 1).
117 During 2011-2013, sampling occurred at four randomly selected 1 km sections (Figure 1). In all
118 years, fish were sampled using two Smith-Root™ 5.0 or 7.5 Generator Powered Pulsators and
119 boom electro-fishers on four consecutive days during late August to early September. Boats
120 fished opposite banks in the downstream direction, and fish were transferred to tubs until the end
121 of the section was reached. Rainbow Trout ≥ 250 mm FL were tagged behind the dorsal fin
122 using individually numbered Floy™ anchor tags, and fish were released in the center of the
123 section they were captured in.

124 *Analysis*—Multi-session capture-recapture models were constructed to obtain derived
125 abundance estimates of Rainbow Trout ≥ 250 mm FL, which were regressed through time to
126 estimate the population trend during 2003-2008 and 2003-2013. Multi-session capture-recapture
127 models generalize a simple closed capture-recapture model to multiple sessions or years, and are

128 useful for combining data from multiple years into a single analysis (Converse and Royle 2012;
129 Kéry and Royle 2015). Our models estimated capture probabilities for each day within each year
130 to account for imperfect detection of fish in our surveys. Data were modeled in an integrated
131 Bayesian framework. The integrated approach propagated uncertainty through the abundance
132 analysis and ultimately into estimates of population trend, rather than analyzing the outputs of
133 models as data (Paul 2012; Maunder and Punt 2013). Additionally, we elected to use the
134 Bayesian framework because it offered more modeling flexibility and for the accounting of the
135 full range of uncertainties related to all models and parameter values (Punt and Hilborn 1997).
136 Standard open population models were not fit because surveys were not conducted in
137 consecutive years throughout the study.

138 A statistical approach known as data augmentation was used to simplify Bayesian
139 abundance estimation. Data augmentation reparameterizes a standard closed capture-recapture
140 model into an occupancy-style model (Royle 2009; Kéry and Schaub 2011). This
141 parameterization removes the abundance parameter N from the model as an estimated parameter,
142 which is useful because it fixes the dimension of the parameter space, and thus enables the use of
143 standard approaches such as Markov-Chain Monte Carlo (Royle and Dorazio 2008). Data
144 augmentation removes N from the model by marginalizing over a $Bin(M, \psi)$ prior distribution for
145 N , where M is an arbitrarily large number of unobserved individuals with all-zero capture
146 histories, and ψ is an inclusion probability to be estimated from the data (Royle 2009). The
147 capture histories of individuals observed in the field are then augmented by the capture histories
148 of the all-zero “potential” individuals, which are said to be present in the population according to
149 a Bernoulli prior with inclusion probability ψ . This approach implies that the marginal prior for
150 N is $Unif(0, M)$, and hence that the expectation of N can be recovered as the derived variable ψM

151 through the estimation of ψ , any relevant capture probabilities, and a Bernoulli latent variable
152 (Royle et al. 2013).

153 The single-year data augmentation scheme described above was expanded to a multi-
154 session framework by introducing a year-specific subscript t to all parameters and values (e.g.,
155 ψ_t , M_t , and N_t). Abundance in each year N_t was assumed to be Poisson distributed with year-
156 specific mean λ_t :

$$(1) \quad N_t \sim Pois(\lambda_t)$$

157 This multi-session framework and Poisson assumption formed the basis for three separate
158 models, as the models could either be used to estimate year-specific abundances (as in Eq. 2
159 below; model 1), or regress the population trend by fixing the trend on the first year of data (as in
160 Eqs. 3 and 4 below; models 2 and 3, respectively). Two trend models were fit to account for
161 potential issues with field sampling: model 2 estimated a trend for years when the surveys
162 occurred in identical locations (i.e., 2003-2008), while model 3 regressed a trend across the
163 entire study period.

164 Model 1 was parameterized as a generalized linear model of the form

$$(2) \quad \lambda_t = e^{\beta_{0t}}$$

165 where β_{0t} are fixed effects that represent independent abundance estimates for each year (i.e.,
166 2003, 2005, 2007, 2008, 2011, 2012, and 2013; Royle et al. 2013). Model 2 regressed a trend
167 through abundance estimates during the first four years of data collection (i.e., 2003, 2005, 2007,
168 and 2008):

$$(3) \quad \lambda_t = e^{\beta_0 + \beta_1(t-t^*)}$$

170 where β_0 was fixed at a single intercept, β_1 is a coefficient describing the log-linear abundance
 171 trend, and t^* is a baseline year that centers the trend. Model 3 regressed a trend term through
 172 abundance estimates during 2003-2013:

$$173 \quad (4) \quad \lambda_t = e^{\beta_0 + \beta_1(t-t^*) + \beta_2 length_t}$$

174 where β_2 is a covariate controlling for the total length (km) of the river sampled in each year.
 175 Additionally, all models featured constraints between the year-specific inclusion parameters ψ_t
 176 and intercept terms (i.e., β_{0_t} or β_0), and ψ_t can be fixed as

$$(5) \quad \psi_t = \frac{\lambda_t}{M_t}$$

177 so that the intercepts are estimable (Royle et al. 2013; Kéry and Royle 2015).

178 Capture probabilities (p) were modeled using a generalized linear mixed model of the
 179 same form for all three models. For each year t , four occasion-specific capture probabilities j ,
 180 and i individual random effects (i.e., $p_{i,j,t}$) were modeled. Capture probabilities were modeled
 181 as additive fixed effects based on the capture occasion (i.e., $\beta_{j,t}$), and the addition of a random
 182 logistic-normal term that represented individual heterogeneity in capture probability, $\alpha_{i,t}$:

$$183 \quad (5) \quad \text{logit}(p_{i,j,t}) = \beta_{j,t} + \alpha_{i,t}$$

$$184 \quad (6) \quad \text{where } \alpha_{i,t} \sim \text{Normal}(0, \sigma_t^* \sigma_{raw_{i,t}})$$

$$185 \quad (7) \quad \sigma_t \sim \text{Normal}(2.5, 1.25)$$

$$186 \quad (8) \quad \sigma_{raw_{i,t}} \sim \text{Normal}(0, 1)$$

187 Thus, σ_t is a year-specific random effect on capture probability drawn from an informative prior
 188 distribution. The specific prior values of σ_t were not of primary interest to this study, but these
 189 priors did alter the variance around the abundance estimates. Data did not contain enough
 190 information to allow use of an uninformative prior for σ_t , and simpler versions of these models
 191 without individual heterogeneity terms failed to pass goodness-of-fit tests. Consequently, we
 192 were left with the choice to use simpler, but potentially ill-fitting models, or to employ an
 193 informative prior and obtain models that passed goodness-of-fit tests. The latter approach was
 194 chosen as it seemed precautionary to err on the side of incorporating more uncertainty in the
 195 models. Values for the informative priors ensured that capture probabilities did not go to zero
 196 and that N_t did not go to infinity, so that the upper limits of the derived density estimates
 197 (abundance/km) corresponded to densities observed in other fluvial wild stock Rainbow Trout
 198 fisheries (Vincent 1996). Lastly, $\sigma_{raw_{i,t}}$ altered the individual random effects to a non-centered
 199 parameterization, which manipulated the geometry of the posterior and improved numerical
 200 performance (Betancourt and Girolami 2013; Monnahan et al. 2017).

201 Estimates of abundance N_t were derived as

$$(9) \quad N_t = n_t + \theta_t$$

202 where n_t is the number of individual fish captured in year t , and θ_t represents the sum of M_t
 203 independent Bernoulli trials with trial-specific success probability equal to

$$(10) \quad \frac{\psi_t \prod_{j=1}^4 (1-p_{i,j,t})}{\psi_t \prod_{j=1}^4 (1-p_{i,j,t}) + (1-\psi_t)}$$

204 Phrased differently, abundance of fish in each year was calculated as the sum of the number of
 205 fish captured in that year and the sum of M_t Bernoulli random deviates describing fish that were

206 present in that year, but never physically captured. A standardized index of Rainbow Trout
 207 density among years (N_{km_t}) was computed by dividing the estimates of N_t by the length (km)
 208 of river sampled in year t . Lastly, the percent decline per year for models 2-3 was derived as:

$$(11) \quad Trend = 100(e^{\beta_1} - 1)\%$$

209 where the *Trend* term represents the per year percent change in N_t during 2003-2008 and 2003-
 210 2013 (denoted as $Trend_s$ and $Trend_l$, respectively).

211 Priors for all additional parameters were set at vague or weakly informative values, and
 212 the sensitivity of the results to a variety of priors was tested during model development. All
 213 predictor variables were centered and standardized prior to analysis (Gelman 2008). For each
 214 model, each year's observed capture-history data was augmented by $M_t = 8\,000$, which implied
 215 $N_t \sim Unif(0, 8\,000)$ priors, and visual inspection of the results showed this bound was sufficiently
 216 large so as to not influence estimates of abundance or the corresponding derived densities (see
 217 also Royle et al. 2013). Occasion-specific capture probabilities for all models were given flat
 218 $\text{logit}(\beta_{j,t}) \sim Unif(0, 1)$ priors. For all three models, intercept terms (β_{0_t}, β_0) were given normal
 219 priors centered at zero, with a prior standard deviation (sd) of 10 to represent a substantial
 220 amount of ignorance regarding the values of λ_t on the log scale. The remaining regression
 221 coefficients (β_1 for models 2 and 3, β_2 for model 3) were given normal priors centered at zero
 222 with a sd of 1. Priors for these remaining regression coefficients were weakly informative as our
 223 predictor variables were also on the unit scale (Gelman et al. 2015), and while these priors did
 224 not truncate estimates of β_1 and β_2 for either model, they did substantially improve the
 225 numerical performance. Final model versions were arrived after fitting several alternative
 226 models that either 1) failed to pass posterior predictive checks, and/or 2) provided identical (or

227 nearly identical) posterior distributions for key parameters. This included models that relaxed
228 the assumption of Poisson-distributed abundances, and models that featured alternative model
229 forms for capture probabilities.

230 Bayesian models were implemented using *RStan* in R (Carpenter et al. 2016; Stan
231 Development Team 2016; R Development Core Team 2017), and an example of the Stan code
232 for model 3 is provided as supplementary material. We ran ten chains for each model, discarded
233 the first 5 000 draws as burn-in, and retained the next 5 000 draws with a thinning rate of 1 to
234 summarize posterior distributions. Starting values were jittered for each model, and chains were
235 started at different random number seeds. Additionally, chains were inspected visually, Gelman-
236 Rubin statistics (\hat{R}) were used to test for convergence to a stable distribution among chains, and
237 tree-depth plots were explored to evaluate step-size and performance of the no-U-turn sampler
238 using ShinyStan (Gelman et al. 2014; Gabry 2015). Model fit was evaluated using posterior
239 predictive p-values (Kéry and Royle 2015), the development of which is described in Appendix
240 1.

241 Results

242 Results from all three models suggest that the abundance of Rainbow Trout ≥ 250 mm FL
243 declined during 2003-2013. Model 1 showed that while year-specific estimates of abundance
244 (i.e., N_t) and derived values of density (i.e., N_km_t) were highly variable, both declined during
245 2003-2008 and 2003-2013 (Appendix Table 2.1 and Figure 2, respectively). Density values from
246 the independent intercepts model declined more sharply during 2011-2013 than during 2003-
247 2008 (Figure 3). The highest derived values for Rainbow Trout density occurred in 2003
248 (median = 414 fish*km⁻¹; 95% Credible Interval (CRI): 290-713), while the lowest density
249 estimates occurred in 2013 (median = 72 fish*km⁻¹; CRI: 57-111; Figure 2). $Trend_s$ was highly

250 variable, but 88% of the posterior mass for this derived variable was < 0 (median = -5.5% per
251 year; CRI: -14.2% to 4.3%; upper panel Figure 4). Values of $Trend_l$ (2003-2013) were less
252 variable than $Trend_s$ (2003-2008), but featured a similar median estimate for the percent change
253 per year, and 99% of the posterior mass was < 0 (median = -6.6% per year; CRI: -10.5% to -
254 2.6%; lower panel Figure 3).

255 Posterior predictive checks indicated that no major deviations from the modeling
256 assumptions existed for all models (i.e., posterior predictive p-values 0.18-0.33; Figure 4), and \hat{R}
257 statistics suggested convergence to a stable distribution among chains for all parameters in each
258 model (i.e., all $\hat{R} = 1$; Appendix Tables 2.1-2.3). Estimates of year- and occasion-specific
259 capture probabilities were low for all three models (i.e., $\beta_{j,t}$ typically ≤ 0.10 ; Appendix Tables
260 2.1-2.3). Additionally, values of ψ_t ranged from 0.03 to 0.39 for all models, which indicated
261 that the abundance estimates were not constrained by our choices for the year-specific data
262 augmentation variables M_t (Converse and Royle 2014; Appendix 2.1-2.3).

263

Discussion

264 Despite uncertainty in both abundance and trend estimates, these results indicate that
265 Rainbow Trout in the LBR likely declined during both assessment periods. The median
266 posterior estimates for a 10-year standardized population trend were -43.0% using $Trend_s$
267 estimated from the 2003-2008 data, and -50.0% using $Trend_l$ estimated from the 2003-2013
268 data. Since the size criteria for tagged fish (≥ 250 mm FL) corresponds approximately to the
269 sizes of mature Rainbow Trout (Rhodes 2005), the estimated decline likely represents a large
270 reduction in the number of mature individuals in this population. The Committee on the Status
271 of Endangered Wildlife in Canada (COSEWIC) guidelines state that “in cases where the declines
272 or its causes are unknown” a decline in the number of mature individuals $\geq 30\%$ or $\geq 50\%$ over a

273 period of ten years would qualify a population as “threatened” or “endangered,” respectively
274 (COSEWIC 2018). Rainbow Trout in the LBR are naturalized, and hence do not qualify for
275 listing as per COSEWIC guidelines; nonetheless, these criteria demonstrate the significance of
276 the magnitude of the decline documented here.

277 The pattern of decline in adult abundance in the LBR appears similar to declines in other
278 high-profile Rainbow Trout fisheries caused by Whirling Disease (Nehring and Walker 1996;
279 Vincent 1996). Whirling disease was first detected in Alberta in 2016 from the Bow River
280 (Canadian Food Inspection Agency 2017). Although timing of its first occurrence in the
281 province is unknown, extensive testing for *Myxobolus cerebralis* (i.e., the causative agent of the
282 disease) from 1997 to 2001 was negative in the province (unpublished data, Fish and Wildlife
283 Policy, Alberta Environment and Parks, Edmonton, Alberta). Whirling disease was detected in
284 Canada for the first time in August 2016, and subsequent monitoring detected the parasite
285 throughout the Bow River watershed in February 2017 (Canadian Food Inspection Agency
286 2017). Therefore, the best available evidence suggested that Whirling Disease arrived in the
287 LBR sometime during 2002-2016. Young-of-year and juvenile Rainbow Trout are particularly
288 susceptible to Whirling Disease, which can consequently cause recruitment failures (Markiw
289 1992; Walker and Nehring 1995; Vincent 1996). However, the impact of Whirling Disease on
290 wild Rainbow Trout populations is highly variable (Bartholomew and Reno 2002). Management
291 response to Whirling Disease has also varied, but has included actions such as stopping or
292 limiting stocking of infected fish into natural waters, emergency bag limit reductions for
293 recreational anglers, and educational campaigns for the public (Modin 1998; Nickum 1999;
294 Nehring 2006).

295 Floods in 2005 and 2013 represent another potential contributing factor to the LBR
296 decline. Although both floods caused extensive damage, peak flows in the LBR during the 2013
297 flood were more than two times those observed during the 2005 flood (Veiga et al. 2014). These
298 flows in 2013 substantially restructured fish habitat throughout the LBR (City of Calgary 2018).
299 Previous studies that have assessed the impact of severe flood events on trout abundances have
300 found responses ranging from dramatic decreases in trout density (Jowett and Richardson 1989;
301 Kitanishi and Yamamoto 2015) to no change between pre- and post-flood measurement periods
302 (George et al. 2015). High flow events leading to food supply limitations and subsequent
303 population collapse were responsible for boom-and-bust population cycles in a tailwater
304 Rainbow Trout fishery below the Glen Canyon Dam in Arizona (Korman et al. 2017). However,
305 this mechanism seems unlikely in the LBR as substantial wastewater inputs have increased
306 biological productivity (Sosiak 2002; Askey et al. 2007), and these inputs have remained
307 relatively constant throughout the study period (see Taube et al. 2016). Intriguingly, abundance
308 declined in both 2005 and 2013 according to post-flood surveys (Figure 3), perhaps because
309 adult fish were displaced downstream. However, the mechanism of downstream displacement
310 was unlikely to have been responsible for the entire decline observed, since declines also
311 occurred in non-flood years.

312 High angling effort on the LBR may also have contributed to the observed decline via
313 post-release mortality. For example, catch-and-release regulations appeared to alter the size
314 distribution of a wild Rainbow Trout fishery relative to a closed-to-fishing section in the South
315 Platte River, Colorado, suggesting that catch and release mortality can structure wild trout
316 populations (Anderson and Nehring 1984). The extent to which Rainbow Trout catch-and-
317 release mortality occurs has been linked to water temperature in the Gallatin and Smith Rivers in

318 Montana. Fish captured on days when daily maximum water temperatures were $> 20^{\circ}\text{C}$ suffered
319 mean mortality rates from 8% to 9%, although mortality was 0% when daily maximum water
320 temperature was $< 20^{\circ}\text{C}$ (Boyd et al. 2010). Maximum water temperatures in the LBR
321 occasionally surpassed 20°C during 2003-2013 in July and August. At present, no estimates of
322 catch-and-release mortality exist in the LBR during the high effort summer fly-fishery. Meta-
323 analysis by Bartholomew and Bohnsack (2005) showed that catch and release mortality of
324 Rainbow Trout ranged from 3-9% when fish were captured once via fly-fishing at water
325 temperatures similar to those observed in the LBR during July-September (i.e., $10\text{-}22^{\circ}\text{C}$; Horak
326 and Klein 1967; Dotson 1982; Schisler and Bergersen 1996). The best available creel survey on
327 the LBR estimated that 49 700 Rainbow Trout were captured and released by anglers during
328 July-September 2006 in a 50-km section of the LBR (Council and Ripley 2006), and our highest
329 estimate of abundance in this section of the river is 20 700 catchable-size trout (Figure 3; 414
330 fish/km x 50 km). While crude, this does correspond to anecdotal information contributed by
331 anglers that suggested individual fish are captured multiple times throughout the fishing season.
332 Given these numbers, the exploitation rate for this fishery was potentially 0.07-0.22 for the
333 summer fishery in 2006 (calculated as dead fish / abundance; Ricker 1975). These values may
334 be high, as they could result in a constant harvest policy that does not scale with decreases in
335 population size (see also Roughgarden and Smith 1996). Importantly, this approximation
336 ignores the potential for sub-lethal effects, such as interactions between the number of times a
337 fish is captured and released and mortality rate (Bartholomew and Bohnsack 2005; Pope et al.
338 2007), and increased susceptibility to disease (Pickering and Pottinger 1989). Thus, it is both
339 prudent and precautionary to suggest that catch-and-release mortality may represent an important
340 stressor in this system.

341 A number of potential concerns exist regarding these data and associated analyses, but we
342 suggest that the trend documented was unlikely to be caused by these issues. For instance, a key
343 study limitation was that no block nets were used during data collection, which was precluded by
344 the large size of the LBR. Consequently, the estimated population sizes may be biased as these
345 were generated using closed population models. Furthermore, the direction and magnitude of this
346 bias depends on the behavior of animals along the periphery of the study area (Van Katwyk
347 2014). However, it is unclear how changes in fish behavior along the periphery of these
348 relatively large study sites could result in the consistent population decline observed across the
349 entire study period. Similarly, the decision to use a multi-session modeling framework ignored
350 the possibility that an individual fish occurred in more than one year (Royle et al. 2013), and we
351 acknowledge that these models feature less ecological resolution than the outputs that would be
352 generated via open population capture-recapture models (see Korman et al. 2017). The approach
353 used here, however, was warranted because Rainbow Trout are short lived (i.e., maximum age of
354 7 years; Rhodes 2005) and have high instantaneous total mortality (van Poorten and Post 2005),
355 which indicated that there was likely high population turnover among years. Additionally, these
356 data did not support the use of an open population model as only nine total recaptures occurred
357 across years. Similarly, no estimates of instantaneous tag loss exist, even though it may have
358 been important (McFarlane et al. 1990; Walsh and Winkelman 2004; Vandergoot et al. 2012).
359 However, tagging crews used the same protocols throughout the study period, and hence
360 differences in instantaneous tag loss among years are unlikely to explain the consistent decline
361 observed. While we acknowledge some weaknesses in the available data, it is unlikely that there
362 was a consistent resultant “year” effect (i.e., consistent changes in animal behavior along the
363 periphery of our study area or with tag loss differences among years).

364 The issues facing the LBR fishery and documented here are germane to many inland
365 recreational fisheries, which are typified by poor or infrequent surveillance-style monitoring
366 (Lester et al. 2003; Nate et al. 2003). For example, fundamental data limitations precluded the
367 ability to determine the cause(s) of the estimated decline, despite compelling evidence that a
368 decline occurred. A paucity of reliable age and length data, along with inconsistent mark-
369 recapture surveys led to an inability to attribute the trend observed to reductions in juvenile or
370 adult survival, and hence to causal variables acting specifically on these life stages. Although
371 additional information can reduce the number of alternative explanations for a decline (see
372 Venturelli et al. 2014), calls to collect more data often fail to recognize key funding and
373 personnel constraints limiting biologists (Canessa et al. 2015). Approaches that explicitly
374 account for the marginal costs of data collection pursuant to management objectives and
375 constraints could provide a strategic framework for triaging monitoring resources (e.g., value of
376 information analysis; Hansen and Jones 2008). Similarly, targeted monitoring that views data
377 collection as a component of a broader structured decision-making process, rather than as a lone
378 activity, would maximize the utility of the data for distinguishing among competing hypotheses,
379 and help guide management actions in the face of uncertainty (Nichols and Williams 2006).
380 Thus, improving the scientific defensibility of inland fisheries management via strategic
381 monitoring and experimental management is necessary (McAllister and Peterman 1992; Post
382 2013; Hansen et al. 2015).

383 The LBR fishery demonstrates the complexities of maintaining inland recreational
384 fisheries in the presence of multiple stressors. A key take-away from this study was that a
385 combination of these stressors may have pushed Rainbow Trout in the LBR on an unsustainable
386 trajectory during 2003-2013. We identified the most plausible causes of the Rainbow Trout

387 decline, and suggest these probably acted in concert to affect the patterns observed, similar to
388 sustainability issues caused by multiple stressors in other inland recreational fisheries (Hansen et
389 al. 2015). We note that the threats facing this fishery include stressors that are both within and
390 beyond the control of local managers, which is similar to the safe operating space (SOS) concept
391 forwarded by Carpenter et al. (2017). Specifically, Whirling Disease and large flood events are
392 uncontrollable from a management standpoint, with high fishing effort remaining as the lone
393 stressor that managers can address. For instance, managers can attempt to reduce catch and
394 release mortality through indirect means such as gear restrictions or warm-weather closures
395 (Cooke and Schramm 2007; Boyd et al. 2010), and indeed, the latter have occurred in the LBR in
396 recent years when average water temperatures exceeded 20°C (i.e., full river closures or
397 voluntary restrictions were instituted in 2015 and 2017, respectively). Similarly, programs
398 seeking to educate anglers on proper catch and release techniques may be helpful (Adams 2017).
399 However, we suggest these may be patchwork solutions to managing release mortality, given
400 that the LBR is a popular open-access fishery that flows through a densely populated urban
401 center.

402 Our findings suggest effort restrictions may represent an important management strategy
403 for inland recreational fisheries that are pushed to undesirable states, or fisheries that are in high
404 effort situations in general. Unfortunately, active management policies that seek to reduce
405 fishing effort are generally unpopular with anglers (Schueller et al. 2012), and hence have rarely
406 been implemented in inland recreational fisheries (Pereira and Hansen 2003). An approach that
407 has been implemented with success, albeit in big-game wildlife management systems, is access
408 limitation via lottery systems (Boxall 1995; Scrogin et al. 2000). Similar limited-entry
409 management systems have been recommended and implemented in coastal sport fisheries (Cox

410 et al. 2002; Abbott and Wilen 2009), and a harvest-tag program (but not effort limitation) is
411 currently used to manage Alberta's high-effort Walleye *Sander vitreus* fisheries (Sullivan 2003).
412 Empirical evaluations of case-studies such as these represent a critical area for future work.
413 Similarly, well-designed adaptive management experiments could reduce key uncertainties
414 associated with limited entry programs in inland fisheries, such as how anglers redistribute effort
415 in response to regulation changes (Cox et al. 2003; Hunt et al. 2011). Management experiments
416 seeking to limit effort may offer exciting opportunities to learn about the dynamics between
417 anglers and fish populations, but will remain challenging to implement.

418 Acknowledgments

419 We acknowledge the significant effort that went into data collection by biologists and
420 technicians. C.L. Cahill acknowledges correspondence with A. Royle and M. Kéry regarding
421 multi-session models, and with D. Gwinn regarding Bayesian goodness-of-fit tests. H. Itô
422 contributed code regarding the non-centered random-effects parameterization. C. Cahill and K.
423 Wilson are supported by Vanier Canada Graduate Scholarship, and S. Mogensen and A. Cantin
424 are supported by NSERC doctoral scholarships. M. Faust, A. Cameron, and XX reviewers
425 greatly improved early versions of this manuscript.

426 References

- 427 Abbott, J.K., and Wilen, J.E. 2009. Rent dissipation and efficient rationalization in for-hire
428 recreational fishing. *Journal of Environmental Economics and Management* **58**(3): 300-314.
- 429 Adams, A.J. 2017. Guidelines for evaluating the suitability of catch and release fisheries:
430 Lessons learned from Caribbean flats fisheries. *Fisheries research* **186**: 672-680.
- 431 Allen, M., Ahrens, R., Hansen, M., and Arlinghaus, R. 2013. Dynamic angling effort influences
432 the value of minimum-length limits to prevent recruitment overfishing. *Fisheries Management
433 and Ecology* **20**(2-3): 247-257.

- 434 Anderson, R.M., and Nehring, R.B. 1984. Effects of a catch-and-release regulation on a wild
435 trout population in Colorado and its acceptance by anglers. *North American Journal of Fisheries*
436 *Management* **4**(3): 257-265.
- 437 Askey, P., Hogberg, L., Post, J., Jackson, L., Rhodes, T., and Thompson, M. 2007. Spatial
438 patterns in fish biomass and relative trophic level abundance in a wastewater enriched river.
439 *Ecology of Freshwater Fish* **16**(3): 343-353.
- 440 Barber, I., Hoare, D., and Krause, J. 2000. Effects of parasites on fish behaviour: a review and
441 evolutionary perspective. *Reviews in Fish Biology and Fisheries* **10**(2): 131-165.
- 442 Bartholomew, A., and Bohnsack, J.A. 2005. A review of catch-and-release angling mortality
443 with implications for no-take reserves. *Reviews in Fish Biology and Fisheries* **15**(1-2): 129-154.
- 444 Bartholomew, J.L., and Reno, P.W. 2002. The history and dissemination of whirling disease,
445 *American Fisheries Society*, pp. 3-24.
- 446 Beamish, R.J., McFarlane, G.A., and Thomson, R. 1999. Recent declines in the recreational
447 catch of coho salmon (*Oncorhynchus kisutch*) in the Strait of Georgia are related to climate.
448 *Canadian Journal of Fisheries and Aquatic Sciences* **56**(3): 506-515.
- 449 Betancourt, M., and Girolami, M. 2013. Hamiltonian Monte Carlo for Hierarchical Models.
450 arXiv preprint arXiv:1312.0906.
- 451 Boxall, P.C. 1995. The Economic Value of Lottery-rationed Recreational Hunting. *Canadian*
452 *Journal of Agricultural Economics/Revue canadienne d'agroeconomie* **43**(1): 119-131.
- 453 Boyd, J.W., Guy, C.S., Horton, T.B., and Leathe, S.A. 2010. Effects of Catch-and-Release
454 Angling on Salmonids at Elevated Water Temperatures. *North American Journal of Fisheries*
455 *Management* **30**(4): 898-907.
- 456 Canadian Food Inspection Agency. 2017. Confirmed detections of whirling disease – Alberta
457 2016. Available from [http://www.inspection.gc.ca/animals/aquatic-
458 animals/diseases/reportable/whirling-disease/alberta-2016/eng/1473443992952/1473443993551](http://www.inspection.gc.ca/animals/aquatic-animals/diseases/reportable/whirling-disease/alberta-2016/eng/1473443992952/1473443993551)
459 [accessed June 2017].

- 460 Canessa, S., Guillera-Aroita, G., Lahoz-Monfort, J.J., Southwell, D.M., Armstrong, D.P.,
461 Chadès, I., Lacy, R.C., and Converse, S.J. 2015. When do we need more data? A primer on
462 calculating the value of information for applied ecologists. *Methods in Ecology and Evolution*
463 **6**(10): 1219-1228.
- 464 Carpenter, B., Gelman, A., Hoffman, M., Lee, D., Goodrich, B., Betancourt, M., Brubaker,
465 M.A., Guo, J., Li, P., and Riddell, A. 2016. Stan: A probabilistic programming language. *Journal*
466 *of Statistical Software* **20**.
- 467 Carpenter, S.R., Brock, W.A., Hansen, G.J., Hansen, J.F., Hennessy, J.M., Isermann, D.A.,
468 Pedersen, E.J., Perales, K.M., Rypel, A.L., and Sass, G.G. 2017. Defining a Safe Operating
469 Space for inland recreational fisheries. *Fish and Fisheries* **18**(6): 1150-1160.
- 470 City of Calgary. 2018. Fish Compensation Program. Available from
471 [http://www.calgary.ca/UEP/Water/Pages/construction-projects/Fish-](http://www.calgary.ca/UEP/Water/Pages/construction-projects/Fish-compensation.aspx?redirect=/fishcompensation)
472 [compensation.aspx?redirect=/fishcompensation](http://www.calgary.ca/UEP/Water/Pages/construction-projects/Fish-compensation.aspx?redirect=/fishcompensation) [accessed Feb 2018].
- 473 Converse, S.J., and Royle, J.A. 2012. Dealing with incomplete and variable detectability in
474 multi-year, multi-site monitoring of ecological populations. Design and analysis of long-term
475 ecological monitoring studies. Cambridge University Press, Cambridge, England, United
476 Kingdom: 426-442.
- 477 Cooke, S., and Schramm, H. 2007. Catch-and-release science and its application to conservation
478 and management of recreational fisheries. *Fisheries Management and Ecology* **14**(2): 73-79.
- 479 COSEWIC. 2018. COSEWIC wildlife species assessment: quantitative criteria and guidelines.
480 Available from [https://www.canada.ca/en/environment-climate-change/services/committee-](https://www.canada.ca/en/environment-climate-change/services/committee-status-endangered-wildlife/wildlife-species-assessment-process-categories-guidelines/quantitative-criteria.html)
481 [status-endangered-wildlife/wildlife-species-assessment-process-categories-](https://www.canada.ca/en/environment-climate-change/services/committee-status-endangered-wildlife/wildlife-species-assessment-process-categories-guidelines/quantitative-criteria.html)
482 [guidelines/quantitative-criteria.html](https://www.canada.ca/en/environment-climate-change/services/committee-status-endangered-wildlife/wildlife-species-assessment-process-categories-guidelines/quantitative-criteria.html) [accessed Feb 2018].
- 483 Council, T., and Ripley, T. 2006. Bow River sport fish population monitoring, 2003 and 2005.
484 Alberta Conservation Association and Alberta Fish and Wildlife, Lethbridge and Calgary,
485 Alberta.

- 486 Cox, S.P., Beard, T.D., and Walters, C. 2002. Harvest control in open-access sport fisheries: hot
487 rod or asleep at the reel? *Bulletin of Marine Science* **70**(2): 749-761.
- 488 Cox, S.P., Walters, C.J., and Post, J.R. 2003. A model-based evaluation of active management of
489 recreational fishing effort. *North American Journal of Fisheries Management* **23**(4): 1294-1302.
- 490 Crowe-Swords, P. 2016. The economic importance of recreational river use to the city of
491 Calgary. Calgary River Users Alliance.
- 492 Dotson, T. 1982. Mortalities in trout caused by gear type and angler-induced stress. *North*
493 *American Journal of Fisheries Management* **2**(1): 60-65.
- 494 Elsayed, E., Faisal, M., Thomas, M., Whelan, G., Batts, W., and Winton, J. 2006. Isolation of
495 viral haemorrhagic septicaemia virus from muskellunge, *Esox masquinongy* (Mitchill), in Lake
496 St Clair, Michigan, USA reveals a new sublineage of the North American genotype. *Journal of*
497 *Fish Diseases* **29**(10): 611-619.
- 498 Gabry, J. 2015. ShinyStan: interactive visual and numerical diagnostics and posterior analysis for
499 Bayesian models. R package version.
- 500 Gelman, A. 2008. Scaling regression inputs by dividing by two standard deviations. *Statistics in*
501 *medicine* **27**(15): 2865-2873.
- 502 Gelman, A., Carlin, J.B., Stern, H.S., and Rubin, D.B. 2014. Bayesian data analysis. Chapman &
503 Hall/CRC Boca Raton, FL, USA.
- 504 Gelman, A., Lee, D., and Guo, J. 2015. Stan: A probabilistic programming language for
505 Bayesian inference and optimization. *Journal of Educational and Behavioral Statistics* **40**(5):
506 530-543.
- 507 George, S.D., Baldigo, B.P., Smith, A.J., and Robinson, G. 2015. Effects of extreme floods on
508 trout populations and fish communities in a Catskill Mountain river. *Freshwater biology* **60**(12):
509 2511-2522.

- 510 Gilmour, W.M. 1950. A study of the lower Bow River trout with special reference to taxonomy,
511 Department of Biological Sciences, University of Alberta, Edmonton, Alberta.
- 512 Glaser, S.M., Fogarty, M.J., Liu, H., Altman, I., Hsieh, C.H., Kaufman, L., MacCall, A.D.,
513 Rosenberg, A.A., Ye, H., and Sugihara, G. 2014. Complex dynamics may limit prediction in
514 marine fisheries. *Fish and Fisheries* **15**(4): 616-633.
- 515 Godwin, S.C., Dill, L.M., Reynolds, J.D., and Krkošek, M. 2015. Sea lice, sockeye salmon, and
516 foraging competition: lousy fish are lousy competitors. *Canadian journal of fisheries and aquatic
517 sciences* **72**(7): 1113-1120.
- 518 Hansen, G.J., Gaeta, J.W., Hansen, J.F., and Carpenter, S.R. 2015. Learning to manage and
519 managing to learn: sustaining freshwater recreational fisheries in a changing environment.
520 *Fisheries* **40**(2): 56-64.
- 521 Hansen, G.J., and Jones, M.L. 2008. The value of information in fishery management. *Fisheries*
522 **33**(7): 340-348.
- 523 Hatai, K., and Hoshiai, G. 1992. Mass mortality in cultured coho salmon (*Oncorhynchus kisutch*)
524 due to *Saprolegnia parasitica* coker. *Journal of Wildlife Diseases* **28**(4): 532-536.
- 525 Hilborn, R. 2016. Correlation and causation in fisheries and watershed management. *Fisheries*
526 **41**(1): 18-25.
- 527 Hilborn, R., and Walters, C.J. 1992. Quantitative fisheries stock assessment: choice, dynamics
528 and uncertainty. *Reviews in Fish Biology and Fisheries* **2**(2): 177-178.
- 529 Holling, C.S. 1973. Resilience and stability of ecological systems. *Annual review of ecology and
530 systematics* **4**(1): 1-23.
- 531 Horak, D.L., and Klein, W.D. 1967. Influence of capture methods on fishing success, stamina,
532 and mortality of rainbow trout (*Salmo gairdneri*) in Colorado. *Transactions of the American
533 Fisheries Society* **96**(2): 220-222.

- 534 Hubert, W., and Quist, M. 2010. Inland fisheries management in North America. American
535 Fisheries Society, Bethesda, Maryland.
- 536 Hunt, L.M., Arlinghaus, R., Lester, N., and Kushneriuk, R. 2011. The effects of regional angling
537 effort, angler behavior, and harvesting efficiency on landscape patterns of overfishing.
538 *Ecological Applications* **21**(7): 2555-2575.
- 539 Johnson, S.C., Bravo, S., Nagasawa, K., Kabata, Z., Hwang, J., Ho, J., and Shih, C. 2004. A
540 review of the impact of parasitic copepods on marine aquaculture. *Zool. Stud.* **43**(2): 229-243.
- 541 Johnston, F.D., Post, J.R., Mushens, C.J., Stelfox, J.D., Paul, A.J., and Lajeunesse, B. 2007. The
542 demography of recovery of an overexploited bull trout, *Salvelinus confluentus*, population.
543 *Canadian Journal of Fisheries and Aquatic Sciences* **64**(1): 113-126.
- 544 Jones, M.L., and Hansen, G.J. 2014. Making Adaptive Management Work: Lessons from the
545 Past and Opportunities for the Future. *In Future of Fisheries: Perspective for Emerging*
546 *Professionals. Edited by W.T. Taylor, A.J. Lynch and N.J. Leonard. American Fisheries Society,*
547 *Bethesda, Maryland. pp. 443-450.*
- 548 Jowett, I.G., and Richardson, J. 1989. Effects of a severe flood on instream habitat and trout
549 populations in seven New Zealand rivers. *New Zealand journal of marine and freshwater*
550 *research* **23**(1): 11-17.
- 551 Kéry, M., and Royle, J.A. 2015. Applied Hierarchical Modeling in Ecology: Analysis of
552 distribution, abundance and species richness in R and BUGS: Volume 1: Prelude and Static
553 Models. Academic Press.
- 554 Kéry, M., and Schaub, M. 2011. Bayesian population analysis using WinBUGS: a hierarchical
555 perspective. Academic Press.
- 556 Kitanishi, S., and Yamamoto, T. 2015. The effects of severe flooding on native masu salmon and
557 nonnative rainbow trout in the Atsuta River, Hokkaido, Japan. *Journal of Freshwater Ecology*
558 **30**(4): 589-596.

- 559 Korman, J., Yard, M.D., and Kennedy, T.A. 2017. Trends in Rainbow Trout recruitment,
560 abundance, survival, and growth during a boom-and-bust cycle in a tailwater fishery.
561 *Transactions of the American Fisheries Society* **146**(5): 1043-1057.
- 562 Lester, N.P., Marshall, T.R., Armstrong, K., Dunlop, W.I., and Ritchie, B. 2003. A Broad-Scale
563 Approach to Management of Ontario's Recreational Fisheries. *North American Journal of*
564 *Fisheries Management* **23**(4): 1312-1328.
- 565 Link, W.A., and Barker, R.J. 2009. Bayesian inference: with ecological applications. Academic
566 Press.
- 567 Lumsden, J., Morrison, B., Yason, C., Russell, S., Young, K., Yazdanpanah, A., Huber, P., Al-
568 Hussine, L., Stone, D., and Way, K. 2007. Mortality event in freshwater drum *Aplodinotus*
569 *grunniens* from Lake Ontario, Canada, associated with viral haemorrhagic septicemia virus, Type
570 IV. *Diseases of aquatic organisms* **76**(2): 99-111.
- 571 Lynch, A.J., Myers, B.J., Chu, C., Eby, L.A., Falke, J.A., Kovach, R.P., Krabbenhoft, T.J.,
572 Kwak, T.J., Lyons, J., and Paukert, C.P. 2016. Climate change effects on North American inland
573 fish populations and assemblages. *Fisheries* **41**(7): 346-361.
- 574 Markiw, M.E. 1992. Experimentally induced whirling disease I. Dose response of fry and adults
575 of rainbow trout exposed to the triactinomyxon stage of *Myxobolus cerebralis*. *Journal of*
576 *Aquatic Animal Health* **4**(1): 40-43.
- 577 Maunder, M.N., and Punt, A.E. 2013. A review of integrated analysis in fisheries stock
578 assessment. *Fisheries Research* **142**: 61-74.
- 579 McAllister, M.K., and Peterman, R.M. 1992. Experimental design in the management of
580 fisheries: a review. *North American Journal of Fisheries Management* **12**(1): 1-18.
- 581 McFarlane, G., Wydoski, R.S., and Prince, E.D. 1990. External tags and marks, pp. 9-29.
- 582 Modin, J. 1998. Whirling disease in California: a review of its history, distribution, and impacts,
583 1965–1997. *Journal of Aquatic Animal Health* **10**(2): 132-142.

- 584 Monnahan, C.C., Thorson, J.T., and Branch, T.A. 2017. Faster estimation of Bayesian models in
585 ecology using Hamiltonian Monte Carlo. *Methods in Ecology and Evolution* **8**(3): 339-348.
- 586 Nate, N.A., Bozek, M.A., Hansen, M.J., Ramm, C.W., Bremigan, M.T., and Hewett, S.W. 2003.
587 Predicting the occurrence and success of walleye populations from physical and biological
588 features of northern Wisconsin lakes. *North American Journal of Fisheries Management* **23**(4):
589 1207-1214.
- 590 Nehring, R.B. 2006. Colorado's cold water fisheries: whirling disease case histories and insights
591 for risk management. Colorado Division of Wildlife, Aquatic Wildlife Research.
- 592 Nehring, R.B., and Walker, P.G. 1996. Whirling disease in the wild. *A Fresh Approach to Stock*
593 *Assessment* **21**(6): 28.
- 594 Nichols, J.D., and Williams, B.K. 2006. Monitoring for conservation. *Trends in ecology &*
595 *evolution* **21**(12): 668-673.
- 596 Nickum, D. 1999. Whirling disease in the United States.
- 597 Ormerod, S., Dobson, M., Hildrew, A., and Townsend, C. 2010. Multiple stressors in freshwater
598 ecosystems. *Freshwater Biology* **55**(s1): 1-4.
- 599 Paukert, C.P., Glazer, B.A., Hansen, G.J., Irwin, B.J., Jacobson, P.C., Kershner, J.L., Shuter,
600 B.J., Whitney, J.E., and Lynch, A.J. 2016. Adapting inland fisheries management to a changing
601 climate. *Fisheries* **41**(7): 374-384.
- 602 Paul, A.J. 2012. Environmental flows and recruitment of walleye (*Sander vitreus*) in the Peace–
603 Athabasca Delta. *Canadian journal of fisheries and aquatic sciences* **70**(2): 307-315.
- 604 Pereira, D.L., and Hansen, M.J. 2003. A perspective on challenges to recreational fisheries
605 management: summary of the symposium on active management of recreational fisheries. *North*
606 *American Journal of Fisheries Management* **23**(4): 1276-1282.

- 607 Pickering, A., and Pottinger, T. 1989. Stress responses and disease resistance in salmonid fish:
608 effects of chronic elevation of plasma cortisol. *Fish physiology and biochemistry* **7**(1-6): 253-
609 258.
- 610 Pope, K., Wilde, G., and Knabe, D. 2007. Effect of catch-and-release angling on growth and
611 survival of rainbow trout, *Oncorhynchus mykiss*. *Fisheries Management and Ecology* **14**(2):
612 115-121.
- 613 Post, J. 2013. Resilient recreational fisheries or prone to collapse? A decade of research on the
614 science and management of recreational fisheries. *Fisheries Management and Ecology* **20**(2-3):
615 99-110.
- 616 Post, J.R., Mushens, C., Paul, A., and Sullivan, M. 2003. Assessment of alternative harvest
617 regulations for sustaining recreational fisheries: model development and application to bull trout.
618 *North American Journal of Fisheries Management* **23**(1): 22-34.
- 619 Post, J.R., Poorten, B.T., Rhodes, T., Askey, P., and Paul, A. 2006. Fish entrainment into
620 irrigation canals: an analytical approach and application to the Bow River, Alberta, Canada.
621 *North American Journal of Fisheries Management* **26**(4): 875-887.
- 622 Post, J.R., Sullivan, M., Cox, S., Lester, N.P., Walters, C.J., Parkinson, E.A., Paul, A.J., Jackson,
623 L., and Shuter, B.J. 2002. Canada's recreational fisheries: the invisible collapse? *Fisheries* **27**(1):
624 6-17.
- 625 Punt, A.E., and Hilborn, R. 1997. Fisheries stock assessment and decision analysis: the Bayesian
626 approach. *Reviews in Fish Biology and Fisheries* **7**(1): 35-63.
- 627 R Development Core Team. 2017. R: A language and environment for statistical computing. R
628 Foundation for Statistical Computing, Vienna, Austria
- 629 Rahel, F.J. 2016. Changing philosophies of fisheries management as illustrated by the history of
630 fishing regulations in Wyoming. *Fisheries* **41**(1): 38-48.

- 631 Rhodes, T. 2005. The immediate and short term impacts of catch-and-release angling on
632 migrating and pre-spawning condition rainbow trout (*Oncorhynchus mykiss*) in the Bow River,
633 Alberta, Department of Biological Sciences, University of Calgary.
- 634 Ricker, W.E. 1975. Computation and interpretation of biological statistics of fish populations.
635 Bull. Fish. Res. Board Can. **191**: 382.
- 636 Roughgarden, J., and Smith, F. 1996. Why fisheries collapse and what to do about it.
637 Proceedings of the National Academy of Sciences **93**(10): 5078-5083.
- 638 Royle, J.A. 2009. Analysis of capture–recapture models with individual covariates using data
639 augmentation. Biometrics **65**(1): 267-274.
- 640 Royle, J.A., Chandler, R.B., Sollmann, R., and Gardner, B. 2013. Spatial capture-recapture.
641 Academic Press.
- 642 Royle, J.A., and Dorazio, R.M. 2008. Hierarchical modeling and inference in ecology: the
643 analysis of data from populations, metapopulations and communities. Academic Press.
- 644 Schueller, A.M., Fayram, A.H., and Hansen, M.J. 2012. Simulated equilibrium walleye
645 population density under static and dynamic recreational angling effort. North American journal
646 of fisheries management **32**(5): 894-904.
- 647 Scrogin, D., Berrens, R.P., and Bohara, A.K. 2000. Policy changes and the demand for lottery-
648 rationed big game hunting licenses. Journal of Agricultural and Resource Economics: 501-519.
- 649 Seber, G.A.F. 1982. The estimation of animal abundance.
- 650 Sosiak, A. 2002. Long-term response of periphyton and macrophytes to reduced municipal
651 nutrient loading to the Bow River (Alberta, Canada). Canadian Journal of Fisheries and Aquatic
652 Sciences **59**(6): 987-1001.
- 653 Stan Development Team. 2016. Rstan: the R interface to Stan.
- 654 Statistics Canada. 2016. Census Profile, 2016 Census. Available from
655 <http://www12.statcan.gc.ca/census-recensement/2016/dp->

- 656 [pd/prof/details/page.cfm?Lang=E&Geo1=POPC&Code1=0115&Geo2=PR&Code2=48&Data=](http://pd/prof/details/page.cfm?Lang=E&Geo1=POPC&Code1=0115&Geo2=PR&Code2=48&Data=Count&SearchText=calgary&SearchType=Begins&SearchPR=01&B1=All)
657 [Count&SearchText=calgary&SearchType=Begins&SearchPR=01&B1=All](http://pd/prof/details/page.cfm?Lang=E&Geo1=POPC&Code1=0115&Geo2=PR&Code2=48&Data=Count&SearchText=calgary&SearchType=Begins&SearchPR=01&B1=All) [accessed Feb 2018].
- 658 Sugihara, G., May, R., Ye, H., Hsieh, C.-h., Deyle, E., Fogarty, M., and Munch, S. 2012.
659 Detecting Causality in Complex Ecosystems. *Science* **338**(6106): 496-500.
- 660 Sullivan, M.G. 2003. Active management of walleye fisheries in Alberta: dilemmas of managing
661 recovering fisheries. *North American Journal of Fisheries Management* **23**(4): 1343-1358.
- 662 Taube, N., He, J., Ryan, M.C., and Valeo, C. 2016. Relative importance of P and N in
663 macrophyte and epilithic algae biomass in a wastewater-impacted oligotrophic river.
664 *Environmental monitoring and assessment* **188**(8): 494.
- 665 Van Katwyk, K.E. 2014. Empirical validation of closed population abundance estimates and
666 spatially explicit density estimates using a censused population of North American red squirrels,
667 University of Alberta.
- 668 van Poorten, B.T., and Post, J.R. 2005. Seasonal Fishery Dynamics of a Previously Unexploited
669 Rainbow Trout Population with Contrasts to Established Fisheries. *North American Journal of*
670 *Fisheries Management* **25**(1): 329-345.
- 671 Vandergoot, C.S., Brenden, T.O., Thomas, M.V., Einhouse, D.W., Cook, H.A., and Turner,
672 M.W. 2012. Estimation of Tag Shedding and Reporting Rates for Lake Erie Jaw-Tagged
673 Walleyes. *North American Journal of Fisheries Management* **32**(2): 211-223.
- 674 Veiga, V.B., Hassan, Q.K., and He, J. 2014. Development of flow forecasting models in the Bow
675 River at Calgary, Alberta, Canada. *Water* **7**(1): 99-115.
- 676 Venturelli, P., Bence, J., Brenden, T., Lester, N., and Rudstam, L. 2014. Mille Lacs Lake
677 Walleye blue ribbon panel data review and recommendations for future data collection and
678 management. Minnesota Department of Natural Resources.
- 679 Vincent, E.R. 1996. Whirling disease and wild trout. *Fisheries* **21**(6): 32-33.

- 680 Walker, P.G., and Nehring, R.B. 1995. An investigation to determine the cause (s) of the
681 disappearance of young wild rainbow trout in the upper Colorado River. Middle Park, Colorado.
682 Colorado Division of Wildlife Report. Denver.
- 683 Walsh, M.G., and Winkelman, D.L. 2004. Anchor and visible implant elastomer tag retention by
684 hatchery rainbow trout stocked into an Ozark stream. North American Journal of Fisheries
685 Management **24**(4): 1435-1439.
- 686 Walters, C.J. 1986. Adaptive management of renewable resources. Macmillan Publishers Ltd.
- 687 Warren, D.R., Ernst, A.G., and Baldigo, B.P. 2009. Influence of Spring Floods on Year-Class
688 Strength of Fall-and Spring-Spawning Salmonids in Catskill Mountain Streams. Transactions of
689 the American Fisheries Society **138**(1): 200-210.
- 690 Welcomme, R. 2008. Inland fisheries: ecology and management. John Wiley & Sons.
- 691
- 692

693 **Figure Captions**

694 FIGURE 1.—Map showing locations sampled via multi-pass electrofishing in the lower Bow
695 River during 2003-2013. Upper insert: location of the study area in Alberta, Canada. Note that
696 sampling locations in 2003, 2005, 2007, and 2008 were identical and are represented by the
697 section of river delineated with vertical black bars (sampling location “1”). Sampling locations
698 were subsequently changed to stratified random locations: 2011= “2”, 2012 = “3”, 2013 = “4.”
699 The Bears paw Dam is indicated by ★.

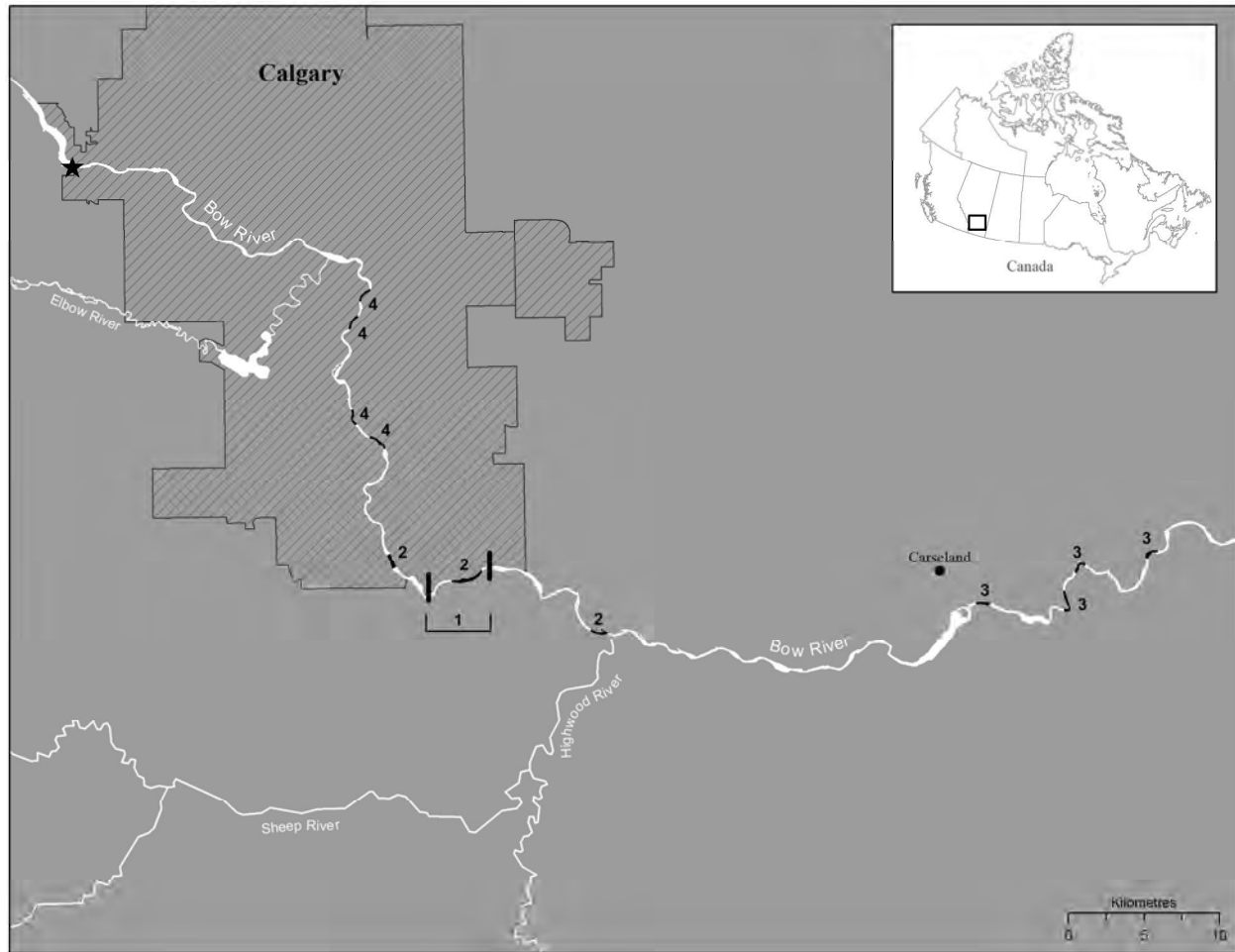
700 FIGURE 2.— Posterior distributions of Rainbow Trout density in the Lower Bow River, Alberta,
701 Canada during 2003-2013. Results are from model 1. Boxplots designate the median (black
702 line), the 25th and 75th percentiles (lower and upper box boundaries), the upper and lower
703 whiskers that extend to 1.5 times the interquartile range, and any remaining “outliers” (open
704 circles).

705 FIGURE 3.— Posterior distributions showing the percent change per year in Rainbow Trout
706 abundance in the lower Bow River, Alberta, Canada during 2003-2008 (upper panel) and 2003-
707 2013 (lower panel). Percent change per year was calculated as a derived variable in our ‘trend
708 model’ analyses.

709 FIGURE 4.— Predictive replicate discrepancy statistics vs. observed test statistics for three multi-
710 session models fit using the no-U-turn sampling algorithm in Stan. Posterior predictive p-values
711 were calculated as the proportion of points above the dashed 1:1 line. Left panel: independent
712 intercepts model. Middle panel: 2003-2008 trend model. Right panel: 2003-2013 trend model

713

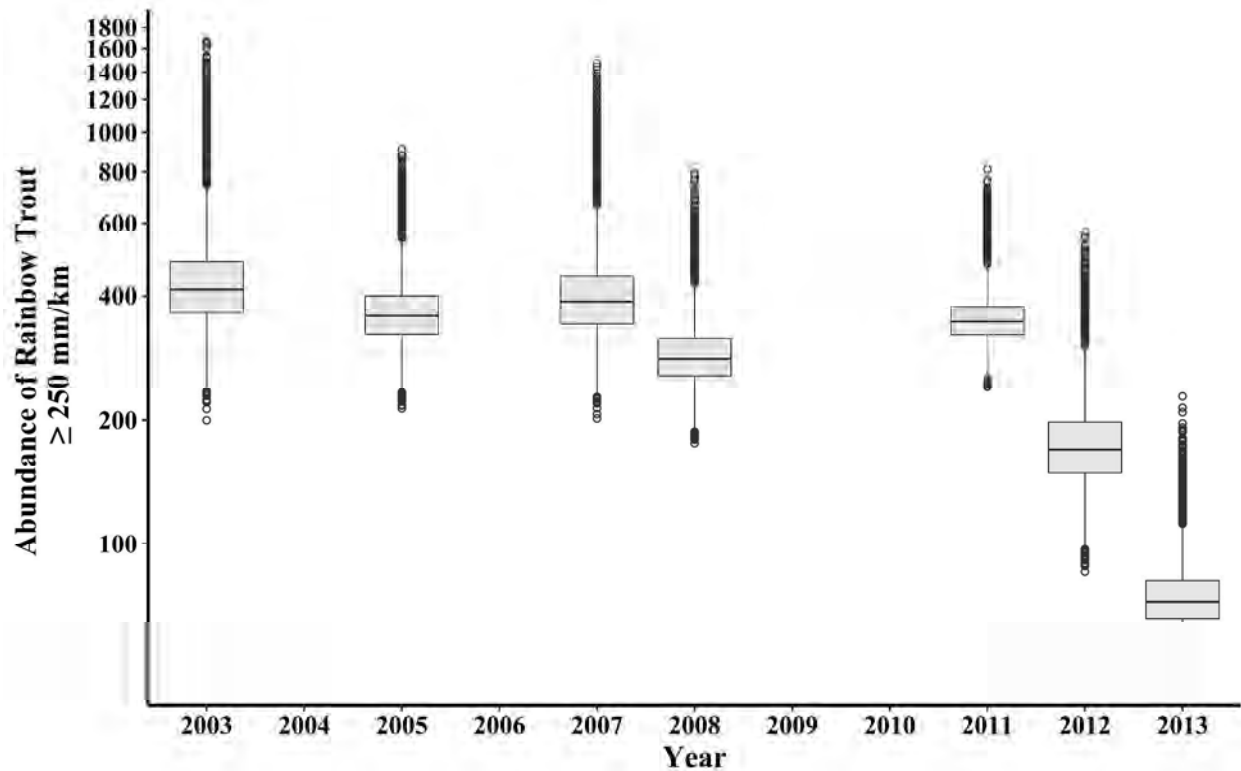
714



715

716 FIGURE 1.—Map showing locations sampled via multi-pass electrofishing in the lower Bow
 717 River during 2003-2013. Upper insert: location of the study area in Alberta, Canada. Note that
 718 sampling locations in 2003, 2005, 2007, and 2008 were identical and are represented by the
 719 section of river delineated with vertical black bars (sampling location “1”). Sampling locations
 720 were subsequently changed to stratified random locations: 2011= “2”, 2012 = “3”, 2013 = “4.”
 721 The Bears paw Dam is indicated by ★.

722



723

724 FIGURE 2.—Posterior distributions of Rainbow Trout density in the Lower Bow River, Alberta,

725 Canada during 2003-2013. Results are from model 1. Boxplots designate the median (black

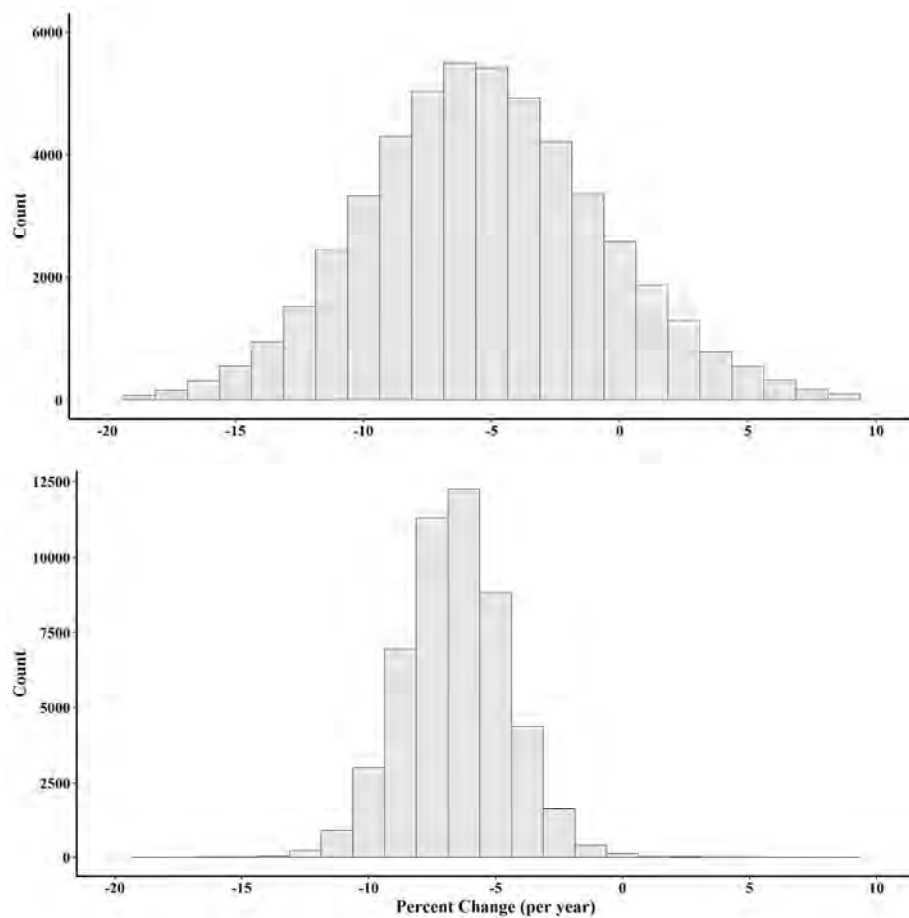
726 line), the 25th and 75th percentiles (lower and upper box boundaries), the upper and lower

727 whiskers that extend to 1.5 times the interquartile range, and any remaining “outliers” (open

728 circles).

729

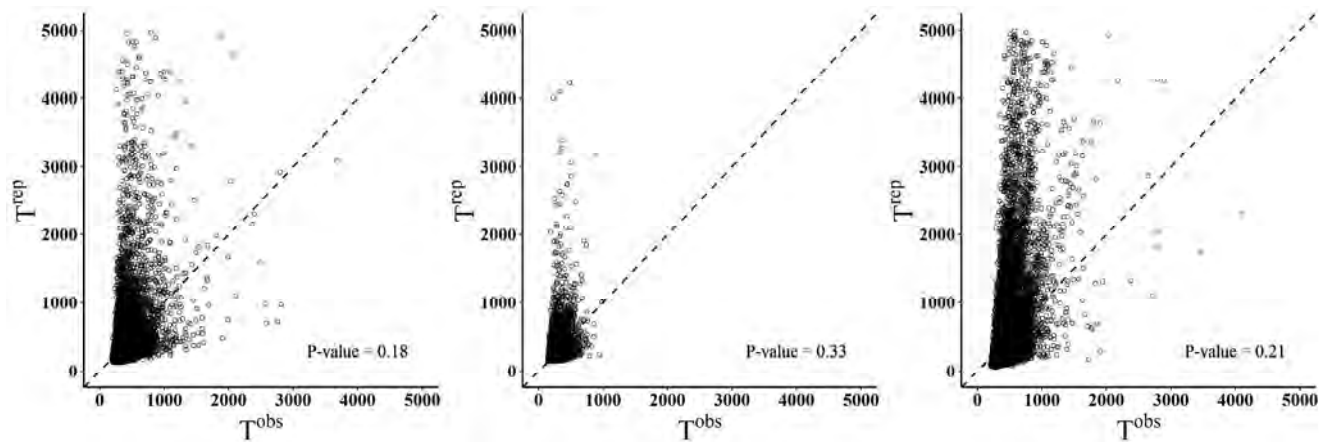
730



731

732 FIGURE 3.—Posterior distributions showing the percent change per year in Rainbow Trout
733 abundance in the lower Bow River, Alberta, Canada during 2003-2008 only (upper panel) and
734 2003-2013 (lower panel). Percent change per year was calculated as a derived variable in our
735 ‘trend model’ analyses.

736



737
738 FIGURE 4.—Predictive replicate discrepancy statistics vs. observed test statistics for three multi-
739 session models fit using the no-U-turn sampling algorithm in Stan. Posterior predictive p-values
740 were calculated as the proportion of points above the dashed 1:1 line. Left panel: independent
741 intercepts model. Middle panel: 2003-2008 trend model. Right panel: 2003-2013 trend model.

742

743

744

745 APPENDIX 1. —Methods used to evaluate goodness-of-fit via posterior predictive p-values for the
 746 multi-session models used in our analyses.

747 We evaluated our models using posterior predictive p-values (Gelman et al. 2014). Seber
 748 (1982) provided an asymptotic discrepancy statistic based on the chi-squared distribution for a
 749 single closed capture-recapture model assuming multinomial sampling:

$$(11) \quad T = \sum_{\omega \in \Omega} \frac{(x_{\omega} - \hat{e}_{\omega})^2}{\hat{e}_{\omega}}$$

750 where x_{ω} is the number of individual fish with capture history ω , \hat{e}_{ω} is the expected number of
 751 animals with that capture history calculated at the parameter estimates, and Ω represents the set
 752 of capture histories excluding the all-zero history of '0000.' Link and Barker (2009) extended
 753 this statistic to a Bayesian posterior predictive check, such that e_{ω} is calculated for each draw (h)
 754 of the posterior. We added an additional summation symbol to the statistic described by Link
 755 and Barker (2009) to evaluate the global fit of the multi-session models for all years considered

$$(12) \quad T_h^{obs} = \sum_{t=1}^7 \sum_{\omega \in \Omega} \frac{(x_{\omega} - e_{\omega}^h)^2}{e_{\omega}^h}$$

756 in our analyses. We calculated our observed test statistics as:

757 where e_{ω}^h corresponds to the expected number of animals with capture history parameter ω
 758 based on the parameter estimates for posterior draw h . We then compared T_h^{obs} to a replicate
 759 test statistic calculated as:

$$(13) \quad T_h^{rep} = \sum_{t=1}^7 \sum_{\omega \in \Omega} \frac{(x_{h\omega}^{rep} - e_{\omega}^h)^2}{e_{\omega}^h}$$

760 where $x_{h\omega}^{rep}$ is drawn from the posterior predictive distribution for x_{ω} (Link and Barker 2009).

761 The posterior predictive p-value for each model was then calculated as the proportion of $T_h^{rep} >$

762 T_h^{obs} (Gelman et al. 2014), and we judged p-values > 0.05 and < 0.95 as indications of sufficient

763 fit (see also Royle et al. 2013).

764

Draft

765 APPENDIX 2.

766 TABLE 2.1. Marginal posterior summaries of parameters (2.5%, 50%, and 97.5% percentiles,
 767 posterior SD) and diagnostic values (Neff = Number of Effective Samples, \hat{R} = Gelman-Rubin
 768 statistic) from the independent intercepts multi-session model 1 fitted to lower Bow River
 769 Rainbow Trout data during 2003-2013.

Parameter	Lower C.I.	Median	Upper C.I.	SD	Neff	\hat{R}
ψ_{2003}	0.16	0.20	0.39	0.06	2998	1
ψ_{2005}	0.15	0.19	0.29	0.04	5342	1
ψ_{2007}	0.15	0.21	0.34	0.05	4176	1
ψ_{2008}	0.12	0.15	0.23	0.03	3810	1
ψ_{2011}	0.15	0.18	0.25	0.03	3823	1
ψ_{2012}	0.07	0.09	0.16	0.02	7360	1
ψ_{2013}	0.03	0.04	0.06	0.01	5750	1
$\beta_{0_{2003}}$	7.13	7.49	8.04	0.23	4348	1
$\beta_{0_{2005}}$	7.07	7.34	7.74	0.17	6097	1
$\beta_{0_{2007}}$	7.08	7.42	7.92	0.21	4725	1
$\beta_{0_{2008}}$	6.85	7.11	7.51	0.17	4171	1
$\beta_{0_{2011}}$	7.08	7.28	7.60	0.13	4205	1
$\beta_{0_{2012}}$	6.27	6.63	7.14	0.22	8221	1
$\beta_{0_{2013}}$	5.52	5.79	6.23	0.18	6248	1
N_{2003}	1256	1789	3083	479.62	3520	1
N_{2005}	1181	1542	2287	283.01	5264	1
N_{2007}	1199	1672	2749	407.29	4134	1
N_{2008}	950	1217	1827	226.03	3733	1
N_{2011}	1200	1458	1995	203.47	3723	1
N_{2012}	532	759	1259	188.93	7262	1
N_{2013}	257	326	501	0.86	5289	1
σ_{2003}	0.02	0.29	0.82	0.22	2945	1
σ_{2005}	0.01	0.23	0.70	0.19	3634	1
σ_{2007}	0.01	0.29	0.81	0.22	2892	1
σ_{2008}	0.01	0.28	0.80	0.21	2992	1
σ_{2011}	0.01	0.24	0.70	0.19	2179	1

σ_{2012}	0.01	0.28	0.80	0.21	5045	1
σ_{2013}	0.02	0.39	0.99	0.26	4676	1
$p_{2003,1}$	0.02	0.05	0.07	0.01	4690	1
$p_{2003,2}$	0.02	0.04	0.07	0.01	4684	1
$p_{2003,3}$	0.03	0.06	0.09	0.02	4586	1
$p_{2003,4}$	0.02	0.04	0.06	0.01	4799	1
$p_{2005,1}$	0.04	0.07	0.10	0.01	6204	1
$p_{2005,2}$	0.04	0.07	0.10	0.01	6084	1
$p_{2005,3}$	0.03	0.06	0.08	0.01	6285	1
$p_{2005,4}$	0.04	0.07	0.10	0.02	5971	1
$p_{2007,1}$	0.03	0.06	0.10	0.02	4670	1
$p_{2007,2}$	0.03	0.06	0.09	0.02	4655	1
$p_{2007,3}$	0.04	0.06	0.09	0.02	4558	1
$p_{2007,4}$	0.02	0.05	0.07	0.01	7573	1
$p_{2008,1}$	0.06	0.11	0.15	0.02	4121	1
$p_{2008,2}$	0.07	0.12	0.16	0.02	4128	1
$p_{2008,3}$	0.05	0.09	0.13	0.02	4360	1
$p_{2008,4}$	0.01	0.05	0.07	0.01	6092	1
$p_{2011,1}$	0.05	0.09	0.11	0.02	4414	1
$p_{2011,2}$	0.06	0.09	0.12	0.02	4430	1
$p_{2011,3}$	0.09	0.14	0.17	0.02	4268	1
$p_{2011,4}$	0.05	0.08	0.10	0.01	4624	1
$p_{2012,1}$	0.01	0.04	0.07	0.01	6534	1
$p_{2012,2}$	0.04	0.08	0.12	0.02	8591	1
$p_{2012,3}$	0.04	0.08	0.13	0.02	8489	1
$p_{2012,4}$	0.05	0.10	0.15	0.03	8261	1
$p_{2013,1}$	0.06	0.13	0.19	0.03	7038	1
$p_{2013,2}$	0.07	0.15	0.21	0.04	6911	1
$p_{2013,3}$	0.10	0.20	0.28	0.05	6515	1
$p_{2013,4}$	0.06	0.12	0.19	0.03	7039	1

770

771

772 TABLE 2.2. Marginal posterior summaries of parameters (2.5%, 50%, and 97.5% percentiles,
 773 posterior SD) and diagnostic values (Neff = Number of Effective Samples, \hat{R} = Gelman-Rubin
 774 statistic) from the multi-session trend model 2 fitted to lower Bow River Rainbow Trout data
 775 during 2003-2008.

Parameter	Lower C.I.	Median	Upper C.I.	SD	Neff	\hat{R}
ψ_{2003}	0.16	0.22	0.32	0.04	5311	1
ψ_{2005}	0.17	0.20	0.24	0.02	4650	1
ψ_{2007}	0.15	0.18	0.22	0.02	4183	1
ψ_{2008}	0.13	0.17	0.23	0.02	4009	1
β_0	6.96	7.19	7.50	0.14	4172	1
β_1	-0.68	-0.25	0.19	0.22	4745	1
N_{2003}	1311	1760	2532	312.61	5300	1
N_{2005}	1320	1579	1958	162.66	4688	1
N_{2007}	1182	1414	1787	155.09	4289	1
N_{2008}	1054	1325	1815	155.09	3976	1
σ_{2003}	0.01	0.27	0.71	0.19	3897	1
σ_{2005}	0.01	0.24	0.61	0.16	4370	1
σ_{2007}	0.01	0.20	0.56	0.15	5676	1
σ_{2008}	0.01	0.36	0.81	0.21	3074	1
$p_{2003,1}$	0.03	0.05	0.07	0.01	5945	1
$p_{2003,2}$	0.03	0.04	0.06	0.01	5974	1
$p_{2003,3}$	0.04	0.06	0.09	0.01	5515	1
$p_{2003,4}$	0.02	0.04	0.06	0.01	5949	1
$p_{2005,1}$	0.05	0.07	0.09	0.01	6954	1
$p_{2005,2}$	0.05	0.07	0.09	0.01	6913	1
$p_{2005,3}$	0.04	0.05	0.07	0.01	7410	1
$p_{2005,4}$	0.05	0.07	0.09	0.01	6902	1
$p_{2007,1}$	0.06	0.08	0.10	0.01	6513	1
$p_{2007,2}$	0.05	0.08	0.10	0.01	6437	1
$p_{2007,3}$	0.07	0.10	0.13	0.01	5944	1
$p_{2007,4}$	0.02	0.05	0.07	0.01	7540	1
$p_{2008,1}$	0.06	0.10	0.13	0.02	4077	1
$p_{2008,2}$	0.07	0.10	0.15	0.02	4017	1

$p_{2008,3}$	0.05	0.08	0.11	0.02	4147	1
$p_{2008,4}$	0.01	0.05	0.07	0.02	5993	1

776

777

Draft

778 TABLE 2.3. Marginal posterior summaries of parameters (2.5%, 50%, and 97.5% percentiles,
 779 posterior SD) and diagnostic values (Neff = Number of Effective Samples, \hat{R} = Gelman-Rubin
 780 statistic) from the multi-session trend model 3 fitted to lower Bow River Rainbow Trout data
 781 during 2003-2013

Parameter	Lower C.I.	Median	Upper C.I.	SD	Neff	\hat{R}
ψ_{2003}	0.18	0.23	0.30	0.03	4158	1
ψ_{2005}	0.17	0.20	0.24	0.02	4105	1
ψ_{2007}	0.15	0.17	0.20	0.01	3767	1
ψ_{2008}	0.14	0.16	0.19	0.01	3458	1
ψ_{2011}	0.15	0.18	0.25	0.02	2950	1
ψ_{2012}	0.06	0.07	0.10	0.01	4145	1
ψ_{2013}	0.04	0.06	0.09	0.01	4194	1
β_0	6.91	7.04	7.19	0.07	3871	1
β_1	-0.83	-0.51	-0.20	0.16	4031	1
β_2	-1.00	-0.69	-0.39	0.16	3831	1
N_{2003}	1423	1810	2413	252.17	4181	1
N_{2005}	1324	1579	1954	160.73	4158	1
N_{2007}	1209	1385	1621	104.82	4061	1
N_{2008}	1133	1285	1492	91.45	3695	1
N_{2011}	1211	1464	1971	197.43	2457	1
N_{2012}	462	589	793	85.53	4320	1
N_{2013}	338	466	683	89.02	4108	1
σ_{2003}	0.02	0.28	0.70	0.19	3485	1
σ_{2005}	0.01	0.24	0.61	0.17	3770	1
σ_{2007}	0.01	0.19	0.52	0.14	6504	1
σ_{2008}	0.02	0.32	0.67	0.18	3608	1
σ_{2011}	0.01	0.25	0.69	0.19	2351	1
σ_{2012}	0.01	0.18	0.55	0.15	8843	1
σ_{2013}	0.24	0.82	1.29	0.26	3407	1
$p_{2003,1}$	0.03	0.05	0.07	0.01	4860	1
$p_{2003,2}$	0.03	0.04	0.06	0.01	5087	1
$p_{2003,3}$	0.04	0.06	0.08	0.01	4718	1
$p_{2003,4}$	0.03	0.04	0.06	0.01	5115	1

$p_{2005,1}$	0.05	0.07	0.09	0.01	5615	1
$p_{2005,2}$	0.05	0.07	0.09	0.01	5552	1
$p_{2005,3}$	0.04	0.05	0.07	0.01	5960	1
$p_{2005,4}$	0.04	0.07	0.09	0.01	5305	1
$p_{2007,1}$	0.06	0.07	0.10	0.01	8200	1
$p_{2007,2}$	0.06	0.08	0.10	0.01	7995	1
$p_{2007,3}$	0.08	0.10	0.13	0.01	7205	1
$p_{2007,4}$	0.02	0.05	0.07	0.01	7540	1
$p_{2008,1}$	0.08	0.10	0.13	0.01	5119	1
$p_{2008,2}$	0.09	0.11	0.14	0.01	5082	1
$p_{2008,3}$	0.06	0.09	0.1	0.01	5371	1
$p_{2008,4}$	0.01	0.05	0.07	0.02	6012	1
$p_{2011,1}$	0.05	0.08	0.11	0.01	3032	1
$p_{2011,2}$	0.06	0.09	0.12	0.02	2870	1
$p_{2011,3}$	0.09	0.14	0.17	0.02	2717	1
$p_{2011,4}$	0.05	0.08	0.10	0.01	3513	1
$p_{2012,1}$	0.01	0.04	0.07	0.01	3701	1
$p_{2012,2}$	0.07	0.10	0.14	0.02	6675	1
$p_{2012,3}$	0.07	0.11	0.15	0.02	6653	1
$p_{2012,4}$	0.09	0.13	0.18	0.02	6140	1
$p_{2013,1}$	0.04	0.08	0.14	0.03	4172	1
$p_{2013,2}$	0.04	0.09	0.15	0.03	4148	1
$p_{2013,3}$	0.06	0.12	0.21	0.04	4025	1
$p_{2013,4}$	0.03	0.07	0.13	0.03	4137	1

Patterns of fish species distributions replicated across three parallel rivers suggest biotic zonation in response to a longitudinal temperature gradient

Jonathan A. Mee | Geneva L. Robins | John R. Post

Department of Biological Sciences,
University of Calgary, Calgary, Alberta,
Canada

Correspondence

Jonathan Mee, Department of Biology,
Mount Royal University, Calgary, Alberta,
Canada.

Email: jmee@mtroyal.ca

Funding information

Canadian Climate Action Fund; National
Science and Engineering Research Council.

Abstract

Environmental gradients determine the distributions of individual species, which, in turn, shape patterns of species assemblage across those gradients. We used species distribution models to study the assemblage of fish species along the three mainstem rivers in the South Saskatchewan River Basin (SSRB) in Alberta, which flow in parallel across an 800-km longitudinal span and down 1400 m from the Rocky Mountains to the Great Plains of North America. We estimated the similarity of species assemblages along each river to identify general patterns of species assemblage associated with temperature and five other physiochemical variables. Mean July water temperature, which ranged from <math><11^{\circ}\text{C}</math> at high elevation to >math>>21^{\circ}\text{C}</math> at low elevation, was strongly associated with the presence-absence of most species in the SSRB. We found that high turnover occurred at two locations along the longitudinal gradient: where mean July water temperature was approximately 15°C and where mean July water temperature was approximately 19 or 20°C. There was also an increase in species richness at lower elevations where water temperatures were higher. Models incorporating forecasted changes in water temperature with climate change will likely provide accurate predictions of changes in the diversity and distribution of riverine fish communities across topographically heterogeneous landscapes.

KEYWORDS

beta diversity, climate change, community continuity, community-unit theory, individualistic hypothesis, river continuum concept

1 | INTRODUCTION

Species distributions are the fundamental units in the study of biogeography. The patterns, causes and implications of species distributions have been investigated for over a century (e.g., von Humboldt & Bonpland, 1805; Macarthur & Wilson, 1967; Wallace, 1876). Despite this long history, ecologists continue to debate the implications of species distributions in the context of species assemblage and community composition (e.g., Agrawal et al., 2007; Ricklefs, 2008). An ecological community is an assemblage of species in a given location at a

particular point in time (Ricklefs, 2008; Whittaker, 1975). Communities may exist, to some extent, due to close associations among species that have adapted to one another (*sensu* Clements, 1916), but communities emerge largely from the influence of regional processes and environmental gradients on the distributions of individual species (Gleason, 1926; Macarthur & Wilson, 1967; Ricklefs, 2008; Whittaker, 1975). Understanding the organisation of communities, therefore, depends largely on understanding the determinants of species distributions. Observational studies of species distributions at the regional scale are a necessary step towards answering questions about the

organisation of species assemblages and towards achieving predictability in ecology (Agrawal et al., 2007), which is important for preparing for the effects of climate change on species and communities.

Spatial distributions of communities and the population dynamics that underlie them are affected by climatic conditions. Each species' spatial distribution is influenced by the range of environmental factors to which it is adapted. At a regional scale, a species will be present where births and immigration exceed deaths and emigration. For example, a species may have a particular physiological response to temperature, which prescribes a zone of tolerance wherein populations have positive instantaneous growth rates; outside of this zone of tolerance, populations will have negative instantaneous growth rates and thus are unable to persist over the long term without immigration. There are assuredly multiple environmental factors that affect population growth rate (e.g., temperature, nutrients) each with varying degrees of importance for different species. Populations are only able to persist in the long term in areas with positive growth rate. We assume that presence and absence data from field studies conducted over several years across a broad geographic scale provides information about a species' zone of tolerance for a suite of environmental factors, although we recognise the potential for immigration and microhabitat refugia to introduce error in our estimation of zones of tolerance. Nonetheless, we can develop species distribution models relating environmental factors and broadscale presence-absence data and then predict or describe species' spatial distributions based on measurements of those environmental variables. These individual species distribution models can then be combined to describe the diversity and distribution of communities.

One challenge in understanding what drives the spatial distribution of species is the large number of physiological and ecological processes that could be important. Population growth rate could be affected by a multitude of abiotic variables and ecological interactions. The effect of a change in one environmental variable, such as temperature, could be potentially catastrophic to fitness and survival (Covich et al., 1997), or it may cause no discernable effect given the myriad of other influences on population dynamics (Davis, Lawton, Shorrocks, & Jenkinson, 1998; Moss et al., 2003). For the purposes of predicting and preparing for changes in diversity as a result of climate change, it is, therefore, desirable to identify the environmental effects that have a particularly strong influence on population dynamics for a given group of species. For example, temperature has a particularly strong effect on feeding, growth, reproduction and survival of fish (Hayward & Weiland, 1998; Wootton, 1990). Increases in temperature are predicted in response to global climate change, and we can potentially use forecasted temperature changes to predict changes in regional fish species assemblage.

Water temperature, due to its strong influence on key bioenergetic processes such as consumption rate, growth, reproduction and survival (Wootton, 1990), is referred to as an ecological resource for poikilothermic organisms (Magnuson, Crowder, & Medvick, 1979). Several species have been found to thermoregulate by actively seeking out areas of cooler water (i.e., tributaries and groundwater discharge zones) when faced with a temperature regime that exceeds their

optimal temperature range (Biro, 1998; Kaya, Kaeding, & Burkhalter, 1977; Mackenzie-Grieve & Post, 2006; Nielsen, Lisle, & Ozaki, 1994; Snucins & Gunn, 1995). Metabolic costs for these organisms typically increase exponentially with temperature (Hanson, Johnson, Kitchell, & Schindler, 1997). Consumption rates typically increase with temperature to a maximum value and then decline rapidly with increasing temperature, potentially falling below their metabolic demands (Hanson et al., 1997). For many species, the difference between their optimal thermal preference and the temperature where lethality or severe functional impairment occurs (critical upper temperature) is only a few degrees (Jobling, 1981). Nonetheless, abundant evidence suggests that distributions of fishes are often determined by a combination of several physicochemical variables, including temperature, and ecological interactions (e.g., Blanchet, Helmus, Brosse, & Grenouillet, 2014; Braaten & Guy, 1999; Brazner et al., 2005; Carvalho & Tejerina-Garro, 2015; Furlan, Esteves, & Quinaglia, 2013; Jackson, Peres-Neto, & Olden, 2001; Jaramillo-Villa, Maldonado-Ocampo, & Escobar, 2010; Lin, Tsai, Lin, Jong, & Wang, 2014; McCleary & Hassan, 2008; McGarvey, 2011; Mercado-Silva, Lyons, Diaz-Pardo, Navarrete, & Gutierrez-Hernandez, 2012; Murray & Innes, 2009; Rahel & Hubert, 1991; Smith & Kraft, 2005; Stevenson, Schnell, & Black, 1974; Troia & Gido, 2013).

Fish communities in river basins with high topographic relief, characterised by steep longitudinal temperature gradients, are excellent systems to study the influence of temperature on species assemblages and diversity (Diana, 2004; Jaramillo-Villa et al., 2010; Moyle, 2002; Rahel & Hubert, 1991), and, potentially, the impacts of climate change on regional diversity (e.g., Keleher & Rahel, 1996). The South Saskatchewan River Basin (SSRB) in southern Alberta, Canada, drains an approximately 300-km span of the east slope of the Rocky Mountains, with fish habitat from high-altitude, fast-flowing, cold mountain streams (maximum elevation 1,963 m) to wide, warm, slow-flowing rivers on the Great Plains (minimum elevation 578 m). The entire SSRB in Alberta drains an area of 112,800 km² (SSRB Water Supply Study Steering Committee 2010), an area slightly larger than Iceland. The mainstem rivers in the basin are the Bow River, Oldman River and Red Deer River, which coalesce with the South Saskatchewan River approximately 900 km from the headwaters (just beyond the eastern border of Alberta). Approximately 1.78 million people live in the South Saskatchewan River Basin, concentrated in the communities of Calgary, Red Deer, Lethbridge and Medicine Hat (Kulshreshtha & Thompson, 2007). Thirty-three species of fish are present in the SSRB mainstem rivers (Nelson & Paetz, 1992) and they represent a wide range of temperature preferences, from cold-water species such as bull trout, *Salvelinus confluentus* Suckley, 1859 (upper lethal temperature 17.7°C; Dunham, Rieman, & Chandler, 2003a), to warmer water species such as quillback, *Carpionodes cyprinus* (Lesueur, 1817) (upper lethal temperature 38.8°C; Cherry & Cairns, 1982; Beiting, Bennett, & McCauley, 2000).

Our study was motivated by two related objectives: to evaluate the predictive power of temperature in species distribution models, and to elucidate the patterns of species assemblage in relation to temperature. Two potential patterns of species assemblage across a river

basin are (i) biotic zonation and (ii) species addition with greater distance from headwaters (Rahel & Hubert, 1991). With biotic zonation, there will be discrete changes in species assemblage identifiable by adjacent locations with high turnover or low similarity. The locations of zone boundaries can then be associated with environmental factors that have particularly strong predictive power in species distribution models. A pattern of species addition, with greater species richness at lower elevation, but no discrete changes in species assemblages or associations with particular environmental factors, would be expected due to increased space, productivity and temporal stability at lower elevations. Our study is an improvement on previous attempts to elucidate these patterns (Jaramillo-Villa et al., 2010; Mercado-Silva et al., 2012; Rahel & Hubert, 1991) because we modelled longitudinal species distributions using extensive fine-scaled sampling along the full length of three replicate parallel mainstem rivers and, thereby, we were better able to draw general conclusions about patterns of species assemblage and the importance of particular environmental variables on species distributions. Also, unlike other studies conducted over similar geographic scales (e.g., Buisson, Blanc, & Grenouillet, 2008; Grenouillet, Pont, & Herisse, 2004; Pont, Hugueny, & Oberdorff, 2005), our aim was not merely to describe species distribution models and local species richness, but to specifically relate species diversity and assemblage to temperature in the context of predicting and preparing for the effects of climate change.

2 | MATERIALS AND METHODS

To quantify the associations between physicochemical variables and the presence or absence of each species, we compiled river physicochemical and fish species presence-absence data into a geographic information system (GIS) geodatabase using ARCGIS software (Environmental Systems Research Institute 2005a). The GIS geodatabase contained spatial information on fish species' presence-absence and environmental parameters. The base map (Figure 1) was created by tiling together National Topographic Service (NTS) maps at a 1:50,000 scale for the SSRB area (Natural Resources Canada 1982-2001). These maps were originally in geographic coordinates and were converted to a 10TM projection (AEP Forestry 10TM coordinates with a NAD83 datum). The 10TM projection has similar properties to the more common UTM projection as they are both Transverse Mercator Projections. The 10TM projection was used since the UTM zones (11U and 12U) divide the study area in half, while 10TM is centred for Alberta and is commonly used for Alberta forestry maps. The Alberta provincial boundary was sourced from the ESRI Geography Network (Environmental Systems Research Institute 2005b). Water temperature monitoring locations in the SSRB are shown in Fig. S1 in Appendix S1.

The South Saskatchewan River starts at the confluence of the Bow River and the Oldman River (Figure 1). For the purposes of our models,

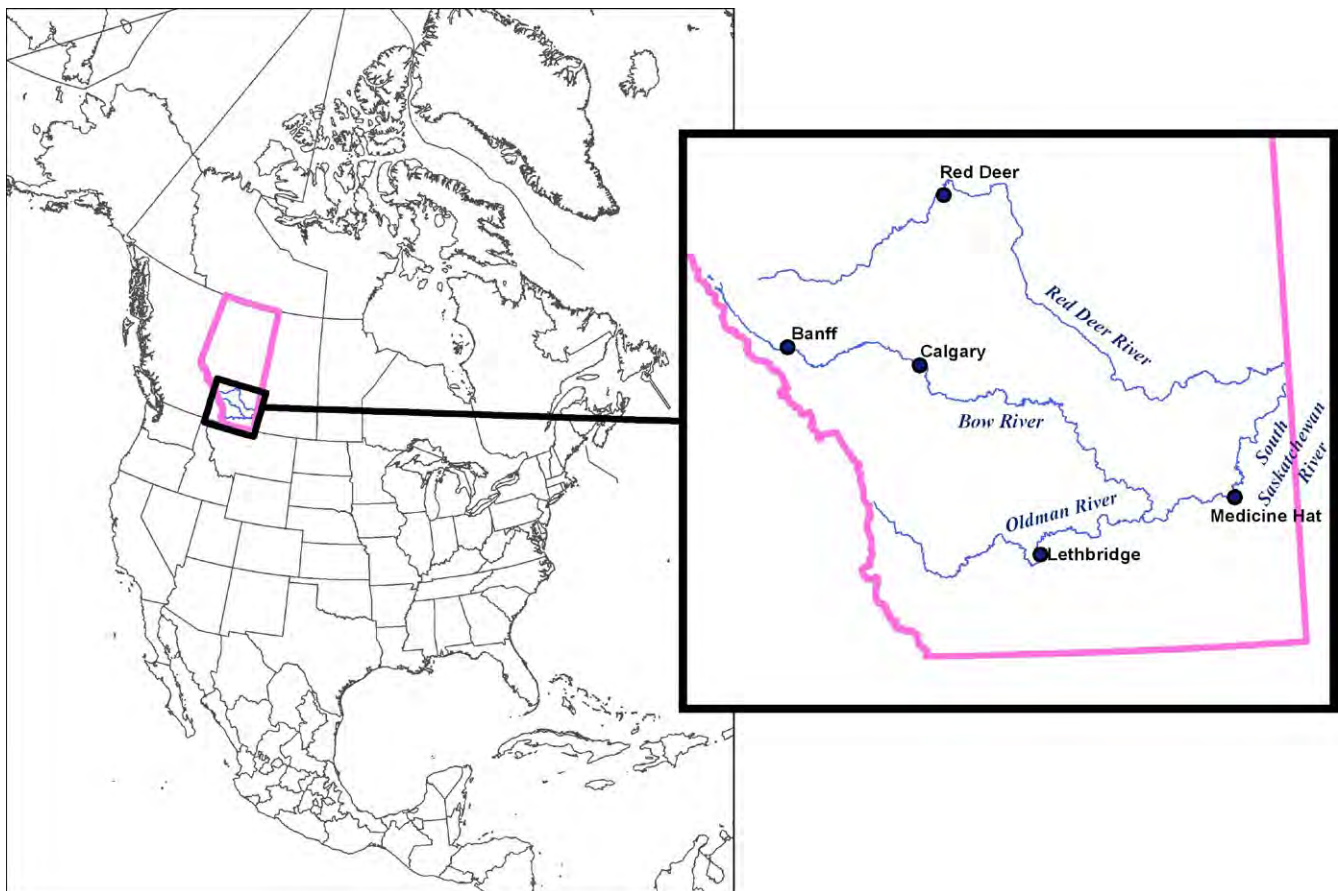


FIGURE 1 Map of the South Saskatchewan River Basin in Alberta, Canada. Provincial boundaries are shown in pink

and the rest of our study, we assumed that the start of the South Saskatchewan River is at the end of the Bow River, 637 km from the headwaters. The alternative was to assume that the start of the South Saskatchewan River was at the end of the Oldman River, 438 km from the headwaters, but neither alternative changed the interpretation of the data (alternative analysis not shown).

Mean July water temperature was expected to be the best predictor of fish species' distributions due to the sensitivity of fish to warm temperatures (Jobling, 1981). Water temperatures in July are typically the warmest of the year in the mainstem rivers of the SSRB. The month of July includes the warmest water temperatures at widely dispersed sites in the river basin. Water temperature data for the mainstem rivers in the SSRB were available from the NCE Water Quality Database. The NCE Water Quality Database was compiled by University of Calgary researchers for the Canadian Water Network from water quality data available in the SSRB from provincial, civic and federal agencies. Water temperatures available in the NCE Water Quality Database were collected by provincial, civic and federal agencies during water sampling events at 174 water monitoring stations throughout the mainstem rivers in the SSRB. Mean July water temperatures were averaged over a forty-year time period (from 1962 to 2001) bracketing the years in which fish presence-absence data were collected (1969–2000; see below). We interpolated mean July water temperatures for each kilometre of the watershed (i.e., between water monitoring stations) by modelling a sigmoidal relationship between mean July water temperature and headwater distance (Robins, 2009).

Phosphorous and nitrogen are limiting for primary producer biomass in the SSRB (Sosiak, 2002). High levels of these nutrients have been linked to high numbers and biomass of invertebrates (Askey et al., 2007). Thus, concentrations of phosphorous and nitrogen in the water of the mainstem rivers were used as indicators of the food environment available to fish in the SSRB. Turbidity may also affect the ability of fish species to capture prey as well as provide a predation refuge for some species and thus affect the relative strength of competition and predation (De Robertis, Ryer, Veloza, & Brodeur, 2003; Rieger & Summerfelt, 1997; Wootton, 1990). Various measures of phosphorous, nitrogen and turbidity were available in the NCE Water Quality Database for the years 1962–2001 in which different analytical methods have been used. For example, phosphorous was measured by fifteen analytical methods, nitrogen by seventeen methods and turbidity by six methods. For all three of these variables, the analysis method that had the greatest data density both spatially and temporally was selected. Total phosphate (mg/L) was used as a measure of phosphorous, dissolved nitrate-nitrite (mg/L) was used as a measure of nitrogen and turbidity was measured in nephelometric turbidity units (NTUs). The majority of data for phosphorous, nitrogen and turbidity were collected during the growing season between May and October, although some samples were taken in the winter months. We restricted our analysis to samples collected in the growing season. Mean values for these variables were calculated for May to October 1962–2001 for each monitoring station. As these variables are related to anthropogenic point sources and to natural processes, there would be high uncertainty in interpolation between sampling locations with a

regression equation. In addition, these variables are influenced by the stream direction (i.e., downstream locations are affected by upstream locations), which would be difficult to capture in a regression equation, which requires independent data points. Therefore, we interpolated phosphorous, nitrogen and turbidity values for each kilometre of the watershed by assigning the value of the closest upstream water monitoring location.

Water velocity has been commonly used in habitat models for lotic fish as the energy required to manoeuvre in fast-flowing water is higher than in slow-flowing water and can represent a limitation for some species (Clipperton, Koning, Locke, Mahoney, & Quazi, 2003; Hughes, Hayes, Shearer, & Young, 2003; Laliberte, Post, & Rosenfeld, 2014; Rosenfeld & Boss, 2001). Water velocity measurements for the entire SSRB were not available, so river slope was used as a proxy of the average water velocity. Slopes were estimated for each kilometre of the watershed from the NTS maps projected in 10TM coordinates based on the elevation contours that crossed the river. The difference in elevation between two contour lines was divided by the downstream distance between the two contours to give the mean slope.

A number of abiotic and biotic variables are correlated with river size and distance from headwaters (Rosenfeld, Post, Robins, & Hatfield, 2007; Vannote, Minshall, Cummins, Sedell, & Cushing, 1980). According to the river continuum concept (Vannote et al., 1980), river ecology, geology and hydrology change in a predictable way from headwaters to mouth. Channel width increases downstream and is correlated to discharge as well as a multitude of other longitudinal variables, which were not measured or available for the rivers in this study. Thus, channel width was included as a correlate of numerous unmeasured variables that change as the rivers increase in size downstream. Channel widths were estimated for each kilometre of the watershed from the NTS maps projected in 10TM coordinates. The channel width was measured directly from the NTS maps in ARCGIS software as the bank-to-bank distance perpendicular to the centre line of the river. Portions of the rivers that are represented as a line feature were estimated to have a channel width of 10 m.

Fish species' presence-absence data were derived from a number of sources. The Alberta Environment and Sustainable Resource Development (AESRD) Fisheries and Wildlife Management Information System (FWMIS) database was accessed on 28 June 2005 (AESRD 2005). Data in the FWMIS database were collected by numerous researchers using a variety of methods and was composed of data from all fish research conducted in the Province of Alberta. In addition, Henderson and Peter (1969) conducted a thorough survey of the fish species present in the rivers in the SSRB using multiple collection methods. Nelson and Paetz (1992) summarised the presence data in Alberta for fish species from University of Alberta collections and government survey data. Rhodes (2005) intensively sampled approximately 180 km of the Bow River for the target species of rainbow trout. These data were also included in the fish presence-absence data set. Where necessary, fish sampling locations were digitised from published maps (Henderson & Peter, 1969; Nelson & Paetz, 1992) into the geodatabase. Digitised data locations had an error of approximately 5 km. Fish locations from the Bow River study (Rhodes, 2005) were

TABLE 1 Species present in the South Saskatchewan River Basin (asterisk denotes non-native species).

Species by family	Abbreviation ^a
Salmonidae	
*Brook trout, <i>Salvelinus fontinalis</i> (Mitchill, 1814)	BKTR
Bull trout, <i>Salvelinus confluentus</i> Suckley, 1859	BLTR
Lake trout, <i>Salvelinus namaycush</i> (Walbaum, 1792)	LKTR
*Brown trout, <i>Salmo trutta</i> Linnaeus, 1758	BNTR
Westslope cutthroat trout, <i>Oncorhynchus clarki lewisi</i> (Suckley, 1856)	CTTR
*Rainbow trout, <i>Oncorhynchus mykiss</i> (Walbaum, 1792)	RNTR
Lake whitefish, <i>Coregonus clupeaformis</i> (Mitchill, 1818)	LKWH
Mountain whitefish, <i>Prosopium williamsoni</i> (Girard, 1856)	MNWH
Cyprinidae	
Finescale dace, <i>Chrosomus neogaeus</i> (Cope, 1867)	FNDC
Fathead minnow, <i>Pimephales promelas</i> (Rafinesque, 1820)	FTMN
Lake chub, <i>Couesius plumbeus</i> (Agassiz, 1850)	LKCH
Pearl dace, <i>Margariscus margarita</i> (Cope, 1867)	PRDC
Flathead chub, <i>Platygobio gracilis</i> (Richardson, 1836)	FLCH
Longnose dace, <i>Rhinichthys cataractae</i> (Valenciennes, 1842)	LNDC
Emerald shiner, <i>Notropis atherinoides</i> Rafinesque, 1818	EMSH
River shiner, <i>Notropis blennioides</i> (Girard, 1856)	RVSH
Spottail shiner, <i>Notropis hudsonius</i> (Clinton, 1824)	SPSH
Hiodontidae	
Goldeye, <i>Hiodon alosoides</i> (Rafinesque, 1819)	GOLD
Mooneye, <i>Hiodon tergisus</i> (Lesueur, 1818)	MOON
Catostomidae	
Longnose sucker, <i>Catostomus catostomus</i> Forster, 1773	LNSC
White sucker, <i>Catostomus commersonii</i> Lacépède, 1803	WHSC
Mountain sucker, <i>Catostomus platyrhynchus</i> Cope, 1874	MNSC
Quillback, <i>Carpiodes cyprinus</i> (Lesueur, 1817)	QUIL
Shorthead redhorse, <i>Moxostoma macrolepidum</i> (Lesueur, 1817)	SHRD
Cottidae	
Spoonhead sculpin, <i>Cottus ricei</i> (Nelson, 1876)	SPSC
Percopsidae	
Troutperch, <i>Percopsis omiscomaycus</i> (Walbaum, 1792)	TRPR
Percidae	
Walleye, <i>Sander vitreus</i> (Mitchill, 1818)	WALL
Sauger, <i>Sander canadensis</i> (Griffith & Smith, 1834)	SAUG

(Continues)

TABLE 1 (Continued)

Species by family	Abbreviation ^a
Yellow perch, <i>Perca flavescens</i> Mitchill, 1814	YLPR
Gasterosteidae	
Brook stickleback, <i>Culea inconstans</i> (Kirtland, 1840)	BRST
Esocidae	
Northern pike, <i>Esox lucius</i> Linnaeus, 1758	NRPK
Acipenseridae	
Lake sturgeon, <i>Acipenser fulvescens</i> (Rafinesque, 1817)	LKST
Lotidae	
Burbot, <i>Lota lota</i> (Linnaeus, 1758)	BURB

^aThis is the standard abbreviation used in the FWMS database, and which we use in Table 2.

included as point locations in the centre of the kilometre subsection where they were captured. We note that given the broad temporal range over which our data was collected (roughly 40 years), our results are expected to be representative of species' average occurrence at the scale of decades.

A location where a species was captured (i.e., a presence) was coded as 1. In order for a species to be classed as absent from a sampling location, and coded as 0, a specified level of fishing effort was required. For the Henderson and Peter (1969) study, all of the sites were sampled with a high level of effort using multiple types of fishing gear. Thus, if a fish species was not captured at one of their locations, it was determined to be absent. For the FMIS data, large fish species were coded as absent only if there were at least 100 fish collected and more than three species recorded at a location for large-bodied species. Small species were coded as absent for the FMIS data if the species was unreported at locations where there were more than 100 small fish collected. If a species was not reported at an FMIS location that did not meet these effort requirements, the species' presence was coded as unknown (999). No information on the level of fishing effort was available for fish locations in Nelson and Paetz (1992). Thus, these locations were coded as unknown (999) if a species was not reported. There was a consistent and high level of effort in the Rhodes (2005) study; thus, if a fish species was caught in other sections, it was coded as absent (0) if it was not caught at a particular location.

A total of 33 species were present in the data sources we used to assess species diversity across the SSRB in Alberta (Table 1). Four of these species (finescale dace, fathead minnow, lake trout and pearl dace) were rare or atypical (e.g., obligate lake species such as lake trout) and were not included in our analysis. To predict the probability of presence for the remaining 29 species at all locations throughout the SSRB, we evaluated multivariate logistic regression models using mean July water temperature (1962–2001), mean slope, mean total phosphate, mean dissolved nitrate–nitrite, mean turbidity and channel width (abbreviated as T, S, P, N, B and C, respectively, in Tables 1 and 2) as correlates of species presence–absence. Among-variable correlations were tested with the Spearman rank correlation coefficient.

TABLE 2 Summary of model averaged coefficients for the physicochemical variables (T = mean July water temperature, S = slope, P = mean total phosphorus, N = nitrate–nitrite, B = turbidity, C = channel width) included in the best logistic regression models predicting the presence of 29 fish species in the SSRB (see Table 1 for species abbreviations).

Species	T	S	P	N	B	C	T^2	S^2	P^2	N^2	B^2	C^2
BKTR	-1.41E+01	7.46E+03	-7.81E+01	1.02E+02	1.74E-01	5.84E-04	3.73E-01	-9.59E+05	4.41E+02	-1.06E+02	-7.83E-04	
BLTR	1.46E+00	-1.54E+03	-1.20E+00	7.45E-02	8.17E-02	-1.22E-02	-9.62E-02	2.28E+05			-4.76E-05	8.19E-06
BNTR	1.51E-02	1.24E+03	3.40E+01	-3.17E+00	-9.74E-02	-7.61E-03		-2.75E+05	-1.21E+02	2.47E+00		9.87E-06
BRST	-1.16E+00	-5.93E+03		-1.01E+00	-5.03E-03	1.05E-02	7.32E-03	1.25E+06		8.06E+00		-3.37E-05
BURB	5.27E-01	2.18E+03	-3.39E+00		-2.55E-02		1.64E-03	-3.32E+05			1.47E-04	
CTTR	-7.16E-01	4.03E+02	-1.26E+01	3.05E+01		-1.74E-02			1.65E+01	-3.71E+01		
EMSH	8.99E-03	3.58E+03	-5.22E+01	4.98E+01	-3.31E-02	1.78E-02	3.78E-02	-9.64E+05	1.62E+02	-8.82E+01	4.69E-04	-5.25E-05
FLCH	2.57E+00	-4.65E+03	1.97E-01	3.78E+00		4.23E-04				-2.05E+01		-1.23E-04
GOLD	5.81E+00	-2.10E+03	-1.89E-01	-1.79E+01	7.19E-03	4.09E-02	-1.59E-01			1.19E+01		
LKCH	9.49E-03	-3.52E+01	6.29E+00		-1.93E-02	-2.56E-04		2.29E+00				
LKST	2.97E+00	-5.92E+03	-2.09E-01	6.43E+00	1.03E-02	8.27E-04	-7.53E-02		5.55E+01	-3.69E+01	1.12E-05	
LKWH	3.18E-01	7.63E+03	-2.68E+01	2.32E+01	3.10E-02			-3.32E+06				3.01E-05
LNDC	4.63E-01	3.07E+03	-1.19E+00		-9.74E-04			-4.10E+05				
LNSC	-2.67E+00	5.13E+03	-1.48E+01	4.97E+00	-7.16E-04	-3.93E-03	1.17E-01	-7.00E+05		-8.86E-01		1.06E-06
MNSC	5.29E-01	3.60E+03	6.58E+01	-7.99E+00	-7.95E-02	-6.13E-04		-4.73E+05	-1.93E+02			
MNWH	4.07E+00	1.18E+03	1.25E-01	-3.90E+00	-6.10E-02	-7.63E-03	-1.20E-01	-2.15E+04		1.48E-01	5.17E-05	4.37E-06
MOON	1.45E+00	2.95E+02	-7.12E+00	2.36E+01	-9.98E-02			-3.34E+05	2.33E+01	-6.37E+01	4.62E-04	
NRPK	1.02E+01	-7.08E+02	-5.41E+01	9.97E+00	9.50E-03	2.44E-02	-2.74E-01	-3.69E+05	1.49E+02	-2.91E+01		-1.07E-04
QUJL	9.32E-01	-3.48E+02	-3.66E+00	1.39E+01	2.09E-02	2.08E-04	2.46E-03		2.11E+00	-1.73E+01	-2.95E-05	
RNTR	1.18E+00	2.74E+02	-1.46E+00	7.42E+00	-1.80E-02	-1.23E-02	-4.04E-02	-2.77E+04		-9.05E-01		
RVSH	1.35E+00	-2.71E+03	-2.72E-01		-1.83E-04	-2.53E-04	1.83E-02	1.86E+05				
SAUG ^a	7.70E+00	-3.68E+02	-1.29E+01	-4.91E+00	1.31E-02	1.72E-02	-1.79E-01		1.35E+01		-2.17E-05	-4.10E-05
SHRD	3.46E+00	2.73E+02	-2.44E+01	2.86E+01	-1.11E-02	-1.45E-02	-2.84E-02		1.69E+01	-4.69E+01	1.36E-05	
SPSC	-1.23E-01	1.09E+04	-2.44E+01	2.37E-01	8.89E-02	1.02E-02		-3.90E+06	2.37E+01		-3.15E-04	-2.68E-05
SPSH	1.95E-01	2.41E+03	-1.12E+01	3.61E+00	-1.01E-03	6.55E-03		-1.48E+06	-2.06E+00	-1.90E-01	-2.53E-05	-1.82E-05
TRPR	3.22E+00	-2.87E+02	-1.36E+01	2.68E+01	-1.23E-02	-3.42E-03	-8.44E-02		1.78E+01	-3.27E+01	-2.33E-06	
WALL	5.82E+00	-1.83E+03	-4.10E+00	8.44E+00	2.46E-02	2.46E-02	-1.64E-01	2.83E+04	5.58E+00	-2.03E+01		-5.72E-05
WHSC	-4.86E+00	5.41E+03	-2.22E+01	6.90E+00	-3.62E-02	-1.13E-03	1.87E-01	-8.21E+05	3.97E+01	-4.26E+00	4.15E-04	2.04E-06
YLPR	1.12E+01	4.25E+02	-7.25E-01	1.10E+01	5.14E-02	-2.89E-01		-4.41E+05		-1.41E+01		-1.05E-04

Bold text indicates significant effects based on Akaike weights >0.95.

^aBest model did not have a good fit. Model averaged parameters based on recalculated delta AIC values using Hosmer and Lemeshow goodness-of-fit test.

Physicochemical variables that were highly correlated with each other (i.e., >0.90 or <-0.90) were not included in the same model in order to avoid problems with multicollinearity, although there still may be some unavoidable multicollinearity due to the nature of rivers changing in a predictable way along the downstream direction (Allison, 2012).

Logistic regression analysis for each species was conducted using PROC LOGISTIC in SAS software, version 9.1 of the SAS System for Windows (Copyright © 2004 SAS Institute Inc., Cary, NC, USA), for all physicochemical variables. Given the possibility of species distributions being restricted to middle portions of the environmental gradients we sampled, we wanted to allow the models to fit a dome-shaped curve. Hence, we also included the cross products of for all physiochemical variables in our models (i.e., T^2 , S^2 , P^2 , N^2 , B^2 and C^2). All of the possible model combinations were compared using Akaike's information criterion, and the corrected Akaike weights (AIC_c) were generated and summed for each parameter. Akaike weights are roughly equivalent to the bootstrapping probabilities of each parameter being selected in the final model and, thus, can be interpreted as probabilities (Burnham & Anderson, 1998, 2004). Parameters with an Akaike weight of 0.95 or greater indicate that the parameter is significant in explaining the variation in the fish presence data. The Hosmer and Lemeshow goodness-of-fit test was also run on the logistic regression results in order to determine how well the model results fit the observed data (Allison, 2012). A model with a Hosmer and Lemeshow goodness-of-fit value that was small (<0.05) was considered to have a poor fit to the data. The final model used for the estimation of fish probability of presence was derived through model averaging. A subset of top models with a ΔAIC_c value of 2 or less relative to the best model, a Hosmer and Lemeshow goodness-of-fit value >0.05 and models with parameters which converged on a reliable solution were used to average the parameters for each variable included in the top model set. The Akaike weights were used to weight each parameter from each model in the model averaging process such that models with a higher Akaike weight (i.e., models that explain more of the variation in the data with the fewest parameters) have a higher influence on the final parameter value for each variable in the final model (Burnham & Anderson, 1998, 2004).

To describe fish species diversity and assemblage across the SSRB, we used the average probability of presence across all species as an index of species richness. To find locations with high turnover in species composition (i.e., high beta diversity), we calculated the mean Czekanowski coefficient among all comparisons of 1-km reaches within a 50-km moving window along each mainstem river (i.e., the mean coefficient within ± 25 km at 5-km steps along each river). To examine assemblage structure, we divided each river into 15-km intervals (i.e., sites), and calculated the mean probability of presence for each species at each of these "sites." We then calculated a dissimilarity matrix among all sites within each river based on 1 minus the Czekanowski coefficient (which is equivalent to the Bray-Curtis or Steinhaus dissimilarity coefficient; Magurran, 2004; Legendre & Legendre, 2012), and used nonmetric multidimensional scaling (NMDS) as an ordination method to look for longitudinal changes in assemblage structure associated with temperature. We also used hierarchical clustering to

delineate sites with similar species assemblages. These analyses were performed in R (R Core Team 2014) using the package *vegan* to perform the ordination analyses (Oksanen et al., 2016).

3 | RESULTS

There was an increase in temperature, turbidity and channel width, and a decrease in slope in the rivers from headwaters to the Alberta border (Figure 2). Total phosphate and dissolved nitrate-nitrite increased as distance from headwaters increased, but there were several spikes in concentrations of these nutrients near major cities, likely due to municipal wastewater discharge (Figure 2). None of the physicochemical variables in our analysis were strongly correlated (above 0.9 or below -0.9) by Spearman rank correlation. While there is some collinearity among the variables, which could affect the results of the parameter fitting and hypothesis tests for the regression modelling, the main concern of this study was to derive a final model that has accurate and reliable predictions. The collinearity present in the data is not expected to cause problems in the derivation of the final model using the information theoretic approach.

Each species' distribution was predicted based on the average values for the physicochemical variables in the best models for that species (Table 2). For seventeen species, mean July water temperature was a significant variable based on Akaike weights (Table 2). Nitrate-nitrite was a significant variable in the final model for 12 species, slope for nine species, phosphate for seven species, turbidity for five species and channel width for four species in the SSRB. Mean July water temperature had the highest average Akaike weight followed by dissolved nitrate-nitrite, mean slope, total phosphate, turbidity and channel width. Temperature was included in all of the final models for all fish species that we evaluated (Table 2).

A dome-shaped distribution pattern (with highest prevalence at intermediate distance from the headwaters) could be caused by a negative coefficient associated with any of the quadratic effects. Six species had a clear dome-shaped distribution pattern (Table 3): rainbow trout, brown trout, spoonhead sculpin, troutperch, spottail shiner and mountain sucker. Whereas temperature was generally an important determinant of species distribution, only two of these six species had a negative coefficient associated with the quadratic term for temperature (Table 2): rainbow trout and troutperch. The dome-shaped patterns for the other four species must, therefore, be caused by the quadratic terms associated with other physiochemical variables. For example, in the case of brown trout, the quadratic coefficients for slope and mean total phosphorous were included in the model predicting probability of occurrence, and had negative values ($-2.75E+05$ and $-1.21E+02$ for S^2 and P^2 , respectively; Table 2). Overall, nonquadratic effects were more prevalent than quadratic effects, and quadratic effects were not necessarily associated with a dome-shaped distribution patterns (Table 2).

Species richness tended to increase downstream and at higher temperatures (Table 3). There was also substantial turnover in composition of species along each of the mainstem rivers in the SSRB. The

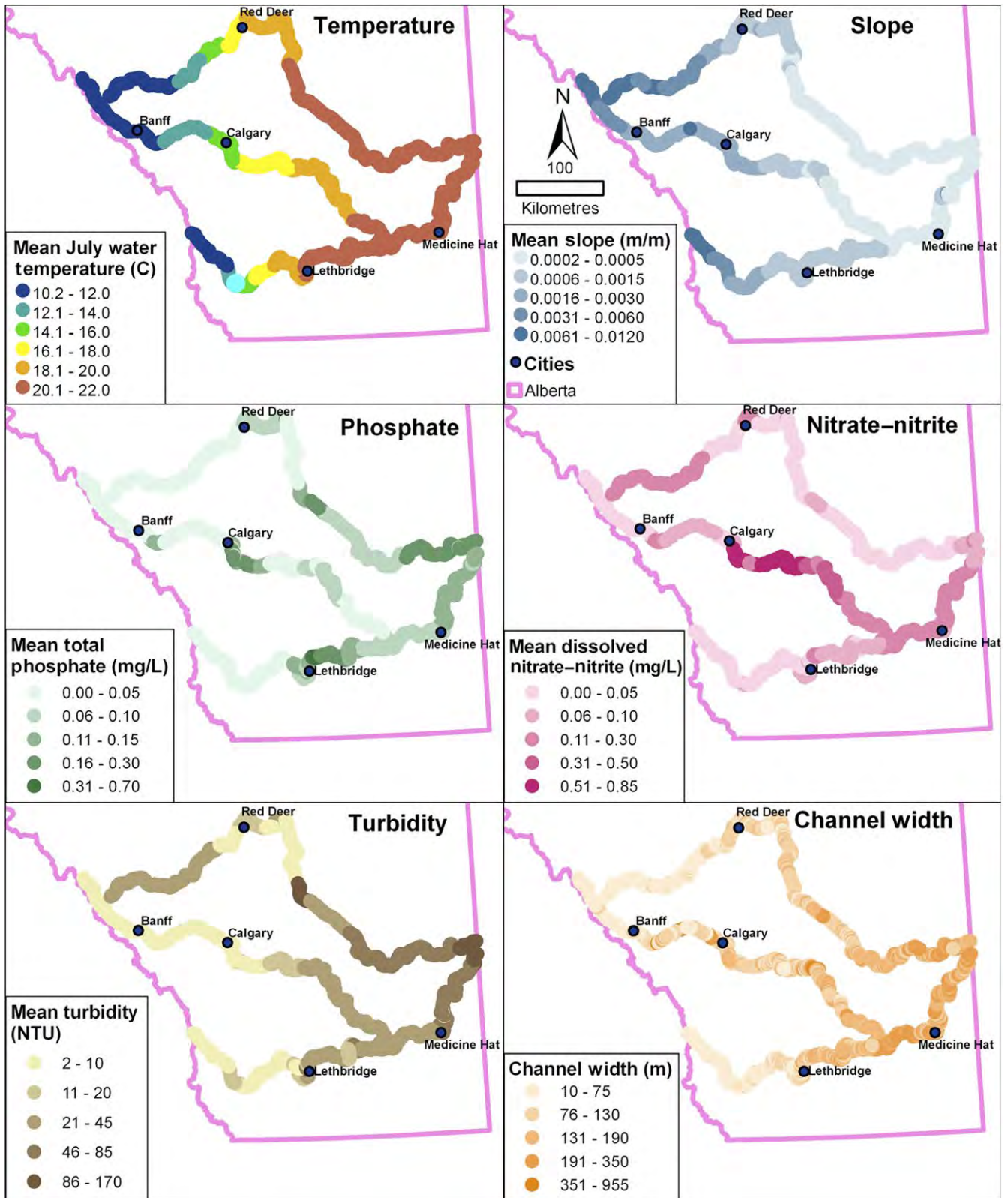


FIGURE 2 Interpolated values for mean July water temperature, slope, phosphate, nitrate-nitrite, turbidity and channel width in the SSRB mainstem rivers

sliding window analysis revealed evidence for high turnover (i.e., low similarity between adjacent locations) at locations where mean July water temperature equalled approximately 15°C in all three mainstem

rivers (Figure 3). There was also evidence for high turnover at locations where mean July water temperature equalled approximately 19–20°C (Figure 3).

TABLE 3 A comparison of species with probability of presence greater than 85% (from the present study) for river locations in the SSRB with different mean July temperatures, presented with thermal guild membership for those species examined in Eaton et al. (1995) and Wehrly et al. (2003), and with sparklines showing longitudinal distribution.

Species	High probability of presence with mean July temperature					Thermal guild	Longitudinal probability of presence
	>10 and <11°C	≥11 and <15°C	≥15 and <20°C	≥20 and <21°C	≥21 and <22°C		
Bull trout	y	y					
Cutthroat trout	y	y				Cold	
Brook stickleback	y	y	y				
Brook trout	y	y	y	y		Cold	
Mountain whitefish	y	y	y	y		Cold	
Rainbow trout		y	y			Cold	
Brown trout		y	y	y		Cold	
Spoonhead sculpin		y		y			
Longnose dace	y	y	y	y	y	Cool	
White sucker	y	y	y	y	y	Cool	
Longnose sucker	y	y	y	y	y		
Troutperch		y	y	y	y		
Spottail shiner			y				
Yellow perch			y			Cool	
Lake chub			y	y			
Northern pike			y	y		Cool	
Mountain sucker			y	y	y		
Emerald shiner			y	y	y		
Lake whitefish			y	y	y		
Goldeye			y	y	y		
Mooneye			y	y	y		
Shorthead redhorse			y	y	y		
Walleye			y	y	y	Cool	
Sauger			y	y	y	Cool	
Quillback			y	y	y		
Lake sturgeon			y	y	y		

(Continues)

TABLE 3 (Continued)

Species	High probability of presence with mean July temperature					Thermal guild	Longitudinal probability of presence
	>10 and <11°C	≥11 and <15°C	≥15 and <20°C	≥20 and <21°C	≥21 and <22°C		
Flathead chub				y	y		
River shiner				y	y		
Burbot				y	y	Cool	

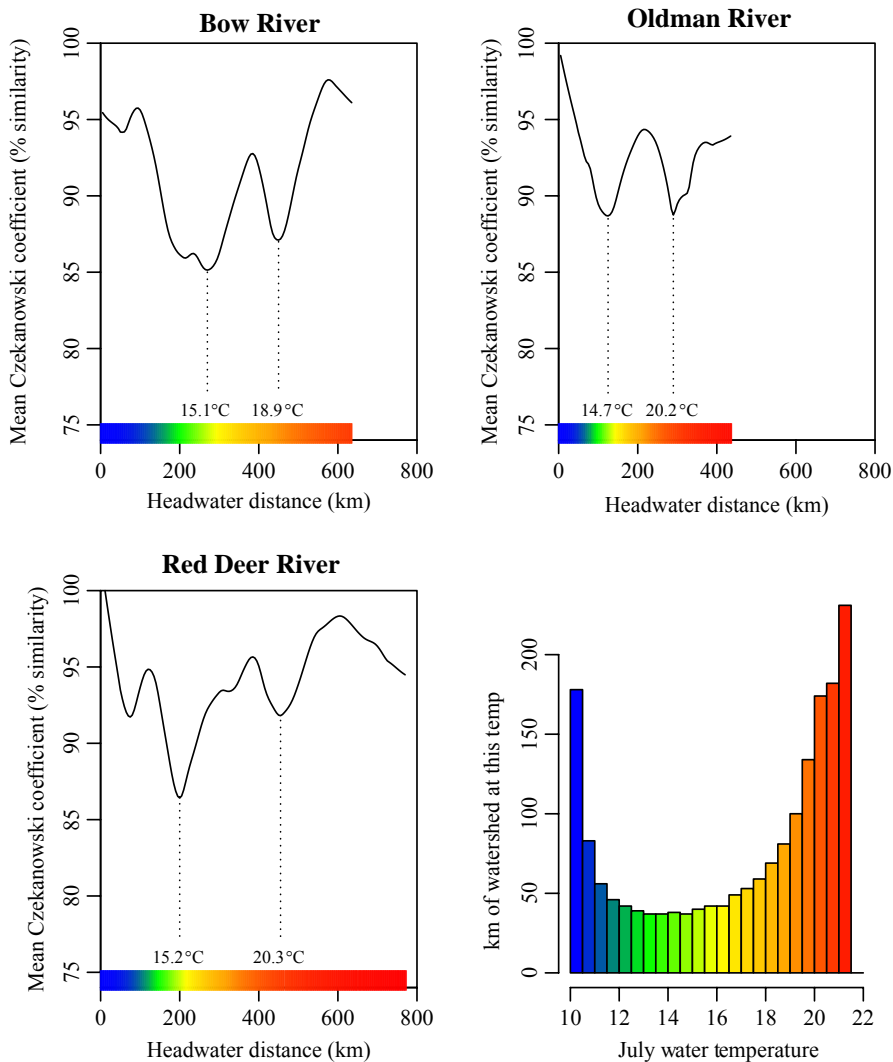


FIGURE 3 The mean Czekanowski coefficient (i.e., per cent similarity) in a 50-km sliding window estimated every 5 km along the Bow, Oldman and Red Deer rivers, based on the predicted probability of presence for 29 fish species at each kilometre of river. The lines have been smoothed by locally weighted regression over 50-km spans using the LOWESS smoother (Cleveland, 1981). The coloured bar at the bottom of the similarity plots shows the mean July water temperature at each kilometre of the rivers. The histogram at the bottom right acts as a legend to interpret the colours at the bottom of the other plots, while also showing the number of kilometres of watershed at each temperature. The specific mean July water temperatures corresponding to the points in the watershed with the greatest turnover are indicated with dotted lines

Ordination using NMDS indicated that headwater sites had distinct communities compared with high stream order sites; scores on the first NMDS axis increased with increasing headwater distance in all three mainstem rivers (Figure 4). In addition, the NMDS analysis, coupled with hierarchical clustering based on community dissimilarity, revealed that the longitudinal structure of species assemblage corresponded closely with the locations of high turnover in each river. Clusters of sites with similar community assemblages identified via hierarchical clustering (i.e., sites connected by short distances along the

green lines in Figure 4) were associated with distinct portions of the temperature gradient (separated by red lines in Figure 4) in each of the three mainstem rivers.

Eleven of the 29 species analysed in our study have previously been classified into thermal guilds (Eaton et al., 1995; Wehrly, Wiley, & Seelbach, 2003). Cutthroat trout, brook trout, mountain whitefish, brown trout and rainbow trout have been classified as cold guild species. Most of these cold guild species had a high probability of presence (>85%) in the coldest reaches of the SSRB (Table 3). Northern

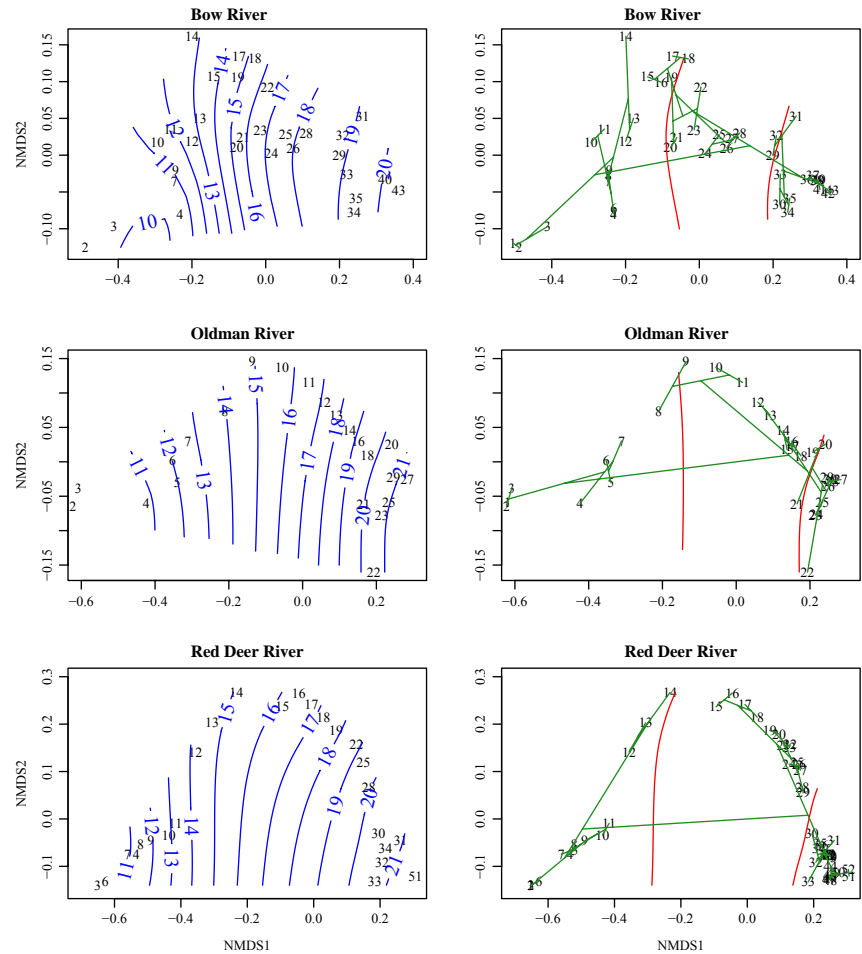


FIGURE 4 Nonmetric multidimensional scaling (NMDS) plots for sites (i.e., 15-km intervals) along each of the mainstem rivers in the SSRB based on the dissimilarity of species assemblages. The small-type numbers (in black) show the location of each site on NMDS ordination axes (NMDS1 and NMDS2). Blue contour lines (and numbers) in the left panels show the association of the temperature gradient in each river with clusters of similar sites. In the left panels only, overlapping site labels have been removed to improve clarity. Red lines in the right panels indicate the temperatures associated with high turnover in each river (see Figure 3). Green lines in the right panels depict the hierarchical clustering of sites based on the dissimilarity of species assemblages (longer distance between sites along the lines indicates greater dissimilarity)

pike, longnose dace, white sucker, walleye, sauger, yellow perch and burbot have been classified as cool guild species. Most of these cool guild species had a high probability of presence in the warmest reaches of the SSRB (Table 3). No warm guild species were found in the SSRB. Three species (longnose dace, white sucker and longnose sucker) had high probability of presence across the full range of temperatures in the SSRB (table 3). The high turnover where water temperature equalled approximately 15°C was associated with a sharp decline in the probability of presence of certain species (e.g., bull trout; Figure 5) and an increase in the probability of presence of others (e.g., northern pike and walleye; Table 3). Similarly, the high turnover where water temperature equalled approximately 19 or 20°C was associated with a sharp decline in the probability of presence of some species (e.g., rainbow trout; Figure 6) and an increase in the probability of presence of others (e.g., flathead chub; Figure 7). Other species generally had varying degrees of thermal niche width, and overlapped continuously along the length of the three mainstem rivers in the SSRB (Table 3).

4 | DISCUSSION

Within the SSRB in Alberta, from headwaters to the Saskatchewan border, there was an increase in water temperature, total phosphate, dissolved nitrate–nitrite, turbidity and channel width and a decrease

in slope, as expected according to the river continuum concept (Vannote et al., 1980). These longitudinal physicochemical changes were associated with changes in the probability of presence of 29 fish species found in the SSRB. Mean July water temperature, in particular, was strongly associated with the presence–absence of most species in the SSRB, and there was a subset of species (most notably bull trout and cutthroat trout) found primarily in the coldest reaches (mean July water temperature <15°C) and a subset of species (most notably flat-head chub and river shiner) found primarily in the warmest reaches (mean July water temperature >19 or 20°C).

Species richness was highest in the low-elevation reaches, and declined towards the headwaters, which is consistent with a pattern of species addition. We also found strong evidence, replicated across all three mainstem rivers in the SSRB, that there is a switch from a cold-water fish assemblage in the headwaters, where mean July water temperature is below 15°C, to a warmer water fish assemblage, where mean July water temperature is above 15°C, and then to an even warmer water assemblage where mean July water temperature is above 19 or 20°C. Generally, the fish that comprise these different assemblages have experimentally determined temperature tolerances that are consistent with the thermal niches inferred in the present study. Within the regional pool of species in the SSRB, those with published mean temperature preferences below 15°C (cutthroat trout, bull trout, mountain whitefish, and longnose sucker; Vigg & Koch, 1980;

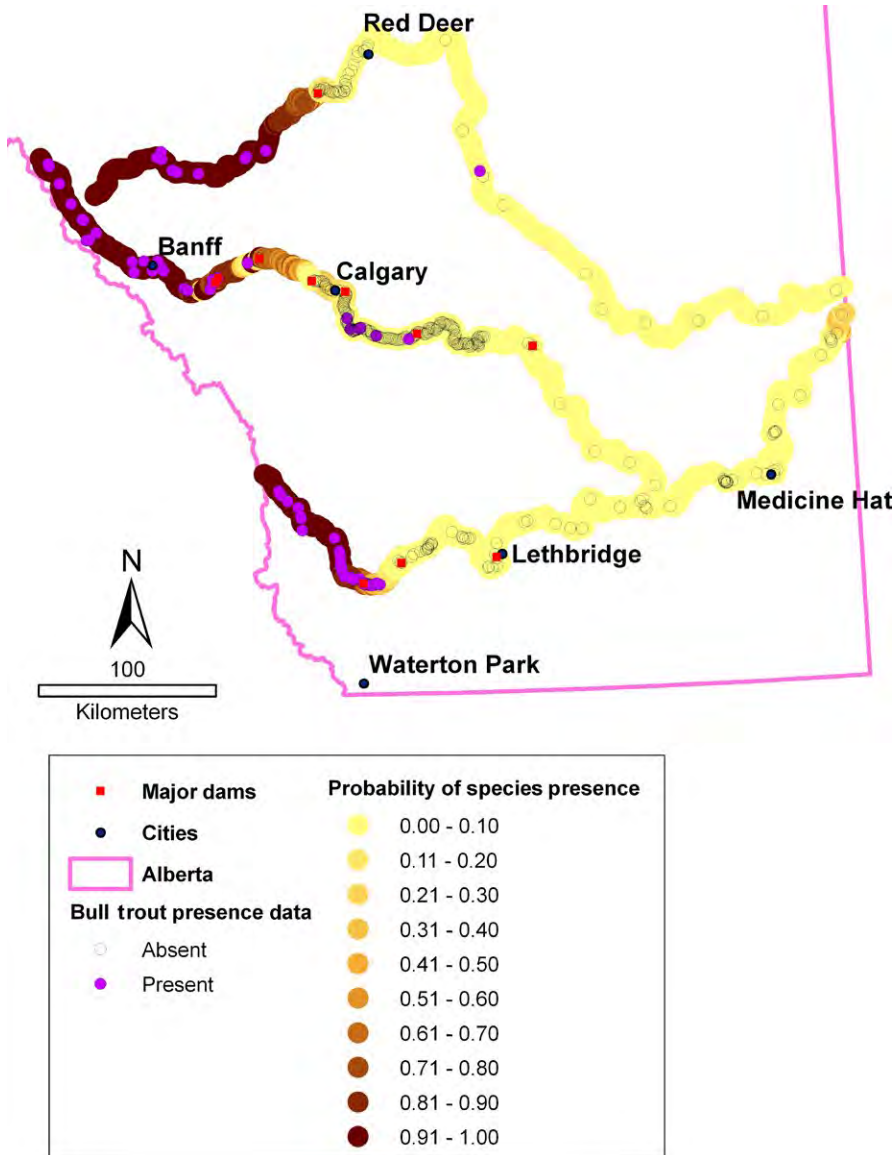


FIGURE 5 Observed presence–absence and probability of presence based on model averaging among the best logistic regression model (see Table 2) predicting the presence of bull trout in the SSRB

Jobling, 1981; Cherry & Cairns, 1982; Ihnat & Bulkley, 1984; Eaton & Scheller, 1996; Dickerson & Vinyard, 1999; Beitinger et al., 2000; BC MELP 2001; Dunham et al., 2003a; Huff, Hubler, & Borisenko, 2005) were all found in the coldest headwater regions of the SSRB. Species with published mean temperature preferences above 18°C (yellow perch, sauger, walleye, lake sturgeon, northern pike, emerald shiner, spottail shiner, quillback, white sucker; Scott & Crossman, 1979; Jobling, 1981; Cherry & Cairns, 1982; Kellogg & Gift, 1983; Cincotta & Stauffer, 1984; US EPA 1995; Eaton & Scheller, 1996; Beitinger et al., 2000; Lester, Dextrase, Kushneriuk, Rawson, & Ryan, 2004; Amadio, Hubert, Johnson, Oberlie, & Dufek, 2005; Benson, Sutton, Elliott, & Meronek, 2005; Amadio, Hubert, Johnson, Oberlie, & Dufek, 2006; Wilson & Nagler, 2006) were all found in the warm lowland regions of the SSRB. Thus, there is substantial evidence for biotic zonation based on temperature driving species assembly in the SSRB.

An important assumption in the species distribution modelling in our study is that the data used for the model selection are unbiased and representative of long-term patterns of fish species' presence.

There can, however, be challenges in using pre-existing historical data due to variable collection methods and biases in sampling effort among different locations (Hortal, Jimenez-Valverde, Gomez, Lobo, & Baselga, 2008). In this study, the results of a detailed presence and absence survey using a high level of effort (Henderson & Peter, 1969) were combined with presence-only data from several sources (Nelson & Paetz, 1992), data with varying levels of effort (AESRD 2005) and data with a high level of effort for large fish (Rhodes, 2005). In particular, many fisheries studies in the FMIS database were focused on one or two target species (mainly trout) and other species are recorded as incidental captures. The bias towards trout in the data set likely influenced the spatial distribution of fish sampling locations, with the greatest density of sampling locations in the stream reaches where trout are known (or suspected) to be present. The mid-reaches of the rivers had a high data density for fish captures with relatively low data density in the lower and upper reaches. But, as many species in this study have a range edge in the mid-reaches of the rivers (i.e., where turnover is highest), oversampling in the mid-reaches of the rivers is

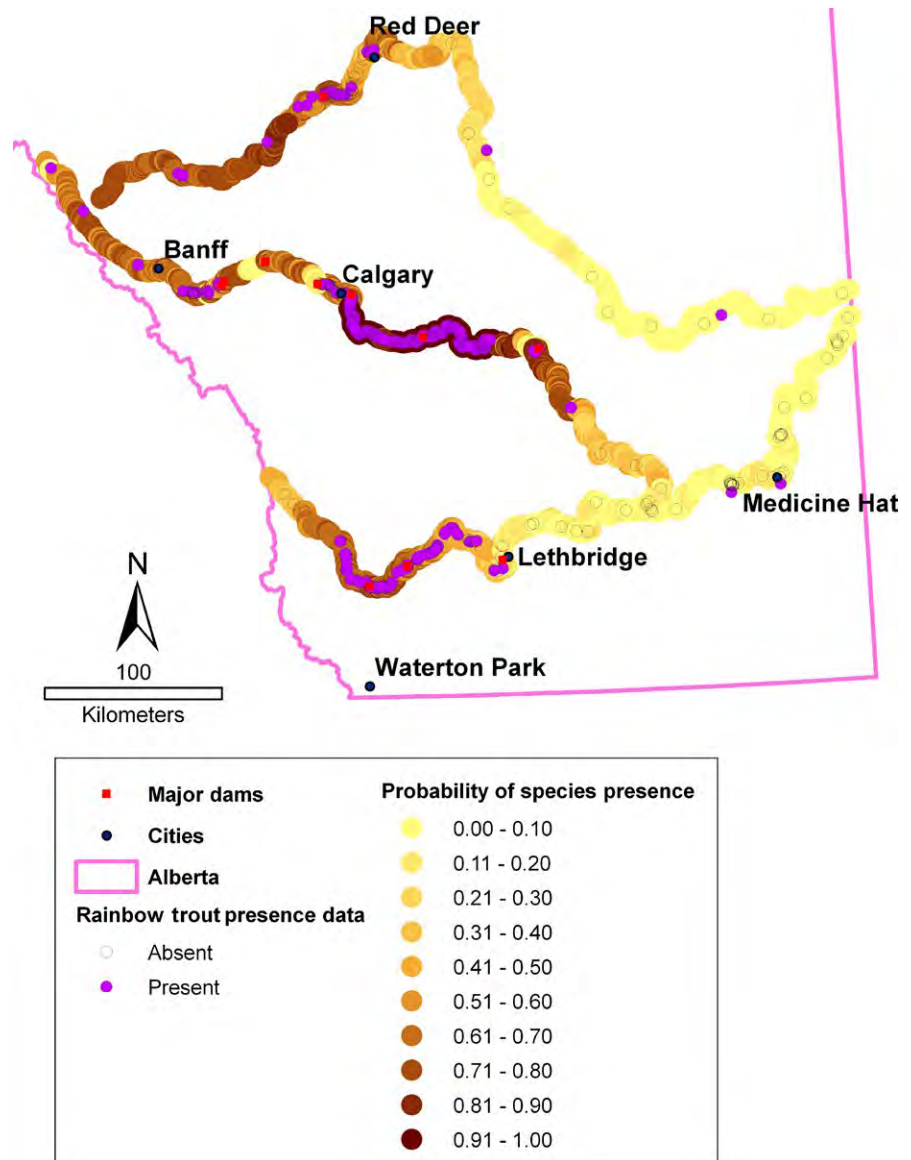


FIGURE 6 Observed presence–absence and probability of presence based on model averaging among the best logistic regression model (see Table 2) predicting the presence of rainbow trout in the SSRB

less likely to cause bias in the modelling results than oversampling in other regions of the rivers.

Our study describes the patterns of species assemblage and diversity in the SSRB, and our correlative results strongly point to species-specific physiological tolerances and environmental preferences as the mechanisms driving these patterns. We have not, however, ruled out processes such as biotic interactions (e.g., competition and predation) and dispersal limitation as contributing factors. For example, Whittaker (1975) suggested that species along a gradient should shift their distributions in response to neighbouring species, resulting in narrower distributions relative to potential distributions in the absence of competition. The removal of a species should, therefore, result in a range expansion of neighbouring species (i.e., ecological release; Terborgh & Weske, 1975; Cox & Ricklefs, 1977), and the addition of a non-native species should cause a range contraction for competitors.

The introduction of non-native species has had profound influences on native species distributions in many systems due to the influence of competition and hybridisation. The best example in the

SSRB is the introduction of rainbow trout to the watershed in the early part of the 20th century, which has been clearly implicated in the contraction of the distribution of cutthroat trout to less than 20% of its native historic range, now largely restricted to high altitude, isolated, headwater regions in small, fragmented populations (Allendorf et al., 2004; Shepard, May, & Urie, 2005; Trotter, 2008). In addition, declines in populations of bull trout in the SSRB are suspected to be due, in part, to competition and hybridisation with introduced brook trout (COSEWIC, 2012).

It is also possible that whereas environmental tolerances may influence the distributions of species along an environmental gradient, the actual boundaries between species distributions are determined (or, at least, reinforced) by direct competitive interaction. In a study of tropical forest birds along an altitudinal gradient in Costa Rica, altitudinal range boundaries at low elevations were strongly influenced by aggressive interactions between competing congeners, whereas range boundaries at the highest elevations were almost entirely the result of environment tolerances related to the cloud forest conditions

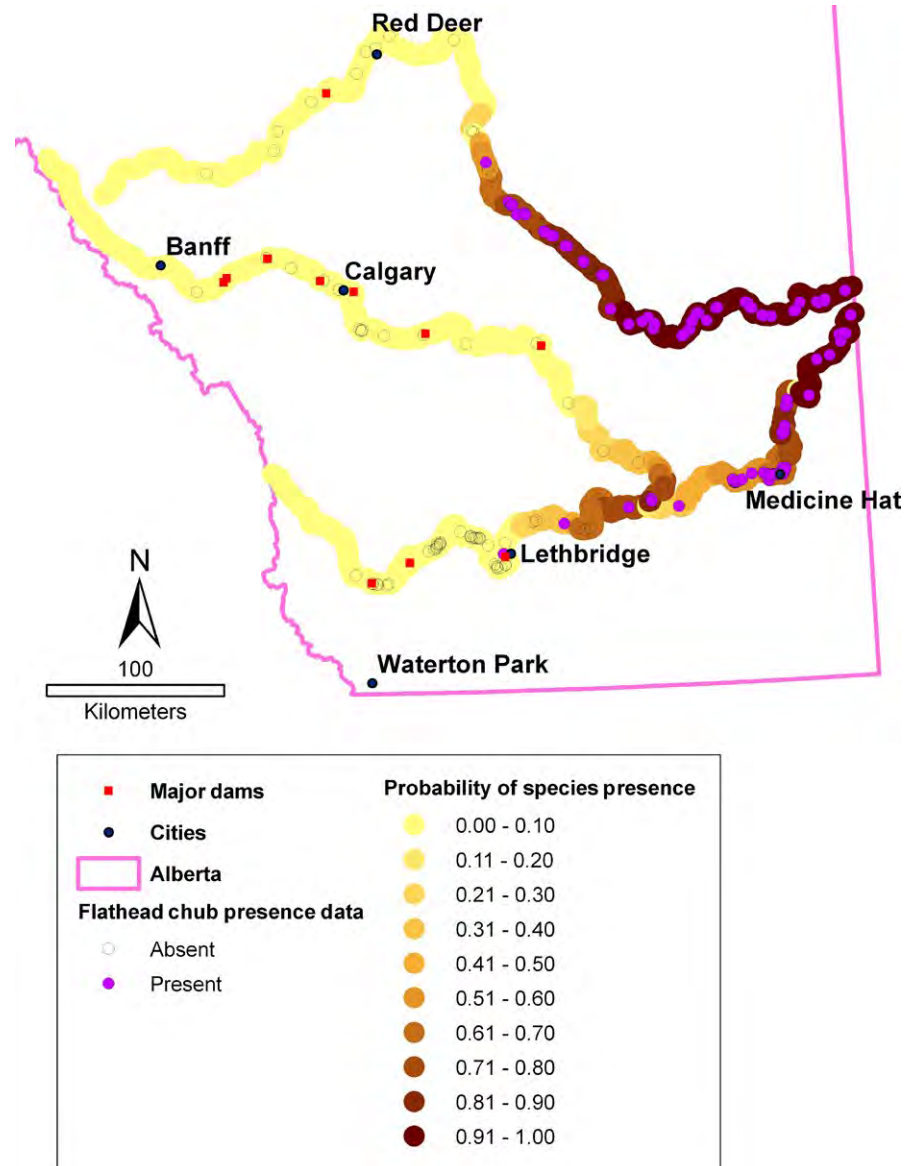


FIGURE 7 Observed presence–absence and probability of presence based on model averaging among the best logistic regression model (see Table 2) predicting the presence of flathead chub in the SSRB

at the mountain tops (Jankowski, Ciecka, Meyer, & Rabenold, 2009; Jankowski, Robinson, & Levey, 2010). In a study of competition for food among three fish species inhabiting different zones along a longitudinal temperature gradient in a mountain river in Wyoming, the cold-water fish was limited primarily by reduced consumption at high temperatures, whereas the warm-water fish was limited by poorer competitive ability at low temperatures (Taniguchi, Rahel, Novinger, & Geron, 1998). Additional studies investigating the relative influence of competitive interactions and environmental tolerances in determining biotic zonation boundaries would contribute greatly to our understanding of mechanisms driving patterns of species assemblages.

Dispersal can influence population dynamics by affecting rates of immigration and emigration. Limitations to dispersal can, therefore, influence species distributions (and, therefore, diversity) in locations where positive population growth depends on immigration. In the SSRB, several dams and weirs inhibit or restrict fish movement, while also altering the physical habitat by widening channels (or creating

reservoirs). In the Bow River, in particular, four dams have been built since 1911 without fishways allowing upstream movement (169.1, 203.3, 245 and 465.5 km from the headwaters; see Figures 4, 5 or 6 for dam locations). These dams may have an effect on local (i.e., within ~10 km of the dam) and regional fish diversity. If river conditions change substantially, perhaps in response to climate change or an acute environmental disturbance, species' environmental tolerances may necessitate movement and relocation throughout the watershed, and the presence of dams without fishways may limit the ability of certain species to relocate to portions of the rivers with suitable environmental conditions. Hence, in anticipation of the effects of climate change, we suggest that monitoring of fish distributions and abundances across the region, and especially in upstream and downstream proximity to dams, should be ongoing.

The fact that temperature emerged as the most predictive environmental factor for species distributions may have important implications. The importance of water temperature has also been shown

in smaller scale studies of longitudinal fish distributions with less replication (Amadio et al., 2005; Dunham, Adams, Schroeter, & Novinger, 2002; Dunham, Schroeter, & Rieman, 2003b; Dunham et al., 2003a; Fausch, Nakano, & Ishigaki, 1994; Hofmann & Fischer, 2002; Jaramillo-Villa et al., 2010; Lester et al., 2004; McCleary & Hassan, 2008; Paul & Post, 2001; Rahel & Nibbelink, 1999; Rich, McMahon, Rieman, & Thompson, 2003; Rieman, Peterson, & Myers, 2006; Smith & Kraft, 2005). It is, therefore, likely to be highly informative to use projected changes in temperature (resulting from climate change) to predict future changes in species distributions and diversity at the regional scale without being overly concerned about unpredicted (or unknown) changes in other physiochemical variables that could affect species distributions. Future directions include a study of predicted changes in fish species distributions in the SSRB based on IPCC predictions for temperature increases across the region. We note that whereas we have focused primarily on upper thermal limits, there are parts of the world where lower thermal limits are more important, and we expect similar processes to act and analogous patterns to emerge regardless of whether upper or lower thermal limits are of greatest importance.

The composition of communities across a heterogeneous landscape can be understood by quantifying the determinants species distributions, especially when those distributions are strongly influenced by the physiology and survival of individuals in response to a particular environmental variable (such as temperature). Our study confirms that temperature can be used to predict both species distributions and species assemblage. This approach to understanding how species and communities are distributed across a landscape could become increasingly important when viewed in the context of climate change.

ACKNOWLEDGEMENTS

We thank Nilo Sinnatamby and three anonymous reviewers for helpful comments on previous versions of this manuscript. This work was supported by a grant from the Canadian Climate Action Fund and a National Science and Engineering Research Council grant to JRP. Thank you to Trevor Rhodes, Jim Stelfox, Linda Winkle and Andrew Paul at Alberta Fish and Wildlife for invaluable access to the Fisheries Management Information System and the Fish and Wildlife library. An additional thanks is in order to Trevor Rhodes for access to his Bow River Study data. Leland Jackson provided crucial access to the water quality database at the Canadian Water Network. Thank you to Nicole Nadorozny and Lauren Hogberg for help with the data and computer time.

REFERENCES

- AESRD (2005). *Fisheries Management Information System*. Edmonton, Alberta: Alberta Environment and Sustainable Resource Development, Fish and Wildlife Division, Fisheries Management Branch.
- Agrawal, A. A., Ackerly, D. D., Adler, F., Arnold, A. E., Caceres, C., Doak, D. F., ... Werner, E. (2007). Filling key gaps in population and community ecology. *Frontiers in Ecology and the Environment*, 5, 145–152.
- Allendorf, F. W., Leary, R. F., Hitt, N. P., Knudsen, K. L., Lundquist, L. L., & Spruell, P. (2004). Intercrosses and the US Endangered Species Act: Should hybridized populations be included as Westslope cutthroat trout? *Conservation Biology*, 18, 1203–1213.
- Allison, P. D. (2012). *Logistic Regression Using SAS®: Theory and Application*, 2nd ed.. Cary, North Carolina, USA: SAS Institute Inc.
- Amadio, C. J., Hubert, W. A., Johnson, K., Oberlie, D., & Dufek, D. (2005). Factors affecting the occurrence of saugers in small, high-elevation rivers near the western edge of the species' natural distribution. *Transactions of the American Fisheries Society*, 134, 160–171.
- Amadio, C. J., Hubert, W. A., Johnson, K., Oberlie, D., & Dufek, D. (2006). Abundance of adult saugers across the wind river watershed, Wyoming. *North American Journal of Fisheries Management*, 26, 156–162.
- Askey, P. J., Post, J. R., Parkinson, E. A., Rivot, E., Paul, A. J., & Biro, P. A. (2007). Estimation of gillnet efficiency and selectivity across multiple sampling units: A hierarchical Bayesian analysis using mark-recapture data. *Fisheries Research*, 83, 162–174.
- BC MELP (2001). *Towards a Water Quality Guideline for Temperature in the Province of British Columbia*. Victoria, BC: British Columbia Ministry of Environment, Lands and Parks, Water Management Branch.
- Beitinger, T. L., Bennett, W. A., & McCauley, R. W. (2000). Temperature tolerances of North American freshwater fishes exposed to dynamic changes in temperature. *Environmental Biology of Fishes*, 58, 237–275.
- Benson, A. C., Sutton, T. M., Elliott, R. F., & Meronek, T. G. (2005). Seasonal movement patterns and habitat preferences of age-0 lake sturgeon in the lower Peshtigo River, Wisconsin. *Transactions of the American Fisheries Society*, 134, 1400–1409.
- Biro, P. A. (1998). Staying cool: Behavioral thermoregulation during summer by young-of-year brook trout in a lake. *Transactions of the American Fisheries Society*, 127, 212–222.
- Blanchet, S., Helmus, M. R., Brosse, S., & Grenouillet, G. (2014). Regional vs local drivers of phylogenetic and species diversity in stream fish communities. *Freshwater Biology*, 59, 450–462.
- Braaten, P. J., & Guy, C. S. (1999). Relations between physicochemical factors and abundance of fishes in tributary confluences of the lower channelized Missouri River. *Transactions of the American Fisheries Society*, 128, 1213–1221.
- Brazner, J. C., Tanner, D. K., Detenbeck, N. E., Batterman, S. L., Stark, S. L., Jagger, L. A., & Snarski, V. M. (2005). Regional, watershed, and site-specific environmental influences on fish assemblage structure and function in western Lake Superior tributaries. *Canadian Journal of Fisheries and Aquatic Sciences*, 62, 1254–1270.
- Buisson, L., Blanc, L., & Grenouillet, G. (2008). Modelling stream fish species distribution in a river network: the relative effects of temperature versus physical factors. *Ecology of Freshwater Fish*, 17, 244–257.
- Burnham, K. P., & Anderson, D. R. (1998). *Model Selection and Inference: A Practical Information-Theoretic Approach*. New York: Springer-Verlag.
- Burnham, K. P., & Anderson, D. R. (2004). Multimodel inference—understanding AIC and BIC in model selection. *Sociological Methods & Research*, 33, 261–304.
- Carvalho, R. A., & Tejerina-Garro, F. L. (2015). The influence of environmental variables on the functional structure of headwater stream fish assemblages: A study of two tropical basins in Central Brazil. *Neotropical Ichthyology*, 13, 349–360.
- Cherry, D. S., & Cairns, J. (1982). Biological monitoring 5. Preference and avoidance studies. *Water Research*, 16, 263–301.
- Cincotta, D. A., & Stauffer, J. R. (1984). Temperature preference and avoidance studies of 6 north-american freshwater fish species. *Hydrobiologia*, 109, 173–177.
- Clements, F. E. (1916). Plant succession, and analysis of the development of vegetation. *Carnegie Institution of Washington Publication*, 242, 1–512.
- Cleveland, W. S. (1981). LOWESS: A program for smoothing scatterplots by robust locally weighted regression. *American Statistician*, 35, 54.
- Clipperton, G. K., Koning, C. W., Locke, A. G. H., Mahoney, J. M., & Quazi, B. (2003). *Instream Flow Needs Determination for the South Saskatchewan River Basin, Alberta, Canada*. No. Report No. T/719. Edmonton, Alberta: Alberta Environment and Sustainable Resource Development.

- Covich, A. P., Fritz, S. C., Lamb, P. J., Marzolf, R. D., Matthews, W. J., Poiani, K. A., ... Winter, T. C. (1997). Potential effects of climate change on aquatic ecosystems of the Great Plains of North America. *Hydrological Processes*, 11, 993–1021.
- Cox, G. W., & Ricklefs, R. E. (1977). Species-diversity and ecological release in Caribbean land bird faunas. *Oikos*, 28, 113–122.
- Davis, A. J., Lawton, J. H., Shorrocks, B., & Jenkinson, L. S. (1998). Individualistic species responses invalidate simple physiological models of community dynamics under global environmental change. *Journal of Animal Ecology*, 67, 600–612.
- De Robertis, A., Ryer, C. H., Velozo, A., & Brodeur, R. D. (2003). Differential effects of turbidity on prey consumption of piscivorous and planktivorous fish. *Canadian Journal of Fisheries and Aquatic Sciences*, 60, 1517–1526.
- Diana, J. S. (2004). *Biology and Ecology of Fishes*. Traverse City, MI: Cooper Publishing Group LLC.
- Dickerson, B. R., & Vinyard, G. L. (1999). Effects of high chronic temperatures and diel temperature cycles on the survival and growth of Lahontan cutthroat trout. *Transactions of the American Fisheries Society*, 128, 516–521.
- Dunham, J. B., Adams, S. B., Schroeter, R. E., & Novinger, D. C. (2002). Alien invasions in aquatic ecosystems: Toward an understanding of brook trout invasions and potential impacts on inland cutthroat trout in western North America. *Reviews in Fish Biology and Fisheries*, 12, 373–391.
- Dunham, J., Rieman, B., & Chandler, G. (2003a). Influences of temperature and environmental variables on the distribution of bull trout within streams at the southern margin of its range. *North American Journal of Fisheries Management*, 23, 894–904.
- Dunham, J., Schroeter, R., & Rieman, B. (2003b). Influence of maximum water temperature on occurrence of Lahontan cutthroat trout within streams. *North American Journal of Fisheries Management*, 23, 1042–1049.
- Eaton, J. G., McCormick, J. H., Goodno, B. E., O'Brien, D. G., Stefany, H. G., Hondzo, M., & Scheller, R. M. (1995). A field information-based system for estimating fish temperature tolerances. *Fisheries*, 20, 10–18.
- Eaton, J. G., & Scheller, R. M. (1996). Effects of climate warming on fish thermal habitat in streams of the United States. *Limnology and Oceanography*, 41, 1109–1115.
- Environmental Systems Research Institute (2005a). *ARCGIS 9.1. Redlands, CA: Environmental Systems Research Institute*.
- Environmental Systems Research Institute (2005b). *ESRI World, ArcIMS Image Service*. Environmental Systems Research Institute: Redlands, CA.
- Fausch, K. D., Nakano, S., & Ishigaki, K. (1994). Distribution of 2 congeneric charrs in streams of Hokkaido Island Japan—considering multiple factors across scales. *Oecologia*, 100, 1–12.
- Furlan, N., Esteves, K. E., & Quinaglia, G. A. (2013). Environmental factors associated with fish distribution in an urban neotropical river (Upper Tiete River Basin, Sao Paulo, Brazil). *Environmental Biology of Fishes*, 96, 77–92.
- Gleason, H. A. (1926). The individualistic concept of the plant association. *Bulletin of the Torrey Botanical Club*, 53, 7–26.
- Grenouillet, G., Pont, D., & Herisse, C. (2004). Within-basin fish assemblage structure: the relative influence of habitat versus stream spatial position on local species richness. *Canadian Journal of Fisheries and Aquatic Sciences*, 61, 93–102.
- Hanson, C., Johnson, J., Kitchell, J., & Schindler, D. E. (1997). *Fish Bioenergetics 3.0*. Madison, Wisconsin: University of Wisconsin Sea Grant Institute.
- Hayward, R. S., & Weiland, M. A. (1998). Gastric evacuation rates and maximum daily rations of rainbow trout fed chironomid larvae at 7.8, 10.0 and 12.8°C. *Environmental Biology of Fishes*, 51, 321–330.
- Henderson, N. E., & Peter, R. E. (1969). Distribution of fishes of southern Alberta. *Journal of the Fisheries Research Board of Canada*, 26, 325–338.
- Hofmann, N., & Fischer, P. (2002). Temperature preferences and critical thermal limits of burbot: Implications for habitat selection and ontogenetic habitat shift. *Transactions of the American Fisheries Society*, 131, 1164–1172.
- Hortal, J., Jimenez-Valverde, A., Gomez, J. F., Lobo, J. M., & Baselga, A. (2008). Historical bias in biodiversity inventories affects the observed environmental niche of the species. *Oikos*, 117, 847–858.
- Huff, D. D., Hubler, S. L., & Borisenko, A. N. (2005). Using field data to estimate the realized thermal niche of aquatic vertebrates. *North American Journal of Fisheries Management*, 25, 346–360.
- Hughes, N. F., Hayes, J. W., Shearer, K. A., & Young, R. G. (2003). Testing a model of drift-feeding using three-dimensional videography of wild brown trout, *Salmo trutta*, in a New Zealand river. *Canadian Journal of Fisheries and Aquatic Sciences*, 60, 1462–1476.
- von Humboldt, A., & Bonpland, A. (1805). *Essai sur la géographie des plantes; accompagné d'un tableau physique des régions équinoxiales, fondé sur les mesures exécutées, depuis le dixième degré de latitude boréal jusqu'au dixième degré de latitude australe, pendant les années 1799, 1800, 1801, 1802 et 1803*. Paris: Levrault, Schoell et Compagnie.
- Ihnat, J. M., & Bulkley, R. V. (1984). Influence of acclimation temperature and season on acute temperature preference of adult mountain whitefish, *Prosopium williamsoni*. *Environmental Biology of Fishes*, 11, 29–40.
- Jackson, D. A., Peres-Neto, P. R., & Olden, J. D. (2001). What controls who is where in freshwater fish communities—the roles of biotic, abiotic, and spatial factors. *Canadian Journal of Fisheries and Aquatic Sciences*, 58, 157–170.
- Jankowski, J. E., Ciecka, A. L., Meyer, N. Y., & Rabenold, K. N. (2009). Beta diversity along environmental gradients: implications of habitat specialization in tropical montane landscapes. *Journal of Animal Ecology*, 78, 315–327.
- Jankowski, J. E., Robinson, S. K., & Levey, D. J. (2010). Squeezed at the top: Interspecific aggression may constrain elevational ranges in tropical birds. *Ecology*, 91, 1877–1884.
- Jaramillo-Villa, U., Maldonado-Ocampo, J. A., & Escobar, F. (2010). Altitudinal variation in fish assemblage diversity in streams of the central Andes of Colombia. *Journal of Fish Biology*, 76, 2401–2417.
- Jobling, M. (1981). Temperature tolerance and the final preferendum—rapid methods for the assessment of optimum growth temperatures. *Journal of Fish Biology*, 19, 439–455.
- Kaya, C. M., Kaeding, L. R., & Burkhalter, D. E. (1977). Use of a cold-water refuge by rainbow and brown trout in a geothermally heated stream. *Progressive Fish-Culturist*, 39, 37–39.
- Keleher, C. J., & Rahel, F. J. (1996). Thermal limits to salmonid distributions in the rocky mountain region and potential habitat loss due to global warming: A geographic information system (GIS) approach. *Transactions of the American Fisheries Society*, 125, 1–13.
- Kellogg, R. L., & Gift, J. J. (1983). Relationship between optimum temperatures for growth and preferred temperatures for the young of 4 fish species. *Transactions of the American Fisheries Society*, 112, 424–430.
- Kulshreshtha, S., & Thompson, W. (2007). Basin Water Use in Regional Economic Perspective: Rationale for Input-Output Analysis. In: *Climate Change and Water: SSRB Final Technical Report*. Ed: Martz, L., Bruneau, J., & Rolfe, J. T. pp. 51–92.
- Laliberte, J. J., Post, J. R., & Rosenfeld, J. S. (2014). Hydraulic geometry and longitudinal patterns of habitat quantity and quality for rainbow trout (*Oncorhynchus mykiss*). *River Research and Applications*, 30, 593–601.
- Legendre, P., & Legendre, L. (2012). *Numerical Ecology*, Third English ed. Amsterdam: Elsevier Scientific Publishing Company.
- Lester, N. P., Dextrase, A. J., Kushneriuk, R. S., Rawson, M. R., & Ryan, P. A. (2004). Light and temperature: Key factors affecting walleye abundance and production. *Transactions of the American Fisheries Society*, 133, 588–605.
- Lin, S.-J., Tsai, S.-T., Lin, J.-H., Jong, K.-J., & Wang, Y.-K. (2014). Changes in structure and function of fish assemblages along environmental gradients in an intensive agricultural region of subtropical Taiwan. *Pacific Science*, 68, 213–230.

- MacArthur, R. H., & Wilson, E. O. (1967). *The Theory of Island Biogeography*. Princeton: Princeton University Press.
- Mackenzie-Grieve, J. L., & Post, J. R. (2006). Thermal habitat use by lake trout in two contrasting Yukon Territory lakes. *Transactions of the American Fisheries Society*, 135, 727–738.
- Magnuson, J. J., Crowder, L. B., & Medvick, P. A. (1979). Temperature as an ecological resource. *American Zoologist*, 19, 331–343.
- Magurran, A. E. (2004). *Measuring Biological Diversity*. Oxford, UK: Blackwell Science Ltd.
- McCleary, R. J., & Hassan, M. A. (2008). Predictive modeling and spatial mapping of fish distributions in small streams of the Canadian Rocky Mountain foothills. *Canadian Journal of Fisheries and Aquatic Sciences*, 65, 319–333.
- McGarvey, D. J. (2011). Quantifying ichthyofaunal zonation and species richness along a 2800-km reach of the Rio Chama and Rio Grande (USA). *Ecology of Freshwater Fish*, 20, 231–242.
- Mercado-Silva, N., Lyons, J., Diaz-Pardo, E., Navarrete, S., & Gutierrez-Hernandez, A. (2012). Environmental factors associated with fish assemblage patterns in a high gradient river of the Gulf of Mexico slope. *Revista Mexicana De Biodiversidad*, 83, 117–128.
- Moss, B., McKee, D., Atkinson, D., Collings, S. E., Eaton, J. W., Gill, A. B., ... Wilson, D. (2003). How important is climate? Effects of warming, nutrient addition and fish on phytoplankton in shallow lake microcosms. *Journal of Applied Ecology*, 40, 782–792.
- Moyle, P. B. (2002). *Inland Fishes of California*. Berkeley: University of California Press.
- Murray, S., & Innes, J. L. (2009). Effects of environment on fish species distributions in the Mackenzie River drainage basin of northeastern British Columbia, Canada. *Ecology of Freshwater Fish*, 18, 183–196.
- Natural Resources Canada (1982–2001). *National Topographic System, 1:50 000 Map Sheets: 072E 01-16; 072L 01-16; 072M 01-16; 082G 01-16; 082H 01-16; 082I 01-16; 082J 01-16; 082N 01-16; 082O 01-16; 082P 01-16; 083A 01-16; 083B 01-16; 083C 01-16; 083G 01-16*. Ottawa, ON: Natural Resources Canada.
- Nelson, J. S., & Paetz, M. J. (1992). *The Fishes of Alberta*. Edmonton, Alberta: University of Alberta.
- Nielsen, J. L., Lisle, T. E., & Ozaki, V. (1994). Thermally stratified pools and their use by steelhead in northern California streams. *Transactions of the American Fisheries Society*, 123, 613–626.
- Oksanen, J., Blanchet, F. G., Kindt, R., Legendre, P., Minchin, P. R., O'Hara, R. B., ... Wagner, H. (2016). *vegan: Community Ecology Package. R package version 2.3-4*. <http://CRAN.R-project.org/package=vegan>.
- Paul, A. J., & Post, J. R. (2001). Spatial distribution of native and nonnative salmonids in streams of the eastern slopes of the Canadian rocky mountains. *Transactions of the American Fisheries Society*, 130, 417–430.
- Pont, D., Hugueny, B., & Oberdorff, T. (2005). Modelling habitat requirement of European fishes: Do species have similar responses to local and regional environmental constraints? *Canadian Journal of Fisheries and Aquatic Sciences*, 62, 163–173.
- R Core Team (2014). *R: A Language and Environment for Statistical Computing*. Vienna, Austria: R Foundation for Statistical Computing. <http://www.R-project.org>.
- Rahel, F. J., & Hubert, W. A. (1991). Fish assemblages and habitat gradients in a Rocky Mountain–Great Plains stream: Biotic zonation and additive patterns of community change. *Transactions of the American Fisheries Society*, 120, 319–332.
- Rahel, F. J., & Nibbelink, N. P. (1999). Spatial patterns in relations among brown trout (*Salmo trutta*) distribution, summer air temperature, and stream size in Rocky Mountain streams. *Canadian Journal of Fisheries and Aquatic Sciences*, 56, 43–51.
- Rhodes, T. (2005). *The Immediate and Short Term Impacts of Catch-and-Release Angling on Migrating and Pre-spawning Condition Rainbow Trout (Oncorhynchus mykiss) in the Bow River, Alberta*. MSc Thesis. Calgary, Alberta: University of Calgary.
- Rich, C. F., McMahon, T. E., Rieman, B. E., & Thompson, W. L. (2003). Local-habitat, watershed, and biotic features associated with bull trout occurrence in Montana streams. *Transactions of the American Fisheries Society*, 132, 1053–1064.
- Ricklefs, R. E. (2008). Disintegration of the ecological community. *American Naturalist*, 172, 741–750.
- Rieger, P. W., & Summerfelt, R. C. (1997). The influence of turbidity on larval walleye, *Stizostedion vitreum*, behavior and development in tank culture. *Aquaculture*, 159, 19–32.
- Rieman, B. E., Peterson, J. T., & Myers, D. L. (2006). Have brook trout (*Salvelinus fontinalis*) displaced bull trout (*Salvelinus confluentus*) along longitudinal gradients in central Idaho streams? *Canadian Journal of Fisheries and Aquatic Sciences*, 63, 63–78.
- Robins, G. L. (2009). *Spatial Distributions of 33 Fish Species in the Mainstem Rivers of the South Saskatchewan River Basin Under Changing Thermal Regimes*. Calgary, Alberta: University of Calgary.
- Rosenfeld, J. S., & Boss, S. (2001). Fitness consequences of habitat use for juvenile cutthroat trout: energetic costs and benefits in pools and riffles. *Canadian Journal of Fisheries and Aquatic Sciences*, 58, 585–593.
- Rosenfeld, J. S., Post, J., Robins, G., & Hatfield, T. (2007). Hydraulic geometry as a physical template for the River Continuum: application to optimal flows and longitudinal trends in salmonid habitat. *Canadian Journal of Fisheries and Aquatic Sciences*, 64, 755–767.
- Scott, W. B., & Crossman, E. J. (1979). *Freshwater Fishes of Canada*. Fisheries Research Board of Canada Bulletin 183, Ottawa, Canada.
- Shepard, B. B., May, B. E., & Urie, W. (2005). Status and conservation of westslope cutthroat trout within the western United States. *North American Journal of Fisheries Management*, 25, 1426–1440.
- Smith, T. A., & Kraft, C. E. (2005). Stream fish assemblages in relation to landscape position and local habitat variables. *Transactions of the American Fisheries Society*, 134, 430–440.
- Snucins, E. J., & Gunn, J. M. (1995). Coping with a warm environment—behavioral thermoregulation by lake trout. *Transactions of the American Fisheries Society*, 124, 118–123.
- Sosiak, A. (2002). Long-term response of periphyton and macrophytes to reduced municipal nutrient loading to the Bow River (Alberta, Canada). *Canadian Journal of Fisheries and Aquatic Sciences*, 59, 987–1001.
- SSRB Water Supply Study Steering Committee (2010). *South Saskatchewan River Basin in Alberta Water Supply Study: Summary*. Lethbridge, Alberta: Alberta Agriculture and Rural Development.
- Stevenson, M. M., Schnell, G. D., & Black, R. (1974). Factor-analysis of fish distribution patterns in western and central Oklahoma. *Systematic Zoology*, 23, 202–218.
- Taniguchi, Y., Rahel, F. J., Novinger, D. C., & Geron, K. G. (1998). Temperature mediation of competitive interactions among three fish species that replace each other along longitudinal stream gradients. *Canadian Journal of Fisheries and Aquatic Sciences*, 55, 1894–1901.
- Terborgh, J., & Weske, J. S. (1975). Role of competition in distribution of Andean birds. *Ecology*, 56, 562–576.
- Troia, M. J., & Gido, K. B. (2013). Predicting community-environment relationships of stream fishes across multiple drainage basins: Insights into model generality and the effect of spatial extent. *Journal of Environmental Management*, 128, 313–323.
- Trotter, P. (2008). *Cutthroat: Native Trout of the East*, 2nd ed. Berkeley: University of California Press.
- US EPA (1995). *Ecological Impacts from Climate Change: An Economic Analysis of Freshwater Recreational Fishing*. No. Report No. EPA 230-R-95-004. Washington, DC: United States Environmental Protection Agency.
- Vannote, R. L., Minshall, G. W., Cummins, K. W., Sedell, J. R., & Cushing, C. E. (1980). River continuum concept. *Canadian Journal of Fisheries and Aquatic Sciences*, 37, 130–137.
- Vigg, S. C., & Koch, D. L. (1980). Upper lethal temperature-range of lahontan cutthroat trout in waters of different ionic concentration. *Transactions of the American Fisheries Society*, 109, 336–339.
- Wallace, A. R. (1876). *The Geographical Distribution of Animals; With a Study of the Relations of Living and Extinct Faunas as Elucidating the Past Changes of the Earth's Surface*. London: Macmillan & Co.

- Wehrly, K. E., Wiley, M. J., & Seelbach, P. W. (2003). Classifying regional variation in thermal regime based on stream fish community patterns. *Transactions of the American Fisheries Society*, 132, 18–38.
- Whittaker, R. H. (1975). *Communities and Ecosystems*. New York: Macmillan Publishing Co., Inc.
- Wilson, S. M., & Nagler, J. J. (2006). Age, but not salinity, affects the upper lethal temperature limits for juvenile walleye (*Sander vitreus*). *Aquaculture*, 257, 187–193.

Wootton, R. J. (1990). *Ecology of Teleost Fishes*. London: Chapman and Hall.

SUPPORTING INFORMATION

Additional Supporting Information may be found online in the supporting information tab for this article.

Predicted spatial distribution of fish species in the South Saskatchewan River Basin
main stem rivers following climate change

Jonathan A. Mee^{1*}, Geneva L. Robins², Anne Farineau², John R. Post²

*Corresponding Author, Email: jmee@mtroyal.ca

¹Department of Biology, Mount Royal University, Calgary, Alberta, Canada

²Department of Biological Sciences, University of Calgary, Calgary, Alberta, Canada

In preparation for Ecology of Freshwater Fish

Introduction

Climate change has been forecasted to cause a worldwide increase in air temperatures, and changes in precipitation and runoff patterns (Bates et al. 2008). Consequently, many aspects of river hydrology may change such as water temperature, discharge, channel morphology, and water quality (Arora and Boer 2001; Jackson et al. 2001; Arheimer et al. 2005; Howarth et al. 2006; Caissie 2006; Lane et al. 2007; Bates et al. 2008). Rivers are likely to become warmer, with lower flows, more extreme events, and higher nutrient levels (Bates et al. 2008).

The forecasted changes in river temperature and hydrology and associated changes to lower trophic level aquatic biota (e.g., algae, macrophytes, invertebrates, Wade et al. 2002; Daufresne et al. 2004; Durance and Ormerod 2009) are likely to have significant impacts on fish. Of the variables that are forecasted to change, water temperature is likely to have notable impacts because of the pervasive effects of temperature on the fitness of fish (Dunham, Rieman et al. 2003; Dunham, Schroeter et al. 2003; Hari et al. 2006; Robillard and Fox 2006; Boughton et al. 2007; Ficke et al. 2007) through its influence on consumption, respiration, growth, reproduction, swimming speed, and behaviour of fish (Wootton 1990). Since it is such a strong determinant of fitness, water temperature changes alone are commonly used to predict the impact of climate change on fish species (Ficke et al. 2007). Several studies indicate the impact of climate change on freshwater fish could be considerable for species with preferences for cold temperatures causing decreased abundance and ranges (Hauer et al. 1997; Milner et al. 2009; Heino et al. 2009). Given the importance that water temperature was found to have on the

current distribution of fish species throughout the SSRB main stem rivers (Mee et al. 2016), the spatial distributions of fish in the SSRB were predicted based on forecasted water temperatures in 2040 and 2080.

Results showed a reduction in the distribution of fish species with colder thermal preferences (<15°C mean July water temperature, Fig. 1, Mee et al. 2016). Fish species such as Cutthroat trout, *Oncorhynchus clarkii*, (Fig. 2) and bull trout, *Salvelinus confluentus*, displayed dramatic retraction of their distributions. Fish with “cool” thermal preferences (Fig. 3) displayed a mixed response to the predicted changes in water temperature. Whereas, rainbow trout, *Oncorhynchus mykiss*, showed little change and a marginal decline in the Red Deer River (Fig. 4), spoonhead sculpin, *Cottus ricei*, was predicted to see local extinctions in the Red Deer, Bow and Oldman Rivers (Fig. 5). On the other hand, fish species with preferences for warmer water temperatures (Fig. 6) displayed an upstream shift in their predicted future distributions with increased predicted presence in the mid-reaches of the main stems. Walleye, *Sanders vitreus*, for example (Fig. 7), was predicted to decrease drastically in the Oldman and South Saskatchewan Rivers by 2080, but increase in the Bow River. Under climate warming scenarios, it is apparent that fish species distributions are likely to undergo dramatic changes, and will have particularly harmful impacts on some of Alberta’s current species of concern (e.g. cutthroat trout, bull trout, spoonhead sculpin). With retractions to distribution predicted here, species are likely to be more susceptible to other environmental and anthropogenic stressors.

Results showed a reduction in the distribution of fish species with colder thermal preferences (<15°C mean July water temperature, Fig. 1, Mee et al. 2016). Fish species such as Cutthroat trout, *Oncorhynchus clarkii*, (Fig. 2) and bull trout, *Salvelinus confluentus*, displayed dramatic retraction of their distributions. Fish with “cool” thermal preferences (Fig. 3) displayed a mixed response to the predicted changes in water temperature. Whereas, rainbow trout, *Oncorhynchus mykiss*, showed little change and a marginal decline in the Red Deer River (Fig. 4), spoonhead sculpin, *Cottus ricei*, was predicted to see

local extinctions in the Red Deer, Bow and Oldman Rivers (Fig. 5). On the other hand, fish species with preferences for warmer water temperatures (Fig. 6) displayed an upstream shift in their predicted future distributions with increased predicted presence in the mid-reaches of the main stems. Walleye, *Sanders vitreus*, for example (Fig. 7), was predicted to decrease drastically in the Oldman and South Saskatchewan Rivers by 2080, but increase in the Bow River. Under climate warming scenarios, it is apparent that fish species distributions are likely to undergo dramatic changes, and will have particularly harmful impacts on some of Alberta's current species of concern (e.g. cutthroat trout, bull trout, spoonhead sculpin). With retractions to distribution predicted here, species are likely to be more susceptible to other environmental and anthropogenic stressors.

References

- Arheimer, B., Andreasson, J., Fogelberg, S., Johnsson, H., Pers, C.B., and Persson, K. 2005. Climate change impact on water quality: Model results from southern Sweden. *Ambio* **34**: 559-566.
- Arora, V.K., and Boer, G.J. 2001. Effects of simulated climate change on the hydrology of major river basins. *Journal of Geophysical Research-Atmospheres* **106**: 3335-3348.
- Bates, B.C., Kundzewicz, Z.W., Wu, S., and Palutikof, J.P. 2008. Climate change and water. IPCC Secretariat, Geneva.
- Boughton, D.A., Gibson, M., Yedor, R., and Kelley, E. 2007. Stream temperature and the potential growth and survival of juvenile *Oncorhynchus mykiss* in a southern California Creek. *Freshwat. Biol.* **52**(7): 1353-1364.
- Caissie, D. 2006. The thermal regime of rivers: a review. *Freshwat. Biol.* **51**(8): 1389-1406.
- Daufresne, M., Roger, M.C., Capra, H., and Lamouroux, N. 2004. Long-term changes within the invertebrate and fish communities of the Upper Rhone River: effects of climatic factors. *Global Change Biol.* **10**(1): 124-140.
- Dunham, J., Rieman, B., and Chandler, G. 2003. Influences of temperature and environmental variables on the distribution of bull trout within streams at the southern margin of its range. *N. Am. J. Fish. Manage.* **23**(3): 894-904.
- Dunham, J., Schroeter, R., and Rieman, B. 2003. Influence of maximum water temperature on occurrence of Lahontan cutthroat trout within streams. *N. Am. J. Fish. Manage.* **23**(3): 1042-1049.

- Durance, I., and Ormerod, S.J. 2009. Trends in water quality and discharge confound long-term warming effects on river macroinvertebrates. *Freshwat. Biol.* **54**(2): 388-405.
- Ficke, A.D., Myrick, C.A., and Hansen, L.J. 2007. Potential impacts of global climate change on freshwater fisheries. *Rev. Fish Biol. Fish.* **17**(4): 581-613.
- Hari, R., Livingstone, D., Siber, R., Burkhardt-Holm, P., and Guttinger, H. 2006. Consequences of climatic change for water temperature and brown trout populations in Alpine rivers and streams. *Global Change Biol.* **12**(1): 10-26.
- Hauer, F., Baron, J., Campbell, D., Fausch, K., Hostetler, S., Leavesley, G., Leavitt, P., McKnight, D., and Stanford, J. 1997. Assessment of climate change and freshwater ecosystems of the Rocky Mountains, USA and Canada. *Hydrol. Process.* **11**(8): 903-924.
- Heino, J., Virkkala, R., and Toivonen, H. 2009. Climate change and freshwater biodiversity: detected patterns, future trends and adaptations in northern regions. *Biological Reviews* **84**(1): 39-54.
- Howarth, R.W., Swaney, D.P., Boyer, E.W., Marino, R., Jaworski, N., and Goodale, C. 2006. The influence of climate on average nitrogen export from large watersheds in the Northeastern United States. *Biogeochemistry* **79**: 163-186.
- Jackson, R.B., Carpenter, S.R., Dahm, C.N., McKnight, D.M., Naiman, R.J., Postel, S.L., and Running, S.W. 2001. Water in a changing world. *Ecol. Appl.* **11**: 1027-1045.
- Lane, S.N., Tayefi, V., Reid, S.C., Yu, D., and Hardy, R.J. 2007. Interactions between sediment delivery, channel change, climate change and flood risk in a temperate upland environment. *Earth Surf. Process. Landforms* **32**(3): 429-446.
- Mee, J.A., Robins, G., and Post, J.R. 2016. Patterns of fish species assemblage replicated across three parallel rivers suggest biotic zonation in response to a longitudinal temperature gradient. *Ecol. Freshwat. Fish* DOI: [10.1111/eff.12322](https://doi.org/10.1111/eff.12322).
- Milner, A.M., Brown, L.E., and Hannah, D.M. 2009. Hydroecological response of river systems to shrinking glaciers. *Hydrol. Process.* **23**(1): 62-77.
- Robillard, M., and Fox, M. 2006. Historical changes in abundance and community structure of warmwater piscivore communities associated with changes in water clarity, nutrients, and temperature. *Can. J. Fish. Aquat. Sci.* **63**(4): 798-809.
- Wade, A., Whitehead, P., Hornberger, G., and Snook, D. 2002. On modelling the flow controls on macrophyte and epiphyte dynamics in a lowland permeable catchment: the River Kennet, southern England. *Sci. Total Environ.* **282**: 375-393.
- Wootton, R.J. 1990. *Ecology of teleost fishes*. Chapman and Hall, London.

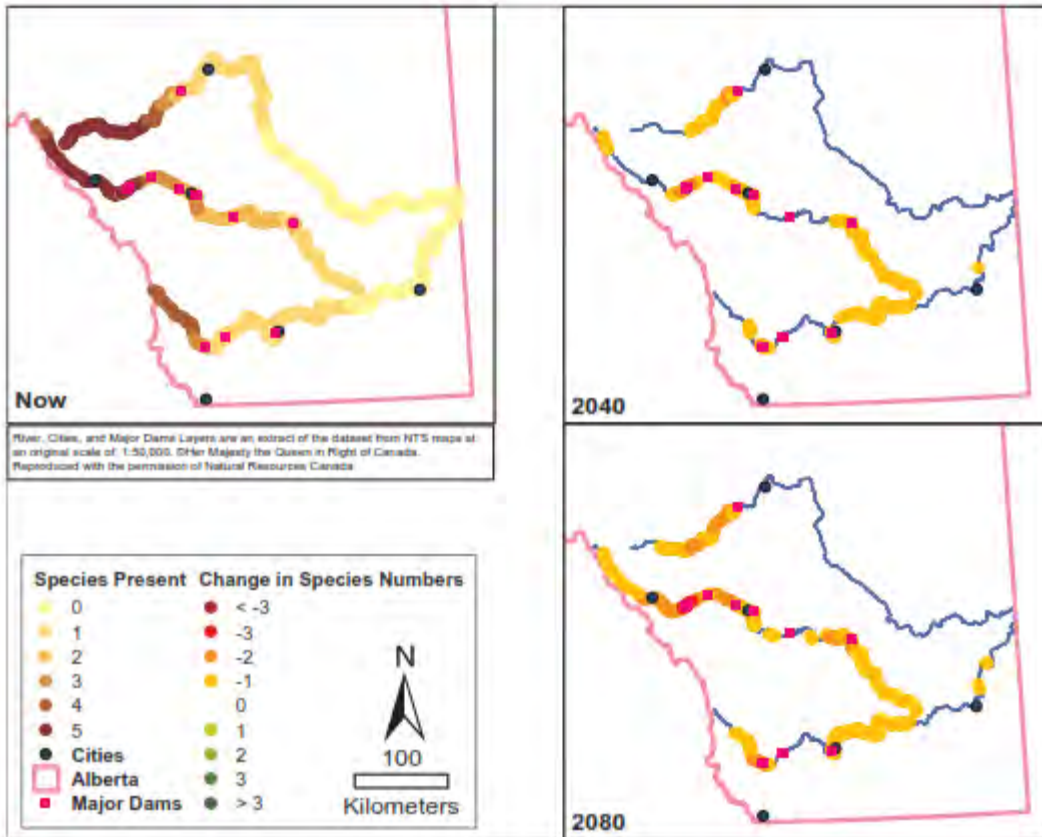


Figure 1. Number of "cold" water fish species present in the SSRB main stem rivers in the present climate (Now) and the change in species' numbers in future climates (2040 and 2080).

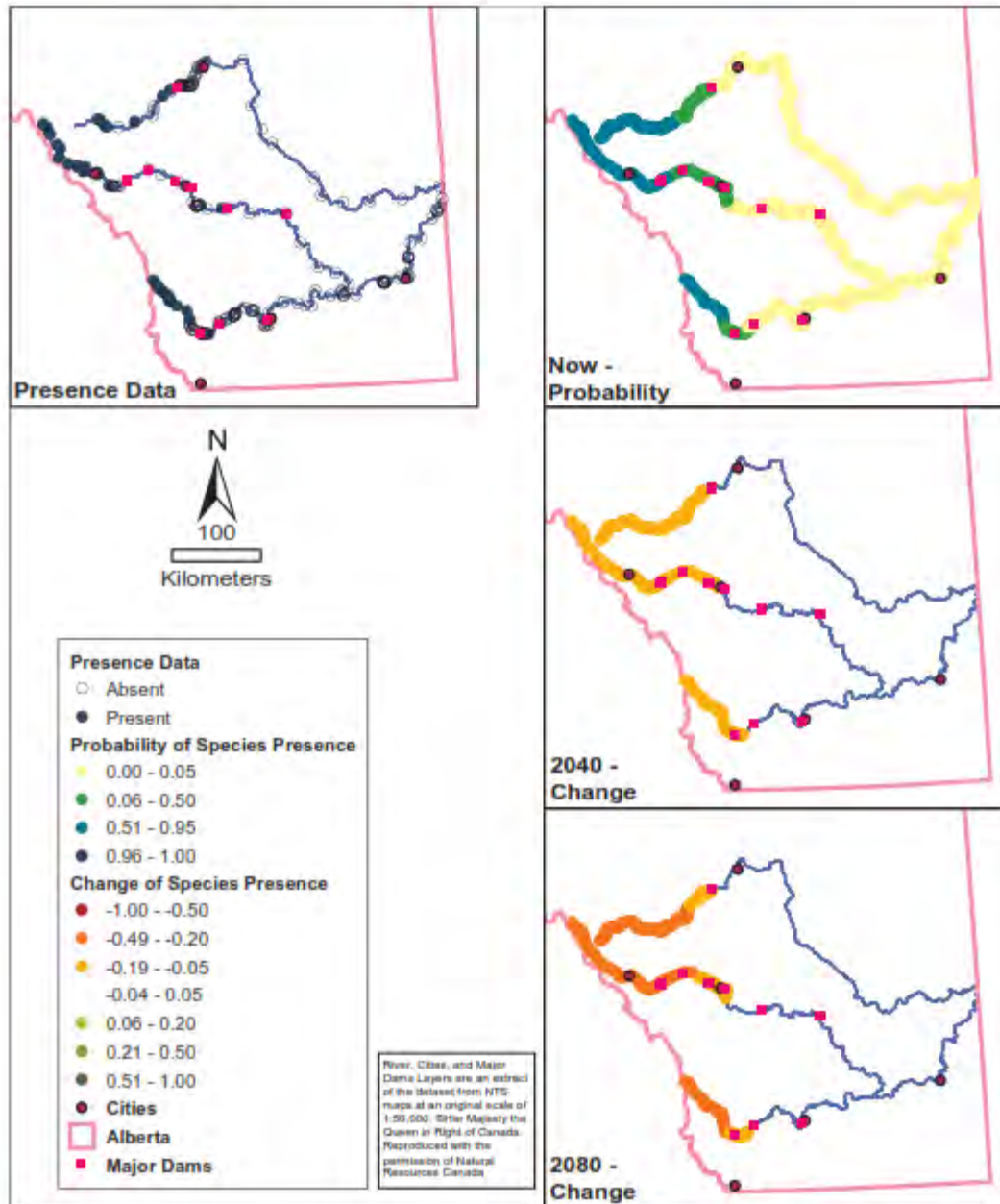


Figure 2. Probability of Cutthroat Trout presence in the SSRB in present day climate and changes in probability of presence in 2040 climate, and 2080 climate.

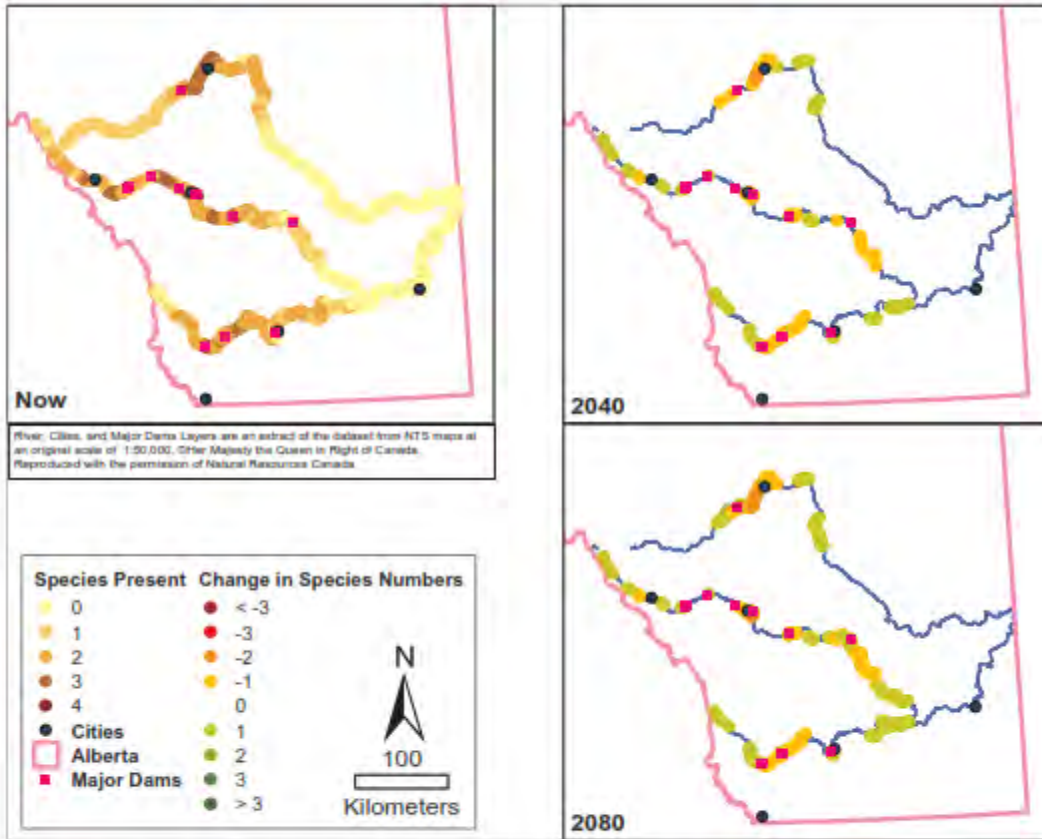


Figure 3. Number of "cool" water fish species present in the SSRB main stem rivers in the present climate (Now) and the change in species' numbers in future climates (2040 and 2080).

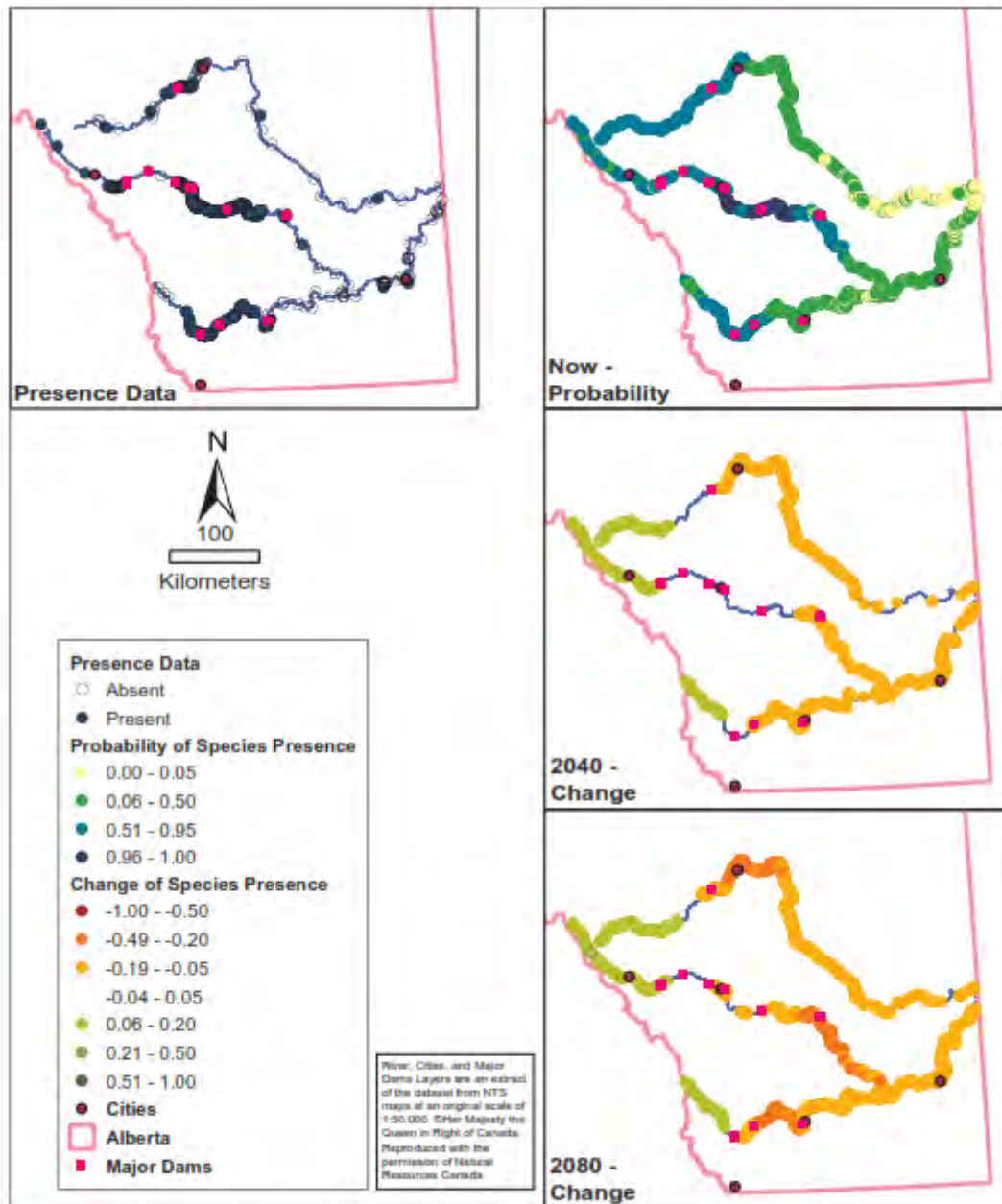


Figure 4. Probability of Rainbow Trout presence in the SSRB in present day climate and changes in probability of presence in 2040 climate, and 2080 climate.

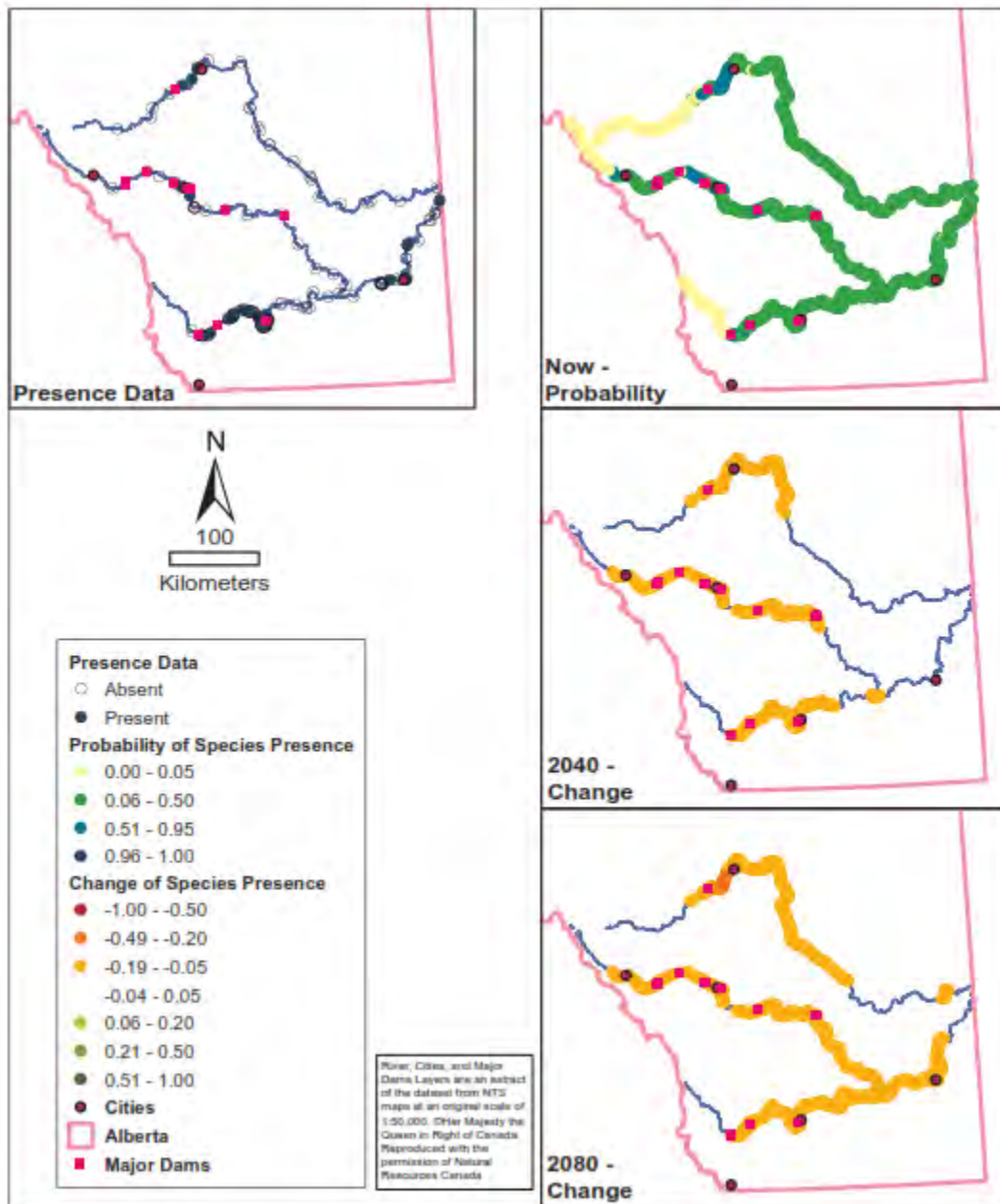


Figure 5. Probability of Spoonhead Sculpin presence in the SSRB in present day climate and changes in probability of presence in 2040 climate, and 2080 climate.

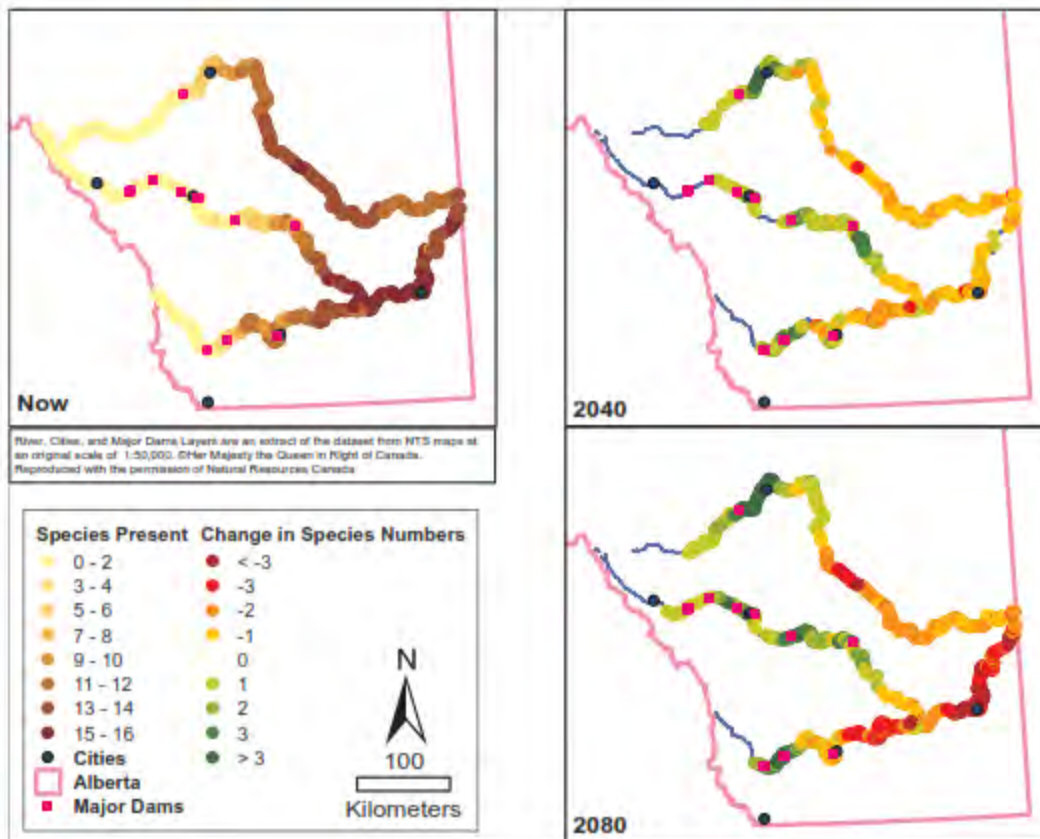


Figure 6. Number of "warm" water fish species present in the SSRB main stem rivers in the present climate (Now) and the change in species' numbers in future climates (2040 and 2080).

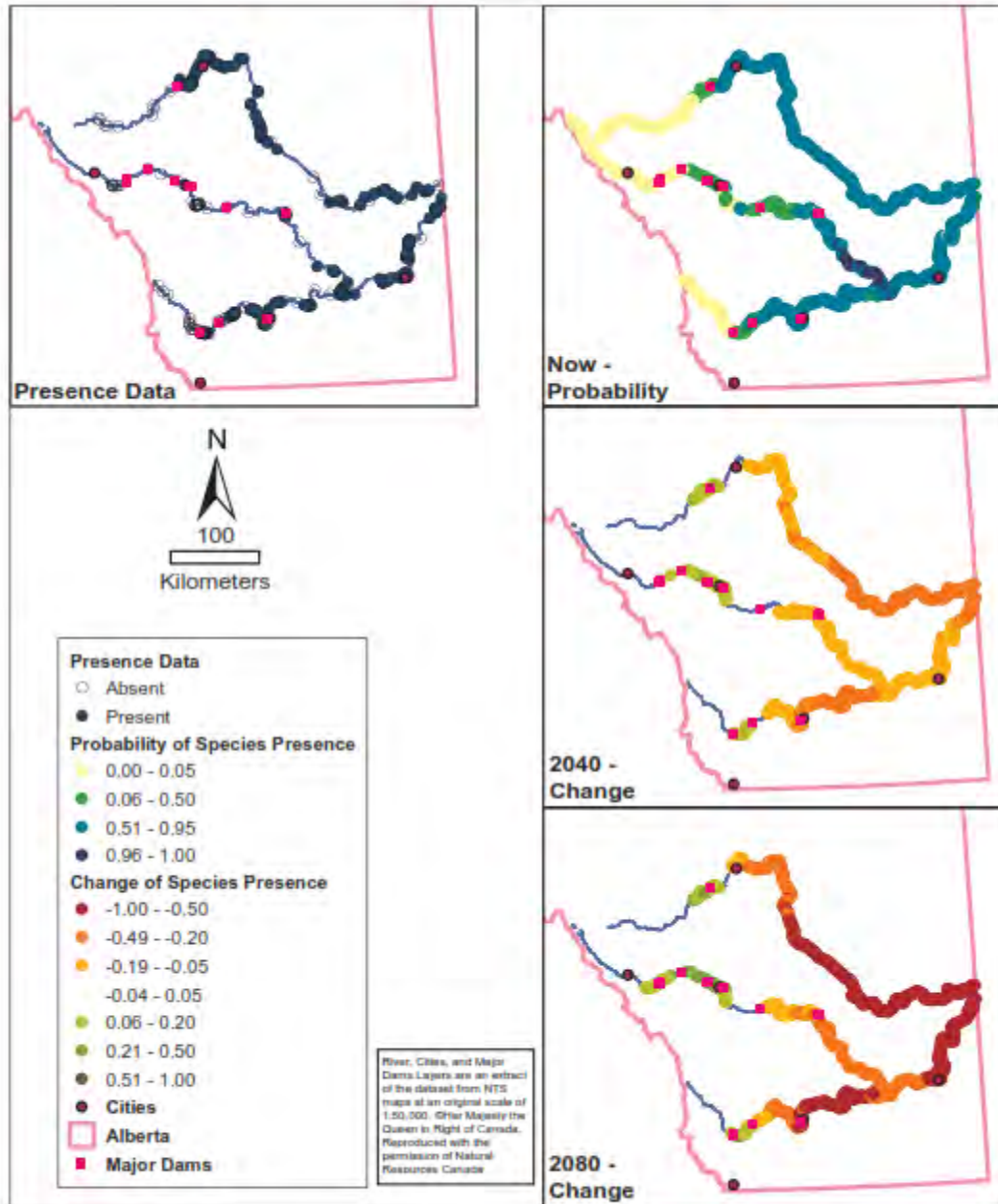


Figure 7. Probability of Walleye presence in the SSRB in present day climate and changes in probability of presence in 2040 climate, and 2080 climate.

From Glaciers to Prairie: Temporal and Spatial Variation in Ecological
Processes in a Large Riverine Ecosystem

R. Niloshini Sinnatamby¹, Bernhard Mayer², Veronique Fau², Stewart Rood³,

Anne Farineau¹, John R. Post¹

In preparation for Total Science of the Environment

¹Department of Biological Sciences, University of Calgary, Calgary, Alberta, Canada, T2N 1N4. Email:

ramila.sinnatamby@ucalgary.ca

²Department of Geoscience, University of Calgary, Calgary, Alberta, Canada, T2N 1N4

³Environmental Science Program, Lethbridge University, Alberta, Canada, T1K 3M4

Introduction

Environmental flows, defined as the 'quantity, timing and quality of water flows required to sustain freshwater and estuarine ecosystems and the human livelihood and well-being that depend on these ecosystems' (Brisbane Declaration, 2007) is a fundamental principle used to guide water allocation decisions to manage healthy rivers and estuaries. Though internationally accepted in principle, the implementation of water management and the methods used to determine when and how much water extraction is permitted, has varied widely both over time and by jurisdiction (Tharme, 2003). There is now general consensus that maintaining the natural flow regime rather than a minimum flow, is vital to maintaining ecosystem function (Poff and Zimmerman, 2010), however, understanding hydroecological relationships, which can vary within and among regions and sites, and over time, remains a fundamental challenge (Poff et al., 2017). This challenge is exacerbated by the vast number of physical, chemical and biological elements that are interconnected and must be considered together to determine impacts of anthropogenic alterations to the quantity, timing and quality of flows. Adding to this complexity is the involvement of multiple stressors typically acting upon any one system. Three key physicochemical factors that tend to vary both naturally and anthropogenically in a system and must be considered in determining environmental flows are discharge, water temperature and nutrients.

To address the challenge of understanding hydroecological relationships in a large glacier-fed, snowmelt-dominated river system, we combine new and existing data on the Bow River, Alberta, Canada. Specifically, we look at how naturally and anthropogenically driven spatial and temporal variations in discharge, water temperature and nutrients effect ecological processes in riparian density and community structure, fish species biomass and distribution and aquatic primary production.

PHYSICAL STRUCTURE OF THE BOW RIVER

The Bow River Basin is one of four sub-basins that comprise the South Saskatchewan River Basin. The main stem of the Bow River is approximately 637 km long, originating at Bow Lake (51°39'2.61"N, 116°25'11.8"W) in the Rocky Mountains, and terminating at the confluence with the Oldman River

(49°56'0.08"N, 111°41'12.62"W, Fig. 1) in the prairies, where they combine to form the South Saskatchewan River. The Bow River is a snow-melt dominated river which is supported by a number of tributaries. Of the larger tributaries, Spray, Cascade, Kananaskis and Elbow Rivers are regulated by upstream dams, whereas Pipestone, Ghost, and Highwood Rivers are free-flowing. On the main stem of the Bow there are two run-of-the-river hydroelectric dams (Kananaskis, Horseshoe, Fig. 1, Fig. 2), two hydroelectric dams with storage reservoirs (Ghost, Bearspaw) and Bassano Dam which diverts water to the Eastern Irrigation District (EID). Harvie passage and Carseland weir divert water to the Western Irrigation District (WID) and the Bow River Irrigation District (BRID), respectively. Harvey passage replaced the City of Calgary weir in 2012.

The Bow River flows through three major natural regions: Rocky Mountain (subalpine and montane subregions), Parkland (foothills parkland subregion), Grassland (foothills fescue, mixed grass, dry mixedgrass subregions, Fig. 2, Alberta Parks, 2015). Its elevation declines gradually from 1983 MAMSL at the mouth of Bow Lake to 706 MAMSL at the confluence with the Oldman River. Consistent with the river continuum concept (Vannote et al., 1980), channel width gradually increases with distance from headwaters. Two exceptions to the expected trend are the area around Canmore where the channel type is frequently braiding and anastomosing, and increased width associated with the reservoirs and other areas immediately preceding dams (excluded from Fig. 2). From the headwaters to Kananaskis Dam, the river is relatively free from anthropogenic alteration. Here, sinuosity values (1-1.5) reflect a fairly straight channel. The channel type was described as a single channel with infrequent braiding in the upper reach, followed by a transition to frequent braiding and anastomosing immediately upstream of Banff. Between the Kananaskis Dam and the inflow of the Highwood River, where the river is characterized by the most anthropogenic alteration found along the river, sinuosity remains low and the channel type was described as a single channel with infrequent braiding. River damming and flow stabilization are known to reduce erosion and sediment transport and deposition, and consequently reduce channel migration and

geomorphic processes that typically occur under natural flow regimes (Williams and Wolman, 1984). In fact, Rood et al (1999), used historical air photos to demonstrate that the Bow River between the City of Calgary and the Highwood River confluence became less geomorphologically dynamic following flow regulation. Further, bank armouring, which is also more prevalent in this reach (City of Calgary, 2016), is known to limit erosion and channel migration (Florsheim et al., 2008). From the confluence of the Highwood River, a large unregulated river, to Bassano Dam, sinuosity is notably higher (2) indicating a meandering river (Dey, 2014), and is similar to a terraced meander belt described by Bridge (2003). This small section of river represents a geomorphologically active section with relatively few anthropogenic alterations. Indeed, Rood et al., (1999) noted the role of the input of unregulated flow from the Highwood River in returning geomorphic channel activity to the Bow River main stem. From Bassano Dam to the confluence with the Oldman River, the channel returns to a single channel river and sinuosity lowers slightly to a value slightly above 1.5 but is still classified as meandering (Dey, 2014).

The Bow River flows through a number of municipalities (Lake Louise, Banff, Canmore, Cochrane, Calgary) and First Nations reserves (Stoney Nakoda, Siksika) with additional population centres within the basin. The City of Calgary accounts for the largest population density with a population of approximately 1,250,000 people in 2017. Water is extracted directly from the Bow River throughout the year by the Town of Cochrane and City of Calgary for municipal use. Water withdrawn and treated by the City of Calgary is used to supply residential users within the city (52%), industrial, commercial and institutional users (34%) and wholesale users (Airdrie, Chestermere, 2%, City of Calgary, 2007). In addition, three of Alberta's irrigation districts are supported through extractions from the Bow River (WID, BRID, EID), which occur primarily from April to October. Six wastewater treatment plants (WWTP) discharge treated effluent directly into the Bow River (Fig. 1). Three of those plants exist within the City of Calgary limits, the largest of the three being the Bonnybrook WWTP, and the most recent being Pine Creek WWTP which began

operation in mid-2008. The three plants treat wastewater from the City of Calgary as well as neighbouring municipalities (Cochrane, Airdrie, Chestermere).

PHYSICOCHEMICAL VARIATIONS ON THE BOW RIVER

SPATIAL VARIATIONS IN WATER TEMPERATURE

Mean July water temperatures measured along the Bow River from 1961 to 2001 ranged between 6.0 and 24.4 °C and demonstrated a gradual increase with distance from the headwater (Fig. 3, Mee et al., 2016). The pattern observed here is typical of a glacier-fed river originating in the mountains and flowing to lower elevations in the prairies (Caissie, 2006).

SPATIAL AND TEMPORAL VARIATIONS IN DISCHARGE

Historical discharge measured at hydrometric stations along the Bow River reflected both spatial and temporal variation (Fig. 4A). Measurements from the first decade on record (1911-1920) illustrated a strong but gradual increase in discharge with distance from headwaters, as expected for increasing drainage size and consistent with the river continuum concept (Vannote et al., 1980). In comparison, during the recent decade (2001-2010) the downstream increase tapers off after the Horseshoe Dam and discharge during the recent decade was substantially lower below the City of Calgary. Municipal withdrawals from the Bow River represent for a relatively small proportion of the total extracted river water, with withdrawal occurring at $\sim 4 \text{ m}^3/\text{s}$ on average throughout the year. In contrast, water withdrawn for irrigation would occur at a rate of approximately $27 \text{ m}^3/\text{s}$ if withdrawals were occurring throughout the year. Instead, agriculture withdrawals occur primarily between April and October at a rate of $46 \text{ m}^3/\text{s}$ during those months. Further, $>90\%$ of water extracted by the city is treated and returned to the Bow River at the wastewater treatment plant outflow locations, in contrast with a return of only $\sim 23\%$ of agriculture water. As such, whereas it is unlikely that municipal extractions contribute appreciably to the lower discharge in the recent decade, agricultural withdrawals, are a likely contributor to the observed pattern. The reduced summer flows are also likely to reflect increased summer storage in the Ghost and Bearspaw Reservoirs when power demand is lower relative to winter.

The hydrometric station on the Bow at Banff (05BB001) is suitable for accessing impacts from climate variability and change because the watershed upstream of the station is free-flowing with a relatively small anthropogenic footprint. Mean annual discharge (m^3/s) between 1911 and 2014 displayed interannual variation and a statistically significant decline of $\sim 0.039 \text{ m}^3/\text{year}$ (Fig. 4B; linear regression: $r^2=0.05$, $p<0.05$; Kendall's τ : $Z=-2.281$, $\tau=-0.152$, $p<0.05$). The decline in discharge observed over the past century reflects a change of $\sim 1\%$ per decade or 10% in total. The observed decline likely reflects a combination of natural and anthropogenic climate variability and change such as warming since the recent Ice age, influence of the Pacific Decadal Oscillation (Rood et al., 2005), and anthropogenically driven climate change. Statistical comparisons of monthly discharge over the same time period indicated significant increasing trends in March, and significant decreasing trends in July-September (Pearson's Correlation $p<0.05$, Kendall's τ $p<0.05$). Increased March flows likely reflect increased March precipitation and/or earlier snowmelt, whereas decreasing July-September flows may reflect reduced snowmelt as a result of reduced snowpack and/or earlier melt, and increased evapotranspiration resulting from warmer spring and summer air temperatures. Glacial wastage is thought to have little relative impact on the observed trends (Hopkinson and Young, 1998; Rood et al., 2005). Discharge trends observed in the Bow River at Banff reflect the same broad-scale patterns as other Nelson River tributaries (Rood et al., 2005).

A comparison of the seasonal hydrograph from the early (1911-1920) and recent decade (2001-2010) at Banff and at the City of Calgary illustrates the increase in anthropogenic impact on the river with increasing distance from headwaters (Fig. 4C). The Banff hydrographs illustrate a modest reduction in summer flows. Since the river at Banff remains free-flowing, and water withdrawals are not a significant part of the upstream river, this change likely reflects changes in climate since the early 1900s and present, and is likely a combination of natural and anthropogenic climate change (Rood et al., 2008). In comparison, the Calgary seasonal hydrograph reflects a drastic decrease in summer discharge and a modest increase in discharge from late fall to early spring. These changes largely reflect anthropogenic

activities, such as river regulation and water withdrawals. River regulation for hydroelectric power generation involves trapping high spring and summer flows, while increasing winter releases when power demands are higher. Water returns from municipal use are not reflected in this plot since the gauging station is upstream of the wastewater treatment plant outflows.

SPATIAL VARIATION IN NUTRIENT FLUX AND SOURCE

Nitrate flux values, combining nitrate concentrations with flow, are low in the headwaters and increase substantially in the City of Calgary followed by a slight decline downstream of the city (Fig. 5A). The substantial increase has been attributed to inputs from wastewater treatment plants in the city (Chao et al., in prep.). The longitudinal profile of boron flux displays a more gradual increase with distance from headwater and continues to increase further downstream of Calgary, declining again towards the confluence with the Oldman River.

Although the large increase in nitrate flux coincident with the City of Calgary WWTP outflow suggest them as the likely source, determining, with certainty the source and the downstream impact of each source is not possible by simply assessing flux. Rather, the dual isotope approach based on the determination of $\delta^{15}\text{N}$ and $\delta^{18}\text{O}$ values of nitrate has improved the ability to identify sources of nitrate in aquatic systems. Comparison of $\delta^{15}\text{N}$ and $\delta^{18}\text{O}$ values from Bow River water samples in the context of stable isotope values of potential sources allows estimation of the percent contribution of each source given enough differentiation in the source stable isotope values. Research in Western Canada and elsewhere has revealed that nitrate derived from manure is usually characterized by $\delta^{15}\text{N}$ values between +8 and +23 ‰ (Fig. 5C, Loo et al., 2017; McCallum et al., 2008; Wassenaar, 1995), while effluent from WWTPs with advanced nitrogen removal technologies usually also have elevated $\delta^{15}\text{N}$ values of nitrate ranging between +8 to >+16 ‰ (Mayer and Wassenaar, 2012). Nitrate from these sources, however, is isotopically distinct from nitrate in atmospheric deposition with $\delta^{15}\text{N}$ values ranging from -5 to +6 ‰ (Proemse et al., 2013), nitrate in synthetic fertilizers with $\delta^{15}\text{N}$ values of 0 ± 2 ‰ (Vitoria et al., 2004), and

nitrate generated via nitrification of organic soil-N, and urea and ammonium-based synthetic fertilizers yielding $\delta^{15}\text{N}$ values between -10 and +5 ‰ (Kendall, 1998; Kendall et al., 2007). Usually, the latter three sources cannot be differentiated by nitrogen isotope analyses alone because of their overlapping ranges of $\delta^{15}\text{N}$ values. However, they do sufficiently differ in $\delta^{18}\text{O}$ values in western sources (nitrate in atmospheric deposition: 50 to 90 ‰, Proemse et al., 2013; nitrate-containing synthetic fertilizers: 22 ± 3 ‰, Vitoria et al., 2004; Wassenaar, 1995; nitrate from soil denitrification: -10 to 10 ‰, Mayer et al., 2001; Mayer and Wassenaar, 2012). Nitrate $\delta^{18}\text{O}$ cannot be used to decipher soil nitrification processes from nitrate in manure and wastewater effluents since they have similarly low $\delta^{18}\text{O}$ values (Mayer and Wassenaar, 2012; Rock and Mayer, 2004). Hence, the combined determination of $\delta^{15}\text{N}$ and $\delta^{18}\text{O}$ values of dissolved nitrate provides a tool for distinguishing between four major nitrate sources: (1) atmospheric nitrate deposition, (2) nitrate-containing synthetic fertilizers, (3) nitrate derived from nitrification e.g. in soils, and (4) nitrate in manure and waste water effluents (see Fig. 5C). Based on nitrate stable isotope values from Bow River water samples collected from upstream, within, and downstream of the City of Calgary, the role of atmospheric deposition and fertilizer as potential sources can be discarded (Fig. 5C). $\delta^{15}\text{N}$ values of the water samples illustrates some spatial variability where upstream values seem to have lower values more indicative of soil nitrification, downstream samples have the highest values leaning towards WWTP or manure sources that cannot be distinguished, and City of Calgary samples fall in between.

Using the isotopic composition of nitrate, it is, in most cases, not possible to distinguish nitrate from WWTP effluent from manure-derived nitrate due to their similar ranges of $\delta^{15}\text{N}$ and $\delta^{18}\text{O}$ values (see Fig. 5C). To distinguish nutrients from these two sources, boron isotope ratios have proven to be a useful co-tracer (Kruk, 2017). In Western Canada and elsewhere, synthetic fertilizers and WWTP effluents have overlapping $\delta^{11}\text{B}$ values ranging from -5 to +10 ‰ (Kruk, 2017; Tirez et al., 2010; Vengosh et al., 1994), while manure-derived boron in Alberta has been found to have distinctly elevated $\delta^{11}\text{B}$ values ranging

between +23 and +28 ‰ (Kruk, 2017), consistent with boron isotope ratios for cow manure reported elsewhere (Komor, 1997; Widory et al., 2004). Therefore, plotting $\delta^{11}\text{B}$ versus $\delta^{15}\text{N}$ values of nitrate is a promising approach to distinguish nitrate from WWTP effluent from manure-derived nitrate and to reveal to what extent nutrient exports through agricultural return-flows contribute to riverine nutrient fluxes. Boron stable isotope values from Bow River water samples collected from upstream, within, and downstream of the City of Calgary indicate that the samples from within the city are more reflective of WWTP effluent as opposed to manure. On the other hand, most downstream samples were characterized by values between those of WWTP effluent and manure. This indicates that WWTP effluent still plays a role downstream of Calgary, but that manure inputs do also become a factor downstream of Calgary.

The approximate percent that each source (soil nitrification, WWTP effluent, and agriculture (manure)) contributes to samples from upstream, within, and downstream of the City of Calgary was estimated based on a nitrate mixing model by Chao et al (in prep.) and the boron stable isotope biplot (Fig. 5B). Results showed that nutrients in upstream samples were predominantly characterized by soil nitrification and less than 1% was from municipal WWTP effluent. Samples within the City of Calgary, on the other hand, reflected approximately 50% soil nitrification sources, and 50% municipal WWTP effluent sources. Downstream of the City of Calgary, the signal from the municipal WWTPs remained an important source (~84 to 92%), and agriculture contributed the remaining nutrients via manure.

SPATIAL VARIABILITY IN RIPARIAN COMMUNITY

An assessment of riparian woodland abundance and coarse composition was conducted using Google Earth satellite imagery (Fig. 6). The riparian woodland community primarily comprised coniferous species in the headwater region. A mixed community of coniferous and deciduous species characterizes the reach from approximately Canmore to Cochrane. And from Cochrane to the confluence with the Oldman River the riparian woodland community is predominately deciduous. The observed shifts in coarse woodland community composition are consistent with expected patterns for a river flowing from the mountains to

the prairies. As well, the riparian woodland community composition is consistent with the major natural regions (Alberta Parks, 2015), which is reflective of larger landscape characteristics rather than being driven strictly by river characteristics.

The riparian woodland abundance index reflects spatial variation along the Bow that likely reflects a combination of natural and anthropogenic characteristics, and can be interpreted as four main reach segments. In the headwater region, from Bow Lake to the Kananaskis Dam, the river is relatively unaltered by anthropogenic activity, and riparian woodland abundances are high (~3.8 on average). Two below average anomalies in this reach occur where the river runs through Hector Lake (lakes and reservoirs were not included in this analysis) and the Town of Banff where alteration was slightly higher. A previous, finer scale, riparian assessment was generally consistent with our findings, reported significant vegetative cover by preferred tree and shrub communities, and one site near Banff that was an exception to the overall rating of “healthy” because of high site use (Alberta Environment, 2007).

In the next reach between Kananaskis Dam and the inflow of Highwood River, areas immediately before the dams were not assessed because the channel is artificially widened, and is represented in Fig. 6 as an index value of zero. Even with these areas excluded, the average index value is lower than the headwater reach (2.1) and contained increased development and human land use (e.g. dams, reservoirs, livestock grazing, population centres, acreage development, urban development, farmland, gravel pits, golf courses, WWTPs and industrial parks, Alberta Environment, 2007). The previous assessment categorized this reach as “healthy with problems” and noted increasing occurrences of invasive or disturbance species (Alberta Environment, 2007). The report also indicated abundant tree and shrub coverage in the upper section of this reach but coverage declined to approximately 25-30% each toward the downstream end of the reach. Particularly in the downstream part of this reach, dewatering from water withdrawals and alterations of peak flows and timing were considered to have some impact on riparian health (Alberta Environment, 2007).

From the inflow of Highwood River to Bassano Dam, riparian woodland abundance increased to index values similar to the pristine headwater reach (3.7). Despite the higher riparian woodland abundances which we observed, the previous report categorizes this reach as “healthy with problems” (Alberta Environment, 2007). Although high coverage by shrubs was reported, a high proportion of grazing resistant species was observed, and only 17% tree cover. The report, however, does note excellent regeneration of cottonwoods and preferred trees and shrubs, and also the largest and densest balsam poplar stand on the river (Alberta Environment, 2007). Land use in this reach is dominated by grazing. The improved riparian community in this reach has been attributed to the return to natural flow regime from the inflow of the Highwood River, which is unregulated (Alberta Environment, 2007; Rood et al., 1999).

The river reach between Bassano Dam and the confluence with the Oldman River, is characterized by the lowest riparian woodland abundances of the entire river (0.4), consistent with the previous report which reported negligible tree communities (<1% cover, Alberta Environment, 2007). Land use in the reach is dominated by grazing, however, this was thought to have negligible impact on the riparian community. Rather, the highly altered flow regime from upstream dams and dewatering from water withdrawals was thought to contribute significantly to the poorer riparian community condition (Alberta Environment, 2007). Flows are the most diminished in this reach relative to the natural flow (>25% withdrawn) as a result of the upstream alterations and withdrawals, but also, importantly, the largest agricultural withdrawal, which occurs at the Bassano Dam (EID). However, while these alterations likely contribute to the poorer riparian community, we suggest that this region is also naturally impoverished. At Bassano Dam, the major natural region switches to dry mixedgrass (Fig. 6) which is the driest subregion in Alberta (Alberta Parks, 2015). This switch marks a large scale regional shift in condition rather than a river-specific shift.

ANNUAL VARIATION: AQUATIC VEGETATION BIOMASS, ANNUAL MAXIMUM FLOWS AND DIEL DO FLUCTUATIONS

Potential eutrophication of the Bow River as a result of effluent inputs from wastewater treatment

plants in the City of Calgary have been a concern for a number of decades (Culp et al., 1992; Sosiak, 2003; Taube et al., 2016). Anthropogenic nutrient inputs to the Bow River have been associated with increased productivity in the system resulting in increased macrophyte and algal production with negative impacts on boat traffic and recreational activities (Chambers et al., 1991). Increases in aquatic primary productivity are often associated with high photosynthesis during the day and high respiration at night, resulting in larger diel fluctuations of dissolved oxygen (DO, Wassenaar et al., 2010). The nutrient input to the Bow River has been suggested to have both beneficial and deleterious impacts on fish biomass (Askey et al., 2007). Specifically, Askey et al., (2007) suggested that rainbow trout and brown trout biomass increased as a direct response to increased productivity in the system. Conversely, productivity-driven changes to habitat structure or lowered DO were suggested as some of the reasons that may have contributed to the observed decline in mountain whitefish biomass (Askey et al., 2007).

Macrophyte and epilithic algae biomass assessments have been conducted by the Alberta government on the Bow River in most years since 1981 and has been the focus of previous studies (Sosiak, 2003; Taube et al., 2016). Authors have demonstrated declines in macrophyte and algae production following upgrades to the City of Calgary WWTPs that resulted in decreased phosphorus entering the river in 1982, and decreased nitrogen between 1990 and 1996 (Sosiak, 2003; Taube et al., 2016). Specifically, Taube et al., (2016) determined that macrophyte biomass responded to reductions in phosphorus, whereas epilithic algae responded more to the nitrogen upgrades. Authors have also noted the role that flow plays on limiting aquatic vegetation (Chambers et al., 1991; Sosiak, 2003; Taube et al., 2016). Most recently, Taube et al., (2016) illustrated that annual maximum flows exceeding 400 m³/s typically scour macrophyte beds, and consequent macrophyte abundances measured in September of the same year are low. Whereas high flows associated with spring freshet have an impact on end of season macrophyte biomass, algae biomass was not influenced by the annual maximum flow (Taube et al., 2016) presumably owing to the quicker regeneration of epilithic algae. Rather, Taube et al., (2016) found that scouring flows

for algae were linked to daily discharge greater than 120 m³/s.

Figure 7 presents an updated time series of aquatic vegetation biomass that includes the 2013 flood event, in the context of maximum discharge and the magnitude of diel fluctuation in DO in the river in September obtained from City of Calgary in-river sondes that measure diel fluctuation. Consistent with relationships identified by Taube et al., (2016), macrophyte biomass tends to be low in years with high flow, and higher in years with low flow. The extreme flood event in 2013 supports this relationship, and even the year following saw no macrophyte growth during river surveys. The diel DO fluctuations show variability among years but tend to hover around a common mean of ~10mg/L, and show no association with macrophyte biomass (linear regression $p > 0.05$). On the other hand, a simple linear regression looking at the diel DO fluctuations vs. algae biomass did produce a significant relationship (Fig. 7B; $r^2 = 0.56$, $p = 0.02$).

SEASONAL VARIATION: AQUATIC VEGETATION BIOMASS, ANNUAL MAXIMUM FLOWS AND DIEL DO FLUCTUATIONS

Figure 8 illustrates both seasonal and spatial variation in discharge, macrophyte and epilithic algae biomass and diel DO fluctuations observed in the City of Calgary. The *Upstream* and *Downstream* panels reflects measurements upstream and downstream of the wastewater treatment plants in Calgary, respectively. The only exception is that discharge in the downstream panel is from the Calgary gauging station. Most notably in the spatial comparison is the very low diel DO fluctuations in the upstream measurements compared to the seasonal patterns observed downstream. The means do not seem to differ drastically, whereas the diel fluctuation is considerably larger downstream. The large fluctuation at the downstream site is likely reflective of photosynthesis and respiration activity in the river (Wassenaar et al., 2010). In fact, in the years with higher fluctuation, the algae biomass is also higher and tends to increase towards the end of the season. As such, the relationship between annual algae biomass and diel DO fluctuations (Fig. 7B) is also supported in the seasonal patterns in the three years presented here. Low fluctuation in the upstream diel DO measurement may be a reflection of lower instream photosynthesis

and respiration activity, or the impact of mixed water released from Bearspaw Dam immediately upstream of the location where DO is measured, or a combination of the two.

SPATIAL VARIATION IN FISH SPECIES DISTRIBUTION AND SPORT FISH BIOMASS

The spatial distribution of fish species was assessed along the Bow River in relation to a number of physicochemical variables such as mean July water temperature, slope, phosphorus and nitrate-nitrite concentrations, turbidity and channel width (Mee et al., 2016). Mean July water temperature was the most common predictor variable describing species distribution along the Bow River. In general, the number of fish species present increased with distance from headwaters, consistent with a species addition pattern of species distribution (Rahel and Hubert, 1991). Authors noted two areas along the Bow River where species composition showed low similarity with adjacent segments of the river, based on the mean Czekanowski coefficient (Fig. 9), marking areas of high community change. These high turnover zones occurred at approximately 260 and 445 km downstream of headwaters on the Bow River, and where mean July water temperatures were approximately 15 and 19 °C, respectively. These high turnover zones, and the temperatures that characterized them were remarkably consistent across the three main stem rivers of the South Saskatchewan River Basin that originate in the Rocky Mountains – Red Deer River, Bow River and Oldman River (Mee et al., 2016).

The role of water temperature in determining current fish species distribution in the SSRB has important implications for species distributions in response to climate change. The findings by Mee et al., (2016) may also provide a new perspective with which to consider the spatial patterns in sport fish biomass in and downstream of the City of Calgary observed in 2000 (Askey et al., 2007).

Given the anthropogenic nutrient inputs to the Bow River in the City of Calgary via WWTP effluent, and the known role of nutrient inputs on biotic productivity, spatial pattern of biomass of mountain whitefish, rainbow trout and brown trout, three dominant sport fish in the region, were assessed over a 177 km section of the Bow River starting at Bearspaw Dam (Askey et al., 2007). As would be expected in

association with a nutrient input, authors observed a drastic increase in rainbow trout biomass (25x) and a smaller but still notable increase in brown trout (5x). However, rather than observing the expected overall increase in sport fish biomass, the increases observed in rainbow trout and brown trout were overshadowed by a remarkable decrease in mountain whitefish. The increase in rainbow trout and brown trout was attributed to nutrient inputs as expected, however the decrease in mountain whitefish was unexpected and several potential factors were suggested as drivers for this change. Authors suggested that changes to habitat structure as a result of the increased macrophyte abundance immediately below the wastewater treatment plants may have altered predator prey interaction with a disproportionate negative impact on mountain whitefish that tend to be more efficient at foraging for invertebrates amongst rocky substrate (Scott and Crossman, 1973). Authors also suggested that the decline in mountain whitefish may be the result of predation by adult trout on young mountain whitefish, that mountain whitefish may be more susceptible to ammonia toxicity, or be more hampered by the Carseland weir. Based on limits to empirical data, these potential hypotheses could not be tested or refuted. The first of the two high species turnover zones identified along the Bow River by Mee et al., (2016), however, occurred within the City of Calgary, immediately upstream of the Bonnybrook WWTP. As such, the large shifts in sport fish biomass by Askey et al., (2007), but mountain whitefish in particular may be related to water temperature and a change in fish community structure.

IMPACT OF TEMPORAL VARIABILITY IN DISCHARGE, TEMPERATURE AND PREY ABUNDANCE ON FISH PRODUCTION POTENTIAL: A CASE STUDY AT JUMPINGPOUND CREEK

Models that simulate physical habitat (e.g. PHABSIM) combine hydraulic stream models with information on species-habitat relationships, and have been a common tool for understanding longitudinal patterns in riverine habitat quality for a number of decades (e.g., Laliberte et al., 2014; Rosenfeld et al., 2007). These models predict the amount of quality habitat that exists in a river reach for a given species and/or life stage at different discharge levels based on longitudinal variations in physical

characteristics (e.g. depth, velocity, wetted width) and habitat suitability indices (Ahmadi-Nedushan et al., 2006). The model outcome is weighted usable area (WUA), which reflects the predicted area of suitable habitat that exists for a given species or life stage within the study reach. In response to critiques that these habitat models rarely accurately predict abundance, and that habitat selection and fitness associations are a rarely supported, bioenergetics models were developed based on mechanistic relationships and consider the energetic costs and benefits of habitat use (Rosenfeld, 2003). Bioenergetics models combine hydraulic models with invertebrate drift models into a single foraging energetics model that also includes information on fish size, water temperature, height of focal point, and probability of prey detection (Hayes et al., 2007; Laliberte et al., 2016). The model produces an estimate of net rate of energy intake (NREI, J_s^{-1}). Production potential (PP) reflects the NREI per 100 m of stream length.

A comparison of weekly mean production potential estimates from a ~500 m reach of a fourth order tributary of the Bow River (Nicoll Ranch reach of Jumpingpound Creek, 51°5'24"N, 114°33'77"W), illustrates variability in the impact that seasonal changes to discharge, temperature and prey densities can have on different life stages of rainbow trout (Laliberte, 2012). Weekly mean of stream discharge measured at the Jumpingpound gauging station (05BH015) in 2008 reflected high discharge due to the spring melt between approximately May 19 and Jun 15 (Fig. 11A). The water temperature profile reflects peak temperatures in July and August. Invertebrate drift densities were highest immediately following the spring freshet and again later in the season in August and early September (Fig. 11B). The resulting modelled production potentials at Nicoll Ranch reach illustrated seasonal variability as well as variability among life stage (Fig. 11C). Production potential was modelled to be highest prior to the spring freshet. This is likely related to the reduced energetic costs associated with swimming because of low discharge and low water temperatures. Production potential values are generally low during the remainder of the season with a small increase during the period immediately following the spring freshet. This small peak likely occurs because of low discharge and because the peak in prey availability is likely large enough to

offset increased metabolic costs associated with temperature. Following week 30, although discharge is low, and prey availability is high, the metabolic costs associated with prolonged high water temperatures is likely unsuitable for high net energy intakes. Compared to seasonal variation, the differences among life stages is relatively small. However, in general, young-of-the-year and juvenile RNTR were found to have slightly higher production potentials throughout most of the season. Adults, on the other hand, likely do not have enough prey to support their greater metabolic requirements. This model based on a real habitat and prey data, illustrates how natural variability in discharge, temperature and prey productivity can impact the fish productivity, with impacts varying with species and life stage requirements. Further, the relationships described here can be applied to predict how fish are likely to respond to anthropogenically driven variations such as flow regulation, climate change or nutrient inputs.

IMPACTS OF VARIABILITY IN WATER QUANTITY, TIMING AND QUALITY ON ECOLOGICAL PROCESSES

The spatial and temporal variation in water quantity, timing and quality in the Bow River contributes to a complex ecological system. Interactions between physical, hydrological and nutrient characteristics of the Bow River reflect the importance of the interplay between natural and anthropogenic drivers. The case studies illustrate how spatial or temporal variation in these characteristics impact ecological processes within the river. Taken together these case studies provide insight into how natural and anthropogenic effects structure river function. This is key to evaluating the river's ability to withstand ongoing anthropogenic change and natural stochastic events.

References

- Ahmadi-Nedushan B, St-Hilaire A, Berube M, Robichaud E, Thiemonge N, Bobee B. A review of statistical methods for the evaluation of aquatic habitat suitability for instream flow assessment. *River Res Appl* 2006;22:503-23.
- Alberta Environment. Aquatic and riparian condition assessment of the South Saskatchewan River Basin 2007.
- Alberta Parks. Natural regions and subregions of Alberta. A framework for Alberta's Parks. Edmonton, Alberta: Alberta Tourism, Parks and Recreation; 2015.
- Askey PJ, Hogberg LK, Post JR, Jackson LJ, Rhodes T, Thompson MS. Spatial patterns in fish biomass and relative trophic level abundance in a wastewater enriched river. *Ecol Freshwat Fish* 2007;16:343-53.
- Bridge JS. Rivers and floodplains: forms, processes, and sedimentary record Malden, Mass: Blackwell Pub; 2003.
- Brisbane Declaration. Summary findings and a global action agenda of the 10th International River Symposium and International Environmental Flows Conference, 2-6 September 2007. Available at: <http://www.watercentre.org/news/declaration> 2007.
- Caissie D. The thermal regime of rivers: a review. *Freshwat Biol* 2006;51:1389-406.
- Chambers PA, Prepas EE, Hamilton HR, Bothwell ML. Current velocity and its effect on aquatic macrophytes in flowing waters. *Ecol Appl* 1991;1:249-57.
- Chao J, Kruk M, Mayer B, Ryan MC. Isotopic apportionment of nitrate sources in the Bow River Alberta, Canada in prep.
- City of Calgary. Calgary Rivers Morphology and Fish Habitat Study 2016.
- City of Calgary. Water efficiency plan: 30-in-30 by 2033 2007.
- Culp JM, Hamilton HR, Sosiak AJ, Davies RW. Longitudinal zonation of the biota and water quality of the Bow River system in Alberta, Canada. In: Becker CD, Neitzel DA, editors. *Water quality in North America river systems*. Columbus, Ohio: Battelle Press; 1992.
- Dey S. *Fluvial hydrodynamics*: Springer; 2014.
- Florsheim JL, Mount JF, Chin A. Bank erosion as a desirable attribute of rivers. *Bioscience* 2008;58:519-29.
- Hayes JW, Hughes NF, Kelly LH. Process-based modelling of invertebrate drift transport, net energy intake and reach carrying capacity for drift-feeding salmonids. *Ecol Model* 2007;207:171-88.

- Hopkinson C, Young G. The effect of glacier wastage on the flow of the Bow River at Banff, Alberta, 1951-1993. *Hydrological Processes* 1998;12:1745-62.
- Kendall C. Tracing nitrogen sources and cycling in catchments. In: Kendall C, McDonnell JJ, editors. *Isotope tracers in catchment hydrology*; Elsevier; 1998. p. 519-76.
- Kendall C, Elliott EM, Wankel SD. Tracing anthropogenic inputs of nitrogen to ecosystems. In: Michener R, Lajtha K, editors. *Stable isotopes in ecology and environmental science*. Oxford, UK: Blackwell Publishing Ltd; 2007. p. 375-449.
- Komor S. Boron contents and isotopic compositions of hog manure, selected fertilizers, and water in Minnesota. *J Environ Qual* 1997;26:1212-22.
- Kruk MK. Tracing sources of nitrate in rivers of southern Alberta using nitrogen, oxygen, and boron isotopes as co-tracers 2017.
- Laliberte JJ. Physical and bioenergetic approaches for modeling instream habitat quality of drift-feeding fish 2012.
- Laliberte JJ, Post JR, Rosenfeld JS. Hydraulic geometry and longitudinal patterns of habitat quantity and quality for rainbow trout (*Oncorhynchus mykiss*). *River Research and Applications* 2014;30:593-601.
- Laliberte JJ, Post JR, Rosenfeld JS, Mee JA. Modelling temperature, body size, prey density, and stream gradient impact on longitudinal patterns of potential production of drift-feeding trout. *River Res Appl* 2016;32:2045-55.
- Loo SE, Ryan MC, Zebarth BJ, Kuchta SH, Neilsen D, Mayer B. Use of $\delta^{15}\text{N}$ and $\delta^{18}\text{O}$ Values for nitrate source identification under irrigated crops: A cautionary Vadose Zone tale. *J Environ Qual* 2017;46:528-36.
- Mayer B, Bollwerk S, Mansfeldt T, Hutter B, Veizer J. The oxygen isotope composition of nitrate generated by nitrification in acid forest floors. *Geochim Cosmochim Acta* 2001;65:2743-56.
- Mayer B, Wassenaar LI. Isotopic characterization of nitrate sources and transformations in Lake Winnipeg and its contributing rivers, Manitoba, Canada. *J Great Lakes Res* 2012;38:135-46.
- McCallum JE, Ryan MC, Mayer B, Rodvang SJ. Mixing-induced groundwater denitrification beneath a manured field in southern Alberta, Canada. *Appl Geochem* 2008;23:2146-55.
- Mee JA, Robins G, Post JR. Patterns of fish species assemblage replicated across three parallel rivers suggest biotic zonation in response to a longitudinal temperature gradient. *Ecol Freshwat Fish* 2016;DOI: 10.1111/eff.12322.
- Poff NL, Tharme RE, Arthington AH. Evolution of environmental flows assessment science, principles, and methodologies. In: Horne AC, Webb JA, Stewardson MJ, Richter BD, Acreman M, editors. *Water for the environment: from policy and science to implementation and management*. London, United Kingdom: Academic Press is an imprint of Elsevier; 2017. p. 203-36.

Poff NL, Zimmerman JKH. Ecological responses to altered flow regimes: a literature review to inform the science and management of environmental flows. *Freshwat Biol* 2010;55:194-205.

Proemse BC, Mayer B, Fenn ME, Ross CS. A multi-isotope approach for estimating industrial contributions to atmospheric nitrogen deposition in the Athabasca oil sands region in Alberta, Canada. *Environ Pollut* 2013;182:80-91.

Rahel FJ, Hubert WA. Fish assemblages and habitat gradients in a Rocky Mountain Great Plains stream - Biotic zonation and additive patterns of community change. *Trans Am Fish Soc* 1991;120:319-32.

Robins GL. Spatial distribution of 33 fish species in the mainstem rivers of the South Saskatchewan River Basin under changing thermal regimes 2009.

Rock L, Mayer B. Isotopic assessment of sources of surface water nitrate within the Oldman River basin, Southern Alberta, Canada. *Water, Air, & Soil Pollution: Focus* 2004;4:545-62.

Rood SB, Pan J, Gill KM, Franks CG, Samuelson GM, Shepherd A. Declining summer flows of Rocky Mountain rivers: Changing seasonal hydrology and probable impacts on floodplain forests. *Journal of Hydrology* 2008;349:397-410.

Rood SB, Samuelson G, Weber J, Wywrot K. Twentieth-century decline in streamflows from the hydrographic apex of North America. *Journal of Hydrology* 2005;306:215-33.

Rood SB, Taboulchanas K, Bradley CE, Kalischuk AR. Influence of flow regulation on channel dynamics and riparian cottonwoods along the Bow River, Alberta. *Rivers* 1999;7:33-48.

Rosenfeld JS. Assessing the habitat requirements of stream fishes: An overview and evaluation of different approaches. *Trans Am Fish Soc* 2003;132:953-68.

Rosenfeld JS, Post JR, Robins G, Hatfield T. Hydraulic geometry as a physical template for the River Continuum: application to optimal flows and longitudinal trends in salmonid habitat. *Can J Fish Aquat Sci* 2007;64:755-67.

Scott WB, Crossman EJ. Freshwater fishes of Canada. *Fisheries Research Board of Canada Bulletin* 1973;184.

Sosiak A. Long-term response of periphyton and macrophytes to reduced municipal nutrient loading to the Bow River (Alberta, Canada). *Can J Fish Aquat Sci* 2003;59:987-1001.

Taube N, He J, Ryan MC, Valeo C. Relative importance of P and N in macrophyte and epilithic algae biomass in a wastewater-impacted oligotrophic river. *Environ Monit Assess* 2016;188:494.

Tharme RE. A global perspective on environmental flow assessment: Emerging trends in the development and application of environmental flow methodologies for rivers. *River Research and Applications* 2003;19:397-441.

Tirez K, Brusten W, Widory D, Petelet E, Bregnot A, Xue D et al. Boron isotope ratio ($\delta^{11}\text{B}$) measurements in Water Framework Directive monitoring programs: comparison between double focusing sector field ICP and thermal ionization mass spectrometry. *J Anal At Spectrom* 2010;25:964-74.

Vannote RL, Minshall GW, Cummins KW, Sedell JR, Cushing CE. River Continuum Concept. *Can J Fish Aquat Sci* 1980;37:130-7.

Vengosh A, Heumann KG, Juraske S, Kasher R. Boron isotope application for tracing sources of contamination in groundwater. *Environ Sci Technol* 1994;28:1968-74.

Vitoria L, Otero N, Soler A, Canals A. Fertilizer characterization: Isotopic data (N, S, O, C, and Sr). *Environ Sci Technol* 2004;38:3254-62.

Wassenaar LI. Evaluation of the origin and fate of nitrate in the Abbotsford aquifer using the Isotopes of ^{15}N and ^{18}O in NO_3^- . *Appl Geochem* 1995;10:391-405.

Wassenaar LI, Venkiteswaran JJ, Schiff SL, Koehler G. Aquatic community metabolism response to municipal effluent inputs in rivers quantified using diel $\delta^{18}\text{O}$ values of dissolved oxygen. *Can J Fish Aquat Sci* 2010;67:1232-46.

Widory D, Kloppmann W, Chery L, Bonnin J, Rochdi H, Guinamant J. Nitrate in groundwater: an isotopic multi-tracer approach. *J Contam Hydrol* 2004;72:165-88.

Williams GP, Wolman MG. Downstream effects of dams on alluvial rivers 1984;Geological Survey Professional Paper 1286.

Figures

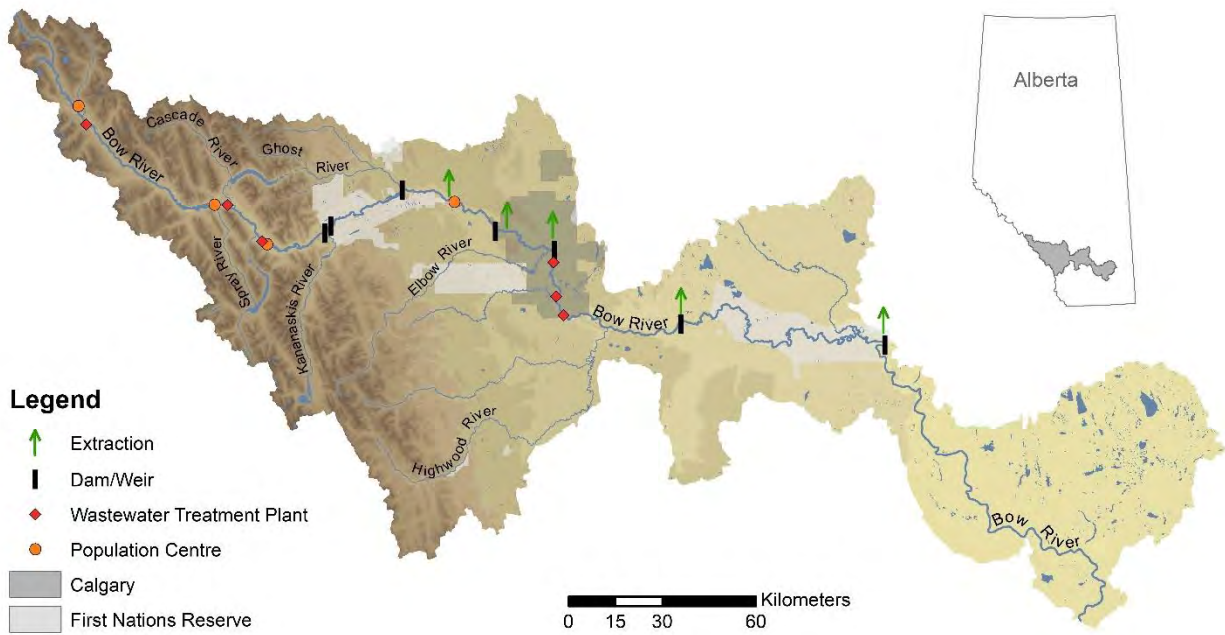


Figure 1. Map of Bow River watershed.

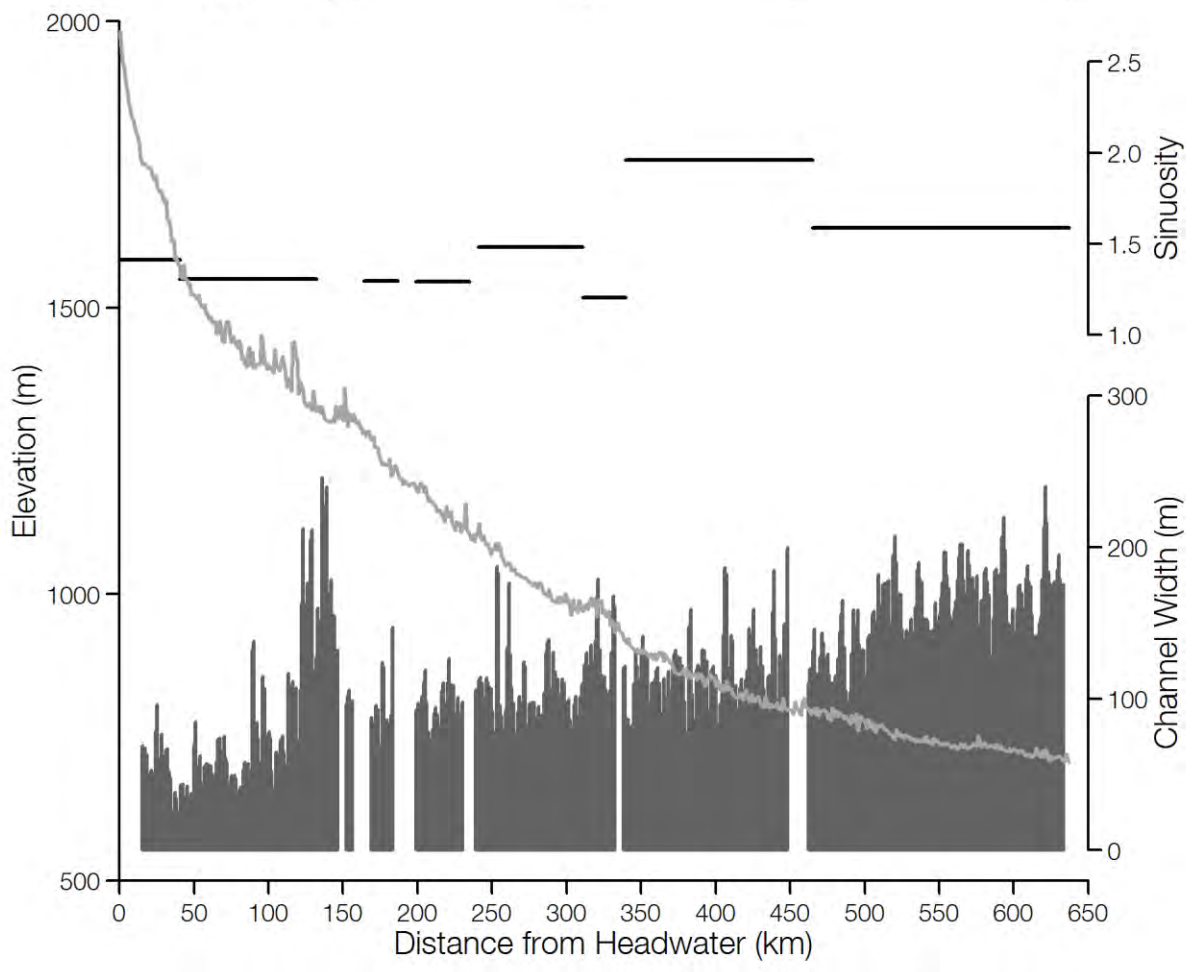
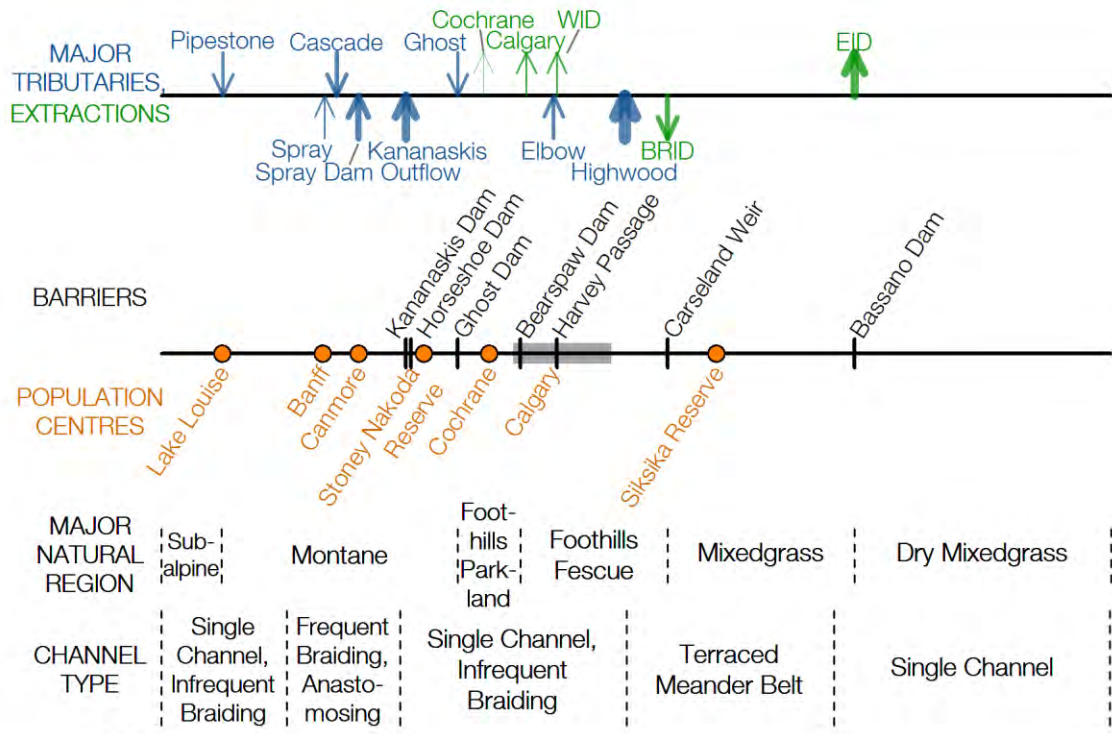


Figure 2. Physical properties of the Bow River from the headwaters at Bow Lake to the confluence with the Oldman River, including elevation (grey line graph), channel width (dark grey bar chart), and sinuosity (horizontal black lines). Major natural regions, and channel type are depicted. Major tributaries, extractions, municipalities, and barriers are illustrated at the top of the figure using the same distance from headwater scale. The orange dots indicate municipalities and reserves except for the City of Calgary, which is represented by the dark grey rectangle. The vertical black bars indicate dams or weirs on the river. The blue arrows indicate main tributaries feeding the Bow River, and the green arrows indicate water withdrawals by Cochrane, the City of Calgary and the irrigation districts. The tributaries and extractions are scaled to represent their approximate annual discharge or withdrawal rate, respectively.

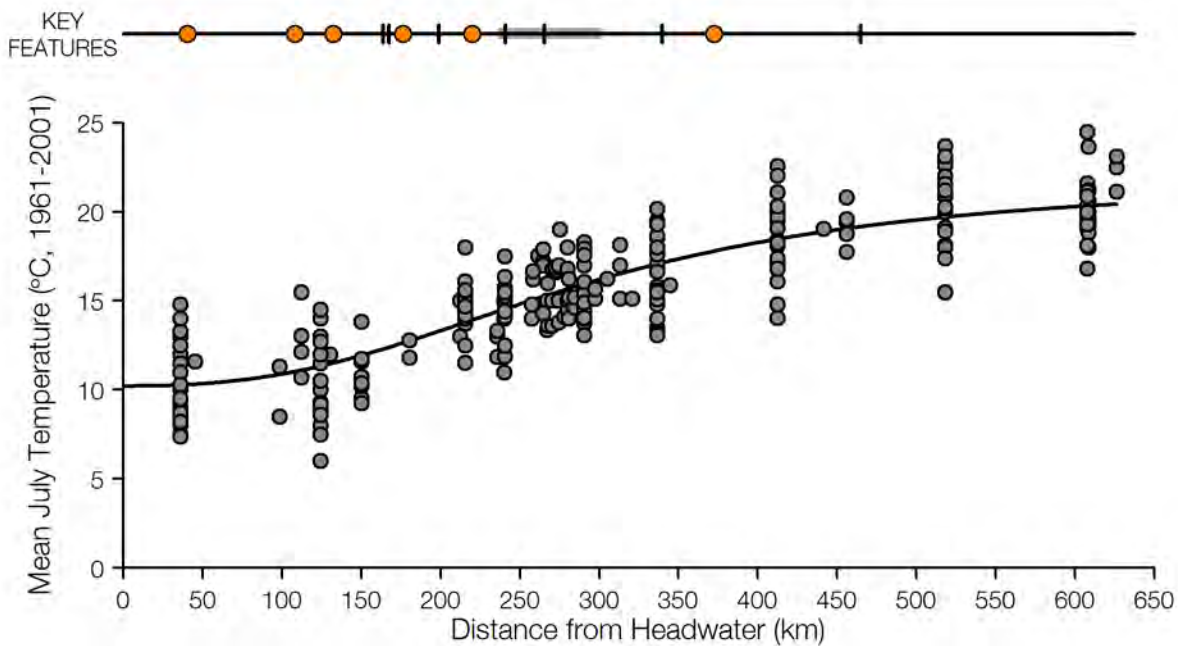


Figure 3. Measured (grey dots) and modelled (black line) water temperature along the Bow River. Water temperatures are measurements from July from water monitoring stations operated by provincial, federal and civic agencies along the mainstem of the Bow River from 1962 to 2001. These data were compiled by University of Calgary researchers for the Canadian Water Network into the NCE water quality database. Key features of the Bow River are illustrated above using the same distance from headwater scale. The orange dots indicate municipalities and reserves except for the City of Calgary, which is represented by the dark grey rectangle. The vertical black bars indicate dams or weirs on the river.

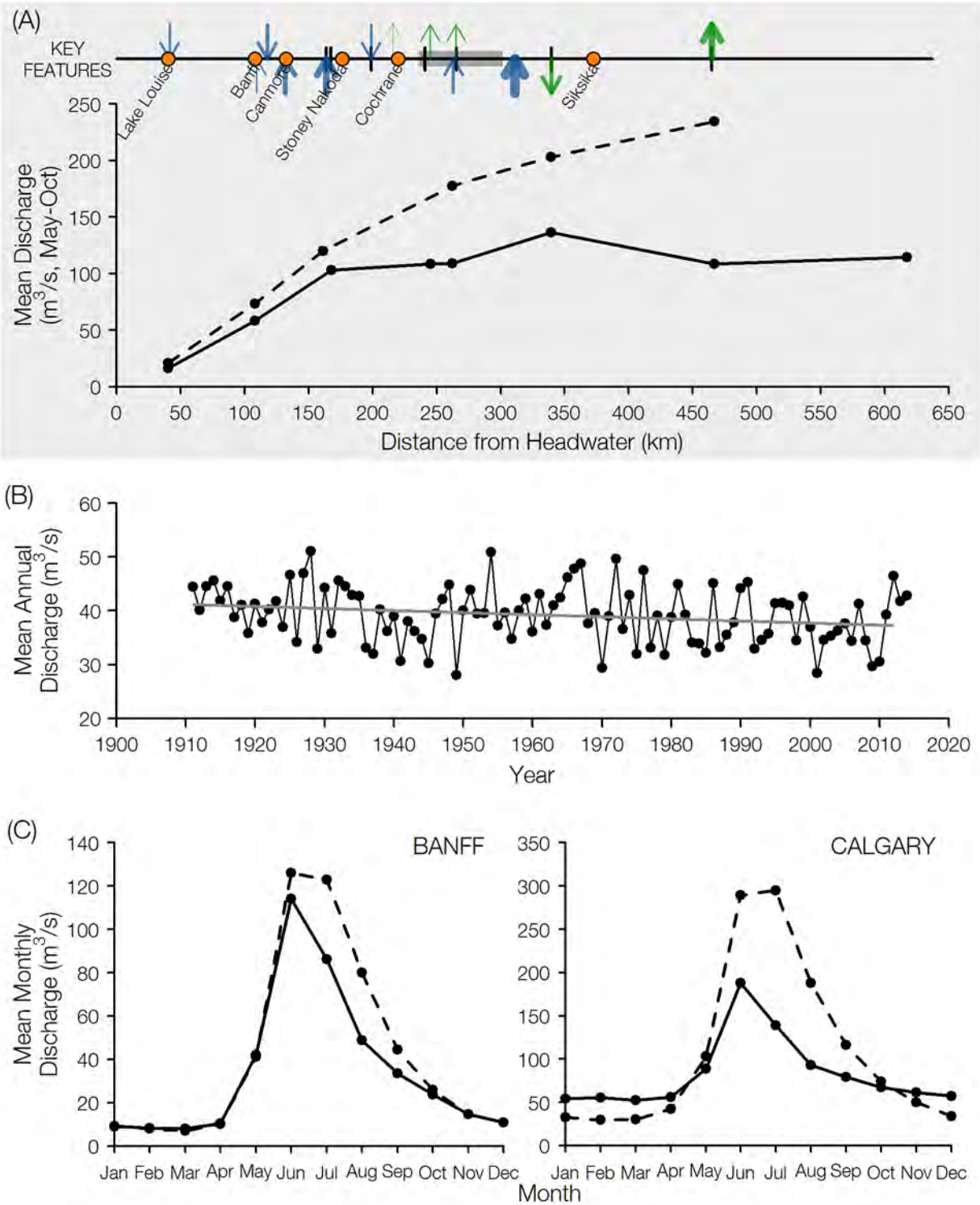


Figure 4. Variability of Bow River hydrology illustrated spatially (Panel A) and temporally (Panels B and C). Panel A shows mean May to October discharge from Lake Louise to near the mouth of the Bow River averaged from early years (1911-1920; dashed line) and from recent years (2001-2010, solid line). Key features of the Bow River are illustrated above using the same distance from headwater scale. The orange

dots indicate municipalities and reserves except for the City of Calgary which is represented by the dark grey rectangle. The vertical black bars indicate dams or weirs on the river. The blue arrows indicate main tributaries feeding the Bow River, and the green arrows indicate water withdrawals by the City of Calgary and the irrigation districts. Panel B shows mean annual discharge measured in Banff between 1910 and 2012. The grey line indicates a significant trend (Mean Annual Discharge = $115.86 - (0.04 * \text{year})$; $r^2 = 0.05$, $p < 0.05$). Panel C shows mean monthly discharge for both Banff and Calgary from the early years (1911-1920; dashed line) and recent years (2001-2010; solid line).

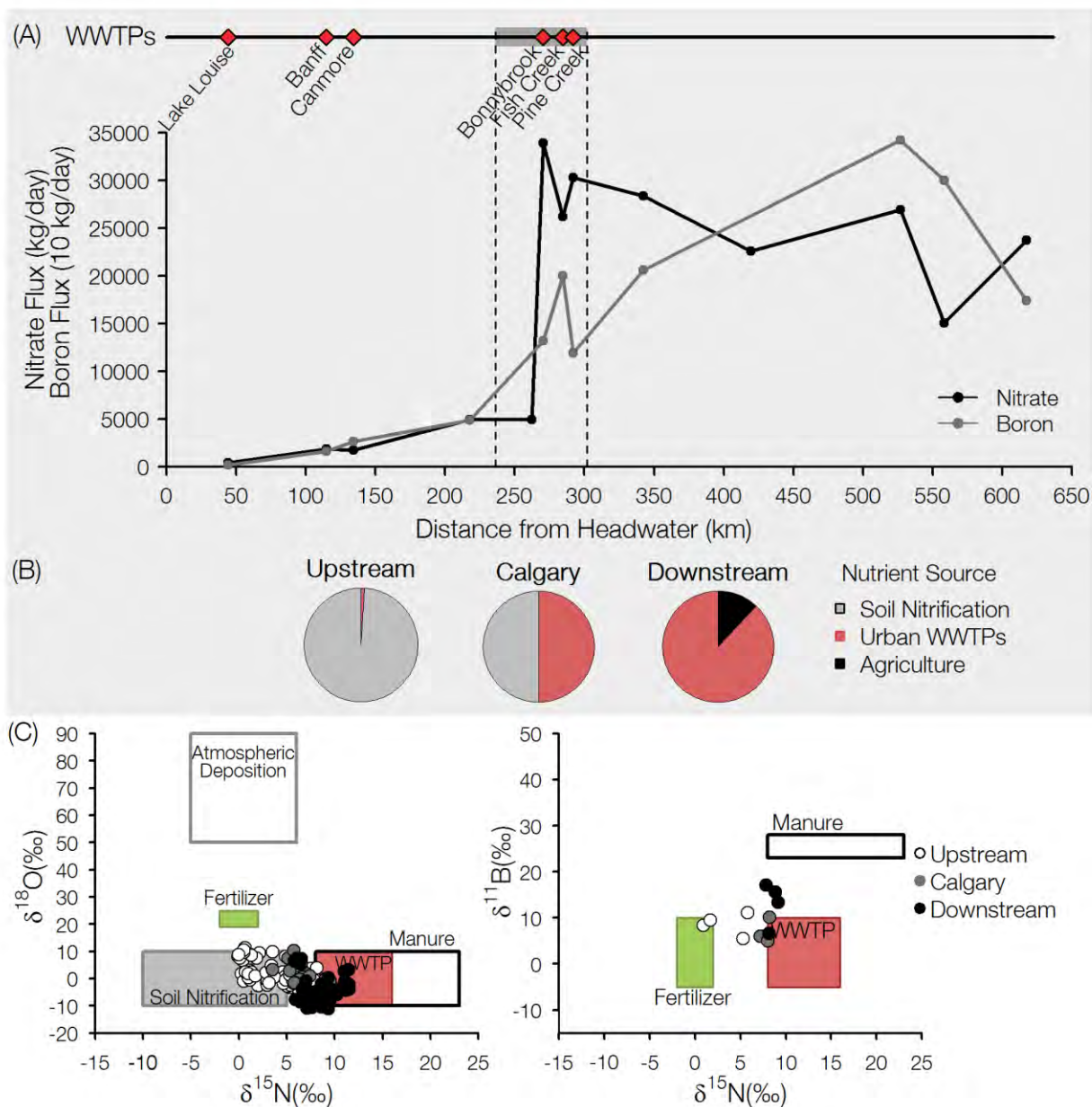


Figure 5. (A) Spatial variability of nitrate and boron flux (concentration x flow) along the Bow. Wastewater treatment plants (WWTPs) are illustrated on the line above using the same scale as the headwater distance scale. The darker grey rectangle along the WWTP line indicates the extent of the City of Calgary. The dashed horizontal lines also present the City of Calgary expanse. (B) Pie charts illustrating the approximated sources of nutrients in the Bow River upstream, within, and downstream of Calgary. (C) Bi-plots depicting stable isotope space of $\delta^{18}\text{O}$ vs $\delta^{15}\text{N}$ (left) and $\delta^{11}\text{B}$ vs $\delta^{15}\text{N}$ (right). The points indicate Bow River water samples with colours indicating the location of the sample. The boxes indicate stable isotope values of the various sources in the Bow River (atmospheric deposition, fertilizer, manure, WWTP, and soil nitrification).

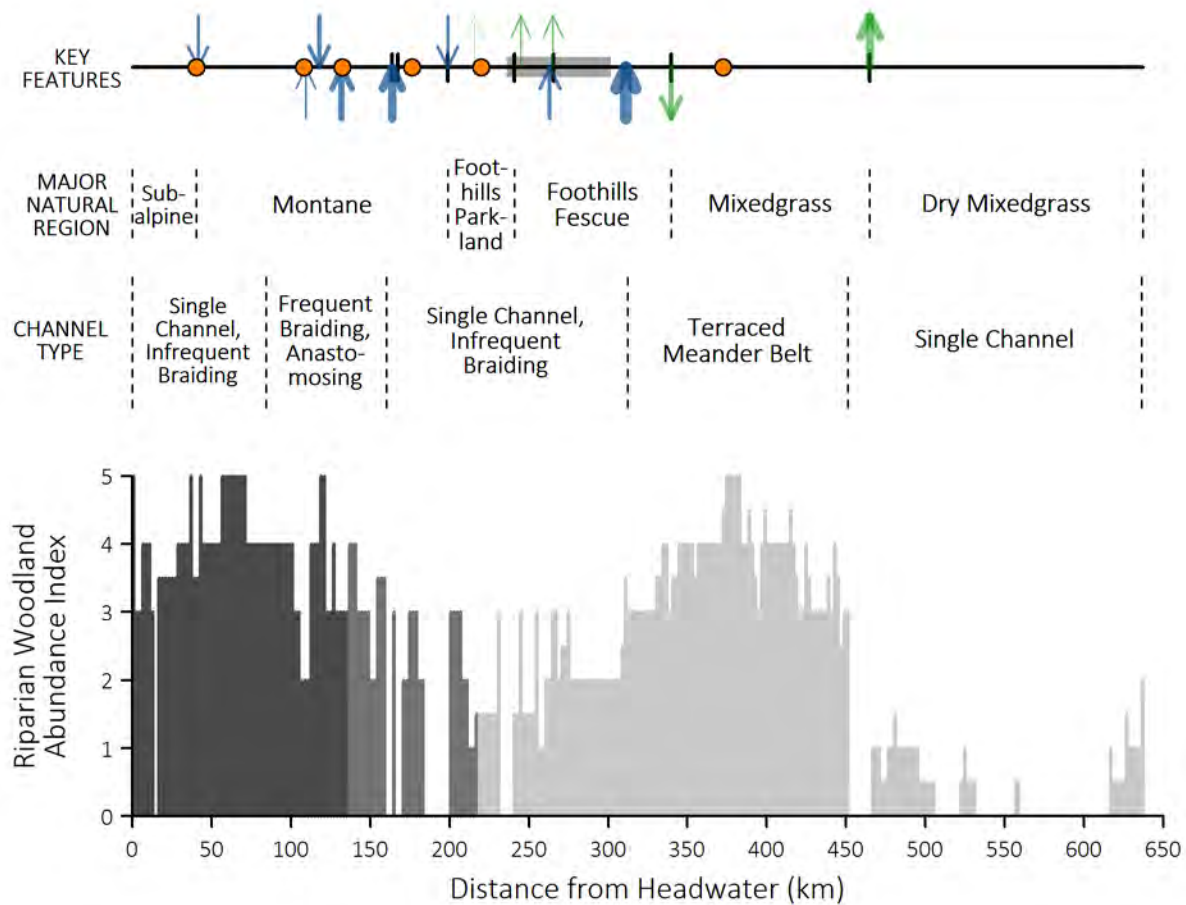


Figure 6. Estimated riparian abundance index along the Bow River from headwaters to the confluence with the Oldman River. The riparian abundance index reflects a visual estimate of density and extent of the riparian forest as observed on Google Earth (0=negligible, 1=very sparse, 2=thin, 3=moderate, 4=dense, 5=very dense and extensive). Dark grey represents a coniferous forest, mid-grey indicates a mixed forest, and light grey indicates a deciduous forest. Key features (municipalities – orange dots, City of Calgary – grey bar, blue arrows – tributaries, green arrows – extractions, vertical black bars – dams/weirs) are illustrated at the top. Major natural regions and channel type are also depicted.

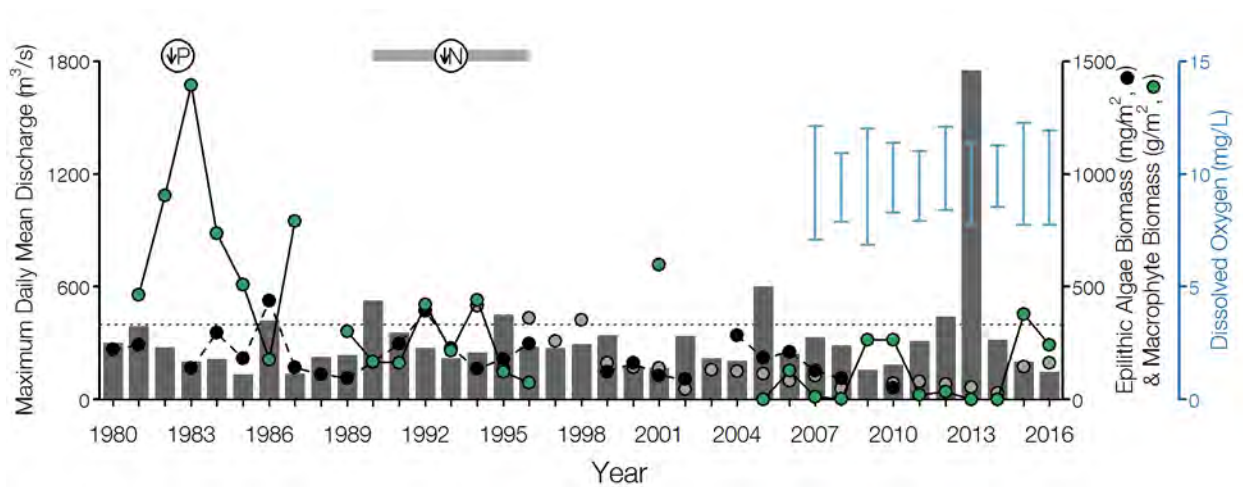


Figure 7A. Annual maximum daily mean discharge measured at the Bow at Calgary gauging station (05BH004; grey bars), mean annual epilithic algae biomass (black points), and mean September macrophyte biomass (green points) in all available years between 1980 and 2016. Dashed and solid lines connect consecutive years of data for algae and macrophyte biomass, respectively. Both algae and macrophyte biomass were measured at sites in the downstream end of Calgary. Since algae sampling at Stiers Ranch stopped after 2010, data from samples measured at a site near Carseland Dam are also shown (grey dots). The horizontal dotted grey line indicates the 400 m³/s discharge level which was suggested by Taube et al (2016) as the threshold above which scouring flows for macrophytes occur. Vertical blue lines indicate upper and lower standard deviation of September DO measured continuously at sites in the downstream end of the City of Calgary.

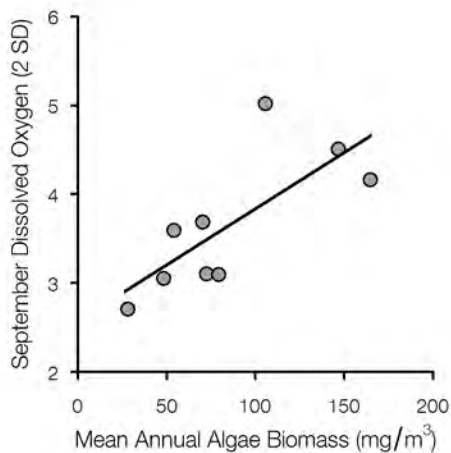


Figure 7B. September diel dissolved oxygen fluctuation (represented by 2SD) vs. mean annual algae biomass.

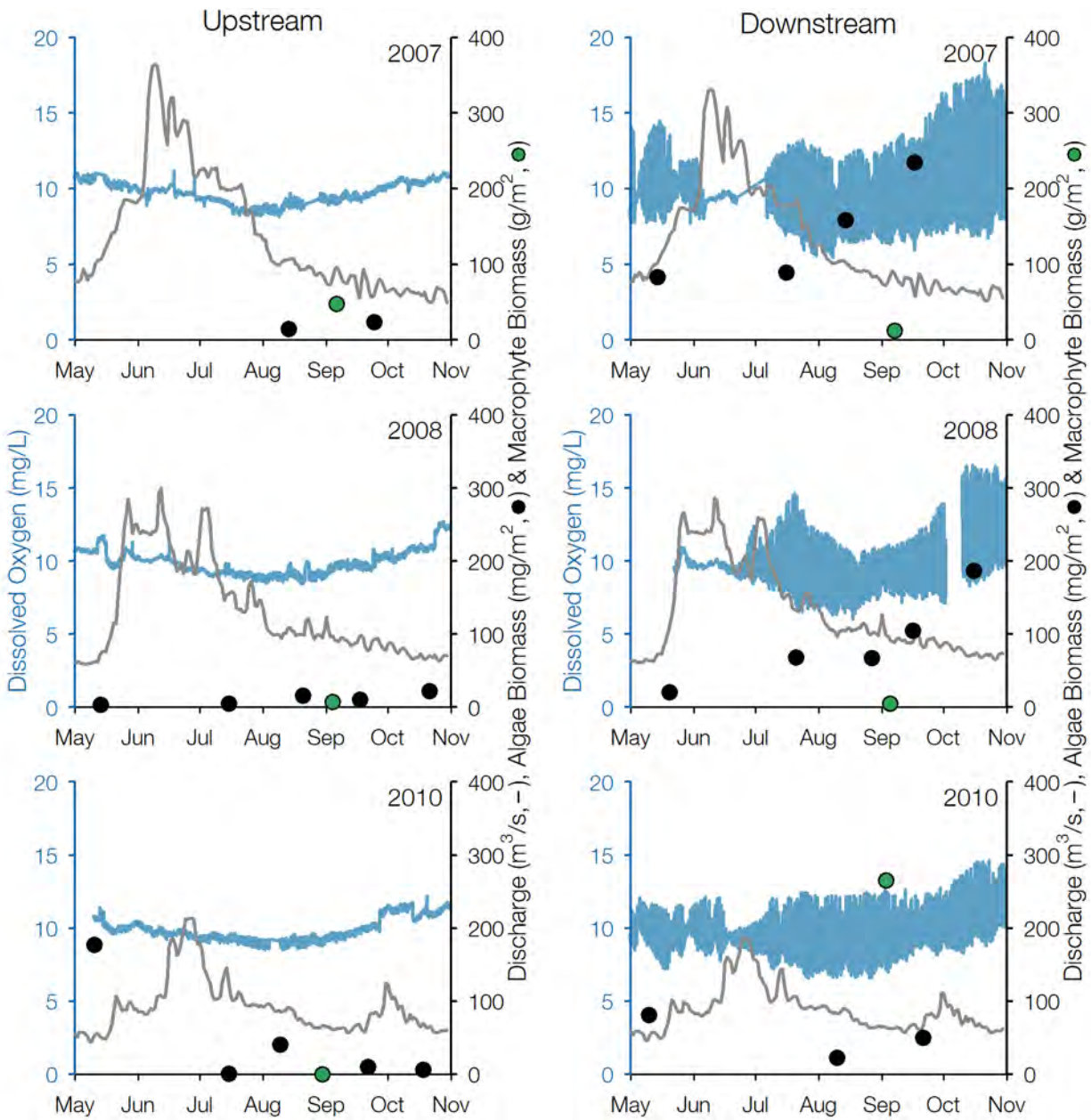


Fig. 8. Seasonal dissolved oxygen measured continuously at sites located upstream (M1) and downstream (M8) of the three WWTP outflows in the City of Calgary (blue line). Seasonal discharge (grey line) measured at Bearspaw (upstream: 05BH008) and Calgary (downstream: 05BH004) gauging stations. Green points indicate mean September macrophyte biomass sampled along both banks at M1 (upstream) and M8 (downstream). Black points indicate monthly epiphytic algae biomass measured at M8 (downstream). The Upstream algae biomass data was taken from a site at Cochrane because it was the closest available upstream data.

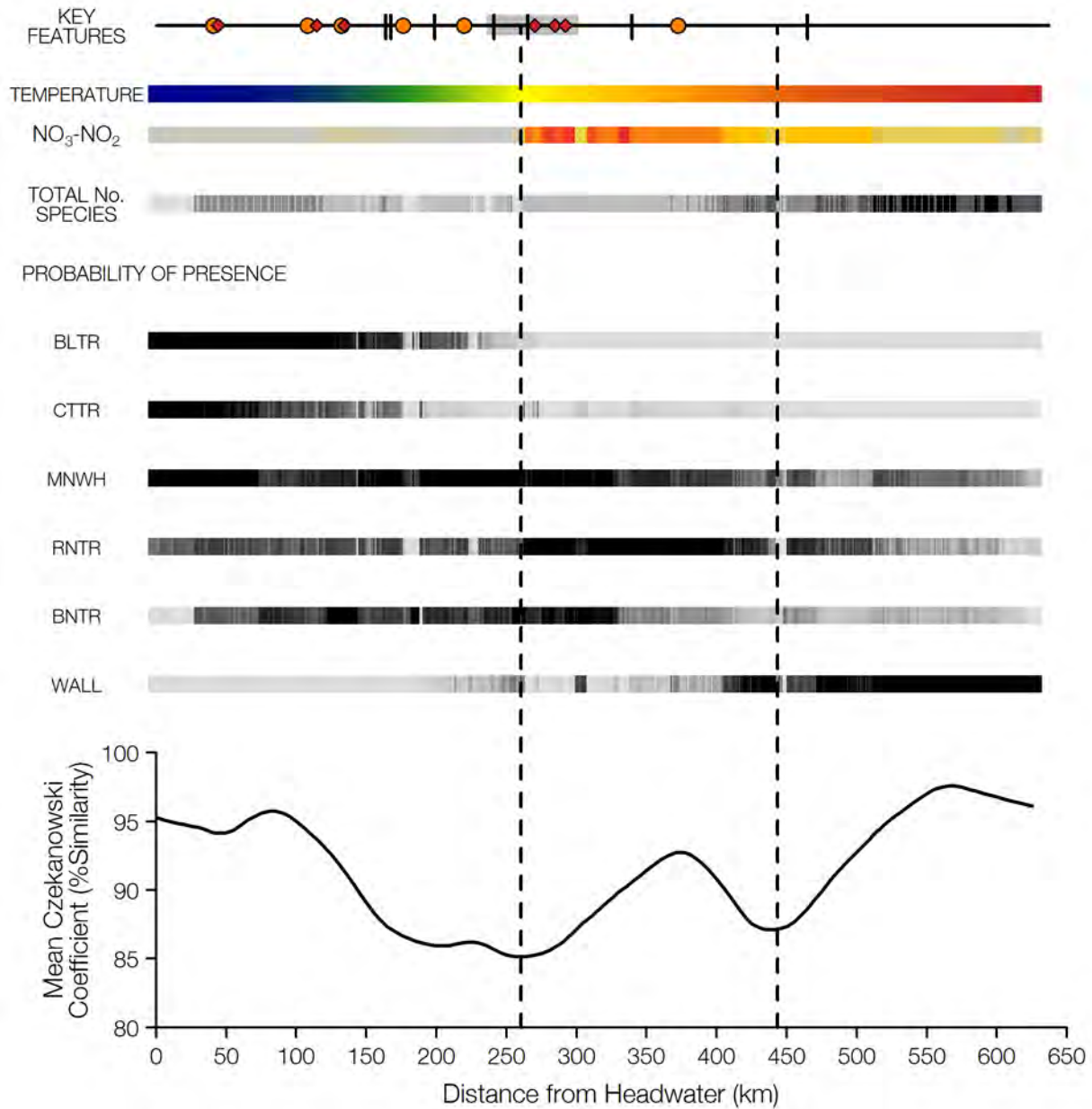


Fig 9. Probability of presence of bull trout (BLTR), cutthroat trout (CTTR), mountain whitefish (MNWH), rainbow trout (RNTR), brown trout (BNTR) and walleye (WALL) along the Bow River from headwaters at Bow Lake to the confluence with the Oldman River, based on logistic regression models based on presence-absence data (Mee et al., 2016). Darker greys indicate higher probability of presence. Total number of species reflect the number of species with predicted probability >0.5 (Robins, 2009). Key features at the top of the figure illustrate locations of population centres (orange dots, City of Calgary is shaded grey bar), WWTP outflows (red diamonds), and dams and weirs (black vertical bars). Mean July water temperature (1961-2001) increases along the Bow River from ~10°C at the headwaters at Bow Lake, to ~20°C at the confluence with Oldman River. The nitrate-nitrite bar indicates variation along the Bow River from 0.03 in grey to 0.8 mg/L in red. The mean Czekanowski coefficient was calculated in a 50-km sliding window estimated every 5 km along the Bow River where low values indicates areas of high species

turnover and high values indicates high similarity in fish species composition (Mee et al., 2016). The vertical dashed lines mark the two points along the Bow River where the highest species turnover occurs – at 15.1°C and 18.9°C.

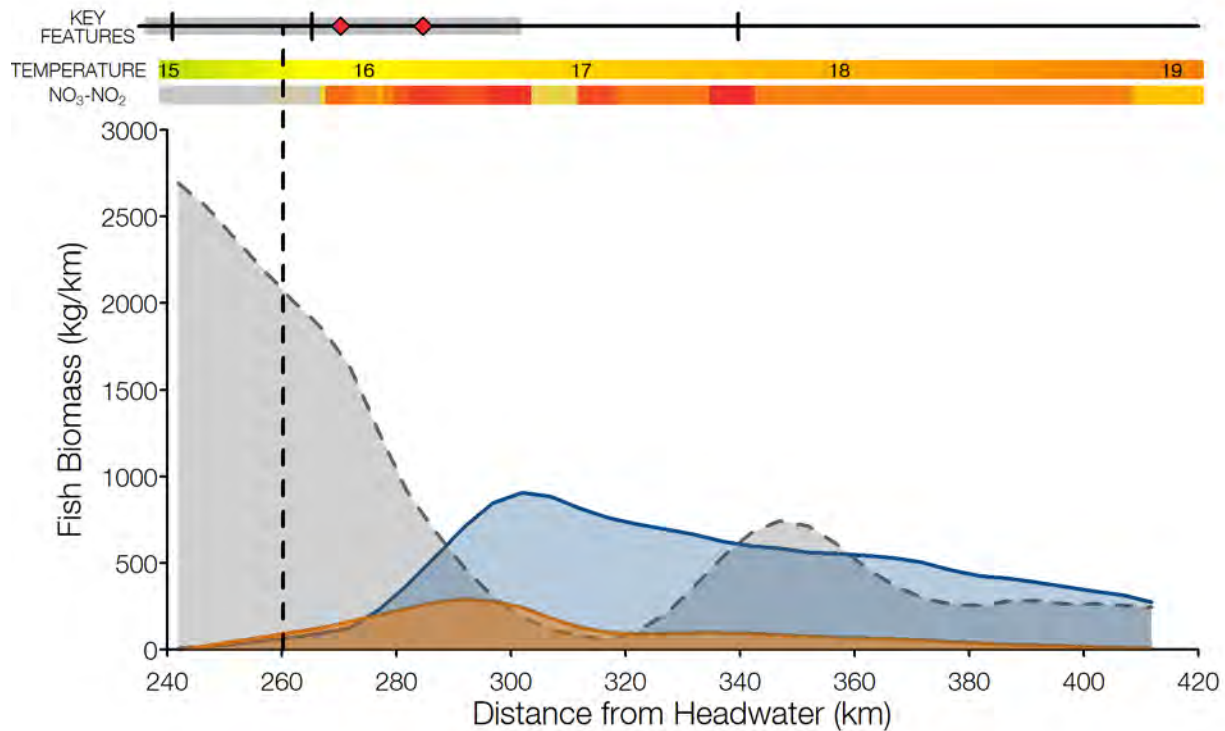


Fig 10. Loess tricube weight functions of biomass (kg/km) of mountain whitefish (grey), rainbow trout (blue) and brown trout (orange) caught in 2001 in the Bow River over a 177 km section (Askey et al., 2007). The vertical dashed line indicates the location of high species turnover estimated by the mean Czekanowski coefficient at 15.1 °C (Fig XA, Mee et al., 2016). Key features are illustrated along the top of the figure indicating the City of Calgary (grey shading), dams and weirs (black vertical bars; Bears paw dam, Calgary weir (which was still in place at the time of sampling) and Carseland weir), WWTPs (red diamond; only Bonnybrook and Fish Creek WWTPs were in existence at the time of sampling). Mean July water temperatures (1961-2001) and dissolved nitrate-nitrite data (1962-2001) presented here were obtained from the NCE Water Quality Database compiled by University of Calgary researchers for the Canadian Water Network from data available from provincial, civic and federal agencies (Mee et al., 2016). For the nitrate-nitrite (mg/L) data, grey indicates lower concentrations and dark red indicates higher concentrations.

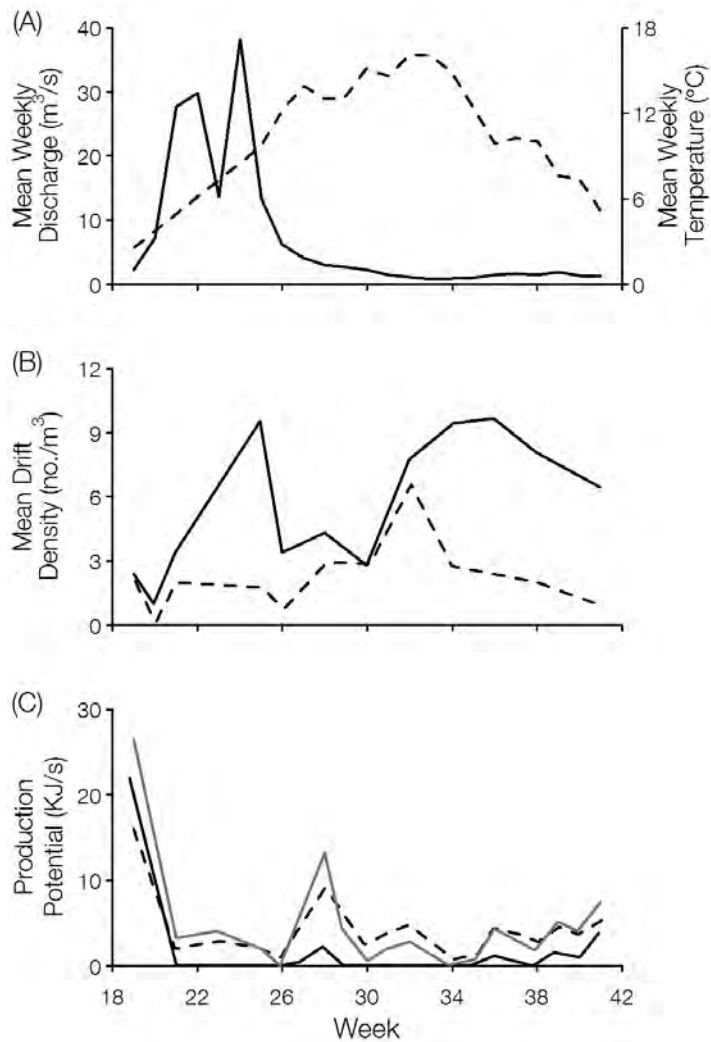


Figure 11. (A) Mean weekly stream discharge (m³/s, solid line) measured at the stream gauging station 05BH015. Mean weekly temperature (°C, dashed line) for Nicoll Ranch reach, Jumpingpound Creek, Alberta were based on in-stream measurements for weeks 26-41. Temperatures from weeks 19-25 were predicted based on a 3-parameter Gaussian function (Laliberte, 2012). (B) Mean weekly drift density of invertebrates in 0-2 mm (solid line) and 2-4 mm (dashed line) size classes. (C) Weekly production potential estimates (sum of positive NREI values) for YOY (dashed, black), juvenile (solid, grey) and adult (solid, black) rainbow trout.